

LOW ENERGY ELECTRON
TRANSPORT COEFFICIENTS AND SCATTERING CROSS SECTIONS
OBTAINED USING SWARM METHODS

A thesis submitted for the degree of
Doctor of Philosophy
of the Australian National University

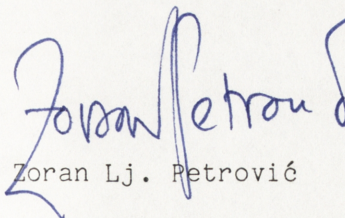
Zoran Lj. Petrović

February 1985

Except where acknowledgements are made in the text and in the present statement the candidate was responsible for all the work reported in this thesis.

The work reported in Chapter 3 was carried out jointly with Dr. G. N. Haddad and candidate's supervisor Dr. R. W. Crompton. The candidate has:

- 1) Suggested Models 3 and 5;
- 2) Carried out the calculations for the real gases and with the negative slope of the momentum transfer cross section;
- 3) Carried out the additional analysis needed to explain the results obtained for Models 1 and 5;
- 4) Developed the criterion and carried out all the comparisons with other available theories;
- 5) Analysed the available literature and compared the present explanation to the other available explanations of the phenomenon;
- 6) Jointly with the coauthors taken part in the development of the conceptual explanation of negative differential conductivity and the formulation of the model calculations (which were initially carried out by Dr. Haddad).


Zoran Lj. Petrović

Canberra 25 February 1985

ACKNOWLEDGEMENTS

Above all, I would like to thank my supervisor Dr. R.W. Crompton for guidance, enthusiasm, countless suggestions and ideas, and tremendous help, which made this work possible.

I would also like to thank Dr. M.T. Elford for numerous discussions, suggestions and help, Dr. G.N. Haddad for help in calculations and for checking some of the present results, Dr. S.J. Buckman for numerous discussions and help, Dr. R. Robson and Mr. K. Ness for very useful correspondence and discussions on various theoretical problems, Dr. K. Kumar for discussions and for reading and giving comments on Chapter 2, Dr. R.A. Cassidy, Dr. J. Reimers and Mr. D.F. Coker for help in use of the computer.

Special thanks are due to Prof. M. Morrison and his coworkers at the Oklahoma University for providing me with their theoretical results for hydrogen, as soon as these were calculated, and for helpful discussions.

I have also greatly benefited from the discussions, correspondence and/or provision of unpublished results from: Prof. A.V. Phelps, Prof. D. Smith, Dr. N. Adams, Prof. F. Linder, Dr. A.D. Stauffer, Dr. P.J. Chantry, Prof. S.C. Haydon, Prof. H. Tagashira, Prof. J. Warman, Prof. H. Blevin, Prof. N. Twiddy, Dr. S.R. Hunter, Dr. O.M. Williams, Dr. D.R.A. McMahon and Dr. W. Roznerski.

I would also like to thank the technical staff of the Ion Diffusion Unit: J. Gascoigne, K. Roberts, K. Jackman and T. Halstead, members of the Electronics Unit especially A. Cullen, N. Esau, P. Smith, D. Gibson and Dr. T. Rhymes, and the members of the Computer Services Centre for their valuable assistance.

Financial support from the Australian National University is gratefully acknowledged.

To all the members of the Ion Diffusion Unit I am grateful for their friendship and support.

Finally I would like to thank my wife and our parents for their patience and understanding and to thank my children for their impatience during the course of this work.

ABSTRACT

In the present work swarm methods were applied to measure electron transport coefficients with the aim of gaining further information about some low energy electron scattering cross sections of topical interest. These data were used either to derive the cross sections or to determine the compatibility of scattering cross section data, experimental or theoretical, with them.

Each case was investigated using the most appropriate swarm technique. Sometimes measurements were made in the pure gas (CO and D₂), but more often mixture techniques were applied (to study H₂O, SF₆, CH₃Br, H₂, Ar). The work with gas mixtures prompted studies of negative differential conductivity and the application of Blanc's Law.

Experimental results derived in this work include: diffusion coefficients for thermal electrons in H₂O and CH₃Br; attachment coefficients for thermal electrons in SF₆ and CH₃Br at different temperatures; drift velocities in CO, D₂ and in Ar-H₂ and He-H₂ mixtures; and finally the values of D_T/μ for CO and D₂. On the basis of these and other available data some low energy elastic and/or inelastic cross sections were either derived or discussed for H₂O, SF₆, CH₃Br, H₂, D₂, CO and Ar.

TABLE OF CONTENTS

ACKNOWLEDGEMENTS	3
ABSTRACT	5
TABLE OF CONTENTS	6
CHAPTER 1 INTRODUCTION	14
CHAPTER 2 THEORETICAL FOUNDATIONS OF ELECTRON SWARM EXPERIMENTS	18
2.1 Introduction	18
2.1.1 Outline of the chapter	18
2.1.2 Basic equations and definitions	20
2.2 Methods for Solving Boltzmann Equation	26
2.2.1 Lin, Robson and Mason's theory	27
2.2.2 Multiterm theories - "exact" solution of Boltzmann equation	36
2.2.3 Monte Carlo simulations	42
2.2.4 The two-term theory and other approximate theories	49
2.3 Determination of Electron Scattering Cross Sections from the Transport Coefficients	56
2.4 Relations Between the Transport Coefficients and the Experimentally Observable Quantities	68
2.5 Electron Transport Under the Influence of Density Gradients	73

CHAPTER 3	NEGATIVE DIFFERENTIAL CONDUCTIVITY IN GASES	82
3.1	Introduction	82
3.2	Qualitative Discussion	85
3.3	A Criterion for Negative Differential Conductivity	88
3.4	Other Theoretical Developments	90
3.5	Model Calculations	94
3.6	General Comments about Model Calculations and Criteria for Negative Differential Conductivity	101
3.7	Negative Differential Conductivity in Real Gases	106
3.8	Conclusions	109
CHAPTER 4	BASIC PRINCIPLES OF THE OPERATION OF THE CAVALLERI DIFFUSION EXPERIMENT	112
4.1	Introduction	112
4.2	Principle of the Operation of the Cavalleri Diffusion Experiment	112
4.3	Processes Governing the Electron Density Decay	123
4.4	Description of the Experiment and the Experimental Procedure	129
4.5	Mechanism of Field Compensation in an All-Glass Cell	134
CHAPTER 5	APPLICATION OF BLANC'S LAW TO THE DETERMINATION OF DIFFUSION COEFFICIENTS FOR THERMAL ELECTRONS: THE CASE OF WATER VAPOUR	142
5.1	Introduction	142
5.2	Analysis of the Application of Blanc's Law to Diffusion Coefficients for Thermal Electrons	144

5.2.1	Basic considerations	144
5.2.2	Deviations from Blanc's law	146
5.2.3	Model calculations	147
5.2.4	"Real" gases	152
5.2.5	Discussion	155
5.3	Measurements of the Diffusion Coefficient for Thermal Electrons in Water Vapour	157
5.3.1	Introduction	157
5.3.2	Experimental procedure	158
5.3.3	Results and discussion	159
5.3.4	A note on thermal electron attachment in water vapour	163
5.4	Conclusion	164
CHAPTER 6	THERMAL ELECTRON ATTACHMENT TO SF ₆ AT ROOM TEMPERATURE AND AT 500 K	165
6.1	Introduction	165
6.2	Electron Attachment to SF ₆	169
6.3	Experimental	178
6.4	Measurement of Attachment Coefficients	179
6.4.1	Introduction	179
6.4.2	The effect of higher-order diffusion modes on the determination of the attachment time constant	181
6.4.3	Results for the attachment rate coefficients obtained using different buffer gases	188
6.4.4	The possible effect of a non-Boltzmann vibrational population on the attachment rate	189
6.5	Temperature Dependence of k_{att}^{th} for SF ₆	196

6.6	Conclusion	201
CHAPTER 7	ATTACHMENT OF THERMAL ELECTRONS TO METHYL BROMIDE	203
7.1	Introduction	203
7.2	Room Temperature Results	205
7.3	Diffusion Coefficient for Thermal Electrons in CH ₃ Br	209
7.4	The Temperature Dependence of k_{att}^{th}	211
CHAPTER 8	MEASUREMENTS OF DRIFT VELOCITIES AND D_T/μ VALUES FOR NON-THERMAL ELECTRONS	215
8.1	Introduction	215
8.2	Measurements of Drift Velocities	215
8.2.1	Principle of the operation and the description of the apparatus	215
8.2.2	Determination of the frequency corresponding to the peak of the transmitted current	218
8.2.3	Sources of systematic errors	222
8.2.4	Preparation of mixtures	222
8.3	Measurements of the D_T/μ values	224
8.3.1	Geometrical and structural considerations	224
8.3.2	Effect of nonuniform surface potentials	226
8.3.3	Measurement of current ratios	230
8.3.4	Electron sources	231
8.3.5	Summary of sources of error	234

CHAPTER 9	ROTATIONAL AND VIBRATIONAL EXCITATION OF HYDROGEN	235
9.1	Introduction	235
9.2	Low Energy Cross Sections for Hydrogen	236
9.2.1	Results based on swarm experiments	236
9.2.2	The beam data	239
9.2.3	Theoretical results	241
9.3	The Swarm Data Used in the Present Analysis	244
9.3.1	Experimental transport coefficients - reliability and accuracy	244
9.3.2	Sources of data	246
9.3.3	Scaling of D_T/μ data for parahydrogen	248
9.4	Analysis	250
9.4.1	Introduction	250
9.4.2	Multiterm transport theory for hydrogen	252
9.4.3	Momentum transfer and total cross sections	254
9.4.4	Rotational cross sections	257
9.4.5	Vibrational excitation: splitting of the cross section into rotationally elastic and inelastic parts	266
9.4.6	Vibrational excitation: comparison of cross sections	268
9.4.7	Sensitivity of the transport data to local perturbations of $\sigma_{vib}(v=0-1)$: analysis of the accuracy of the swarm cross section	276
9.4.8	Electron transport coefficients in argon-hydrogen mixtures	279
9.5	Electron Transport Coefficients in a Helium-Hydrogen Mixture	284

9.5.1	Introduction	284
9.5.2	Results and analysis	288
9.6	Conclusion	292
CHAPTER 10	VIBRATIONAL EXCITATION OF DEUTERIUM BY LOW ENERGY	
	ELECTRONS	294
10.1	Introduction	294
10.2	Experimental Details and Results	296
10.2.1	Drift velocities	296
10.2.2	D_T/μ values	299
10.2.3	Corrections for longitudinal diffusion and ionization	302
10.2.4	Discussion	305
10.3	Derivation of the Vibrational Excitation Cross Section	305
10.3.1	The basic set of cross sections	305
10.3.2	Low energy analysis	307
10.3.3	Multiterm corrections for deuterium	311
10.3.4	Analysis at higher energies	312
10.4	Conclusion	316
CHAPTER 11	VIBRATIONAL EXCITATION OF CARBON MONOXIDE	319
11.1	Introduction	319
11.2	Measurement of Transport Coefficients	320
11.2.1	Available transport data	320
11.2.2	Measurements of D_T/μ	321
11.2.3	Measurements of drift velocities	327
11.3	Swarm-Derived Cross Sections	328
11.3.1	Available cross section data	328

11.3.2	Analysis	332
11.3.3	Non-resonant vibrational excitation	338
11.4	Conclusion	339
CHAPTER 12	LOW ENERGY ELASTIC SCATTERING OF ELECTRONS BY ARGON	342
12.1	Introduction	342
12.2	Cross Sections for Electron-Argon Scattering	344
12.2.1	Theoretical results	344
12.2.2	Modified effective range theory	345
12.2.3	Experimental results obtained using electron beams	346
12.2.4	Swarm-derived cross sections	350
12.3	Data used in the Present Analysis	350
12.3.1	Drift velocities and D_T/μ values in pure argon	350
12.3.2	Pressure dependence of the transport coefficients	351
12.3.3	Drift velocities in Ar-H ₂ mixtures	354
12.4	Analysis	358
12.4.1	Introduction	358
12.4.2	Method of Calculation	358
12.4.3	Comparison of cross sections	362
12.5	Conclusion	368
Appendix 1	Requirements for the Computer-Interface for Controlling the Cavalleri Diffusion Experiment	371
Appendix 2	Electron Thermalization	375
Appendix 3	The Experimental Data used in the Analysis to Determine the Cross Sections in Hydrogen	377
Appendix 4	Scaling Factor for Rotational Cross Sections	383

Appendix 5	Energy Losses in Rotationally Inelastic Vibrational Transitions	385
Appendix 6	Populations of the Rotationally Excited Levels in Molecules	387
	REFERENCES	389

CHAPTER 1: INTRODUCTION

In a recently published review article on the elastic scattering of electrons by molecules, the authors (Csanak et al. 1984) stated the following: "Secondly, in the electron energy region where the results obtained by the two different methods (i.e. beam and swarm techniques) can be directly compared ($\approx 0.1-5$ eV), such a comparison provides invaluable insight into the validity of the particular approach used to solve the Boltzmann equation". There are several similar statements in recently published papers presenting results obtained using beam methods. They all show a certain lack of understanding of the principle and of the merits of the swarm technique. As a comment on the statement given above it can be said that in most cases beam results are not accurate enough to be used to test various techniques used to solve the Boltzmann equation. In fact quite the opposite is true, swarm results can normally be used quite validly, irrespective of the numerical technique applied in the analysis, to test various beam and theoretical results.

However, as the accuracy of beam experiments improves and the energy range of these experiments is extended downwards the interaction between scientists using the two technique increases, and the complementarity of the two experimental techniques, supported by theoretical research, has been recognized (see, for example, Crompton 1983, 1984a). In recent years some of the disagreements between swarm-derived cross sections and other data have been resolved (e.g for elastic scattering in H₂, He, Ne and Ar) and in all the cases known to the author the swarm-derived cross sections turned out to be correct.

In the present work a variety of experimental swarm techniques were

used in order to provide additional swarm data as a basis for deriving low energy electron scattering cross sections or, if that were not possible, to check the consistency of some other sources of data with accurate transport data.

The thesis can be divided into three parts. The first does not involve any experimental work and consists of a theoretical introduction and an analysis of negative differential conductivity. An attempt has been made to present the theoretical introduction as a personal view of the merits and the drawbacks of various theoretical/numerical methods used in swarm physics and to discuss in as much detail as possible the problems that exist in the analysis of swarm experiments. The next chapter on negative differential conductivity contains a conceptual description and semi-quantitative analysis of one of the most interesting features in electron transport, especially in gas mixtures. This is supported by results of model calculations which clearly demonstrate the validity of the physical picture that has been developed.

In the second part, work is described on measurements of diffusion coefficients and attachment rates for thermal electron swarms. First, the "Cavalleri Diffusion Experiment" is described and some of its features, such as charge compensation in an all-glass cell, are discussed in detail. Next, a measurement of the diffusion coefficient for thermal electrons in water vapour is described together with an analysis of the data from these experiments. Since mixtures of H_2O and N_2 were used, an examination is made of the validity of Blanc's law as applied to mixtures of gases in which the energy dependences of the electron momentum transfer cross sections are very different. In the next two chapters measurements of electron attachment rates in SF_6 and CH_3Br at several temperatures are

presented. A detailed examination of the validity of the results for attachment rates obtained from the Cavalleri diffusion experiment is made. All these results are used to comment on some features of attachment cross sections for these gases.

Finally, non-thermal electron transport data are used to derive or check low energy cross sections in hydrogen, deuterium, carbon monoxide and argon. Where necessary, additional measurements were made in the pure gas (D_2 , CO) or in some appropriately chosen gas mixtures (H_2 , Ar).

The common feature in all the work presented in this thesis is the existence of some controversy about results either for the transport coefficients or for the cross sections. While it cannot be claimed that the present results have settled the dispute in every case they at least provide or strengthen the swarm standpoint. The philosophy behind the present work was, therefore, to apply the swarm techniques best suited to help resolve the controversy about the values of the transport data and low energy cross sections. Efforts were made to provide a much wider basis for the comparison between the swarm and the beam or theoretical results, or to provide data that would complement data from other experimental techniques or theory (e.g. to provide data for normalization).

Since one of the aims of the present work was to make a comparison between beam and swarm-derived cross sections an attempt is made to provide the reader who is not fully acquainted with the swarm method with a discussion of the basic principles of swarm techniques and of the problems that occur in the analysis of swarm data. Therefore Chapter 2 contains a discussion that may be too detailed for a specialist in swarm physics. For the same reason all the other chapters contain a brief review of the available data and possible applications, mainly in gas discharge physics.

The diversity of the problems that were analysed made the project very enjoyable and interesting, and increased the benefits to the author. Nevertheless this diversity created the problem of coping with a wide range, and a large quantity, of material. Therefore some of the accounts of the work are necessarily brief, while some minor aspects of it are not discussed at all.

Throughout the present work an attempt was made to use SI units as much as possible, but some units outside that system were used also such as the Townsend ($1 \text{ Td} = 10^{-21} \text{ Vm}^2$; see Huxley et al. 1966) and, occasionally, the Torr ($1 \text{ Torr} = 1/7.5 \text{ kPa}$). Standard notation was generally used wherever it exists, but notation for some quantities (such as the cross sections) is, for convenience, different in the theoretical introduction.

CHAPTER 2: THEORETICAL FOUNDATIONS OF ELECTRON SWARM EXPERIMENTS

2.1: Introduction

2.1.1: Outline of the chapter. As mentioned in Chapter 1 it is hoped that the present work will also be of interest to an audience outside swarm physics, most importantly physicists involved in the theory of electron scattering and in electron beam experiments. It is apparent that the methods applied in swarm physics are not sufficiently well known, with the consequence that problems inherent in swarm experiments and their interpretation are sometimes poorly understood or overstated. A rather lengthy chapter on the theoretical basis of swarm physics is therefore included in the present work together with summary of the principle underlying the extraction of cross sections from the experimental data.

The chapter commences with an outline of approximations involved in the development of the Boltzmann equation in the form used to analyse the swarm data. In the same section the transport coefficients are also defined.

In the next section the multiterm theory of Lin et al. (1979), which was used in the present work, is outlined. This is followed by a discussion of the difficulties that are sometimes encountered in its application.

In the following section (2.2.2) other multiterm theories are briefly outlined with a short description of the numerical methods that are used. The methods are compared by means of a table summarizing their characteristics.

Another way of relating the macroscopic properties of the swarm to collision processes is the method of Monte Carlo simulation. This method

is described next. It is usually believed that this technique invariably produces the correct results, the results being subject only to statistical uncertainty. Without wishing to diminish the merits of this technique, some problems in its implementation are discussed.

The so called "two-term" theory was the first theory that was developed to study electron swarms, and it was, and still is, used in the majority of papers published in this field. Nevertheless in the present work this theory is presented as a special case of a more general multiterm theory. For that reason its presentation follows rather than precedes (as is usually the case) the presentation of the multiterm theory.

A detailed exposition is given next of the swarm method for determining cross sections. Problems such as lack of uniqueness and the need to use highly accurate data are discussed but it should not be inferred from this discussion that the swarm technique is unreliable in general. On the contrary, if one is aware of its limitations, a correct assessment of the uniqueness and accuracy of the derived cross sections can be easily made.

A special branch of swarm theory that is of central importance to the interpretation of swarm experiments deals with solutions of the electron density continuity equation for geometries and boundary conditions that are appropriate to real experiments. The formulae that are derived from these solutions enable the experimentally observable quantities to be related to the transport coefficients.

Finally an account is given of a recently discovered problem in the interpretation of diffusion coefficients. Some calculations were performed to investigate a claim that the formula for the diffusion coefficient derived from the two-term theory gives incorrect results even when the electron distribution function is accurately calculated.

Since a wide range of topics is covered in this chapter it is not always possible to give detailed and explicit definitions of some of the quantities that are used. Appropriate references are given in such cases. For the same reason it was not possible to repeat some equations which would have assisted the reader.

2.1.2: Basic equations and definitions. Some excellent reviews of the theory of swarms have been published recently and in this chapter only the outline and the basic assumptions of the development of existing swarm theories will be given. In doing so the papers of Lin et al. (1979), Kumar et al. (1980) and Kumar (1984) will be mainly followed.

First, the meaning of the term swarm will be defined. It is an ensemble of charged particles that are moving in a neutral gas, and conditions are such that the probability of interaction between the charged particles is practically zero. The spatial and the time development of the ensemble are governed by collisions with the gas, the electric field and by the vessel that contains the swarm. In addition the gas is not significantly perturbed from thermal equilibrium by the presence of the swarm.

This definition has important implications for the form of the transport equation that describes the behaviour of such an ensemble of particles.

Second, it will be assumed that the motion of the charged particles is governed by the laws of classical mechanics. Quantum mechanical effects may occur for a period that is short compared to the free time between collisions, and occur only during the collisions. The number of particles is not necessarily conserved, in fact conservation is only possible for

swarm of electrons drifting and diffusing in an infinite medium under conditions that do not allow ionizing or attaching collisions to occur. This apparently idealized situation is far from being unrealistic since many swarm experiments try to simulate it by careful design and choice of operating conditions. Even the sampling of the electron swarm can be achieved without absorbing electrons on the boundary as in Cavalleri's electron density sampling technique (see Chapter 3). However any sampling of the swarm (except that which depends on measurements of the light emission from the gas excited by swarm at high E/N - see Blevin et al. 1976; 1978a and 1978b) means that it is significantly perturbed, and ceases to exist as such.

The dynamics of the system of N particles with 3N degrees of freedom can be described by Liouville's equation (see Liboff 1969 or Resbois and Leener 1977). Its solution is a function proportional to the density of ensemble points in phase space and can be related to the function $f_N(q_1, \dots, q_N, p_1, \dots, p_N, t)$ whose product with $dq_1, \dots, dp_N = dpdq$ represents the probability of finding the system in the state (q_1, \dots, p_N) . Generalized coordinates are denoted by q and the corresponding momentum by p while f_N is known as the N particle distribution function. The ensemble average of a dynamical property G of the system is then given by $\langle G \rangle = \int f_N G dpdq$.

It is possible to renormalize the distribution function to s particles using:

$$F_s = V^s \int f_N dq_{s+1}, \dots, dq_N, dp_{s+1}, \dots, dp_N \quad (2.1)$$

where V is the volume of a cell in the phase space. Consequently a whole hierarchy of equations relating F_s to F_{s+1}, \dots, F_N is produced (BBGKY -

equations).

In principle we are not concerned about microscopic properties of an ensemble. Most macroscopic properties can be described using a single particle distribution function $f(\underline{q}_1, \underline{p}_1, t)$. One form of the differential equation for f is known as Boltzmann Equation (BE). It can be derived from the BBGKY hierarchy by one of the available techniques (due to Bogoliubov, Kirkwood, Grad,...-see Liboff 1969). In doing so it must be assumed that correlations between the particles are small in comparison with the kinetic part. BE can also be formulated directly in phase space by balancing the flux of particles in and out of a small element (see Liboff 1969 or Huxley and Crompton 1974) - so it is a continuity equation in phase space. The important difference between BE and the BBGKY-single particle equation is that the former is irreversible. Irreversibility was introduced by the so called "molecular chaos" assumption that was used to relate F_2 to F_1 (or f) in order to make an equation closed in f .

The basic form of BE that describes electron swarms is (Kumar et al 1980):

$$\left\{ \frac{\partial}{\partial t} + \underline{c} \frac{\partial}{\partial \underline{r}} + \underline{a} \frac{\partial}{\partial \underline{c}} \right\} f(\underline{r}, \underline{c}, t) = -Jf(\underline{r}, \underline{c}, t) \quad (2.2)$$

where J is the collision operator and from this point on the variables \underline{c} (particle velocity) and \underline{r} (spatial coordinate) will be used instead of \underline{p} and \underline{q} . In principle J is a nonlinear function of f , dependent on $(f_1' f_1' - f_1 f_1) d\underline{c} d\underline{r}$ where ' denotes the precollision situation and subscript 1 refers to the other particle taking part in the collision process.

The definition of the electron (and ion) swarm enables us to linearize the collision operator since f_1 is taken to be the Maxwellian distribution

function for the gas particles (at the known gas temperature T). Once electron-electron collisions become important this linearity is in principle lost, but in that case it is also possible to formulate a workable BE by using the Fokker-Planck collision integral (Braglia 1970; Gould 1974; Kunc 1983). Under conditions relevant to electron swarms, it is possible to write the collision operator as (Lin et al. 1979; Kumar et al. 1980):

$$J(f) = \sum_i \sum_j \int [f(\underline{c})F_i(\underline{C}) - f(\underline{c}')F_j(\underline{C}')] g \sigma(ij;g,\Omega) d\underline{g}' d\underline{C} \quad (2.3)$$

where i, j denote the internal degrees of freedom of the (molecular) collision partner, C is the thermal velocity of the molecule (the background gas is at rest) and F_i is the corresponding distribution function

$$F_m(C) = \frac{N}{Z} e^{-\frac{\epsilon_i}{kT}} \left(\frac{M}{2\pi kT}\right)^{3/2} e^{-\frac{MC^2}{2kT}} \quad (2.4a)$$

$$Z = \sum_i e^{-\frac{\epsilon_i}{kT}} \quad (2.4b)$$

The relative velocity of the collision partners is g , and Ω is the scattering angle. The differential elastic and inelastic cross sections are $\sigma(ii;g,\Omega) = \sigma(i;g,\Omega)$ and $\sigma(ij;g,\Omega)$ respectively; ϵ_i is the energy of the internal level i . From this point on N represents the gas particle number density.

Equation (2.3) includes the superelastic collisions $j \rightarrow i$. Cross sections for superelastic and inelastic collisions are related by the microscopic reversibility relation (for non-degenerate states, or sums over

degenerate states):

$$(g')^2 \sigma(ji;g',\Omega) = g^2 \sigma(ij;g,\Omega) \quad (2.5a)$$

with

$$\frac{1}{2} mg^2 + \epsilon_i = \frac{1}{2} m(g')^2 + \epsilon_j \quad (2.5b)$$

Apart from the above mentioned property of linearity and the assumption that led to irreversibility, there is another set of inherent assumptions. Collisions are treated as if their duration is short enough, or interaction strong enough, that boundary effects, the influence of external forces, the spatial variation of the distribution function and multiple collisions may be neglected (Ness 1977). Conditions under which the binary collisions approximation is violated will be discussed in more detail later on (see Section 12.3.2).

It is desirable to represent the motion of swarms by macroscopic transport coefficients. Starting from the initial conditions, or following some very fast perturbation, it is possible to follow the short-time development of swarms (Kumar 1981). At such early times it is difficult to define those coefficients, as they are functions of the spatial coordinates and time. Normally these functions decay to coefficients dependent only on the field intensity and on the characteristics of the gas (N,T). This situation is the so called hydrodynamic regime. In this regime it is possible to factorize the distribution function in the following way:

$$f(\underline{r}, \underline{c}, t) = \sum_{k=0}^{\infty} \underline{f}^{(k)}(\underline{c}) * (-\nabla)^k n(\underline{r}, t) \quad (2.6)$$

Here $\underline{f}^{(k)}(\underline{c})$ are tensor functions of the rank k and $*$ is a k -fold scalar product. The distribution function is normalized thus:

$$\int f(\underline{r}, \underline{c}, t) \, d\underline{r} \, d\underline{c} = \int n(\underline{r}, t) \, d\underline{r} \quad (2.7)$$

$$\int f^{(k)}(\underline{c}) \, d\underline{c} = \delta_{k0} \quad . \quad (2.8)$$

Therefore we are able to split the velocity (energy) and the spatial/time dependence. The continuity equation for $n(\underline{r}, t)$ is:

$$\left(\partial_t - \sum_{k=0}^{\infty} \underline{\omega}^{(k)} * (-\nabla)^k \right) n(\underline{r}, t) = 0 \quad (2.9)$$

where $\underline{\omega}^{(k)}$ are tensorial transport coefficients that can be determined from (Kumar et al. 1980; Kumar 1984)

$$\underline{\omega}^{(0)} = - \int J^R f^{(0)}(\underline{c}) \, d\underline{c} \quad (2.10a)$$

$$\underline{\omega}^{(k)} = \int \underline{c} f^{(k-1)}(\underline{c}) \, d\underline{c} - \int J^R \underline{f}^{(k)}(\underline{c}) \, d\underline{c} \quad . \quad (2.10b)$$

J^R is the reactive part of the collision operator - the part of J that describes non-conservative processes.

It should be noted that there is an ever-present possibility that hydrodynamic conditions are not reached even in a steady state situation. In that case the coefficients are not easily defined and experiments produce results that are dependent on the geometry of the apparatus. Such situations are encountered when diffusion or attachment cooling occur (Rhymes and Crompton 1975; Leemon and Kumar 1975; Robson 1976b; Hegerberg and Crompton 1983; Skullerud 1983). Experiments that fail to simulate an infinite volume are usually prone to such effects. Under these conditions the influence of the boundaries is felt deep inside the apparatus and it becomes critical to define the boundary conditions carefully in order to be

able to model the experiment.

Precise analysis of electron transport phenomena that occur close to absorbing boundaries is one of the most challenging tasks faced by electron transport theorists. Results of a limited number of either analytical (Robson 1981; McMahon 1983c) or numerical solutions (Hall and Lowke 1975; Lowke et al. 1977, see also Chantry 1982a) supported by Monte Carlo simulations (Braglia and Lowke 1979) indicate that all the transport coefficients deviate significantly from the spatially independent values. It appears that the mean distance for momentum transfer D/v_{dr} describes very well the thickness of the transition region close to the boundary. A novel approach to the treatment of the boundary effects was suggested by Kumar (1984). It is to treat the boundary as an additional, localized, term in the collision operator. Thus the need to specify the higher order boundary conditions (higher order derivatives) is avoided.

2.2: Methods for solving Boltzmann Equation

The basic requirements for the theory of swarm experiments will now be listed together with some procedures that have been developed to satisfy those needs.

a) First, it is necessary to develop theory that links the macroscopic, transport coefficients to the microscopic events that is, collisions and their cross sections.

b) Coefficients should be well defined and it should be possible to calculate them to a very high accuracy (desirably better than $\pm 0.1\%$).

c) The procedures for doing so should be reasonably fast because they have to be repeated many times during the process of adjustment of the

cross sections to fit the experimental data.

d) The theory must also link the experimental observables to the transport coefficients. These observables include: the frequency dependence of the current transmitted through the shutters of a drift tube (see Chapter 8), the ratios of currents falling on the segments of the divided anode of a Townsend-Huxley experiment (see Chapter 8), the time dependence of the current of a pulsed discharge, the ratios of light intensities emitted from the Cavalleri's diffusion experiment (see Chapter 4),

2.2.1: Lin, Robson and Mason's theory. The first step in the analysis is to expand the distribution function into a series of spherical harmonics (Lin et al. 1979):

$$f(\underline{r}, \underline{c}, t) = \sum_{\ell=0}^{\infty} \sum_{m=-\ell}^{\ell} f_{\ell m}(\underline{r}, \underline{c}, t) Y_{\ell m}^*(\underline{c}/c) \quad (2.11a)$$

where

$$Y_{\ell m}(\underline{c}/c) = P_{\ell}^{|m|}(\cos\theta) e^{im\phi} \quad , \quad (2.11b)$$

θ and ϕ are the polar angles, and $*$ denotes a complex conjugate. $f_{\ell m}$ depend only on the magnitude of c . The expansion (2.11) can be applied to any function of \underline{c} , in particular also to the function $f^{(k)}(\underline{c})$. An important property of the collisional operators used in swarm physics is their rotational invariance. It has the effect that $J(f(\underline{c})Y_{\ell m}) = Y_{\ell m}J_{\ell}(f(\underline{c}))$ so that the collision operator is "transparent" to $Y_{\ell m}$ and therefore:

$$J(f(\underline{c})) = \sum_{\ell=0}^{\infty} \sum_{m=-\ell}^{\ell} Y_{\ell m}(\underline{c}/c) J_{\ell}(f(c)) \quad (2.12)$$

where J_{ℓ} is the projection of J onto $Y_{\ell m}$. This procedure plus the orthogonality of the spherical harmonics enables one to perform the expansion (2.11) on the left hand side of BE (Equation 2.2) and, by equating the factors that are multiplying the harmonics, to determine the equations for various coefficients of the expansion, that is, the functions $f_{\ell m}$.

The transport of electrons through gases is a special case of a more general problem, that is, of the transport of charged particles of an arbitrary mass (ions). In many ways the introduction of the small mass ratio m/M ($< 1/1836$) simplifies the situation, but on the other hand it is easier for electrons to reach higher energies for the same value of E/N and then numerous inelastic channels (both conservative and not) become accessible.

Difficulties encountered in the theory of ionic transport led to much faster development of "exact" solutions of BE. Especially successful was the multi-temperature moment method developed on the basis of the work of numerous authors (see Kumar et al. 1980; Weinert 1982; and Skullerud 1984 for general ideas and references). Lin, Robson and Mason (LRM) have successfully modified this approach to suit electron transport. Their theory will be presented in greater detail than the other theories, since their method has been used in all the "multi term" calculations presented in this work.

First, the distribution function is expanded in a series of spherical harmonics (2.11). The next step is to expand $f_{\ell m}$ into a series of Sonine polynomials S (see Chapman and Cowling 1960 for details of Sonine

polynomials):

$$f_{\ell m}(\underline{c}) = n g^{(0)}(\underline{w}) \sum_{\ell=0}^{\infty} f_{\ell m}^{(r)} w^{\ell} S_{\ell+1/2}^{(r)}(w^2), \quad (2.13)$$

where

$$g^{(0)}(\underline{w}) = \left(\frac{m}{2\pi k T_b} \right) e^{-w^2} \quad (2.14)$$

is the Gaussian weight function (for a more detailed and general discussion see Kumar et al. 1980; Weinert 1982; and Skullerud 1984), and

$$\underline{w} = \left(\frac{m}{2\pi k T_b} \right)^{1/2} \underline{c}. \quad (2.15)$$

T_b is a parameter with the dimension of temperature, but in general $T_b \neq T$ (T is the gas temperature). Choosing $T_b = T$ would be adequate for the "low field - low gradient" situation (Kumar 1984).

Combining the previous expansions we get:

$$f(\underline{c}) = n g^{(0)}(\underline{w}) \sum_{r=0}^{\infty} \sum_{\ell=0}^{\infty} \sum_{m=-\ell}^{\ell} f_{\ell m}^{(r)} \Psi_{\ell m}^{(r)}(\underline{w}) \quad (2.16)$$

where $\Psi_{\ell m}^{(r)}(\underline{w}) = w^{\ell} S_{\ell+1/2}^{(r)}(w^2) Y_{\ell m}(w/w)$ is a tensor function (see Lin et al. 1979). Coefficients of the expansion $f_{\ell m}^{(r)}$ can be found using the orthogonality of $\Psi_{\ell m}$ (LRM). We shall proceed by substituting (2.16) into (2.2), multiplying the result by $\Psi_{\ell m}^{(r)}$ and integrating over all \underline{c} 's. After some algebraic manipulations an infinite set of moment equations may be obtained (for detailed exposition and definitions see LRM):

$$\begin{aligned} \left(\langle \underline{v} \Psi_{\ell m}^{(r)} \rangle - \langle \underline{v} \rangle \langle \Psi_{\ell m}^{(r)} \rangle \right) \underline{\nabla} \ln(n) - \frac{e}{m} \underline{E} \langle \underline{\nabla} \Psi_{\ell m}^{(r)} \rangle \\ = - N \sum a_{rs}(\ell) \langle \Psi_{\ell m}^{(r)} \rangle \end{aligned} \quad (2.17)$$

where

$$a_{rs} = \frac{N_{s\ell}}{N_{r\ell}} J_{rs}^\ell = \frac{N_{s\ell}}{N_{r\ell}} \sum_{\lambda\mu\nu} \langle lrs | \lambda\mu\nu \rangle U_{\mu\nu}^\lambda \quad (2.18)$$

$$N_{r\ell} = \frac{2\pi^{3/2} r!}{\Gamma(r+\ell+3/2)} \quad (2.19)$$

$$U_{\mu\nu}^\lambda = \frac{w_j}{Z} e^{-(\epsilon_j/kT)} \left\{ V_{\mu\nu}^\lambda(j) + \sum_k \left[\frac{w_k}{w_j} e^{-(\epsilon_k - \epsilon_j)/kT} V_{\mu\nu}^\lambda(jk) \right] \right\} \quad (2.20)$$

$$Z = \sum_j w_j e^{-\epsilon_j/kT} \quad (2.21)$$

(where w_j is the statistical weight of the level j).

Matrix elements in equation (2.20) are separated into elastic:

$$V_{\mu\nu}^\lambda(j) = \left(\frac{2kT_b}{m}\right)^{1/2} N_{\mu\nu}^\lambda \int_0^\infty e^{-x} x^{\lambda+1} S_{\lambda+1/2}^{(\mu)}(x) S_{\lambda+1/2}^{(\nu)}(x) \\ \times [\sigma_0(j; kT_b x) - \sigma_\lambda(j; kT_b x)] dx \quad (2.22)$$

inelastic:

$$V_{\mu\nu}^\lambda(jk) = \left(\frac{2kT_b}{m}\right)^{1/2} N_{\mu\nu}^\lambda \int_0^\infty e^{-x_{kj}} x_{kj}^{\lambda/2+1} S_{\lambda+1/2}^{(\nu)}(x_{kj}) \\ \times [\sigma_0(jk; kT_b x_{kj}) x_{kj}^{\lambda/2} S_{\lambda+1/2}^{(\mu)}(x_{kj}) \\ - \sigma_\lambda(jk; kT_b x_{kj}) x^{\lambda/2} S_{\lambda+1/2}^{(\mu)}(x)] dx \quad , \quad (2.23)$$

and superelastic parts:

$$\begin{aligned}
 V_{\mu\nu}^{\lambda}(kj) &= \left(\frac{2kT_b}{m}\right)^{1/2} N_{\mu\nu}^{\lambda} \int_0^{\infty} e^{-x} x_{kj} x^{\lambda/2} S_{\lambda+1/2}^{(\nu)}(x) \\
 &\quad \times \left[\sigma_0(jk; kT_b x_{kj}) x^{\lambda/2} S_{\lambda+1/2}^{(\mu)}(x) \right. \\
 &\quad \left. - \sigma_{\lambda}(jk; kT_b x_{kj}) x_{kj}^{\lambda/2} S_{\lambda+1/2}^{(\mu)}(x_{kj}) \right] dx , \quad (2.24)
 \end{aligned}$$

where

$$N_{\mu\nu}^{\lambda} = \left(\frac{\mu! \nu!}{\Gamma(\mu+\lambda+3/2) \Gamma(\nu+\lambda+3/2)} \right)^{1/2} , \quad (2.25)$$

$$x = \epsilon/kT_b \quad , \quad x_{kj} = x + (\epsilon_k - \epsilon_j)/kT_b \quad (2.26)$$

and

$$\sigma_{\lambda}(jk; \epsilon) \equiv 2\pi \int_0^{\pi} P_{\lambda}(\cos\theta) \sigma(jk; \epsilon, \theta) \sin\theta d\theta . \quad (2.27)$$

Here $\sigma(jk; \epsilon, \theta)$ is the energy dependent differential scattering cross section, and θ is the scattering angle.

At this point the total (σ_T) and the momentum transfer (σ_m) cross sections will be defined:

$$\sigma_T = \sigma_0 \quad ; \quad \sigma_m = \sigma_0 - \sigma_1 . \quad (2.28)$$

The formulae relating the energy dependent differential cross section and σ_m and σ_T are obtained as follows. First, the angular dependence of $\sigma(jk; \epsilon, \theta)$ is separated from its energy dependence using

$$\sigma(jk; \epsilon, \theta) = \sigma(jk; \epsilon) I(\theta) , \quad (2.29)$$

with

$$I(\theta) = \sum_{\ell=0}^{\infty} a_{\ell} P_{\ell}(\cos\theta) \quad (2.30)$$

From (2.27) we then obtain:

$$\sigma_T(jk; \varepsilon) = 4\pi a_0 \sigma(jk; \varepsilon) \quad (2.31)$$

and

$$\sigma_m(jk; \varepsilon) = 4\pi (a_0 - a_1/3) \sigma(jk; \varepsilon) \quad (2.32)$$

The expression for the coefficients $\langle \ell rs | \lambda \mu \nu \rangle$ in (2.18) is quite complicated (Lin et al. 1979) and it is unnecessary to present it here. However, for electrons (low mass ratio m/M) these coefficients can be simplified; for example (see Lin et al. 1979), for a gas in which there are only elastic collisions in the relevant energy range, equations (2.18) and (2.20) can be simplified to give:

$$J_{rs}^{\ell} = V_{rs}^{\ell} + O(m/M) \quad (2.33)$$

where $O(m/M)$ is a term approximately m/M times smaller than the other term on the right hand side of (2.33). It should be noted that in all the equations above the effective mass μ_{eff} was replaced by the mass of the electron m , which is a very good approximation throughout.

Terms $V_{\mu\nu}^{\lambda}(j)$ represent elastic, $V_{\mu\nu}^{\lambda}(jk)$ inelastic, and $V_{\mu\nu}^{\lambda}(kj)$ superelastic collisions. The same notation for indices jk is used for cross sections.

Once all the matrix elements J_{rs}^{ℓ} are calculated one can proceed to solve the set of equations (2.17). However in order to produce a set that

can be solved numerically some additional assumptions are implemented (LRM). The most important is that the spatial gradients are small and therefore that the moment equations can be linearized in ∇n . Thus one produces a set of equations for the spatially homogeneous moments $\langle \psi_1(r) \rangle^{(0)}$, and two sets for the spatially inhomogeneous moments, one, $\langle \psi_1(r) \rangle^{(z)}$, parallel to the field and the other, $\langle \psi_1(r) \rangle^{(\rho)}$, perpendicular to it, where $\rho^2 = x^2 + y^2$.

The drift velocity and the diffusion coefficients are related to appropriate moments (see LRM for full definitions) thus:

$$v_{dr} = m \langle v_z \rangle = \left(\frac{2kT_b}{m} \right)^{1/2} \langle \psi_1^{(0)} \rangle^{(0)} \quad (2.33)$$

$$D_L = \left(\frac{kT_b}{eE} \right) \left(\frac{2kT_b}{m} \right)^{1/2} \langle \psi_1^{(0)} \rangle^{(z)} \quad (2.34)$$

$$D_T = \left(\frac{kT_b}{eE} \right) \left(\frac{kT_b}{m} \right)^{1/2} \langle \psi_1^{(0)} \rangle^{(\rho)} \quad (2.35)$$

The procedure for solving the moment equations is not trivial, but it will not be discussed here since it does not provide any further physical insight into the method. We simply note that an infinite set of equations is necessarily truncated. Typical values for the maximum number of the Legendre polynomials used are between 2 and 6, and for the Sonine polynomials between 20 and 32. The convergence with respect to the Sonine polynomials is very slow. It has been established that it is strongly dependent on the choice of T_b .

In some cases (Ness 1984a) even the final result becomes dependent on the choice of T_b . Ness showed that this anomaly is related to the choice of the method of integration for the matrix elements. The form of these

integrals suggests that the so called "Gauss" integration technique should be applied. However, Ness (1984a) showed that for rapidly varying cross sections, this method is inadequate and leads to the anomalous dependence of the final results on T_b . In such a situation it is necessary to use a much more time consuming Simpson integration or some other algorithm. The speed of calculation in this case critically depends on the number of points that are used, but so does the accuracy of the integration and consequently of the final results. Typically, the number of points for the Simpson integration has to lie between 300 and 5000.

An alternative method for solving the problem of obtaining adequate accuracy for the numerical integration of the matrix elements when the cross sections are varying rapidly with the energy can be suggested along the following, rather pragmatic, lines. Normally in analyses of this kind the cross sections are tabulated at a certain number of energies typically 10 to 60. Values of the cross section at intermediate energies are obtained by interpolation using some low order polynomial (linear or cubic). Therefore the transport coefficients are not being calculated for the real cross section but for a model cross section that corresponds to the real cross section only at tabulated points. The adequacy of such a representation is questionable in some cases (see Section 12.4.2) but normally presents no problem. It would be useful for practical purposes to have analytical solutions for integrals in equations (2.22-2.24), bounded between arbitrary limits ϵ_a and ϵ_b and for some simple form of the energy dependence of the cross section. In principle the time necessary for calculation at each ϵ_a and ϵ_b point need not be longer than for the integrand in (2.22-2.24) for the Simpson integration. On the other hand the number of points i.e. calculations, would be reduced by a factor of 5

to 10, and an "exact" value of the integral would be obtained. Ness (1984b) has shown that the implementation of this procedure is possible by deriving analytical expressions for the matrix elements for some simple forms of the momentum transfer cross section both from 0 to ∞ and from ϵ_a to ϵ_b . One should note that in situations where the Gauss integration is sufficiently accurate, it is advisable to retain it since it is much faster than the Simpson integration. Also the problems mentioned above are often related to the momentum transfer cross section and not to the inelastic cross sections. Therefore it is possible to limit the application of the Simpson integration to σ_m only.

The LRM (or moment) method is easier to implement than most other methods and appears to be one of the fastest. However it has some disadvantages. Apart from the above mentioned difficulty in achieving a sufficient numerical accuracy for cross sections that are strongly energy dependent, and sometimes the necessity to invert large matrices, an additional problem encountered with the moment method is the representation of the high energy tail by a single temperature (T_b) parameter. This may prove inadequate for calculations of the rate coefficients for processes with thresholds much higher than the average electron energy (McMahon 1983a). Also it has been frequently suggested that it is very difficult to obtain accurate electron energy distribution functions (EDF) using this method (e.g. see comments in Braglia 1980). This is not strictly speaking correct since the EDF can be represented accurately once a sufficient number of moments is known. For instance the isotropic EDF is (Ness 1984b):

$$f_0(\epsilon) = (kT_b)^{-3/2} e^{-x} \sum_{s=0}^{\infty} \frac{s!}{\Gamma(s+3/2)} S_{1/2}^{(s)}(x) \langle \psi_0^{(s)} \rangle^{(0)} \quad (2.35)$$

with

$$\int_0^{\infty} \epsilon^{1/2} f_0(\epsilon) d\epsilon = 1. \quad (2.36)$$

It is, however, true that the EDF is not calculated during the calculation of the transport coefficients and one has to make an additional effort to obtain it. In a similar way one may obtain the excitation rate coefficients (Ness 1984b):

$$v_{\text{exc}}(jk) = N \left(\frac{2kT_b}{m} \right)^{1/2} \sum_{s=0}^{\infty} \frac{s!}{\Gamma(s+3/2)} v_{s0}^0(jk) \langle \psi_0^{(s)} \rangle^{(0)}. \quad (2.37)$$

Finally one should add that some alternative forms of the weight function could be implemented in a situation where a cross section decreases rapidly. Skullerud (1984) has suggested one form and shown that it improves the convergence properties of the moment method as applied to ions. A Gaussian weight function performs much better as the mass ratio decreases, but nevertheless one could perhaps still benefit from some alternative choice designed to suit the special situations sometimes encountered in electron transport.

2.2.2: Multi term theories - "exact" solutions of Boltzmann

equation. BE for electrons is a partial integro-differential equation. The integral part - the collision operator - is rather complicated and contains terms for at least three types of collisions that are treated in quite a different manner (i.e., elastic, conservative inelastic and superelastic, and nonconservative collisions). This section contains an attempt to make a rather brief comparison of the methods that are used to overcome the difficulty resulting from the complexity of the collision operator. The term "exact" means that the method should make it possible,

given sufficient resources, to produce a solution of an arbitrary accuracy. Methods that have inherent limitations will be discussed in the following section, since they can be treated as special cases of the more general theories.

During the 1960s it became evident that, even when the two term theory is used, it is necessary to include effects of spatial gradients (Parker and Lowke 1969; see also Penetrante and Bardsley 1984). Expansion (2.6) is usually developed to the second (linear) term and therefore using cylindrical symmetry one is left with three coefficients (EDFs), one for the spatially homogeneous part $f^{(0)}$ and two for the linear terms in V , one in direction of the field $f^{(z)}$ and the other perpendicular to the field $f^{(\rho)}$. This procedure is usually called gradient expansion. An equivalent approach is to apply Fourier transformation, the Fourier coefficients being energy and time dependent distribution functions.

Having made this step one is left with a set of partial-integro-differential equations that have one less variable (r). In principle it is possible to treat the initial form of BE without expanding the EDF in series with respect to the gradients - i.e. to perform iterations with respect to the spatial variables.

The next step to be considered is how to represent anisotropy. Usually spherical harmonics are employed to achieve a representation of the non-isotropic EDF. The consequences of the truncation of the series (2.11) after the second term (the so called "two term" approximation TTT) has been one of the major issues of the theory of electron swarms in the past few decades. If one takes only two Legendre polynomials, the theoretical description becomes relatively simple since it is possible to transform BE into a set of two ordinary differential equations for the two coefficients

f_0 and f_1 of the expansion (Huxley and Crompton 1974). However, for some real and model gases this is inadequate and even for those examples when one expects the two term theory to be adequate it is useful to have some guidance about the magnitude of the higher order terms. This can be achieved either by using more than two terms (in the Legendre polynomial expansion) or by iterating with respect to the angular variable.

Once one solves the problems related to the representation of the spatial gradients and the angular dependence one is left with the most important step - the representation of the velocity (energy) dependence. Up to this point the collision operator played only a limited role (see equation 2.12) but now it becomes the dominant source of difficulties. There are two approaches to solving the BE with respect to velocity (energy).

The first is the iterative technique applied to the integro-differential equation. Alternatively it is possible to transform BE to a purely integral equation (Braglia 1980) and then to perform the iteration.

The other approach is to expand the EDF in a series of some specially chosen functions (polynomials). One example of such a procedure is given in (2.13). It is not necessary for these functions to form an orthogonal set. When the expansion is substituted into BE a set of linear algebraic equations is produced, and a matrix inversion is necessary to construct the solution. In some situations the matrices to be inverted become large and excessive computer time is necessary for the inversion.

Electron distribution functions are normally the first results of calculations. They are then related to the observable macroscopic quantities through relations such as (2.10). It is, however, possible to formulate the procedure in such a way that moments of the EDF are directly

calculated. These moments can be directly related to the transport coefficients without the derivation of EDF as in the work of LRM.

Following some attempts to improve the two term theory (TTT) by adding one additional term or refining some other aspects of the theory (see Baraff and Buchbaum 1963; Parker and Lowke 1969), the first "exact" theory was developed by Kleban and Davis (1977; 1978; see also Kleban et al. 1980). Their approach is based on a technique originally devised for electron transport in semiconductors (Rees 1969). Initially gradient expansion is applied and then integral equations for the EDFs are derived. Iteration is performed for both the velocity and the angular distributions (the components of the velocity c_z and c_ρ are actually used to perform the iteration). Kleban and Davis applied their theory with limited success to analyse CH_4 and some other molecular gases but the accuracy of their results was challenged by other methods, (Lin et al. 1979; Braglia 1981b). Their procedure was never really verified although some attempts to vindicate the basic ideas behind the iterative approach were published (Kleban et al. 1980; Skullerud and Kuhn 1983) and it is now established that the inaccuracy of some of their results was caused by inadequate normalization rather than the failure of the whole procedure.

Along similar lines and independently at the same time Tagashira and coworkers developed another "exact" method (Kitamori et al. 1978; Tagashira et al. 1978; Kitamori et al. 1980). Their work was aimed at relatively large E/N values where ionization losses become very important and definitions of the transport coefficients become dependent on the experimental technique adopted. The first step in their analysis is to apply a Fourier expansion. Then the whole BE is expanded using finite differences for c , θ and t without employing the factorization given by

(2.6), and thus the time development of transport coefficients can be followed. Even though their work was aimed at high E/N it is, of course, applicable throughout the entire E/N range.

Historically the method of Lin, Robson and Mason (1979) came next, but it should be pointed out again that all these methods were developed independently and concurrently. The LRM theory has already been discussed in detail, and we shall just summarize it here. Spatial gradients are represented by gradient expansion and anisotropy of the EDF by Legendre polynomials. The distribution function is expanded using Sonine polynomials with a Gaussian weight function and the set of linear equations is solved to produce a set of moments of the EDF.

Methods developed by Pitchford and coworkers (Pitchford et al. 1981; Pitchford and Phelps 1982; Pitchford 1983) appears to be the most logical extension of approximate methods. A gradient expansion is applied first and then a Legendre polynomials expansion. A series of integro-differential equations is developed coupling the j^{th} coefficient of the Legendre polynomial expansion to coefficients $j+1$ and $j-1$. The EDF is then expanded into a series of cubic B splines and again a set of linear equations for the coefficients of the expansion is produced. This technique for solving partial differential equations is known as Galerkin's method (Schryer 1976). It is worth noting that cubic B splines are not a set of orthogonal polynomials (see Kumar 1984).

Segur and his coworkers (Segur et al. 1983a and 1984) have developed a new method that is particularly well suited to the analysis of effects of ionization and attachment. It is also relatively fast and can be implemented on a small computer (even a minicomputer). Using a gradient expansion they were able to derive integro-differential equations that

correspond to SST, PT and TOF conditions (steady-state Townsend, pulsed Townsend and time of flight respectively; for further explanations see Tagashira 1981; Blevin and Fletcher 1984). (As it turned out all these equations have the same general form, which is similar to that of some equations of neutron and radiation transport). They then apply finite difference methods taken from other fields of kinetic theory and derive the distribution function.

The method developed by McMahon (1983a; 1983b) is similar to that of Kleban and Davis. However, the starting point of his analysis is a modified BE that has an additional term

$$s \{ f(\underline{r}, \underline{v}, t, s) - g(\underline{r}, \underline{v}, t, s) \} \quad . \quad (2.38)$$

There is an extra variable s in the EDF while g is an additional function. Both s and g are chosen in such a way as to improve the accuracy and the speed of convergence of the iterative procedure but so that the calculated transport coefficients and the EDF are not affected. Solution of the modified BE is achieved by the application of finite differences to the energy variable. The choice of this numerical procedure was justified by the fact that a certain number of mesh points is equivalent to the same number of splines (McMahon 1983a). Sonine polynomials would have some advantage due to the use of a single parameter T_b but in the situation where the accuracy of the high energy tail becomes critical, the basis sets become very large in order to overcome the difficulty of representing EDF at high energies by a single parameter (Kumar 1984).

McMahons technique also has one other interesting feature. The procedure is formulated so that only the corrections to the TTT results for the transport coefficients (or those calculated by some other approximate

method) are calculated. Usually the differences between the two term results and the multiterm results are small (between 1 and 20%). Therefore one does not need the same mesh density and accuracy for the calculation of the multi-term corrections as for the the calculation of the initial values, and the procedure can be therefore relatively faster.

Another interesting approach was suggested by Sevel'ev (1983). It is to expand the transport coefficients into series, rather than the EDF itself. In one way it appears to be similar to the LRM theory since the EDF is not the direct result of the calculation. At the time of writing only a limited set of results for some models exists. These comprise the velocity averages ($\langle v_z \rangle$, $\langle v^2 \rangle$, ...). Therefore one has to wait until this method is developed to the level where it can be used to calculate the transport coefficients (including diffusion coefficients) for some more complicated model or real gases in order to be able to judge its merits.

In order to summarize, the basic characteristics of the "exact" theories are presented in Table 2.1.

2.2.3: Monte Carlo simulations. An alternative to solving BE by using numerical methods is to simulate the motion of electrons i.e. to apply a Monte Carlo technique. Numerous such studies have been performed for electron transport through gases (Itoh and Musha 1960; Thomas and Thomas 1968; Englert 1971; Sakai et al. 1972 and 1977; McIntosh 1974; Braglia 1977; 1981a; and 1981b; Saelee and Lucas 1977; Milloy and Watts 1977; Friedland 1977; Reid 1977 and 1979; Hunter 1977a and 1977b; Braglia and Biaocchi 1978; Reid and Hunter 1979; Kucukkarpci and Lucas 1979; Davies et al. 1979 and 1984; Braglia et al. 1981; Hayashi 1983; Dincer and Govinda Raju 1983). A good review of the early history of the development of these method has been given by Hunter (1977a).

Table 2.1: Comparison of Multi-Terem theories

	Kleban & Davis	Tagashira	LRM	Pitchford	Segur	McMahon
spatial	GE	FE	GE	GE	GE	FE
angular	A-IT	A-IT	LP	LP	A-IT	A-IT
energy	IE-IT	IDE-IT ^a	MI	MI	IDE-IT	IE-IT ^b
basis of numerical procedure	FD	FD	SP-GW	B-SP	FD	FD
primary result	EDF	EDF	MOM	EDF	EDF	EDF

^a with time relaxation

^b modified BE

GE -gradient expansion

FE -Fourier expansion

A-IT -iteration for angular dependence

LP -spherical harmonics (Legendre polynomials) expansion

IE -integral equation

IDE -integro-differential equation

IT -iterations

MI -matrix inversion

FD -finite differences

SP-GW-Sonine polynomials with Gaussian weight function

B-SP -cubic B splines

EDF -electron distribution function

MOM -moments of EDF

First it may be noted that there is a correlation between the path integral method for solving BE (see Reif 1965; Kleban and Davis 1977 and 1978; Braglia 1980; Kumar et al. 1980; McMahon 1983a; Skullerud and Kuhn 1983) and the Monte Carlo method. The choice of paths in the second case is random and consequently the procedure is much more time consuming; the results are also subject to statistical uncertainty. On the other hand the MC method does not suffer from the problems caused by complicated numerical procedures that normally demand a huge computer memory, even though less

computer time is required for their execution. The MC method is also much simpler to program and interpret. Both methods gained by the introduction of the null-collision technique (Skullerud 1968, see also Lin and Bardsley 1977 and 1978; Reid 1979; for a "generalized" null-collision method see Penetrante and Bardsley 1983).

Before discussing the null collision technique in greater detail, the standard MC scheme will be briefly outlined. Monte Carlo simulations for electron transport through gases consist of several steps:

- 1) An electron is released with a certain energy and direction of motion.
- 2) Its motion through the gas is followed until it collides with a molecule.
- 3) The type of collision is randomly selected, taking account of the ratio of the cross sections for the possible collision processes at that energy. The type of collision determines the electron speed after collision, while its direction of motion is randomly selected, taking account of the angular scattering for that process at that energy (if known).
- 4) The transport coefficients are calculated from the characteristics of the motion of the electron (see equations 2.42 and 2.43).
- 5) Steps 2), 3) and 4) are repeated until a satisfactory statistical quality of the results is achieved.
- 6) In some cases (especially in the analysis of non-conservative processes) many electrons are followed. When there is ionization the newly created electrons are included in the simulation.

All the decisions about whether a collision has occurred, and its type, and about the direction of motion of the electron following the collision

are made on the basis of random numbers. However, the choice of the procedure relating the random number to the characteristics of the event that is to be randomly selected is very important and can be a cause for difficulties when the MC technique is applied.

Two methods have been used to determine the time and position of the collision that terminates a free path. In the first, the mean free path corresponding to the instantaneous energy of the electron is first calculated. This is then divided appropriately (usually by a number between 10 and 40) and a random number is used to decide whether a collision has occurred at the end of the first segment of the mean free path. If there is no collision the mean free path corresponding to the energy of the electron at the end of the segment is calculated and the procedure outlined above repeated. The accuracy of this method depends on the number of subdivisions (especially for gases such as Ar and CH₄) but so does the duration of the calculation.

The second method is based on calculating the time of the next collision rather than its position. The probability that n electrons out of an initial population of n_0 will survive a time T is given by

$$\frac{n}{n_0} = \exp \left(- \int_0^T \nu(c) dt \right) \quad (2.39)$$

where $\nu(c)$ is the total (i.e. summed over all processes) collision frequency. Given n/n_0 (from the random number generator) the time T of the next collision can be found, and hence the position and velocity of the electron at that time. However, this involves the rather time-consuming task of solving (2.39) by iteration. Hence, like the first method, this procedure is time consuming and therefore costly. However, a variant of it, the so-called null-collision method, results in considerable

time-saving. In the null-collision method, advantage is taken of the fact that (2.39) can be solved directly when $v(c) = \text{const} = v$. In this case the time of the next collision is given by

$$T_c = - \frac{1}{v} \ln(\rho) , \quad (2.40)$$

where ρ is a random number, and the calculation of T_c is then trivial. Since realistic cross sections do not, in general lead to a constant collision frequency, a cross section is added that makes up the difference between the real cross section and one that gives a constant collision frequency equal to the maximum collision frequency for the real cross section (see Fig. 2.1). Once the time of the next collision is established an additional random number is used to decide whether a real collision has occurred or whether the electron continues its trajectory - the null collision. The cross section for this null-collision process is, of course, equal to the added cross section (see Fig. 2.1).

The null collision technique was introduced to remove one of the greatest sources of arbitrariness in the MC technique, namely the choice of the length of the segments in the first method. It also improves the speed of the codes. It is also possible to optimize the choice of the constant collision frequency by splitting the energy range into at least two regions (Reid 1977 and 1979).

The discussion of the null collision method has been given here partly because some calculations were performed in this work using the MC code developed by Reid (1979), and partly to point out that MC simulations are, contrary to a widespread opinion, prone to some inaccuracies if implemented without great care. This care is necessary because approximations and inaccuracies that are sources of error are much less visible than in the

numerical procedures for solving BE. The basic physics is relatively simple and therefore subtle inaccuracies tend to be overlooked. Especially critical are: the analysis of the collision event (Reid 1979 and the corrigendum 1982), the choice of the sampling times, either before or after the collision or at fixed time intervals (Friedland 1977; Braglia 1981), and the choice of the formulae for calculating the transport coefficients (Braglia 1982; Ikuta et al. 1983).

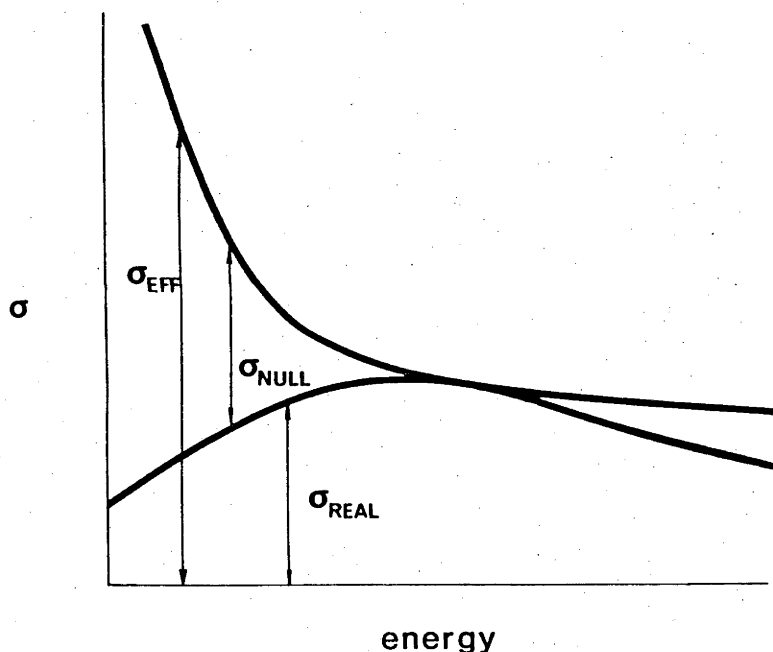


Figure 2.1 The real collision cross section and the null-collision cross section that is added to the real one to produce the effective cross section with the constant collision frequency.

In the code that was used a single electron was followed through numerous collisions (which makes it inadequate for situations when non-conservative processes are present - see Thomas and Thomas 1968). It

is easy to define the drift velocity:

$$v_{dr} = z/t, \quad (2.41)$$

while the diffusion coefficient is calculated from:

$$D_T = \lim_{\tau \rightarrow \infty} \frac{1}{4\tau} \langle \{x(t+\tau) - x(t)\}^2 + \{y(t+\tau) - y(t)\}^2 \rangle. \quad (2.42)$$

In addition the EDF derived by MC technique may be used together with the two-term formula for D_T (see 2.56), although this introduces one of the approximations inherent in the TTT. Quite often the expression for D_T is presented in an equivalent form:

$$D_T = \frac{1}{4} \frac{d\langle \rho^2 \rangle}{dt}, \quad (2.43)$$

where ρ is the radial displacement. D_T is calculated from the slope of the radial displacement at sufficiently large times since the contribution from the autocorrelation function to the mean square displacement then becomes negligible in comparison with the diffusion term (Skullerud 1974).

It has been suggested that MC methods could compete with numerical techniques for solving BE (Braglia 1981) in speed and accuracy. The optimum choice for the formulation of the procedure appears to be a generalized null-collision method (Penetrante and Bardsley 1983) and sampling before the collisions (Friedland 1977; Braglia 1981), with an additional sampling at fixed time intervals for the determination of D_T (whose accuracy puts the most stringent conditions on the performance of a MC code). It is, however, uncertain that it would be feasible to use MC

methods for cross section determination (see Section 2.3) even using very fast computers or microprocessors dedicated to MC simulations. This is so especially for gases with small elastic energy losses. For gases that have large energy losses MC simulations might prove sufficiently fast and accurate. Moreover it is very difficult to include the temperature of the background gas (e.g. for ions see Skullerud 1973) which would be essential if calculations are to be performed that correspond to real conditions.

The greatest value of the MC technique so far is that it has provided independent, relatively reliable benchmarks against which to test the two- and multi term theories. Also it provides a means of examining a great number of phenomena that are either difficult or impossible to analyse with other available methods. These phenomena include: boundary effects (Burch and Whealton 1977; Braglia and Lowke 1979; Braglia et al. 1984) and other related non-hydrodynamic phenomena (Boeuf and Marode 1982; Hayashi 1982; Segur et al. 1983b); electron transport greatly influenced by non-conservative processes (Penetrante and Bardsley 1983; Boeuf and Marode 1984); effects of attachment cooling (Koura 1982), electron energy relaxation (Koura 1984) and the development of the gas discharges (Kunhardt and Tzeng 1985). All these phenomena are related to a certain degree and this division is somewhat arbitrary. They are listed simply to give an indication of the possibilities open to MC methods.

2.2.4: The two-term theory and other approximate theories. If we retain only two terms in the expansion (2.11a) we obtain what is known as the two term theory (TTT). It has been a basic tool of swarm physics for the last thirty years.

Early developments of electron swarm theory (the work of Lorentz,

Pidduck, Davydov, Druyvesteyn, Allis and coworkers and Chapman and Cowling) were reviewed in the Introductory chapter of the book by Huxley and Crompton (1974) (see also Healy and Reed 1941; Loeb 1955; Allis 1956). A short survey will be given here of the more recent developments, some of which are important for the present work. A full development of equations and details of the theoretical ideas will not be presented since the subject is extremely well covered by a great number of publications (e.g. Shkarofsky et al. 1966; Gilardini 1972; Huxley and Crompton 1974) including some textbooks (Cherrington 1979; Smirnov 1981).

Earlier work of Holstein (1946), Allis (1956) and Ginzburg and Gurevich (1960 - see also Huxley 1981) led to the development of the basic equations and especially to the refinement of the collision operator which was, up to that time, treated according to various models that were investigated. The applications of the TTT to the derivation of cross sections from the results of swarm experiments began once suitable numerical methods for the solution of the equations and appropriate computers became available. The backward prolongation technique developed by Sherman (1960) was used extensively by Phelps and coworkers in the analysis of cross sections for various atomic and molecular gases (Frost and Phelps 1962; Phelps 1979), and later on by some other authors (e.g. Garamoon and Ismail 1977). It is basically a finite difference technique, but the novelty is that integration of the EDF is performed backwards from the highest energy where the EDF is very well represented by the distribution function that corresponds to elastic collisions only.

A quite different approach was adopted by Lucas (1969) and, following his work, by some other authors (e.g. El Hakeem and Mathieson 1979). It is to iterate the EDF, starting from an assumed initial function until

sufficient stability of the result is achieved. The final result must of course be independent of the initial choice.

Crompton and Jory (see Huxley and Crompton 1974 and Crompton et al. 1967) developed a technique similar to that developed by Frost and Phelps (1964) for determining elastic (momentum transfer) cross sections from electron transport data in monoatomic gases where the basic problems caused by the presence of inelastic and superelastic collisions do not exist. In such a case, as we shall see later on, the EDF can be calculated relatively simply by integration (see equation 2.52).

A method was developed by Gibson (1970) for situations where superelastic collisions are non-negligible; it is a combination of the backward prolongation and the iteration techniques. The two term calculations for the present work were carried out using the program developed by Gibson with some modifications.

The basic equations involved in the TTT are now summarized. Having neglected ∂_t and ∂_r terms in (2.2) and having performed expansions (2.11) and (2.12) and retained only the first two terms f_0 and f_1 one obtains two equations. The first one, the so called scalar equation (Huxley and Crompton 1974), can be combined with the vector equation

$$\underline{f}_1 = \frac{e \underline{E}}{N \sigma_m(\epsilon)} \frac{\partial}{\partial \epsilon} [f_0(\epsilon)] \quad (2.44)$$

to give

$$\frac{E^2}{3N} \frac{d}{d\epsilon} \left(\frac{\epsilon}{\sigma_m(\epsilon)} \frac{df_0}{d\epsilon} \right) + \frac{2mNkT}{M} \frac{d}{d\epsilon} \left(\epsilon^2 \sigma_m(\epsilon) \frac{df_0}{d\epsilon} \right) +$$

$$\frac{2mN}{M} \frac{d}{d\epsilon} \left(\epsilon^2 \sigma_m(\epsilon) f_0(\epsilon) \right) +$$

$$\begin{aligned}
& \sum_k N_j \{ (\epsilon + \epsilon_{jk}) f_0(\epsilon + \epsilon_{jk}) \sigma(jk; \epsilon + \epsilon_{jk}) - \epsilon f_0(\epsilon) \sigma(jk; \epsilon) \} + \\
& \sum_k N_k \{ (\epsilon + \epsilon_{jk}) f_0(\epsilon + \epsilon_{jk}) \sigma(kj; \epsilon - \epsilon_{jk}) - \epsilon f_0(\epsilon) \sigma(kj; \epsilon) \} = 0,
\end{aligned} \tag{2.45}$$

where

$$N_k = \frac{w_k}{w_j} N_j e^{-\epsilon_{jk}/kT}, \quad \sigma(kj) = \frac{w_j}{w_k} \frac{\epsilon}{\epsilon - \epsilon_{jk}} \sigma(jk), \tag{2.46}$$

$$\int_0^{\infty} \epsilon^{1/2} f_0(\epsilon) d\epsilon = 1 \tag{2.47}$$

and N_i represents the population of the state i of the gas.

The first term in (2.45) represents the energy gained by the field (σ_m in this term is the total momentum transfer cross section $\sigma_m(\epsilon) = \Sigma \sigma_m(j; \epsilon)$), the second is the term describing the energy gained in collisions with the background molecules at the temperature T , and the third term is due to the energy loss in elastic collisions (here σ_m is purely elastic but it is normal to retain the first interpretation of σ_m for both terms). The fourth and the fifth terms represent the inelastic and the superelastic collisions respectively. Some difficulties in solving (2.45) are due to the "non-locality" in ϵ , that is to the $\epsilon - \epsilon_{jk}$ and $\epsilon + \epsilon_{jk}$ factors. Integrating (2.45) over all energies one obtains:

$$a(u) f_0(u) + b(u) \frac{df_0}{du} + c(f_0, u) = 0 \tag{2.48}$$

where u is the energy and :

$$a(u) = \left(\frac{2m}{M} \right) u^2 \sigma_m(u) \tag{2.49}$$

$$b(u) = \frac{1}{3} \left(\frac{E}{N} \right)^2 \frac{u}{\sigma_m} + kT a(u) \quad (2.50)$$

$$c(f_0, u) = \sum_{j,k} N_j \int_u^{u+\epsilon_{jk}} e^{-\sigma(jk; \epsilon)} \left\{ f_0(\epsilon) - e^{-\epsilon_{jk}/kT} f_0(\epsilon - \epsilon_{jk}) \right\} d\epsilon \quad (2.51)$$

Neglecting the inelastic collisions results in the following solution (i.e. for a "purely elastic" gas) :

$$g(\epsilon) = \exp\left(- \int_0^\epsilon \frac{a(u)}{b(u)} du \right) \quad (2.52)$$

It can be shown that for very large ϵ ($\epsilon \rightarrow \infty$) the solution for (2.48) with the inelastic collision term included is still given by (2.52). For an arbitrary energy the solution is:

$$f_0(\epsilon) = g(\epsilon) \left\{ 1 + \int_0^{\epsilon_{\max}} \frac{c(f_0, u)}{b(u) g(u)} du \right\} \quad (2.53)$$

where ϵ_{\max} is the maximum energy for the integration and should be chosen in such a way that the EDF is sufficiently small at that energy and also that $f_0(\epsilon_{\max}) \cong g(\epsilon_{\max})$.

From the equation (2.45) when finite differences have been incorporated (i.e. $\epsilon_i = i\epsilon_{\max}/n_s$ where n_s is the number of grid points) we get:

$$f_0(\epsilon_i) = \sum_{m=1}^{n_s} I_m^i f_0(\epsilon_m) + \sum_{m=0}^i S_m^i f_0(\epsilon_m) \quad (2.54)$$

where the first term is a sum due to inelastic and the second term due to superelastic collisions, while I_m^i and S_m^i are the corresponding coupling coefficients. In Gibsons hybrid scheme integration for $f_0(u_i)$ starts from

the maximum energy but the contribution of the superelastic collisions is calculated on the basis of the EDF obtained in the previous iteration.

The transport coefficients are calculated using the following TTT formulae (for the derivation of these formulae and their range of validity see Huxley and Crompton 1974):

$$v_{dr} = - \frac{eE}{3N} \left(\frac{2}{m} \right)^{1/2} \int_0^{\infty} \frac{\epsilon}{\sigma_m(\epsilon)} \frac{df_0}{d\epsilon} d\epsilon \quad (2.55)$$

$$ND_T = \frac{1}{3} \left(\frac{2}{m} \right)^{1/2} \int_0^{\infty} \frac{\epsilon}{\sigma_m(\epsilon)} f_0(\epsilon) d\epsilon \quad (2.56)$$

$$\frac{D_T}{\mu} = \frac{E}{N} \frac{ND_T}{v_{dr}} \quad (2.57)$$

$$\langle \epsilon \rangle = \int_0^{\infty} \epsilon^{3/2} f_0(\epsilon) d\epsilon \quad (2.58)$$

$$v_{jk} = N \left(\frac{2}{m} \right)^{1/2} \int_0^{\infty} \epsilon \sigma(jk; \epsilon) f_0(\epsilon) d\epsilon \quad (2.59)$$

The two term theory for low energy electron transport has been well established for some time now. Apart from the large number of codes that have been developed for individual laboratories there is a number of codes that are generally available (Luft 1975; Thomson et al. 1976; Morgan 1979; Rockwood and Greene 1980). Most of these codes were written in order to model gas laser (and other) discharges and some of them can be coupled to a system of kinetic equations describing the population densities of various excited neutral molecules, ions and products of chemical reactions (Davies et al. 1975; Roberts 1979; Capitelli and Molinari 1980). Under discharge conditions electron swarms perturb the background gas and the resulting excited particles effectively act as a new species that can introduce large

inelastic losses with relatively low thresholds (Judd 1976). Also if excessive populations of excited levels are present they can effectively "heat" the electron swarm through superelastic collisions during the post-discharge relaxation (Capitelli et al. 1981; 1982; 1983). The possible implications of this effect on one of our experiments will be discussed in Chapter 6.

Two term codes were also extended to include the temporal development of the discharge (e.g. Morgan 1979) and some interesting effects were observed (Ingold 1984).

Another area of research has received a great attention lately. It is electron transport in the presence of non-conservative processes. Two problems occur in such a case: how to include the non-conservative processes in the collision integral of the TTT (e.g. see Brunet and Vincent 1979 and Yoshida et al. 1983) and how to define the EDF and the transport coefficients according to the actual experimental conditions (Crompton 1967; Thomas 1969; Tagashira 1981; Blevin and Fletcher 1984).

It had already been pointed out by Holstein (1946) that the TTT is applicable only when the inelastic cross sections are small compared to the elastic one, i.e. when the degree of anisotropy of the EDF is small. Numerous attempts were made to extend the TTT to further terms in order to gain some knowledge about the accuracy of the results obtained using it (Wilhelm and Winkler 1969; Ferrari 1975 and 1977; Makabe and Mori 1980; Cavalleri 1981; Braglia et al. 1984). Baraff and Buchsbaum (1963) have also calculated the degree of anisotropy of the EDF under certain conditions, by adopting an iterative procedure (to determine the axial and radial components of the electron velocity). All these investigations pointed out that TTT is sometimes inadequate. However, when it was shown

to be so, there was no way of knowing whether the extended theory was sufficient or not. Therefore there were numerous pointers to the need for developing methods for calculating transport coefficients for an arbitrary degree of anisotropy. This does not mean the use of an infinite number of Legendre polynomials, but just a sufficient number to be able to go at least one step beyond the point where the number of terms is satisfactory in order to verify the reliability of the result. As pointed out by Phelps (1984, see also Pitchford and Phelps 1982), the lower order transport coefficients ($\omega^{(0)}$, $\omega^{(1)}$, $\omega^{(2)}$, see equation 2.10) which are the ones we are basically interested in, may be calculated accurately with a limited number of terms in the Legendre expansion (2.11) even though the higher order coefficients are still quite inaccurately determined.

2.3: Determination of Electron Scattering Cross Sections from the Transport Coefficients.

In the previous section we have briefly summarized methods for solving BE and therefore relating the transport coefficients to the electron scattering cross sections. In this section we shall discuss the existing procedures to derive the cross sections from the transport coefficients, while in the next section we shall present the very well known formulae that relate those coefficients to the experimentally observable quantities.

Probably the first attempt to relate the energy dependence of the cross sections to the observed transport data was made by Townsend in relation to the discovery of the Ramsauer - Townsend effect (Townsend 1947). Modern methods for obtaining electron scattering cross sections have been reviewed many times (Phelps 1968; Crompton 1969; Huxley and Crompton 1974; Phelps

1979; Crompton 1983; 1984a; and 1984b). Also some comprehensive compilations of the transport data exist (Gilardini 1972; Christophorou 1971; Huxley and Crompton 1974; Dutton 1975; Gallagher et al. 1982), while the cross sections derived from these data have been compiled together with the data obtained from electron beam techniques (Kieffer 1973; Hayashi 1981).

The development of gas lasers and other applications of gas discharges created interest in, and urgent need for, accurate low energy electron scattering cross sections. It was evident that beam experiments were not able to provide absolute data of any accuracy at low electron energies, although the data at higher energies, if needed, came almost exclusively from beam experiments. This duality reflects the basic limitations of beam experiments at low energies and swarm experiments at higher energies.

Analysis of the data obtained in swarm experiments is a multi-step process (Crompton 1983 and 1984b).

1) First, one has to accurately determine the transport coefficients from the quantities that are measured in swarm experiments.

2) Once a set of transport coefficients is established it is possible to commence the derivation of cross sections. Normally drift velocities v_{dr} and characteristic energies eD_T/μ at numerous E/N values are used, although important information about very low energy cross section can also be obtained from diffusion coefficients for thermal electrons ND^{th} and their temperature dependence. Transport coefficients in the presence of magnetic fields and longitudinal diffusion coefficients ND_L are of limited use because the accuracy of the experimental data for these coefficients is lower than for v_{dr} and D_T/μ . In addition various rate coefficients that can be determined experimentally are used under certain circumstances.

3) The next step is to assume a set of cross sections and calculate the corresponding transport coefficients using some solution to the BE.

4) Comparison of the experimental and the calculated set of transport coefficients and other swarm data indicates how to adjust the cross sections in order to reach a better agreement. Steps 2) and 3) are repeated until the difference between experimental and calculated values does not exceed the experimental uncertainty. The resultant set of cross sections is then consistent with the transport data although the set may not be unique.

The swarm technique is not a direct way to determine the cross sections. Also the electron swarm has a wide spread of energy and is under the influence of various inelastic processes at a single value of E/N . Therefore the sensitivity of the transport data to a certain process is reduced. In order to achieve satisfactory accuracy for the derived cross sections the accuracy of the transport data needs be much higher than the accuracy to which the cross section is to be determined. For example the drift velocities that were measured by Pack and Phelps (1961; see also Phelps et al. 1960) and used to derive the momentum transfer cross section (Frost and Phelps 1964) for electrons in helium were known to within $\pm 5\%$. Further improvement of the experimental techniques enabled the drift velocities to be measured to within $\pm 1\%$ (Crompton et al. 1967 and 1970; Milloy and Crompton 1977) and, since elastic scattering is the only process present, the cross section could then be determined to within $\pm 2\%$. In Fig. 2.2a the drift velocities from both sources are presented. It is difficult to see a significant difference (unless tabulated data are compared). However, the cross sections that best fit these data are quite different, as can be seen from Fig. 2.2b.

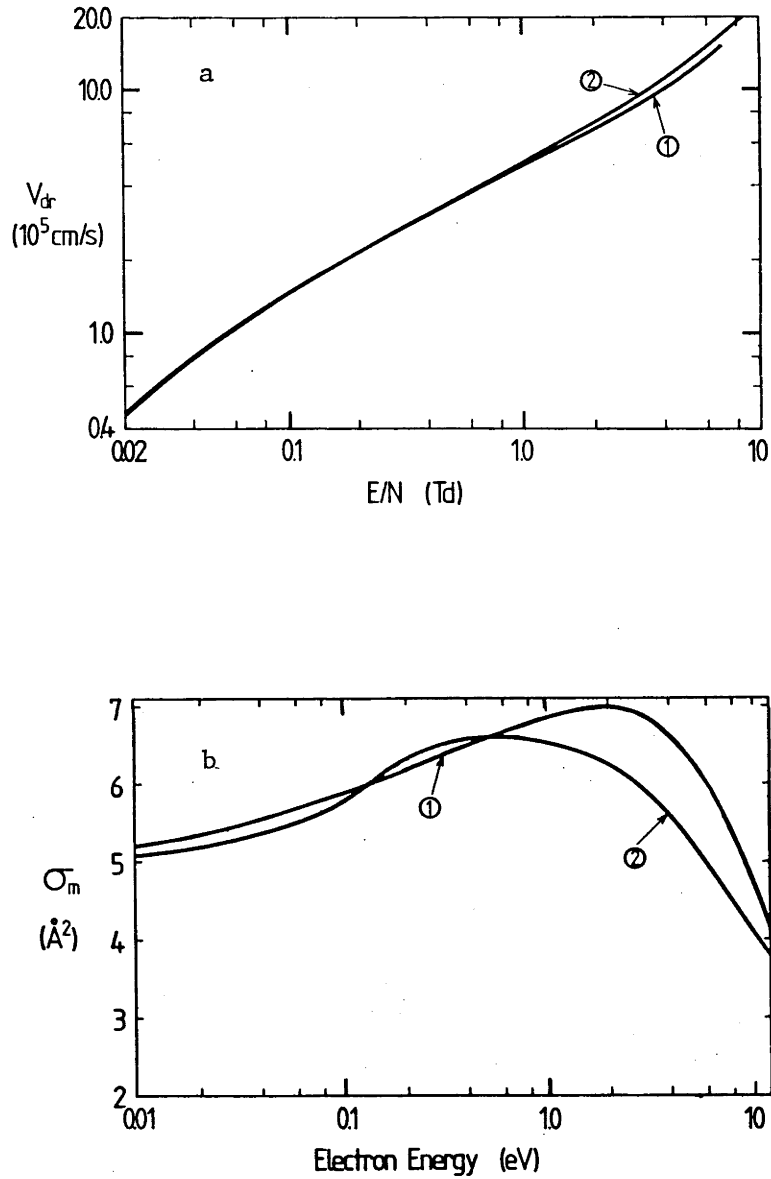


Figure 2.2 (a) Two sets of experimental drift velocities and (b) the cross sections that were derived (see text).

In this example one can uniquely determine the momentum transfer cross section for elastic scattering because for a very wide range of E/N values the EDF does not extend to the thresholds of the cross sections for inelastic processes. Moreover a single set of transport data can be used to derive the cross section (e.g. v_{dr}) leaving data for D_T/μ to provide an independent check. The resultant cross section (Crompton et al. 1967; Milloy and Crompton 1977a and 1977b; see also Nesbet 1979) still stands as the most accurate experimentally determined electron scattering cross section (see Fig. 2.2).

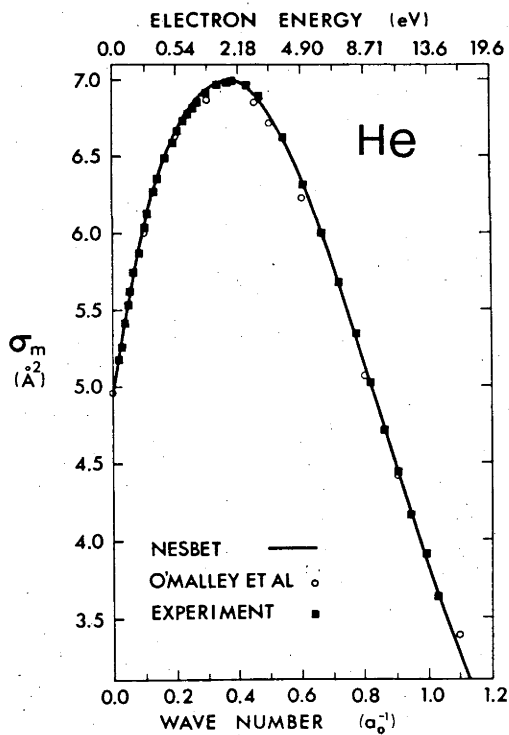


Figure 2.3 Momentum transfer cross section for electrons in helium. Theoretical results of Nesbet (1979) and O'Malley et al. (1979) are compared with the results obtained on the basis of the swarm data.

If there is one additional (inelastic) process in the E/N region that is being used to determine the cross sections, two sets of transport coefficients will suffice. However any further cross section will cause

loss of uniqueness of the cross sections that are derived. Inelastic processes influence electron transport mainly through the energy loss and not through the momentum transfer. Therefore the influence is through the term $\sum \epsilon_i v_i = \sum \epsilon_i N \langle \sigma_i \rangle$ where ϵ_i is the energy loss for that process. Thus if there are two processes j and k to which adjustments are to be made. Changing cross section for one process σ_k by $\Delta\sigma_k$ and for the other σ_j by $-\Delta\sigma_k \epsilon_j/\epsilon_k$ does not alter the sum if all the other cross sections are not altered. Since $\Delta\sigma_k$ can be of arbitrary magnitude the derived cross sections are not uniquely determined. In Fig. 2.4 such a situation is shown where an original arbitrary set of model cross sections (consisting of one elastic and two inelastic processes) was modified to give identical transport coefficients in order to illustrate the problem of non-uniqueness. It should be noted that changes of σ_k and σ_j do, however, lead to a change in σ_m by an amount $\Delta\sigma_k (1-\epsilon_j/\epsilon_k)$ which could be noticed if one had infinitely accurate transport coefficients, but often, as in our example, σ_m is much larger than σ_k or σ_j . The corresponding change in σ_m is then very small and has an unobservable influence on the coefficients.

There are four ways to solve the problem of lack of uniqueness in situations where a large number of cross sections exists. The first is to seek some additional information about the relative magnitude of the cross sections either from electron scattering theory or from electron beam experiments. In this case swarm experiment can provide easy and accurate normalization of the relative cross sections. The second approach (usually applied to the monatomic gases) is to produce a single effective inelastic cross section (Thomas 1969; Jacob and Mangano 1976; Specht et al. 1980). This is normally done by using the fact that the calculated Townsend ionization coefficient is a very sensitive function of the effective

excitation cross section, and that both the ionization coefficient and the ionization cross section can be accurately measured. An effective excitation cross section is therefore found which leads to agreement between calculated and experimental data for the ionization coefficients. This approach is useful if the derived cross section set is to be used in some further calculations of swarm data but it gives very limited information about the shape and magnitude of the real cross sections.

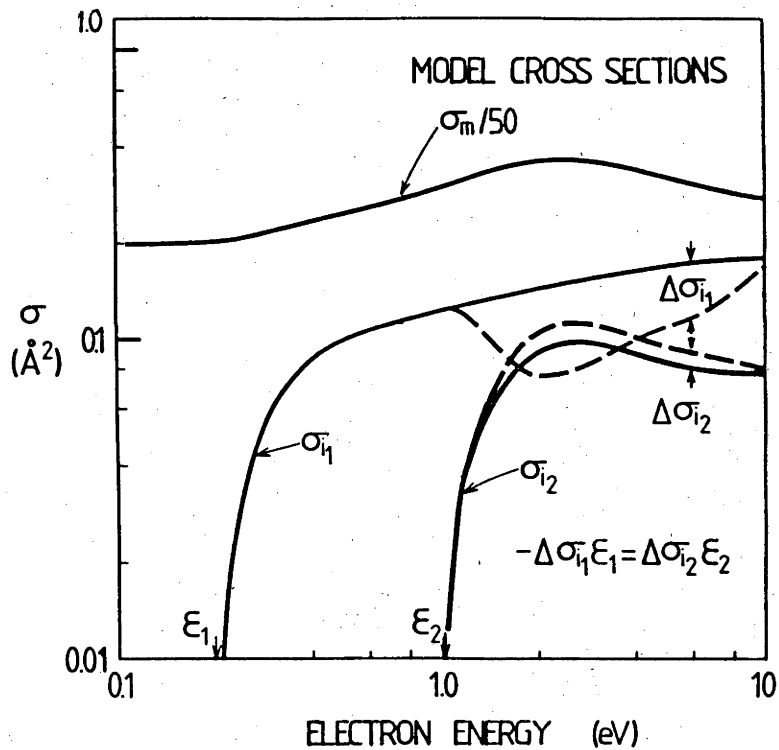


Figure 2.4 An example chosen to show the problem of non-uniqueness of swarm cross sections. A small change in the cross section with a higher threshold (i.e. inelastic energy loss) can be compensated by somewhat larger adjustment to the cross section with a lower threshold (compare dashed to solid lines for each cross section).

The third approach has been exploited only partially and only recently. It is to extend the set of swarm data by measuring a number of excitation

coefficients for various inelastic processes and matching calculated data for these coefficients, as well as for the transport coefficients, to the experimental data. For electronic levels that radiate in the easily accessible spectral range (Tachibana and Phelps 1978; Urosević et al. 1983) it is relatively simple to interpret the experimental data, but for metastable electronic levels (Bozin et al. 1983; Lawton and Phelps 1978) and for vibrational levels (Bulos and Phelps 1976; Buckman and Phelps 1985) the kinetics of the excited levels becomes very complicated and the analysis depend on some heavy particle collision data. Also special experimental techniques are needed. One example is the tracer technique. In this technique a small amount of some other gas is added to the gas that is being studied and emission from the tracer gas is measured, the emission being in a spectral range that can be investigated with the available experimental techniques. In this case additional assumptions must be made, and that is that the tracer does not significantly affect the electron transport in the buffer gas and that direct excitation of the radiating levels of the tracer can be neglected compared to the energy transfer from the excited molecules/atoms of the buffer gas. Up to the present time the accuracy of the experimentally determined excitation coefficients hardly matches the accuracy of the other data. Moreover, it is practically impossible to provide excitation coefficients for all the levels, and it is usual to combine this method with the first.

The fourth method of increasing the accuracy of the cross sections derived from swarm experiments is to use gas mixtures. Transport coefficients are measured in mixtures of the gas that is under investigation with a gas whose cross sections are well known (Engelhardt and Phelps 1964; Haddad and Crompton 1980; Haddad and Milloy 1983; Haddad

1983 and 1984). Examples of the application of this technique are described in Chapters 9, 11 and 12.

Another disadvantage of the swarm method compared with beam methods is that it is difficult, and often impossible, to resolve the fine structure of a cross section since the energy spread of the swarm is fairly large. This statement is in principle true, but it deserves closer scrutiny. At average energies of a few electron volts the "width" of the EDF is much larger than the energy spread of an electron beam of comparable energy, but if the field and the gas temperature are reduced (see Fig. 2.5) widths of a few meV are achieved at energies of 8 to 10 meV. Thus it is in principle possible to analyse the fine structure of cross sections at very low energies.

As for the possibility of detecting fine structure at higher energies it is true that the accurate shape of a resonance cannot be determined uniquely but it is sometimes possible to verify its shape and magnitude once its profile has been measured in a beam experiment (for discussions of a hypothetical resonance in He see Huxley and Crompton 1974, and for resonances in CO see Haddad and Milloy 1983). On the other hand the swarm technique makes it possible to study the threshold behaviour of cross sections that are too small to be accessible to beam methods; e.g. nonresonant vibrational excitation of N_2 and CO (see Chapter 11).

It is important to note that the entire swarm procedure is critically dependent on the accuracy of calculations of the transport coefficients from a given set of cross sections. As we have already seen the two term approximation is not adequate in many cases. The following illustrations shows that large errors in determinations of the cross sections are made if one applies TTT in situations when it is not sufficiently accurate. The

ramp inelastic cross sections of Reid (1979) (Fig. 2.6) were chosen, and using the LRM code the transport coefficients were calculated for a range of values of E/N . These data were then analyzed using the two term code in an attempt to determine the cross sections that would best fit the data. The result of this procedure, shown in Fig. 2.6, clearly indicates that large errors can result from the use of inaccurate methods for calculating the transport coefficients.

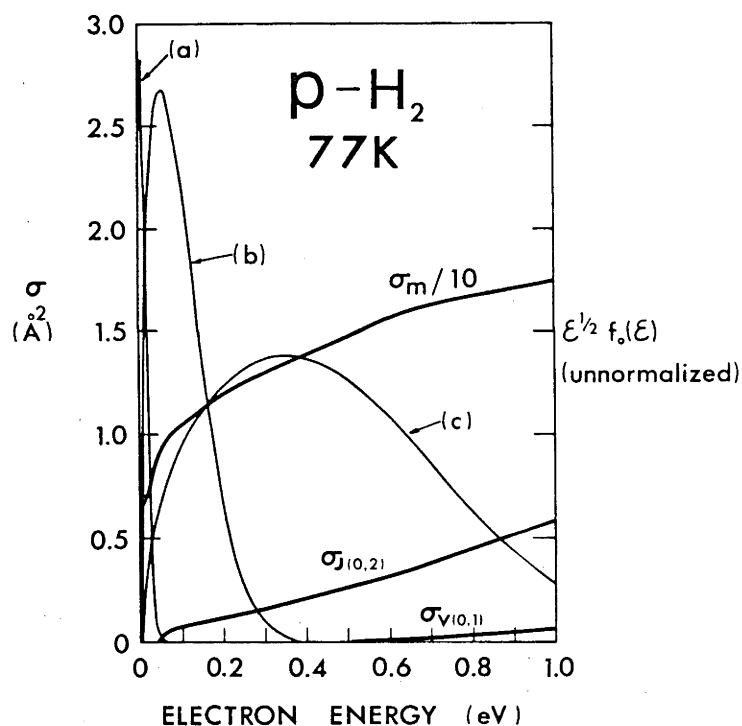


Figure 2.5 Electron energy distribution functions in para-hydrogen at 77 K :

(a) $E/N = 0.01$ Td, $\langle \epsilon \rangle = 0.0111$ eV, $\nu_m = 9.9 \cdot 10^9$ s $^{-1}$, $\nu_{rot} = 3.6 \cdot 10^4$ s $^{-1}$, $\nu_{vib} = 0.0$ s $^{-1}$.

(b) $E/N = 1.00$ Td, $\langle \epsilon \rangle = 0.1007$ eV, $\nu_m = 4.7 \cdot 10^9$ s $^{-1}$, $\nu_{rot} = 3.5 \cdot 10^7$ s $^{-1}$, $\nu_{vib} = 1.7 \cdot 10^1$ s $^{-1}$.

(c) $E/N = 7.00$ Td, $\langle \epsilon \rangle = 0.478$ eV, $\nu_m = 1.4 \cdot 10^{10}$ s $^{-1}$, $\nu_{rot} = 3.2 \cdot 10^8$ s $^{-1}$, $\nu_{vib} = 1.7 \cdot 10^7$ s $^{-1}$.

The cross sections for para-hydrogen are also shown (see Chapter 9) and the pressure is 1kPa.

One would expect that the introduction of multiterm methods would resolve all these problems, but between the formulation of a multiterm theory and its realization in the form of a computer code lie many numerical difficulties. Initially, instead of improving the situation in swarm physics, the introduction of multiterm techniques added somewhat to the confusion. The results for a particular gas or model sometimes differed by almost as much as the difference between the two term and multiterm results (see McMahon 1983a; Braglia 1981; Braglia *et al.* 1982; Segur *et al.* 1984). As a result an international benchmarking exercise was initiated and it is still going on (Crompton 1984b). It is now well established that some of the differences were caused by the use of different cross section sets for to the same gas.

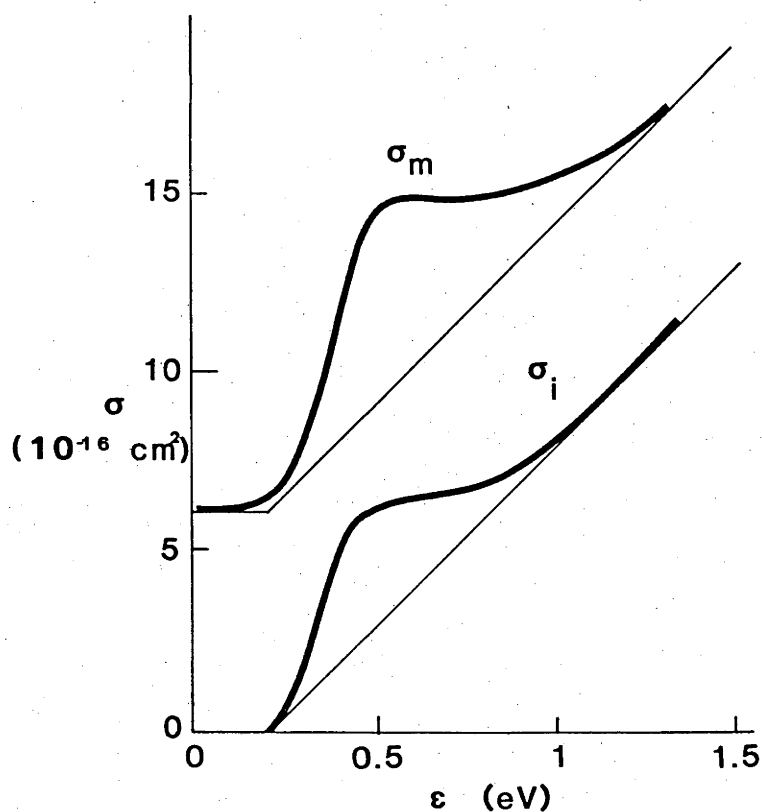


Figure 2.6 Reid's ramp model (thin line) and the cross sections that can be derived from the "exact" values of the transport coefficients (in a limited E/N range) if one uses the two term theory (thick line).

Most of the results are now in very good agreement (except for ND_L in some cases; see for examples Penetrante and Bardsley 1984), and this lends confidence to the results derived from swarm experiments provided an adequate theory and method of calculation is being used. It seems that, following the benchmarking exercise, the next step should be the development of "black box" multiterm codes that could be applied without specialized knowledge of the details of transport theory and without the need to modify the code except in exceptional circumstances. It is also desirable that the code could be used on computers of moderate speed with a fast memory of moderate size. It should be possible to extend such a code to analyse nonconservative situations. Finally, the accuracy of the calculated coefficients should be better than the accuracy of the experimental data. If the performance claimed in the papers by Segur et al. (1983a and 1984) is correct, the method developed by these authors appears to be the closest to achieving the goals mentioned above.

A different approach of using multiterm theory in the derivation of cross sections was used extensively by Haddad (1983; 1984; see also Haddad and Crompton 1980 and Haddad and Milloy 1983). It is to use the much faster two term code to do the cross section fitting and to use the multiterm code only twice, at the beginning and at the end of the iterative process. In this way the corrections to the two term results for the transport data are calculated. The corrections are first based on the initial set of cross sections, but when the final fit is achieved the resultant set is used to recalculate the corrections and, if necessary, another iteration is performed. This is usually unnecessary. It may be added that, since the highly accurate but time consuming and expensive calculations need be performed only a small number of times, even Monte

Carlo codes could be used in this scheme. The approach presented in this paragraph will be used in present work.

The accuracy that has recently been achieved by multiterm methods matches the accuracy of the experimental data (i.e. does not produce any limitation on the accuracy of the analysis of these data). However, one should be aware of the problems discussed above both in applying two term theory and in the operation of some of the multiterm codes.

It is worth noting that if one uses the TTT for some application with the cross sections obtained using the same theory, accurate results for transport coefficients that were not used to derive the cross section will be derived even when the theory is not strictly applicable. However, it is clearly not possible to make a valid comparisons of the cross sections obtained using the theory with the corresponding cross section data from the scattering theory or beam experiments when the approximations of the theory break down.

2.4: Relations Between the Transport Coefficients and the Experimentally Observable Quantities

Swarm experiments are usually designed to observe the space/time distribution of the electron swarm. The set of equations (2.6-2.10) shows the procedure that is usually employed to separate the spatial and temporal development of the swarm from the distribution of electron energies within it, and to describe the former (2.9) on the basis of transport coefficients calculated using the energy distribution function (equations 2.10, 2.33-2.35, 2.54-2.58).

If we take the general expansion of the continuity equation (2.9, see

Kumar and Robson 1973) only up to the second term we obtain the form of the continuity equation that is usually used to analyse swarm experiments (Huxley and Crompton 1974):

$$-\frac{\partial n}{\partial t} + (v_i - v_{att})n - v_{dr} \frac{\partial n}{\partial z} + D_T \left(\frac{\partial^2}{\partial x^2} + \frac{\partial^2}{\partial y^2} \right) n + D_L \frac{\partial^2}{\partial z^2} n = 0 \quad . \quad (2.60)$$

In this equation the z axis is parallel to the electric field. The solution of (2.60), for a swarm of electrons drifting and diffusing between two electrodes separated by h and with boundary conditions $n(h)=n(0)=0$, is (Huxley 1972; Huxley and Crompton 1974)

$$\begin{aligned} n(\underline{r}, t) = & \frac{n(0) \exp[(v_i - v_{att})t]}{(4\pi D_T t) (4\pi D_L t)^{1/2}} \exp\left[-\frac{x^2 + y^2}{4D_T t}\right] \frac{1}{v_{dr} t} \\ & \times \left\{ z \exp\left(-\frac{(z-v_{dr}t)^2}{4D_L t}\right) + (z - 2h) \exp\left(-\frac{(z-v_{dr}t)^2 + 4h(h-z)}{4D_L t}\right) \right. \\ & \left. + \dots \right\} \quad (2.61) \end{aligned}$$

where $n(0)$ is the electron density at the source ($z=0$) and at time $t=0$, h the distance between the two electrodes and $z=v_{dr}t$ is the position of the centroid of the travelling group of electrons.

The first term in the brackets {} of the equation (2.61) is the so called dipole term that satisfies the boundary condition $n=0$ over $z=0$ at all times t. The addition of the image term (the second term in 2.61) gives the correct condition $n=0$ at $z=h$ but somewhat spoils the $z=0$ condition. A whole hierarchy of images would be necessary to satisfy both conditions, but it is usually sufficiently accurate to use only one image.

Equation (2.61) provides us with a means to analyse swarm experiments such as v_{dr} measurements using Bradbury Nielsen shutters or D_T/μ measurements using the Townsend-Huxley technique (Huxley and Crompton 1974).

In the Bradbury-Nielsen time of flight experiment the gating frequency applied to the shutters is varied until the frequency f_m is found that maximises the transmitted current. If f_m is the lowest such frequency, then the drift velocity is given approximately by $v_{dr} = 2hf_m = h/t_m$ where t_m is the time interval between successive shutter open times that leads to maximum transmitted current. However, to determine v_{dr} accurately from f_m one must integrate $n(\underline{r}, t)$ over the collecting electrode behind the second shutter and then find the maximum of the corresponding current. The drift velocity is then given by (Crompton et al. 1957; Lowke 1962):

$$v_{dr} = \frac{h}{t_m} \left(1 - C' \frac{D_L/\mu}{U} \right) = \frac{h}{t_m} \left(1 - C \frac{D_T/\mu}{U} \right) \quad (2.62)$$

where U is the total voltage applied across the drift distance h and C is a constant. The value of C can be derived from the procedure just described (2.61) but it is better to keep it as an unknown experimental parameter and obtain it from the pressure dependence of the data measured at the same E/N . This is because the value of C depends on the nature of the boundary conditions which may not be exactly those used in the derivation of (2.61) (see Huxley and Crompton 1974). In this way one can also account to first order for the small but still important influence from nonequilibrium effects at the shutters (Lowke 1962; Elford 1984). These effects are especially big for some atomic gases, but for molecular gases the nonequilibrium effects are relatively smaller and therefore the value of C' varies little for different gases. This is because the mean distance for

energy exchange, and consequently the width of the nonequilibrium region, is much smaller for molecular gases at low energies. With careful design of the experiment it is possible to work under conditions where the correction factor is very small - of the order of the experimental uncertainty. In the presence of nonconservative processes the correction $CD_T/\mu U$ is modified (Pack and Phelps 1966) and is then also dependent on the attachment or ionization collision frequency.

In the Townsend-Huxley experiment a steady swarm is produced from a point source in the cathode. The ratio of the lateral diffusion coefficient to mobility is determined from the ratio of two currents, one falling on the central disk of a divided anode and the other falling on the remaining outer annular segment. This is a steady state experiment and therefore we should either use equation (2.60) with $\partial n/\partial t=0$ and solve it for appropriate boundary conditions, or integrate the travelling group solution (2.61) from $t=0$ to $t=\infty$. The equivalence of these two approaches is a result of the fact that electrons do not interact with each other, and this equivalence is preserved even when longitudinal gradients due to ionization (and/or attachment) become large provided the correct definitions of the transport coefficients are used (Blevin and Fletcher 1984).

The derivation of the formula relating R (the ratio of the current falling on the central disc to the total current) proved to be a very difficult problem and has an interesting history (Crompton 1972; Huxley and Crompton 1974). The basic formula (the so-called Huxley formula) is:

$$R = 1 - \frac{h}{d} \exp[- \lambda_T(d-h)] \quad (2.63)$$

where

$$\lambda_T = \frac{v_{dr}}{2D_T} \quad \text{and} \quad d^2 = h^2 + b^2, \quad (2.64)$$

and b is the radius of the inner disc. This formula for R can be derived under the assumption that $D_T = 2D_L$ (which applies when σ_m is constant—Parker and Lowke 1969) from the more general formula:

$$R = 1 - \left[1 + \left(\frac{1}{2} - \frac{D_L}{D_T} \right) \left(\frac{b}{d} \right)^2 \right] \left(\frac{h}{d} \right) \exp[- \lambda_T (d-h)]. \quad (2.65)$$

The formula can be derived by following either of the procedures outlined above, i.e. by using the steady state solution of (2.60) or by integrating (2.61). In the presence of ionization/attachment the following formula can be derived:

$$R = 1 - \left[1 + \left(\frac{1}{2} - \frac{D_L}{D_T} \right) \left(\frac{b}{d} \right)^2 \right] \left(\frac{h}{d} \right) \exp[- \lambda_T \left(1 - \frac{\alpha_T}{\lambda_L} \right) (d-h)] \quad (2.66)$$

where

$$\lambda_L = \frac{v_{dr}}{2D_L} \quad (2.67)$$

and α_T is the Townsend ionization coefficient.

All the formulae mentioned above are only approximate. Their accuracy and the range of validity have been checked experimentally (see Crompton and Jory 1962) and by Monte Carlo simulations (Braglia and Lowke 1979). Huxley's formula (2.63), or (2.65) if $2D_L = D_T$, or (2.66) in the presence of ionization are sufficiently accurate under normal experimental conditions. To ensure their accuracy the drift length h should be made large enough compared to b and to the size of the hole in the cathode (for the analysis of the effect of the finite hole see Huxley 1973 and Huxley and Crompton

1974 and the references therein). When (2.65) is used it is important to check its accuracy, especially when the term $(1/2 - D_L/D_T)(b/d)^2$ is not small. The general lack of data for D_L/μ makes the application of this formula difficult in these circumstances; theoretical formulae for the ratio D_L/D_T are then useful (Parker and Lowke 1969; Robson 1984).

A brief review has been given in this section of the theory relating the relevant transport coefficients to the quantities determined experimentally in the two experiments used in the present work to study the transport of non-thermal electrons. The theoretical foundation of the third experiment, which was used to study thermal electrons, will be discussed at greater length in Chapter 4.

2.5: Electron Transport Under the Influence of Density Gradients

Any treatment of electron swarms has to confront the problem of the presence of the density gradients and its influence on the distribution function. A satisfactory explanation of anisotropic diffusion depends on the correct treatment of the density gradients in a pulse of electrons travelling in an electric field (Skullerud 1969; Parker and Lowke 1969; Lowke and Praker 1969; Huxley 1972; Francey and Jones 1976; Penetrante and Bardsley 1984). As has been already mentioned, if nonconservative processes are present the resulting longitudinal gradient has a major influence on the values of the transport coefficients (see Tagashira 1981; Blevin and Fletcher 1984).

Another influence of spatial gradients, this time perpendicular to the electric field, has recently been analysed by Ikuta and coworkers (Ikuta and Itoh 1982; Ikuta et al. 1983; Itoh et al. 1983; Ikuta 1984). These

authors suggested that up to the present time the transverse diffusion coefficient has been inaccurately determined due to an error in the standard two-term formula for ND_T (equation 2.56). It is claimed that the error persists even when the TTT accurately predicts the EDF.

The somewhat surprising findings of Ikuta et al. (1983) are discussed in this section. First, a brief description of the work of these authors will be given and their explanation will be briefly outlined. The results of the present work are shown in Table 2.2 and compared to the results of Ikuta et al. Finally, the implications of the effect described by Ikuta et al. for the application of the swarm technique will be analysed. The primary concern is whether the available swarm-derived cross sections for "real" gases should be reanalysed. One of the conclusions of this work is that, in the author's opinion, the physical picture of the phenomenon given by Ikuta et al. is still not satisfactory. It is possible that the presentation, of their argument in this work is not adequate. If this is the case the reader is referred to the original articles for a more detailed exposition.

Ikuta et al. (1983) made calculations and Monte Carlo simulations for gases that have the following characteristics: a) a purely elastic scattering; b) isotropic scattering; c) zero temperature; d) a mass ratio $m/M=10^{-2}$ or 10^{-4} ; and e) a simple power law energy dependence of the cross section ($\sigma_m=\sigma_{m0}\epsilon^n$). They found that transverse diffusion coefficients calculated using either the TTT or a three-term theory differed from the results of their MC simulation.

These results were somewhat surprising as it was usually assumed that the breakdown of the TTT does not occur unless some inelastic processes are present. A similar observation to that of Ikuta et al. was made (for

argon) even earlier by Kitamori et al. (1980) but no explanation of the effect was given.

Ikuta et al. proposed the following explanation. First, they point out that there is a fundamental difference between the diffusion coefficients obtained on the basis of two different approaches. In the first approach the coefficient (ND_T) is calculated from time averages in real space (see equation (2.43)) while in the second the coefficient (ND_V) is calculated from the averages made in velocity space (2.56) over the entire ensemble. They claimed that the difference is the result of the inadequate calculation of the mean free time in the second approach because when the ensemble average, as given by equation (2.56), is made, the effects of the curved electron orbits due to the field are lost. Since the curved orbits result in the displacement perpendicular to the field being somewhat reduced, the ensemble-averaged diffusion coefficients ND_V are larger than the "real space" diffusion coefficients ND_T . The degree of anisotropy of the distribution function determines the magnitude of the effect. Therefore a difference between ND_V and ND_T is only observed for model gases that have unrealistically large mass ratios m/M (namely 10^{-2}) if the cross section is not strongly dependent on energy. For realistic mass ratios a rapidly increasing momentum transfer cross section is necessary for the difference to occur. The results of Ikuta et al. for some of their model gases are presented in the Table 2.2.

Table 2.2 Comparison of the diffusion coefficients for the model gases proposed by Ikuta et al. (1983)

$\sigma_m = 1$ (in 10^{-16}cm^2) $E/N = 1 \text{ Td}$ $m/M = 10^{-2}$ (ND in $10^{23} \text{cm}^{-1} \text{s}^{-1}$)					
	2 Term	3 Term	4 Term	5 Term	MC
Ikuta <u>et al.</u>					
ND _V	1.23	1.21			1.22
ND _T					1.16
PRESENT					
MC ND _V					1.22
ND _T					1.14
TTT ND _V	1.22				
LRM ND _T	1.24	1.20	1.20		
$\sigma = 1$ $m/M = 10^{-4}$					
	2 Term	3 Term	4 Term	5 Term	MC
PRESENT					
MC ND _V					3.84
ND _T					3.89
TTT ND _V	3.87				
LRM ND _T	3.87	3.87	3.87		

$$\sigma = 1.8 \epsilon \text{ (in } 10^{-16} \text{ cm}^2 \text{ when } \epsilon \text{ in eV)} \quad m/M = 10^{-2}$$

	2 Term	3 Term	4 Term	5 Term	MC
Ikuta <u>et al.</u>					
ND _V	2.05	2.05			2.05
ND _T					1.58
PRESENT					
MC ND _V					2.05
ND _T					1.60
TTT ND _V	2.05				
LRM ND _T	2.02	1.61	1.65	1.64	

$$\sigma = 1.8\epsilon \quad m/M = 10^{-4}$$

	2 Term	3 Term	4 Term	5 Term	MC
Ikuta <u>et al.</u>					
ND _V	1.15	1.15			
ND _T					1.06
PRESENT					
MC ND _V					1.14
ND _T					1.06
TTT ND _V	1.14				
LRM ND _T	1.12	1.08	1.08	1.08	

The estimated inaccuracy of the MC results is smaller than $\pm 1\%$ for $m/M = 10^{-2}$ and $\pm 2\%$ for $m/M = 10^{-4}$. For the results of the LRM code the inaccuracy is smaller than $\pm 1\%$ (but having in mind that there could be an additional uncertainty due to inadequacy of the theory as applied in the LRM code for large values of m/M).

One may make the following comments about the work of Ikuta et al. (1983). The two and the three term formulae used by them are only approximate and do not include some higher order terms in m/M . Moreover some other approximations are made in their derivation (see Braglia and Caraffini 1980). The formulae tested by Ikuta et al. are only valid for small values of the mass ratio, that is, for ratios that are similar to the ratios for real gases. Therefore it is inappropriate to look for the effects discussed by Ikuta et al. using mass ratios that render these formulae inaccurate. For this reason the results obtained by Ikuta et al. (1983) for the mass ratio of 10^{-4} are the most important. For the model gas that has a linearly increasing cross section with the energy these authors found the difference between ND_V and ND_T to be 8.5% for $E/N=1$ Td.

Present calculations using the Monte Carlo code developed by Reid (1979) have confirmed the results of the MC simulations of Ikuta et al. - see Table 2.2. Agreement was also found with the results (ND_V - MC (EDF)) obtained using the EDF obtained from the MC simulations and the formulae for ND from the two or three term theories. The two-term results calculated using the standard code also agree well with the results calculated from the analytical formulae by Ikuta et al. However, it is interesting to discuss the LRM code results. An important feature of that code is that the transport coefficients are calculated in "real space", therefore ND_T is being calculated. Table 2.2 shows that there is a small difference between the two-term LRM results and the TTT results for the cases when the momentum transfer cross section increases rapidly. It is not clear whether this difference is a genuine difference between the TTT values for ND_V and the "real space" results of ND_T , or a result of some

problems in the numerical procedure. Three and four term results obtained using the LRM code agree well with the values of ND_T , and disagree with the three term results for ND_V of Ikuta et al. This is an indication that the standard formulae for two and three term calculations are in error in the cases that were analysed. However, it must be pointed out again that more importance should be given to the results with $m/M=10^{-4}$ because all the numerical codes (including the LRM code) were developed by taking the advantage of the small electron to molecule mass ratio. Unfortunately the results for $m/M=10^{-4}$ are difficult to obtain using the MC codes since the energy losses are small and electrons come to equilibrium with the field only after a large number of collisions (Milloy and Watts 1977).

A different approach to the analysis of the relationship between the "real space" and the "ensemble" averages in electron transport was adopted by Makabe and Mori (1984). These authors constructed a three-term theory that includes effects of spatial gradients, perpendicular to the electric field, on the calculation of the EDF. The diffusion coefficient is represented as a tensor that consists of two terms - one the standard "ensemble" average term, and the other a term representing the correction due to the effects of the curvature of electron orbits. It appears that the three-term theory that includes the full gradient expansion of the EDF is the lowest order theory that can give these correction terms. Apart from applying their theory to the models proposed by Ikuta et al., Makabe and Mori (1984) analysed diffusion coefficients for the realistic case of argon. They found a differences between ND_V and ND_T of up to 9% even at E/N values where the inelastic processes are negligible (see Milloy 1975). It is interesting to note that Haddad (1985-personal communication) obtained values of ND_T for Ar at 0.5 Td that differ by less than 2% from

the two-term result (both obtained by the LRM code), compared to the difference of 8% calculated by Makabe and Mori. At the moment it is uncertain whether the results for argon presented by Makabe and Mori are correct.

The following conclusion may be made:

- 1) The calculations of Ikuta et al. were confirmed in the present work.
- 2) For realistic gases some effects may appear for argon and perhaps for neon and krypton. Therefore any analysis at moderate and high E/N values should take into account the proper definition of the diffusion coefficient.

- 3) Standard multiterm theories give the correct results for ND when 3 or more terms are used. In fact the difference between ND_V and ND_T may be regarded as another correction term to the TTT. Therefore in addition to the correction that results from the inaccurate determination of the EDF, a correction must also be made for the inadequacy of the formula that is used to calculate ND. In that sense all the TTT results that were corrected using the multiterm theories or MC simulations do not require reanalysis. In the present work the distinction between ND_V and ND_T will not be made because all the TTT results are normally checked using the LRM theory and/or MC simulations.

- 4) The physical picture of the phenomenon described in this section is still not satisfactory. It is not clear that the representation of the curved electron orbits (which is inherent in BE through the field term) is lost in the process of the development of the TTT, and if so exactly which approximation leads to this loss. Conceptually it is much easier to accept the phenomenon as a consequence of neglecting the higher-order terms in the gradient expansion perpendicular to the field.

Nevertheless, the analysis performed by Ikuta et al. (1983) deserves attention and more work is required before a full explanation can be given for the discrepancies between results based on the different definitions of ND.

CHAPTER 3: NEGATIVE DIFFERENTIAL CONDUCTIVITY IN GASES

3.1: Introduction

Negative differential conductivity (NDC), that is, decreasing electron drift velocity (hence conductivity) with increasing electric field strength, occurs in semiconductors and gases. It has received considerable attention because, on the one hand, a number of applications are dependent on it, while on the other it can cause undesirable instabilities. The role of NDC in gas discharges has been stressed by Lopantseva et al. (1979)(see also Petrushevich and Starostin 1981), who made both experimental and theoretical studies of instabilities in externally sustained discharges in Ar-N₂ and Ar-CO mixtures and in pure Ar. Investigations of the phenomenon are particularly important in relation to the operation of Ar-N₂ lasers (Searles 1974; Ault et al. 1974; Ault 1975; Bychkov et al. 1980), CO lasers (Willett 1974; Garscadden 1981) and diffuse discharge switches (Christophorou et al. 1982a; Schoenbach et al. 1982; Christophorou and Hunter 1984), and to the detection of nuclear radiation (Mathieson and El-Hakeem 1979; Al-Dargazelli et al. 1981).

In the gas phase, NDC has been most commonly observed in very dilute mixtures of molecular gases with argon. There were some early reports of NDC in pure argon but it is now known that these were the result of the presence of molecular impurities (Long et al. 1976, and references therein) and it is well established that NDC is not present in the pure gas (Robertson 1977). The phenomenon has also been observed experimentally and/or predicted "theoretically" in a number of other gas mixtures and even in pure gases; Table 3.1 lists some examples.

Table 3.1: Occurrence of NDC in various pure gases and gas mixtures

Reference	Theory	Experiment
Pack and Phelps (1961)		N ₂ (77 K)
Pack <u>et al.</u> (1962)		CO (77 K)
Lowke (1963)		N ₂ (77 K)
Hurst <u>et al.</u> (1963)		H ₂ O-CH ₄ , H ₂ O-N ₂
Klots and Reinhardt (1970)		Various hydrocarbons
Christophorou (1971)		Data and references for various gases
Long <u>et al.</u> (1976)	Ar-N ₂ , Ar-CO	
Kleban and Davis (1977)	CH ₄	
Kleban and Davis (1978)	CH ₄ , CD ₄	
El-Hakeem and Mathieson (1978)		Ar-CH ₄
Mathieson and El-Hakeem (1979)	CH ₄ , Ne-CH ₄ , Ar-CH ₄ , Ar-CO ₂	
Lopantseva <u>et al.</u> (1979)		Ar-N ₂ , Ar-CO
Lin <u>et al.</u> (1979)	CH ₄	
Elford (1980)		Hg (due to presence of mercury dimers)
Foreman <u>et al.</u> (1981)		Ar-CH ₄ , He-CH ₄
Kleban <u>et al.</u> (1981)	He-CH ₄ , Ar-CH ₄	
Garscadden (1981)	CO-Ar-He	
Christophorou <u>et al.</u> (1982a)		Ar-C ₃ F ₈ , Ar-CF ₄
Haddad (1983)		Ar-N ₂
Haddad and Milloy (1983)		Ar-CO
Haddad (1985)		CH ₄

Almost all investigations of NDC relate it to the presence of a Ramsauer-Townsend minimum in the electron momentum-transfer cross section σ_m , which is exhibited by some atomic and molecular gases, and one or more inelastic energy loss processes in the region of that minimum. This situation may be present in a single molecular gas (e.g. methane) or it may be produced by adding a small quantity of a molecular gas to a heavy monatomic gas.

A more general situation that arises when small quantities of molecular gas are added to an atomic gas is that of enhanced electron conductivity, that is the value of the drift velocity (and conductivity) for the mixture exceeds the values for both constituent gases at the same E/N (Long et al. 1976; Garscadden et al. 1981; Foreman et al. 1981).

Explanations of two examples of NDC in gases have recently been given, one by Long et al. (1976) and the other by Kleban and Davis (1977; 1978). Long et al. based their argument on the variation with E/N of the mean collision frequency for momentum transfer $\langle v_m \rangle$, while Kleban and Davis were concerned with the effect of the degree of anisotropy of the electron velocity distribution function. Both groups of authors dealt with the situation when a Ramsauer-Townsend minimum is present.

The aim of this work is to point out the importance of certain features of the elastic and inelastic collision cross sections in inducing NDC. Initially the desire was to understand better the variation of drift velocity for some gases and gas mixtures that were investigated. For example why NDC is observed in CO-Ar mixtures but not in H₂-Ar mixtures. However, it was soon discovered that the situation in those mixtures was too complicated to enable a real understanding to be gained due to the large number of collision processes occurring simultaneously. Also there

did not appear to be any explanation in the literature that was satisfactory in terms of generality and simplicity. In fact one could not help the feeling that the analyses of both Long et al. and Kleban and Davis, which were restricted to specific gases, did little to provide a general concept of NDC in gases. Moreover, it could be inferred from their work that the presence of a Ramsauer-Townsend minimum was essential for the occurrence of NDC. Model calculations were therefore made in an attempt to gain a deeper insight into the cause of the phenomenon, since the use of simple models rather than the cross sections for real gases enables one to get a much clearer physical picture of the situation.

3.2: Qualitative discussion

The physical situation that leads to NDC for low electric field strength can be understood in general terms in the following way. The well-known formula for the drift velocity in terms of the electron speed c (based on the "two-term approximation"):

$$v_{dr} = - \frac{4\pi}{3} \frac{eE}{m} \int_0^{\infty} \frac{c^3}{v_m(c)} \frac{df_0}{dc} dc, \quad (3.1)$$

can be transformed by partial integration to

$$v_{dr} = \frac{eE}{3mN} \left\langle c^{-2} \frac{d}{dc} \frac{c^2}{\sigma_m(c)} \right\rangle \quad (3.2)$$

provided that $c^3 f_0(c)/v_m(c) \rightarrow 0$ in the limit $c \rightarrow 0$ or $c \rightarrow \infty$ (Huxley and Crompton 1974). In these formulae $\sigma_m(c)$ and $v_m(c) = N\sigma_m(c)c$ are the energy-dependent momentum-transfer cross section and momentum-transfer

collision frequency respectively. It follows that provided the cross section does not vary too rapidly the formula for v_{dr} reduces to

$$v_{dr} = \frac{FeE}{m\langle v_m \rangle} \quad (3.3)$$

where F is a factor near unity (e.g. $F=0.8$ if σ_m is constant) which is constant or varies slowly with E/N (Huxley and Crompton 1974; see also Long et al. 1976; Lin et al. 1979).

We use (3.3) to predict qualitatively the variation of the drift velocity with E/N for the simple situation illustrated in Fig. 3.1. For low values of E/N essentially all the electrons have energies below the inelastic threshold. Therefore, because elastic scattering is the only energy loss process, the mean electron energy and $\langle v_m \rangle$ rise relatively rapidly with increasing E/N , and v_{dr} increases only slowly. At a sufficiently large value of E/N a significant fraction of the electrons in the swarm have energies above the threshold. There is now a much larger average energy loss per collision, the average energy and $\langle v_m \rangle$ increase less rapidly with E/N , and v_{dr} therefore increases more rapidly than it would if there was no inelastic channel (see equation 3.3). This is illustrated in Fig. 3.1b. At very large values of E/N , elastic scattering again becomes the dominant energy loss process, since the average energy loss per elastic collision increases linearly with electron energy, whereas the energy loss per inelastic collision remains constant, so that the drift velocity must approach asymptotically the dashed curve which corresponds to the case of no inelastic scattering. At intermediate values of E/N there is at least the possibility that v_{dr} will decrease with increasing E/N , as shown in Fig. 3.1b. Whether or not this actually occurs depends on the combination of elastic and inelastic cross section and the threshold energy

of the inelastic process.

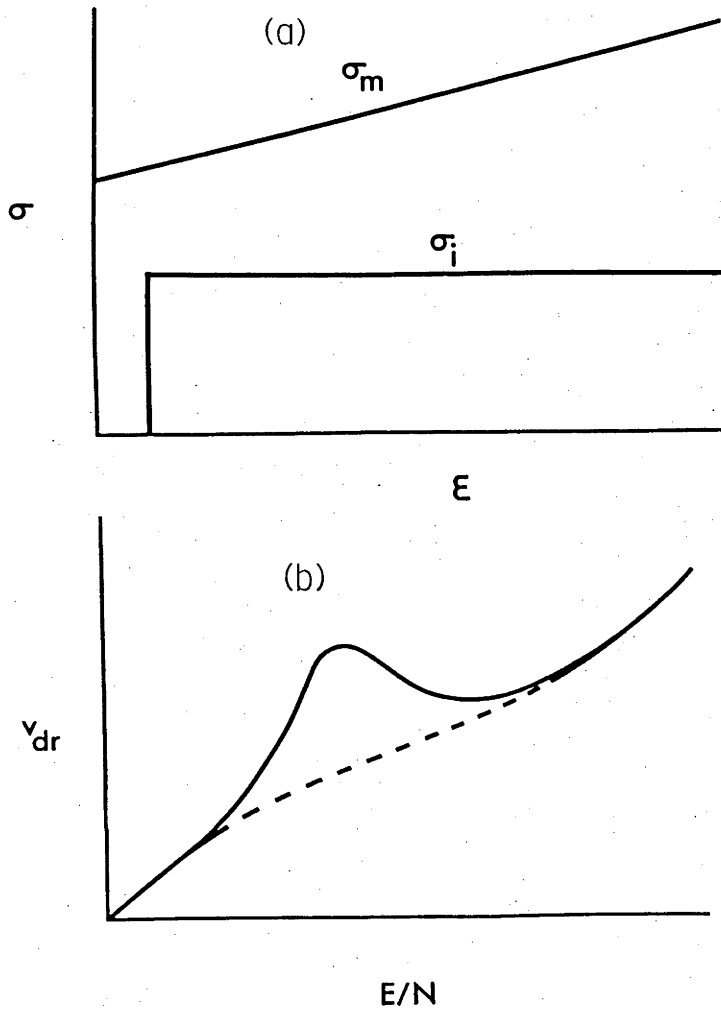


Figure 3.1 Simple model cross sections (a) and the corresponding drift velocity (b) used to illustrate the primary cause of NDC. The dashed curve in (b) shows the drift velocity that would be expected if there was no inelastic scattering.

Explanations of NDC as observed in specific cases have been given by several authors. Kleban and Davis (1977; 1978) discussed the phenomenon in terms of the degree of anisotropy of the velocity distribution. They considered gases such as methane where the threshold of vibrational excitation coincides with a Ramsauer-Townsend minimum in σ_m . In the range of value of E/N where the maximum in the distribution of electron speed is somewhat above that corresponding to the excitation threshold, the average electron energy is kept relatively low by inelastic collisions even though E/N is relatively large. Moreover, because σ_m is small the frequency of

elastic collisions, whose effect is to randomize the direction of the velocity vectors without significantly reducing their magnitudes, is small. Under these conditions the distribution function may become markedly anisotropic, a condition which Kleban and Davis described as "streaming anisotropy". At higher values of E/N , where the distribution of electron speeds has its maximum in the region where σ_m is large, there is enhanced elastic scattering, especially of those electrons whose motion is predominantly in the direction of the electric force and whose velocities are therefore largest. The consequence is enhanced randomization of the velocities and reduced anisotropy. Thus, although the average electron speed is increased, the average velocity (the drift velocity) may be reduced, i.e. NDC may occur.

While affording a new insight into the nature of the phenomenon, the Kleban and Davis description does not provide the basis for a criterion for its occurrence, whereas the preceding argument and equation (3.1) can provide at least an approximate criterion (see Section 3.3).

A somewhat different approach was taken by Long et al. (1976) who based their argument on equation (3.3) but implied that NDC occurs in a transition region where the mean energy of the swarm lies between two inelastic processes with widely separated thresholds.

The argument presented at the beginning of this section suggests that NDC has a simpler explanation than that given by Long et al., and the model calculations described in Section 3.6 support this view.

3.3: A Criterion for Negative Differential Conductivity

Lopantseva et al. (1979) also based their discussion on equation (3.3)

and used a relatively simple argument to develop from it a criterion for NDC. This equation predicts that NDC will occur when $\langle v_m \rangle$ increases more rapidly than E (see Section 3.5), but does not say anything about the characteristics of the elastic and inelastic cross section(s) that will lead to this situation. Following Lopantseva et al., we write an approximate energy balance equation in the form

$$\langle v_i \rangle \epsilon_i = v_{dr} e E \quad , \quad (3.4)$$

where $\langle v_i \rangle$ is the mean inelastic collision frequency, ϵ_i is the energy loss per inelastic collision and, for the sake of simplicity in this discussion, the energy loss in elastic scattering is neglected. Combining (3.1) and (3.2) we get

$$\frac{\partial v_{dr}}{\partial (E/N)} = \frac{F \epsilon_i}{2m v_{dr}} \frac{\langle v_i \rangle}{\langle v_m \rangle} \left(\frac{1}{\langle v_i \rangle} \frac{\partial \langle v_i \rangle}{\partial (E/N)} - \frac{1}{\langle v_m \rangle} \frac{\partial \langle v_m \rangle}{\partial (E/N)} \right), \quad (3.5)$$

or using the logarithmic derivatives ($d(\ln y)/d(\ln x) = \hat{y}(x)$):

$$\hat{v}_{dr} = \frac{F \epsilon_i}{2m v_{dr}^2} (\hat{\langle v_i \rangle} - \hat{\langle v_m \rangle})$$

where it is assumed that $F(E/N)$ is constant.

While the many approximations contained in the derivation of equation (3.5) make it far from adequate in a realistic situation, nevertheless it is useful as a guide to the relationship between elastic and inelastic processes that lead to NDC. It is clear, for example, that a rapid increase of $\langle v_m \rangle$ or decrease of $\langle v_i \rangle$ with E/N will induce a negative slope of v_{dr} versus E/N , i.e. NDC.

Equation (3.4) is only an approximation and it is inadequate in the

situation when elastic collisions are a significant energy loss because these energy losses have been neglected in the equation (3.4). They can be easily included approximately by adding, thus:

$$\langle v_i \rangle \epsilon_i = v_{dr} eE - \frac{2m}{M} \langle \epsilon v_m \rangle \cong v_{dr} eE - \frac{2m}{M} \langle \epsilon \rangle \langle v_m \rangle . \quad (3.6)$$

In that case the condition in (3.5) becomes:

$$\frac{\partial v_{dr}}{\partial (E/N)} = \frac{F \epsilon_i}{2m v_{dr}} \frac{\langle v_i \rangle}{\langle v_m \rangle} \left(\frac{1}{\langle v_i \rangle} \frac{\partial \langle v_i \rangle}{\partial (E/N)} - \frac{1}{\langle v_m \rangle} \frac{\partial \langle v_m \rangle}{\partial (E/N)} \right) + \frac{F}{M v_{dr}} \frac{\partial \langle \epsilon \rangle}{\partial (E/N)} . \quad (3.7)$$

3.4: Other Theoretical Developments

Robson (1984) independently worked on the problem of NDC and derived criterion for its occurrence. His derivation (for the spatially uniform case i.e. $\nabla n=0$) starts from the momentum and energy conservation equations (momentum transfer theory) in the following form

$$v_{dr} = \frac{eE}{\mu \langle v_m \rangle} \quad (3.8)$$

and

$$\langle \epsilon \rangle = \frac{3}{2} kT + \frac{1}{2} M v_{dr}^2 - \Omega \quad (3.9)$$

where μ is the effective mass ($=m_e$ for electrons) and

$$\Omega = \frac{M}{m+M} \sum_i \frac{\epsilon_i \{ \langle v_i \rangle - \langle v_{se} \rangle \}}{\langle v_e \rangle} . \quad (3.10)$$

Here v_{se} is the collision frequency of the superelastic collisions and v_e

is the collision frequency for the elastic energy transfer

$$\langle v_e \rangle = \frac{M}{m+M} \langle v_m \rangle \quad . \quad (3.11)$$

It is then possible to derive:

$$m v_{dr}^2 \hat{v}_{dr} = \left(1 + \frac{d\Omega}{d\langle \epsilon \rangle} \right) \langle \epsilon \rangle \langle \hat{\epsilon} \rangle \quad . \quad (3.12)$$

Since the average energy has to increase with the increase of the field, the only way that NDC can occur is to have

$$\left(1 + \frac{d\Omega}{d\langle \epsilon \rangle} \right) < 0 \quad . \quad (3.13)$$

The usual approximation of momentum transfer theory is the replacement of $\langle v(\epsilon) \rangle$ by $v(\langle \epsilon \rangle)$. This approximation may be adequate for v_m but is not adequate for v_i close to threshold. Consequently Robson proposes averaging on the basis of the Maxwellian distribution function

$$\langle v_i(\epsilon) \rangle = v_i(\langle \epsilon \rangle) (1 + \xi) \exp(-\xi) = v_i(\langle \epsilon \rangle) S(\xi) \quad (3.14)$$

where $\xi \approx 3\epsilon_i/2\langle \epsilon \rangle$. Using $v=Nv\sigma$ Robson has obtained:

$$\Omega(\epsilon) = \frac{M}{2m} \epsilon_i \frac{\sigma_i(\langle \epsilon \rangle)}{\sigma_m(\langle \epsilon \rangle)} S(\xi) \quad . \quad (3.15)$$

The criterion (3.13) is better than the criterion (3.5) since it includes the elastic energy losses and superelastic collisions. Also the term $S(\epsilon)$ enables one to make a good estimate of the average inelastic collision frequency $\langle v_i(\epsilon) \rangle$. It is, however, possible to use (3.14) in our criteria (3.5) and (3.7) and derive formulae in terms of cross sections.

Part of Robson's motivation for studying NDC was its importance as the

most stringent test of generalized Einstein relations (see Klots and Reinhardt 1970; Robson 1972; Kumar et al. 1980; Robson 1984)

An alternative approach to the derivation of a criterion for NDC was proposed by Chantry (1983 - personal communication). He uses the momentum transfer relation (3.3) only. It can be presented in the following form:

$$v_{dr} = \frac{e}{\sqrt{(2m)}} \frac{1}{\langle \sqrt{\epsilon} \sigma_m(\epsilon) \rangle} \frac{E}{N} \quad (3.16)$$

After making an approximation: $\langle \epsilon^{1/2} \sigma_m(\epsilon) \rangle = \langle \epsilon \rangle^{1/2} \sigma_m(\langle \epsilon \rangle)$ it is possible to differentiate (3.16) with the respect to E/N . The final result is:

$$\hat{v}_{dr} = 1 - \langle \hat{\epsilon} \rangle (E/N) \left[\frac{1}{2} + \hat{\sigma}_m(\langle \epsilon \rangle) \right] \quad (3.17)$$

where the round brackets imply "a function of". The necessary condition for the occurrence of NDC is that $\hat{\sigma}_m > -1/2$ and sufficient conditions are $\hat{\sigma}_m \geq 0$ and $\langle \hat{\epsilon} \rangle > 2$. One can see that it is not absolutely necessary for σ_m to increase with ϵ but it favours NDC and that the occurrence of NDC is also favoured by a rapid increase of $\langle \epsilon \rangle$.

It is possible to plot the curve $\hat{v}_{dr}=0$, i.e.:

$$\langle \hat{\epsilon} \rangle (E/N) = \frac{1}{1/2 + \hat{\sigma}_m(\langle \epsilon \rangle)} \quad (3.18)$$

This curve represents the boundary between the positive (PDC) and the negative differential conductivity (Fig. 3.2). It is possible to use D_T/μ instead of $\langle \epsilon \rangle$, but it is rather difficult to give the meaning to $\hat{\sigma}_m(\langle \epsilon \rangle)$ in the case of realistic rapidly changing cross section. Once this problem is overcome this approach provides a very good visual presentation of the dependence of the occurrence of NDC on some parameters. Inelastic cross

sections are, however, hidden in the dependence of the average energy but the relationship is not hard to find. Chantry's criterion is equivalent to ours since the basic equation is identical. Additional approximation is only made when the collision frequency is split (see the line following equation 3.16). On the other hand no commitment to the particular form of the energy balance equation is made.

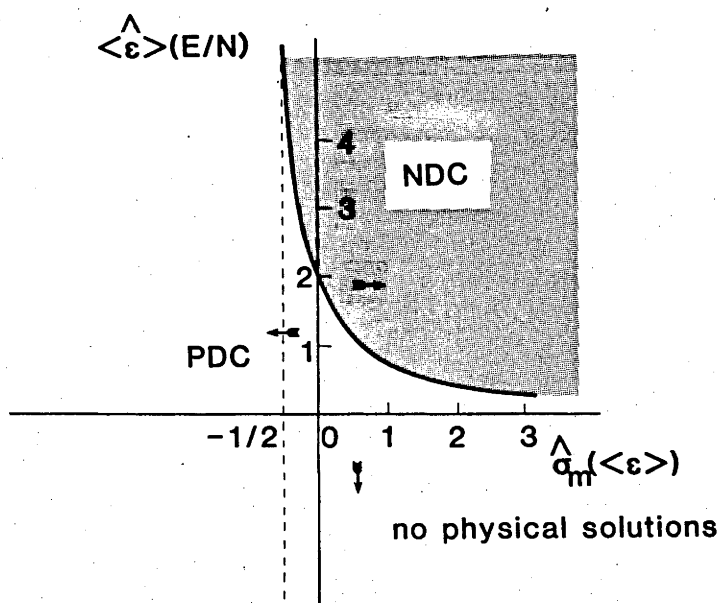


Figure 3.2 The curve representing condition $\hat{v}_{dr}=0$ in the space of parameters $\langle \hat{\epsilon} \rangle$ as a function of E/N and $\hat{\sigma}_m$ as a function of $\langle \epsilon \rangle$. The shaded area corresponds to conditions that lead to NDC and the area that is not shaded to the positive differential conductivity (PDC). Negative values of $\langle \hat{\epsilon} \rangle$ are not allowed because the law of the conservation of energy would be violated.

Lopantseva et al. (1979) have taken the energy loss per collision to be the characteristic energy ϵ_k . Consequently their NDC criterion differs from (3.5). However, apart from this apparently incorrect step, their physical reasoning is correct and their conclusion that NDC is related to

"overheating" of electrons enables them to relate NDC to the stability of the discharge. It is possible that eventual applications of NDC will be impeded by the ever present chance of an instability and therefore this problem deserves much attention, although it is not within the scope of the electron swarm physics.

3.5: Model Calculations

A number of calculations were performed using model cross sections to explore the conclusions of the Section 3.2. One conclusion was that a Ramsauer-Townsend minimum in σ_m was not a necessary condition for NDC, although it has almost always been taken to be so in the literature. The models were constructed with the intention of verifying this conclusion as well as investigating more generally the features of the elastic and inelastic cross section that lead to the phenomenon. The choice of the models was guided by the general arguments given in the Sections 3.2 and 3.3.

Model 1. We chose for the first model a momentum-transfer cross section that linearly increases with energy and is given by

$$\sigma_m = 5 + 1.95\varepsilon$$

(all cross sections are in 10^{-16} cm² when the energy ε is given in eV), and an inelastic cross section that is constant above a threshold energy ε_T , i.e.

$$\begin{aligned} \sigma_i &= 0 & (\varepsilon < \varepsilon_T) \\ &= 0.03 & (\varepsilon \geq \varepsilon_T) \end{aligned}$$

This model corresponds to that on which the discussion at the beginning of Section 3.2 is based. The threshold energy is the parameter in this model and was given the values 0.05, 0.1 and 0.2eV. The inelastic energy loss was taken to be equal to ϵ_T . Room temperature and a molecular mass of 28 a.m.u. were assumed. Drift velocities were calculated using the usual two-term spherical harmonics representation of the velocity distribution function. The results are shown in Fig. 3.3. As predicted, NDC occurs even with cross sections as unspectacular as those for this model and where there is no Ramsauer-Townsend minimum. Note that as ϵ_T increases NDC is postponed to higher E/N, but the effect is much more pronounced. This is because the larger inelastic losses in the region of maximum loss further suppress the mean electron energy, leading to a reduction in $\langle v_m \rangle$ and increase in v_{dr} . Since the drift velocities converge at high E/N, such an increase must lead to enhanced NDC.

It might be argued that the observed decrease of the NDC effect as the threshold energy (inelastic energy loss) becomes smaller is actually the result of "thermal" effects. As has already been stated superelastic collisions were neglected for this calculation, and therefore the molecular motion can only influence the transport of electrons through the term in the Boltzmann equation that takes into account the energy gained by the electrons in elastic collisions with the molecules. In order to check whether the onset and the magnitude of the region of NDC for this model were influenced by the molecular motion the temperature was reduced to 77 K and the calculations repeated. Drift velocities in the region just before the local maximum and in the NDC region were not affected at all even though values at much lower E/Ns were considerably affected. This proves that the transport was dominated by inelastic collisions in the region of

NDC and just before it and that the conclusion about the importance of the inelastic energy loss in inducing NDC is correct.

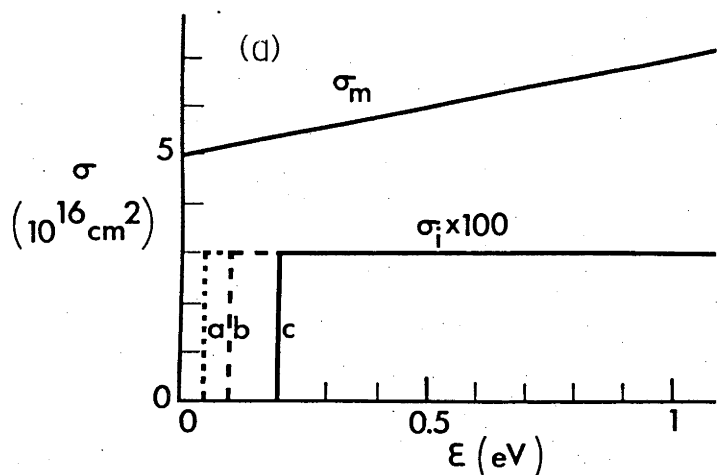
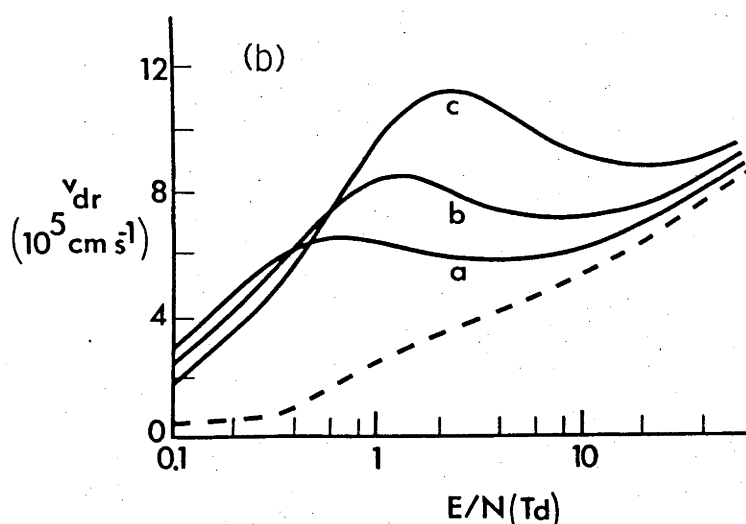


Figure 3.3 Model 1. (a) Cross sections, where the inelastic thresholds are: a, $\epsilon_T = 0.05$ eV; b, $\epsilon_T = 0.1$ eV; c, $\epsilon_T = 0.2$ eV. (b) Calculated drift velocities, where the dashed curve shows results for the case when only the elastic process is present.



Model 2. Here σ_m and σ_i were chosen to have the same form as in Model 1, but the inelastic energy loss per collision ϵ_i was kept the same in all cases (0.05 eV per collision). The threshold energies for the inelastic process were 0.05, 0.3 and 1.0 eV. The results are shown in Fig. 3.4. As the difference between ϵ_i and ϵ_T increases, NDC becomes less pronounced until, in case C, the dependence of v_{dr} on E/N becomes monotonic. This is because the delay in the onset of inelastic scattering allows the mean

electron energy to rise to a point where the elastic energy losses become comparable with the inelastic losses, so that the situation is little different from that for pure elastic scattering where NDC cannot occur.

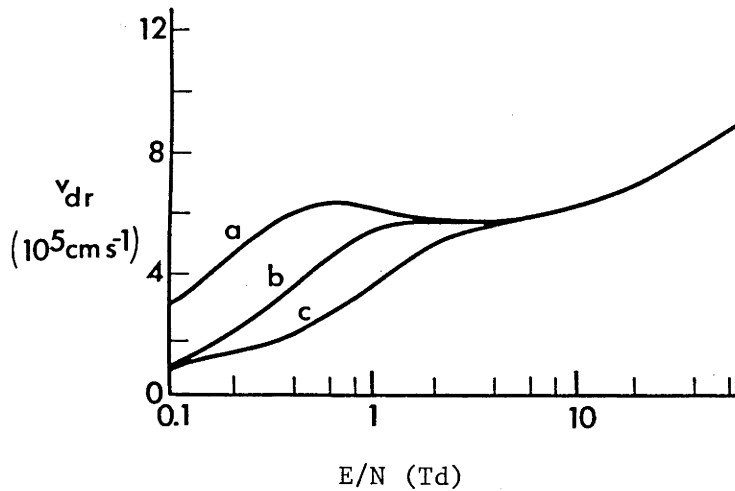


Figure 3.4 Calculated drift velocities for Model 2 with the threshold energy values: a, $\epsilon_T = 0.05$ eV; b, $\epsilon_T = 0.3$ eV; c, $\epsilon_T = 1$ eV. In each case the inelastic energy loss is $\epsilon_i = 0.05$ eV.

Model 3. The third model was designed to show how a sudden decrease of σ_i induces NDC (see equation 3.5). Initially the inelastic cross section of Model 1, case b was used and the slope of σ_m reduced (to 0.15) until no NDC was observed (case d in Fig. 3.5b). Then σ_i was set to zero above different "cut-off" energies ϵ_c . The set of cross sections (in 10^{-16} cm²) is :

$$\sigma_m = 5 + 0.15\epsilon$$

$$\sigma_i = 0 \quad (\epsilon < 0.1\text{eV}; \epsilon > \epsilon_c)$$

$$= 0.3 \quad (0.1\text{eV} \leq \epsilon \leq \epsilon_c)$$

where the parameter ϵ_c has the values 1.0, 3.0, 9.0 eV and ∞ , and $\epsilon_i = 0.1$ eV. The results shown in Fig. 3.5 demonstrate that NDC can be induced by reducing the cut-off energy, and that it becomes more pronounced

as ϵ_c is further reduced. This is evidently due to the fact that above ϵ_c a situation is rapidly reached, as E/N increases, when inelastic scattering is unimportant; that is, one reaches the asymptotic region discussed under Model 1 much more rapidly. Correspondingly, NDC can occur with a momentum-transfer cross section that increases much less rapidly with energy when the inelastic cross section has this form.

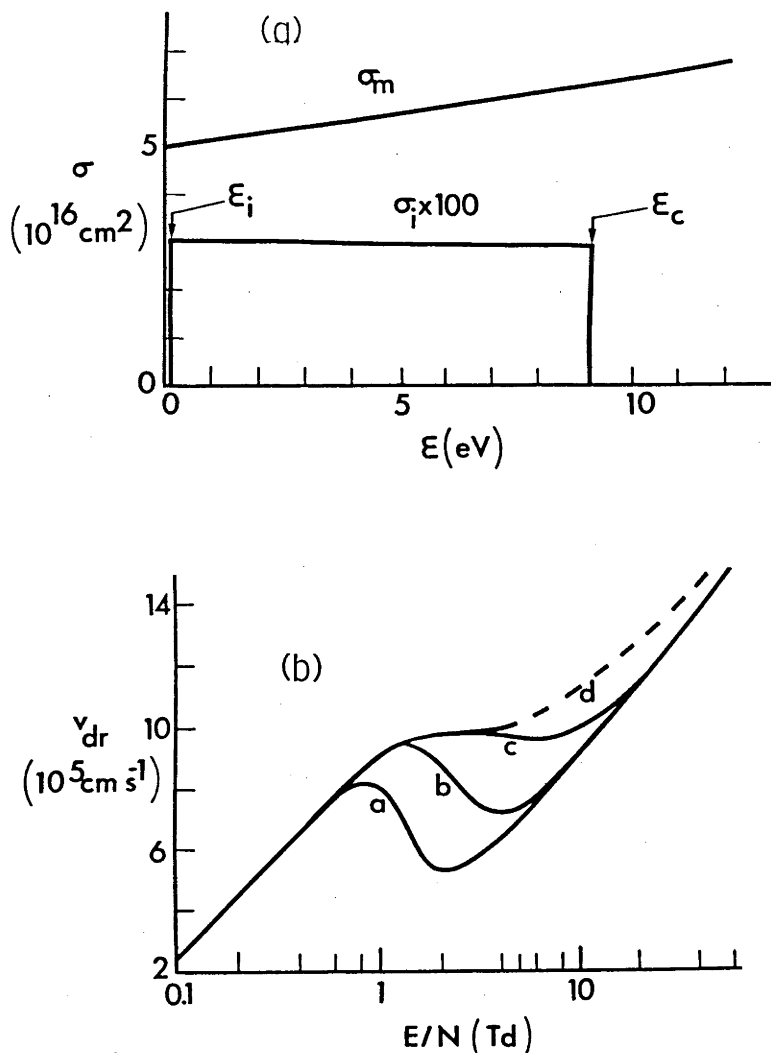


Figure 3.5 Model 3: (a) Cross sections, where the inelastic cross section cut-offs have the values a, $\epsilon_c = 1$ eV; b, $\epsilon_c = 3$ eV; c, $\epsilon_c = 9$ eV (illustrated); d, $\epsilon_c = \infty$. In each case $\epsilon_i = \epsilon_T = 0.1$ eV. (b) Calculated drift velocities, where the dashed curve for d shows the case of no cutoff.

Model 4. It was evident from earlier work that NDC is enhanced when σ_m increases rapidly with energy. This can be illustrated by using the

following model cross sections:

$$\sigma_m = 5 + A\epsilon$$

$$\sigma_i = 0 \quad (\epsilon < 0.1 \text{ eV})$$

$$= 0.03 \quad (\epsilon \geq 0.1 \text{ eV})$$

where A is a parameter taking the values 9.95, 0.45 and 0. The results presented in Fig. 3.6 not only show that NDC is promoted by a steeply rising σ_m , but that the phenomenon can occur with an energy dependence that is much weaker than that usually found on the high energy side of a Ramsauer-Townsend minimum. The model also shows that if σ_m increases too slowly with energy the reduced anisotropy of the velocity distribution function as E/N increases will be more than offset by the increased average speed of the electrons, thus eliminating NDC.

Model 5. The final model demonstrates a perhaps unexpected result that NDC can occur even when σ_m is not increasing. The model has the following characteristics:

$$\sigma_m = 5, \quad \sigma_i = 0 \quad (\epsilon < 0.1)$$

$$\text{Case a:} \quad \sigma_i = 0.03 \quad (\epsilon > 0.1)$$

$$\text{Case b:} \quad \sigma_i = 0.03 \quad (0.1 < \epsilon < 1.0)$$

$$= 0 \quad (\epsilon > 1.0)$$

$$\text{Case c:} \quad \sigma_i = 0.01 \quad (0.1 < \epsilon < 1.0)$$

$$= 0 \quad (\epsilon > 1.0)$$

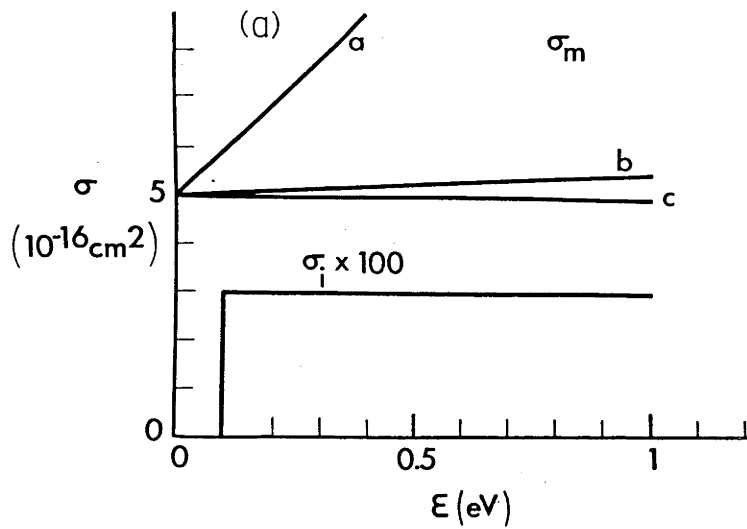
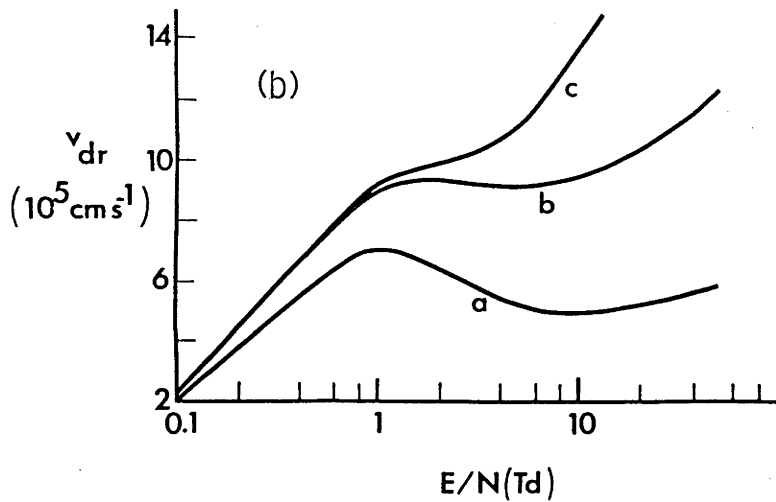


Figure 3.6 Model 4: (a) Cross sections, where the slopes of σ_m have the values: A, $A = 9.95 \cdot 10^{-16} \text{ cm}^2 \text{ eV}^{-1}$; B, $A = 0.45 \cdot 10^{-16} \text{ cm}^2 \text{ eV}^{-1}$; C, $A = 0.0$ (b) Calculated drift velocities.



As shown in Fig. 3.7, case b shows that NDC can in fact occur in this situation. Note that a cut-off in σ_i is essential for NDC to occur in this case (compare curves a and b in Fig. 3.7b), and that this cross section must be sufficiently large (compare curves b and c). Both conditions are necessary to ensure a sufficiently rapid decrease in anisotropy with increasing E/N .

One can extend the example further and introduce a negative slope to σ_m , keeping the same σ_i as for the case b. NDC becomes less and less pronounced but still exists. For a σ_m that linearly decreases from 5 at

$\epsilon=0$ to 3 at 10 eV there is a sharp NDC (see Fig. 3.8).

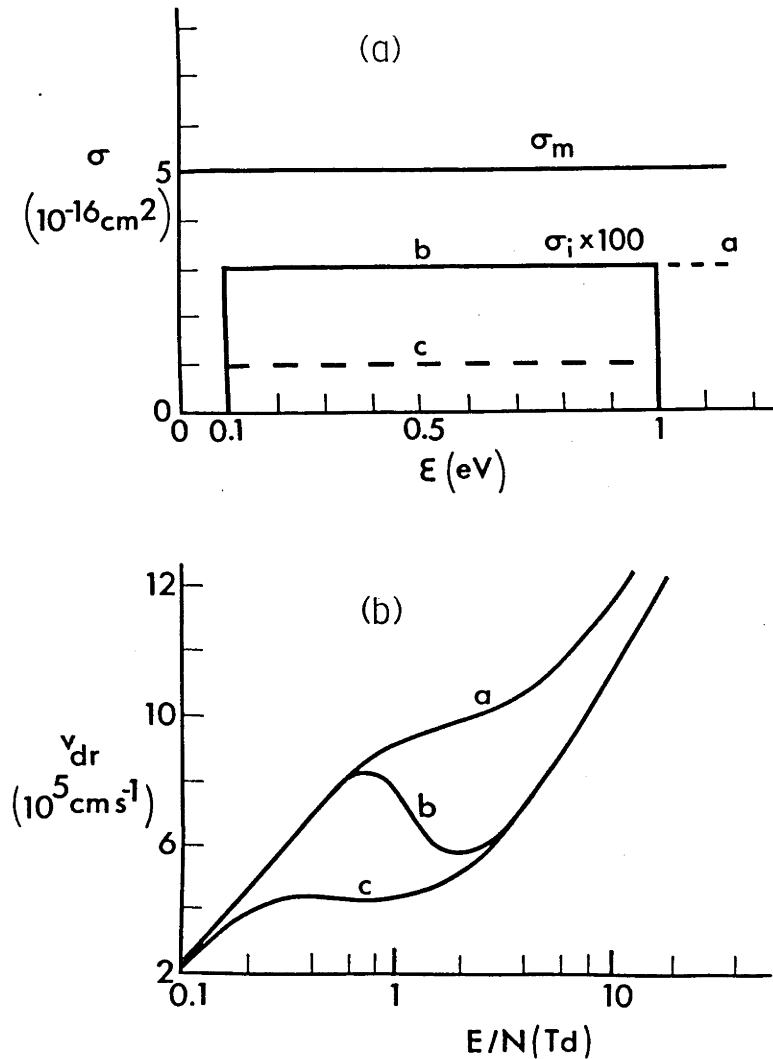


Figure 3.7 Model 5 (see text): (a) Cross sections. (b) Calculated drift velocities.

3.6: General Comments about Model Calculations and Criteria for Negative Differential Conductivity

The results presented in the previous section were obtained using the Boltzmann code developed by Gibson (1970). In order to determine the significance of errors arising from the two-term approximation inherent in

the solution of Boltzmann's equation upon which Gibson's code is based (Holstein 1946), v_{dr} was recalculated using a multiterm code (Lin et al. 1979; see also Haddad et al. 1981) for the typical case of Model 5, case b.

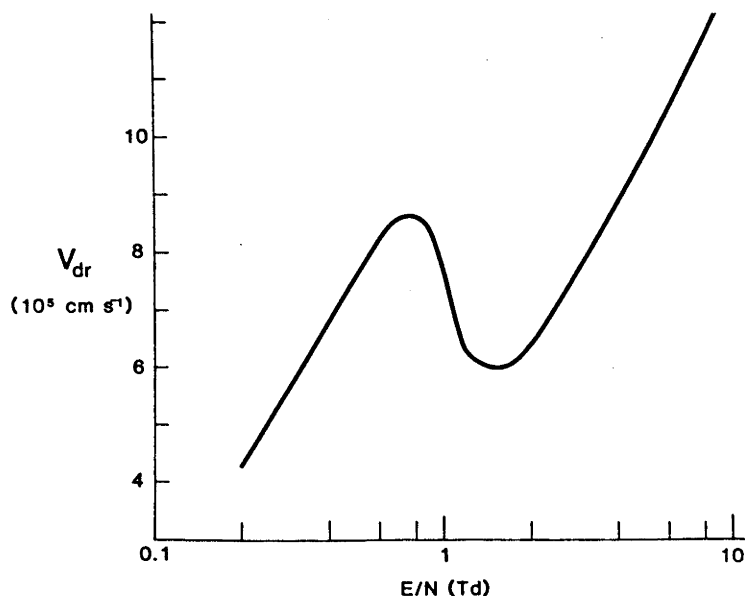


Figure 3.8 Calculated drift velocities for the model cross section with a negative slope of σ_m as explained in the text.

The results are compared with the two-term results in Fig. 3.9a. This figure also shows results for D_T/μ , the ratio of transverse diffusion coefficient to mobility, which is more subject to error from this approximation. The error arising from the approximation are negligible in each case, a result which is not surprising given the ratio of the elastic and inelastic cross sections (Reid 1979). The validity of the two-term approximation in this instance also shows that the degree of anisotropy required for NDC to occur need not be large.

Gibson's (1970) code was also used to calculate $\langle v_m \rangle$; the ratio $\langle v_m \rangle/E$

is plotted in Fig. 3.9b. The range of E/N where $\langle v_m \rangle$ increases more rapidly than E (labeled R) corresponds to the region of NDC, in accordance with (3.3). This illustrates the adequacy of the explanation based on this formula despite the approximations inherent in its derivation. In all the calculations both for the model and for real gases there was extremely good agreement between the range of R and the range of NDC.

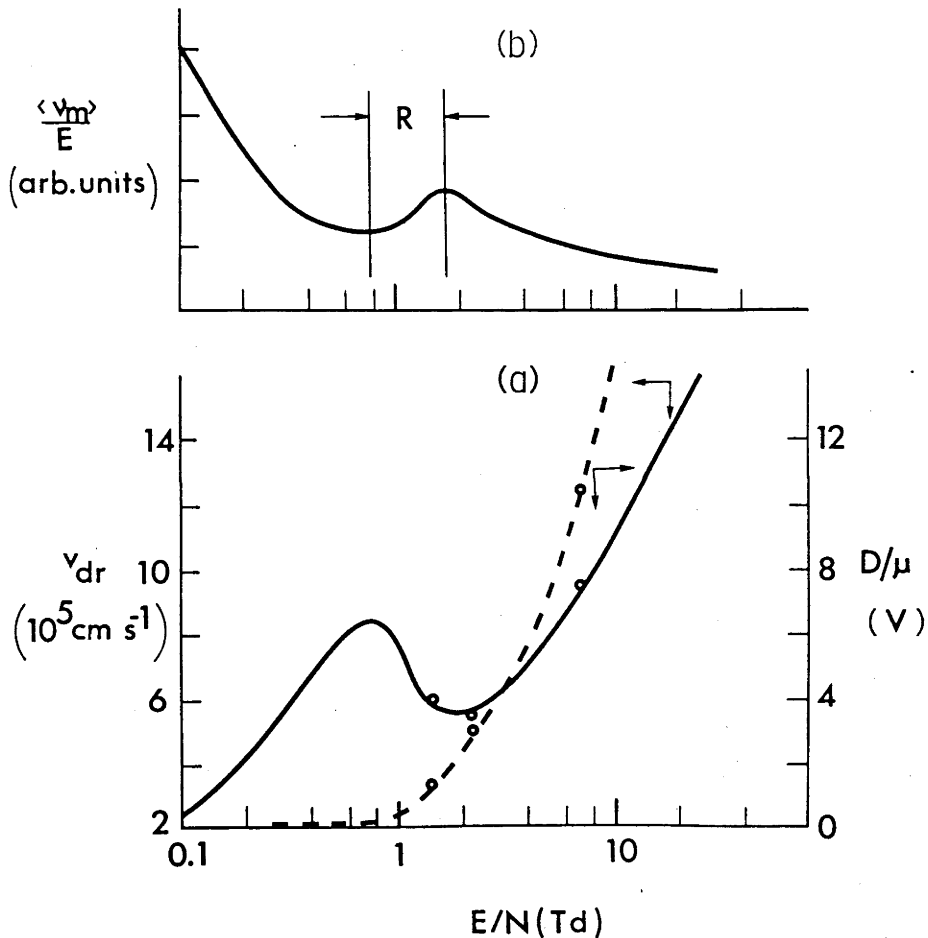


Figure 3.9 Model 5, case b: (a) Calculated drift velocities (solid curve) and the ratio D_T/μ (dashed curve). The multiterm calculations for both v_{dr} and D_T/μ are represented by circles on the corresponding curves. (b) The E/N dependence of $\langle v_m \rangle / E$. The region where $\langle v_m \rangle$ rises more rapidly than E , leading to NDC, is indicated by R.

Initially the criterion (3.5) was developed just to guide the choice for the model calculations. The addition of the elastic energy losses produces a more accurate criterion that somewhat narrows the range of NDC but does not give much more physical insight into the causes of NDC than the (3.5). The reason is that the assumptions (equations 3.3 and 3.4) in the derivation of (3.5) are quite adequate for the peak of the v_{dr} -E/N curve where inelastic collisions dominate the energy transfer. Whether NDC will occur or not is "decided" at this point, i.e. v_{dr} can continue its increase, can remain constant or decrease. Drift velocity of the purely elastic gas is the lower limit to the v_{dr} and therefore NDC cannot start from the purely elastic curve (this is evident from (3.5) or/and from Robson's criterion but it is rather hard to see it from Chantry's criterium unless someone actually performs calculations and plots the results.

The adequacy of criteria (3.5) and (3.7) can be judged on the basis of Fig. 3.10. Here, the calculations of drift velocities for Model 5 case b carried out by Robson (1983-personal communication) are displayed. In the region of the local maximum of v_{dr} both criteria agree very well with the calculations based on BE. As can be expected, the criterion (3.5), which does not include the energy losses in elastic collisions, breaks down at high E/N values, but is sufficiently accurate at the maximum. Similar checks were made during the course of the present work when the mass of the model gas was varied from 28 to 100 then to 500 atomic units in order to show that the drift velocity in the region of the maximum was not affected by energy loss in elastic collisions.

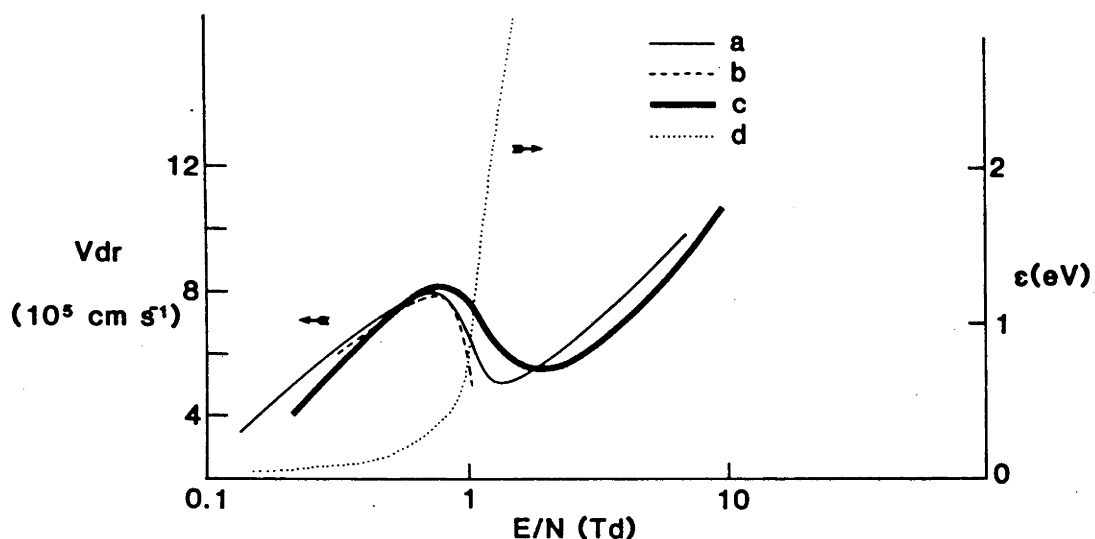


Figure 3.10 Model 5, case b: Drift velocities calculated on the basis of: (a) equation (3.7) (or equations 3.10-3.15); (b) equation (3.5); (c) by a solution to the Boltzmann Equation. The corresponding values of D_T/μ are also presented (d). These are the results of calculations carried out by Robson (1983-personal communication).

It is relatively easy to apply Chantry's criterion to our models. For the constant σ_m it can be seen from Fig. 3.2 or from (3.18) that the logarithmic derivative of $\langle \epsilon \rangle$ should be greater than 2 for NDC to occur. In Fig. 3.11 we have presented the log-log plots of the calculated D_T/μ vs. E/N and the plot of the corresponding finite difference ratios. The notation is the same as in Fig. 3.7. We see that the curve B reaches the value of 3 between 1 and 1.7 Td, while the curve C reaches the peak of 2.06 below 1 Td. This is in very good agreement with the observed behaviour of the drift velocities (see Fig. 3.7) where the curve C only just shows NDC, while B has a very pronounced minimum. We should also add that Chantry's

criterion is consistent with our conclusion that it is possible to have NDC with a decreasing σ_m , and it even gives a limit of $\hat{\sigma}_m(\langle \epsilon \rangle) > -1/2$ to the negative slope.

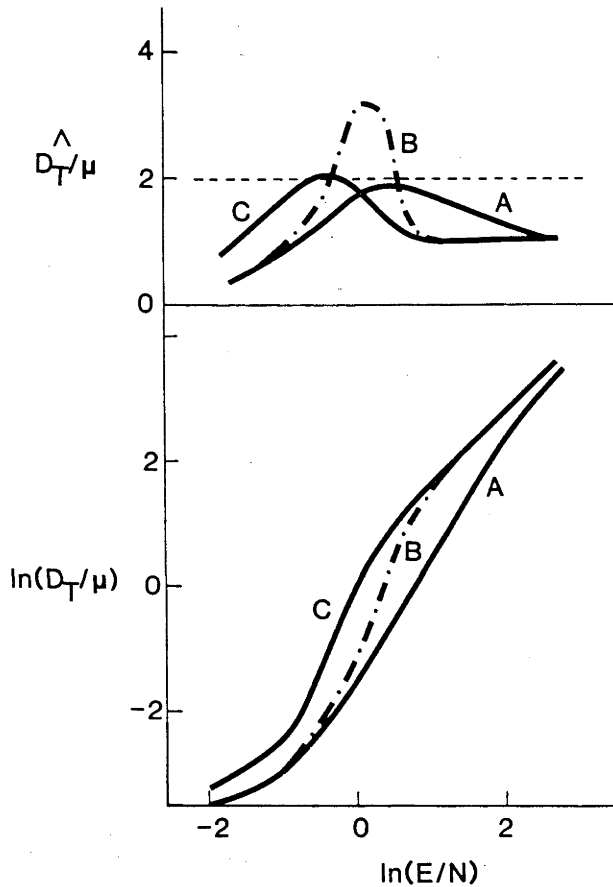


Figure 3.11 Model 5: Dependence of $\ln(D_T/\mu)$ and D_T/μ on $\ln(E/N)$ as an illustration of Chantry's criterion for the occurrence of NDC. The notation is the same as in Fig. 3.7.

3.7: Negative Differential Conductivity in Real Gases

Most studies of NDC have concentrated on gases or gas mixtures in which the thresholds for vibrational excitation lie near or above a Ramsauer-Townsend minimum. Consequently such conditions are generally taken to be

necessary for the phenomenon to occur. However, its occurrence in nitrogen and carbon monoxide at 77 K for small values of E/N (Pack and Phelps 1961; Pack et al. 1962; Lowke 1963) shows that a Ramsauer-Townsend minimum is not necessary, and also suggests that rotational rather than vibrational excitation may be the relevant inelastic process in these instances. Moreover, in the case of CO, where σ_m decreases with increasing energy in the relevant range of electron swarm energies, the fact that NDC occurs confirms one of the conclusions reached with the models, namely that σ_m need not increase with energy for the effect to occur.

From an examination of experimental data for v_{dr} and D_T/μ in N_2 , it seems to us unlikely that vibrational excitation is responsible for NDC in the 77 K data for this gas. We investigated this more fully using the two-term Boltzmann code together with rotational excitation cross section calculated using the Gerjoy and Stein (1955) formula (Born approximation) and the momentum transfer and vibrational excitation cross sections of Pitchford and Phelps (1982). We could show that the phenomenon is entirely due to the rotational excitation by suppressing the vibrational cross sections (see Fig. 3.12a); in fact their removal considerably increases the range of E/N over which NDC occurs without affecting its onset. Thus, in this case the presence of the second inelastic process reduces NDC rather than promotes it (Long et al. 1976).

In real gases superelastic collisions with rotationally excited molecules also have a considerable influence on NDC. In N_2 at 293 K, NDC is not observed experimentally, and our calculations show that it does not occur even when the vibrational cross sections are suppressed (see Fig. 3.12b). Thus, its disappearance cannot be accounted for by the reduction in the energy gap between the threshold for rotational excitation of the

most populated state and the lowest vibrational threshold that result from the higher temperature. On the other hand, as shown by curve b in Fig. 3.12b, the suppression of superelastic cross sections restores the phenomenon at this temperature even when vibrational losses are included. This is in accordance with the criterion of Robson (1984) that predicts that the superelastic collisions have a negative effect on NDC.

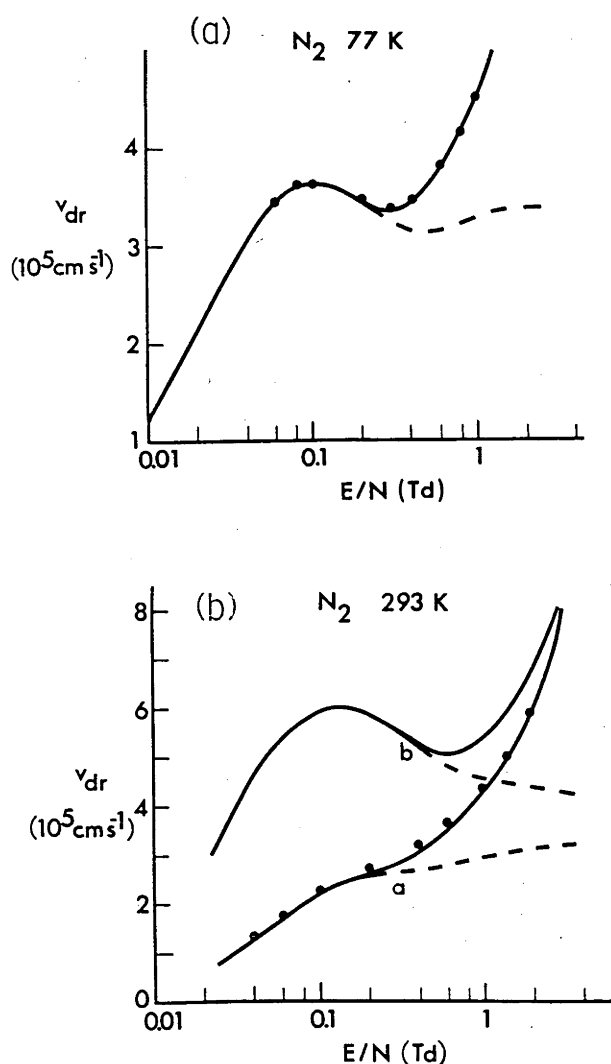


Figure 3.12 Drift velocities in N_2 at low values of E/N for (a) $T = 77$ K and (b) $T = 293$ K. The solid curves correspond to the inclusion of all the relevant processes, and dashed curves to the omission of vibrational excitation. The points are the experimental results of Lowke (1963). In (b) curves a and b correspond respectively to when superelastic processes are included and omitted.

The energy dependence of σ_m in the relevant energy range is clearly less favourable for NDC in CO than it is in N_2 . On the other hand, the

decrease in the rotational excitation cross sections at higher energies, which is characteristic of polar molecules (Takayanagi 1966), favours NDC so that our discussion of the phenomena for N_2 is expected to be valid for CO also.

3.8: Conclusions

From the general arguments developed in this section and the illustrations provided by the model calculations the following conclusions can be drawn:

- 1) NDC cannot take place in the absence of an inelastic process (see criteria of Robson and/or equations 3.5 and 3.7). As mentioned above physical explanation of this is the fact that the elastic drift velocity is the minimum of the drift velocity and $\langle v_m \rangle$ cannot increase faster than E in that case.
- 2) The more rapid the increase of σ_m with energy, the more likely is NDC to occur.
- 3) An inelastic cross section that rapidly decreases with increasing energy enhances NDC or may even produce it under favourable conditions: for example when σ_m does not increase with energy. It has been shown that it is possible to induce NDC with a constant or decreasing σ_m .
- 4) The relative magnitude of σ_m and σ_i plays a key role. It is not necessary to have such a low σ_m as is usually encountered at a Ramsauer-Townsend minimum. NDC can also occur when the inelastic cross section is small compared with the elastic cross section, that is under conditions when the degree of anisotropy is never very large and a

two-term theory is valid. On the other hand NDC may fail to occur even if there is an apparently appropriate combination of characteristics of σ_m and σ_i .

5) It is also worth noting that the presence of the superelastic collisions reduces a chance of NDC.

Finally it should be noted that all the results presented here can be explained using arguments developed by Kleban and Davis (1977) unless by their use of their term "streaming anisotropy" they are implying that NDC is associated with the breakdown of the two term approximation (in the case that they have analysed CH_4). This interpretation of their work may be encountered quite often and one should point out that the transport of electrons is governed by electric field and the cross sections of the gas (including of course effects of temperature). It is very difficult to accept that inadequacy of a numerical procedure that is used to analyse the transport of electrons could affect the transport itself and consequently that could affect the observable experimental results. So whatever the theory that is being used, NDC either exists or does not exist and one can calculate it more or less accurately. Even for methane the maximum deviation of the two term theory from the multiterm results is of the order of 10% for v_{dr} (Haddad 1985). The NDC region has a difference of the order of 20% between the peak and the lowest point. Therefore even if the two term theory made a 10% error at one E/N and none at the neighbouring E/N (which is very unlikely) it would still predict NDC (see Mathieson and El-Hakeem 1979).

In those terms it is believed that the causes of NDC as described in this work (preferred term would be "the conditions that lead to") are the basic ones. It is however possible that some secondary effect may

determine whether NDC will occur or not but only if the favourable conditions already exist. For instance having a model gas that has isotropic cross sections and a calculated $v_{dr}-E/N$ curve that shows a plateau. Then an inclusion of some anisotropy could induce NDC, but already conditions as mentioned above have been satisfied. For the case of methane where the two-term theory is inadequate it is evident that the cross sections satisfy very well the conditions as given above and therefore CH_4 is just an example of rather extreme conditions for electron transport but is certainly covered by present analysis.

Present results are also consistent with the argument developed by Long et al. (1976) (see also Lopantseva et al. 1979). However it should be noted that the presence of the second inelastic process is not necessary for NDC to occur, although in certain situations it could play an important role if the thresholds of the two processes are close to each other. Its role would be then to suppress the NDC produced by the first process rather than promote it.

Finally it should be stressed that in our opinion the essential part of the work presented in this chapter is to demonstrate that NDC may occur in a much wider set of circumstances than has previously been discussed and that its underlying causes may be simply conceptualized. Also it was rewarding to realise that independently of the present work some other authors have at the same time reached similar conclusions (though in a very different way and with somewhat different motivation).

CHAPTER 4: BASIC PRINCIPLES OF THE OPERATION OF THE CAVALLERI
DIFFUSION EXPERIMENT

4.1: Introduction

Direct measurement of electron diffusion coefficients was the last swarm technique to be developed, though one of the two methods that exist now proves to be perhaps one of the conceptually least complicated swarm techniques. The field was reviewed by Huxley and Crompton (1974) and Rhymes (1976) and here we shall give only a brief account.

The drift-dwell-drift technique was devised by Nelson and Davis (1969) on the basis of a technique for measuring drift velocities and longitudinal diffusion coefficients that had been developed at the Oak Ridge National Laboratory (Wagner et al. 1967). In this experiment a swarm of electrons is produced by a pulsed UV source in the presence of a drift field that drives the swarm to the centre of the chamber. Once it gets there the field is switched off and a period of field free diffusion commences (dwell-period). The centre of mass of the swarm does not move but its width increases. At the end of a suitable time interval the drift field is applied again and the swarm drifts to the anode where its arrival time distribution is sampled by a particle multiplier.

The spread of the swarm on arrival at the anode results from diffusion during two drift periods and that in the dwell period (in addition the width of the initial swarm must be accounted for). Analysis of the results of this technique is rather involved as various corrections are applied: those for the initial pulse width, the dead time of the detector, diffusion during the sampling and electronic fluctuations. In addition boundary

effects should be accounted for although this was not done by Nelson and Davis (1969).

The results obtained in Nelson and Davis' experiment were in a good agreement with available data for the nine gases that were analysed but the statistical scatter was between 5 and 10% (and in the case of neon as much as 30%).

Two major difficulties of this technique are the production of the swarm and the determination of its shape, and both were solved in the other approach to the direct measurement of the diffusion coefficients which is known as the Cavalleri's Diffusion Experiment (CDE). The first difficulty was avoided by the production of electrons in the gas directly, rather than at the cathode. The determination of the shape of the swarm was replaced by the sampling of the total number of electrons in the experimental cell and this was the most important achievement of this new technique. Therefore the need for the two "drift" periods was removed and only the "dwell" period remained.

Historically speaking the development of this technique was not as straightforward as suggested above. Initially it was proposed as an alternative method of particle detection (Cavalleri et al. 1962). Soon it was realised that this technique could produce values of the thermal diffusion and attachment rate coefficients (Cavalleri et al. 1964, 1965). Culmination of the work of Cavalleri (and his colleagues) was reached when they developed the apparatus which could accurately measure diffusion coefficients for both thermal and nonthermal electrons (see Fig 4.1). A constant RF field was applied to electrodes (in addition to the sampling pulses - see section 4.2) to increase the effective energy of the electron swarm. It was possible to relate the RF field intensity to the equivalent

DC values (Holstein 1946, Gilardini 1972 and Huxley and Crompton 1974).

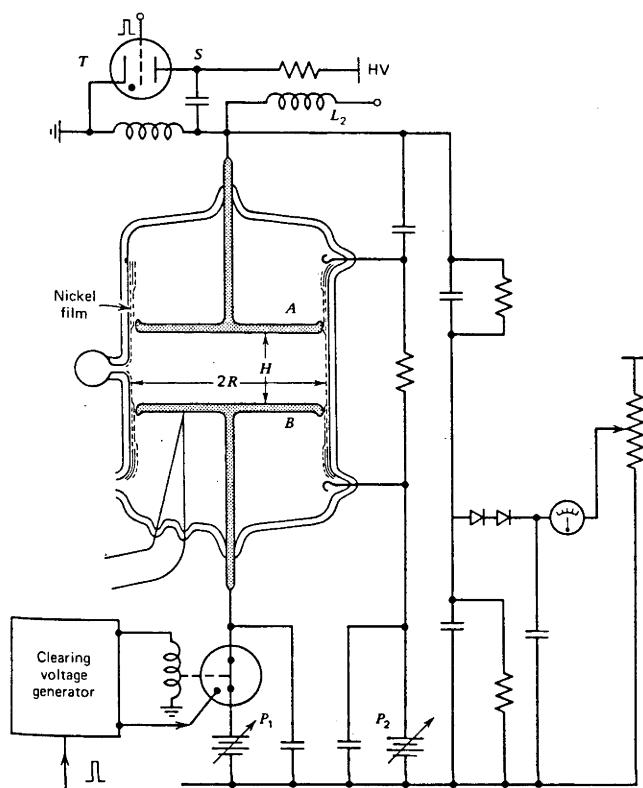


Figure 4.1 Experimental apparatus used by Cavalleri (1969) to measure the diffusion coefficients in pure helium for a wide range of electric fields.

In this version of the CDE the electrodes were inside the glass cell. The glass walls were coated with a thin film of nickel in order to produce a uniform contact potential of the surface, while the contact potential differences between the walls and the electrodes and between the electrodes were compensated by the application of DC potentials ($\approx 100\text{mV}$).

Researchers at IDU - ANU solved problems with contact potentials in a different way. In order to achieve field free conditions, a design was adopted that is quite similar to the initial design of Cavalleri. Electrodes were put outside the cell, and the glass walls of the cell were

not coated by the film of conductive material. Thus charges produced during the sampling pulse would fall on the walls and compensate the effect of the patches of nonuniform work function (Section 4.5).

Having achieved field free conditions in experiments of this type the technique was first applied to measure the diffusion coefficient of thermal electrons in various gases (He, Gibson et al. 1973; Ne, Rhymes et al. 1975; Ar, Rhymes and Crompton 1975; Hg and H₂, Hegerberg and Crompton 1980; CO₂, Hegerberg et al. 1980). It was also applied to determine the Penning ionization coefficient for Ar in Ne (Rhymes 1976) and to measure the attachment coefficient for thermal electrons in O₂, CFCl₃ and SF₆ (Hegerberg and Crompton 1983 and Crompton and Haddad 1983).

In this work the CDE was applied to measure both the diffusion and the attachment coefficients for electrons in various gases. This chapter contains first a detailed discussion of the principle of the operation of CDE. The basic theoretical foundation of the experiment is then given which includes the derivation of the relations necessary to relate the observable quantities to the transport coefficients. (A special situation with a high degree of attachment will be dealt with in the following chapter.) Some details of the experimental procedure are discussed next and following that the compensation of the "stray" fields in the cell. Appendix 1 contains some details of the computer-interface system that was built to control the experiment.

4.2: Principle of the Operation of the Cavalleri Diffusion Experiment

This section contains a description of the operation of the CDE as presently configured and used in this work.

The most important feature of Cavalleri's technique is a novel approach to the electron density sampling. It was designed especially to suit situations when the electron density is too small for standard microwave or other diagnostic techniques. These conditions are necessarily met when one attempts to study free rather than ambipolar electron diffusion.

The sampling consists of the application of a high frequency (RF) voltage to electrodes that are either inside or outside the experimental cell. All the electrons inside the cell are able to follow the rapidly oscillating electric field (20-30MHz), but not the ions. The amplitude of the field is large enough so that electrons gain energies sufficient to excite and ionize the molecules but the RF field is sufficiently highly damped that this period of excitation lasts only for a very short time (over a few oscillation of the field, $\leq 1\mu\text{s}$). The rapid oscillations also ensure that electrons are localized and therefore that each one produces a minute avalanche. The size of the avalanches and the light intensity produced by them are very small and cannot be observed by an adapted human eye. However a high gain photomultiplier can detect the light output even from a single avalanche. The integrated intensity of the light leaving the cell $I(t)$ is proportional to the electron number $N(t)$ at the time at which the RF field is applied.

The basic scheme of the CDE is shown in Fig. 4.2. A glass cell of extremely well defined geometry is filled with the gas to a known pressure p . A pulse of X-rays ionizes the gas and produces a certain number of electrons (and positive ions) $N_e(0)$. The duration of the X-ray pulse (X) can be varied, and therefore also $N_e(0)$. These electrons are in fact secondary electrons produced by very high energy primary electrons. The secondary electrons have initial energies of the order of 20 eV.

The pressure of the gas is chosen to be high enough to provide both efficient initial ionization and fast thermalization (see Gibson et al. 1973; Rhymes et al. 1975; see Appendix 2). Once the electrons have thermalized the only possible processes that can alter their population are:

- 1) Free diffusion to the walls
- 2) Attachment
- 3) Creation of new electrons by Penning ionization (in gas mixtures).

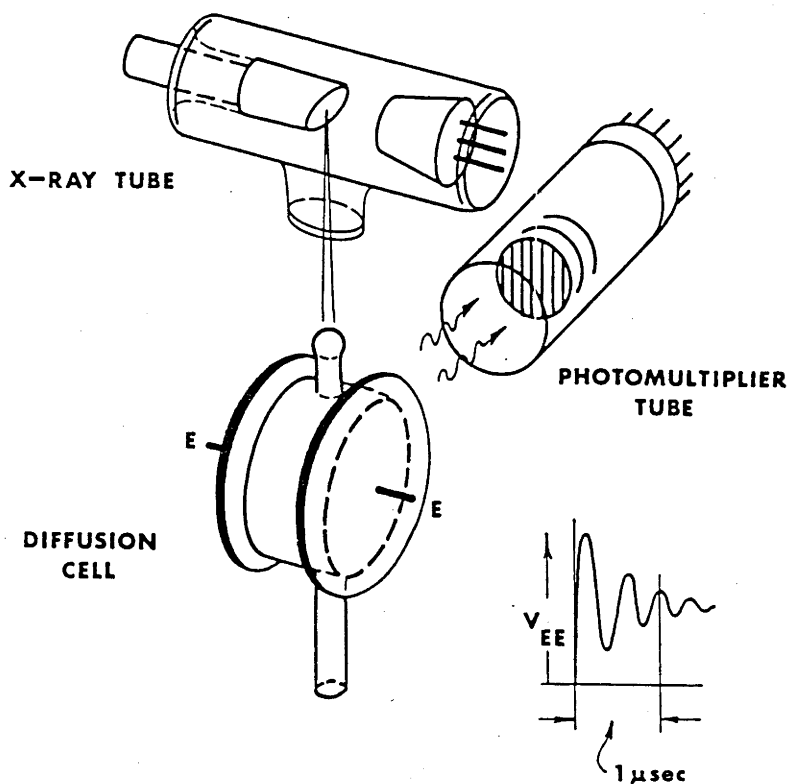


Figure 4.2 A schematic diagram of the CDE.

The kinetics of heavy particles can play a role only in the third process, while all the other types of collisions that could lead to electron production or loss, such as recombination, can be neglected because

the conditions are chosen in such a way that populations of excited states, densities of ions etc. are extremely small. For the same reason (that is the electron density $n(t)$ is very small, i.e. $n(0) \leq 10^2$) collective effects (i.e. in our case ambipolar diffusion) can also be neglected. Therefore we start our experiment with a swarm of electrons (ions are irrelevant for our discussion) whose population decays only through process 1 and possibly 2 and/or 3.

After a time S ("the starting time") following the X-ray pulse, a sampling RF pulse is applied to the electrodes (E) that are outside the glass cell. The signal which is proportional to the intensity of the corresponding radiation from the cell is stored in one memory location and it is proportional to the number of electrons in the cell at the time S . The next X-ray pulse is followed by the sampling RF pulse after the time $S+D$ has expired (D being a delay time). The measured intensity of radiation is proportional to the electron density at this time and is stored in another memory location of the microcomputer that controls the experiment. The ratio of the two values stored can be used to determine the time constant for the decay of the electron population.

The times X and S are of the order of microseconds ($X=1-20\mu\text{s}$, $S=1-1000\mu\text{s}$). However, following the sampling pulse one has to wait for at least $0.5-2\text{s}$ (the "repetition time" R) before the next pulse is applied. This is to give sufficient time for all the charged particles to diffuse to the walls and recombine.

In between the measurements of the electron number at times S and $S+D$, sampling pulses without the initial X-ray ionization are applied. The signals at times S and $S+D$ are also stored and later subtracted from the corresponding signal resulting from the electron avalanche to account for

background noise (eg pickup associated with the sampling pulse itself).

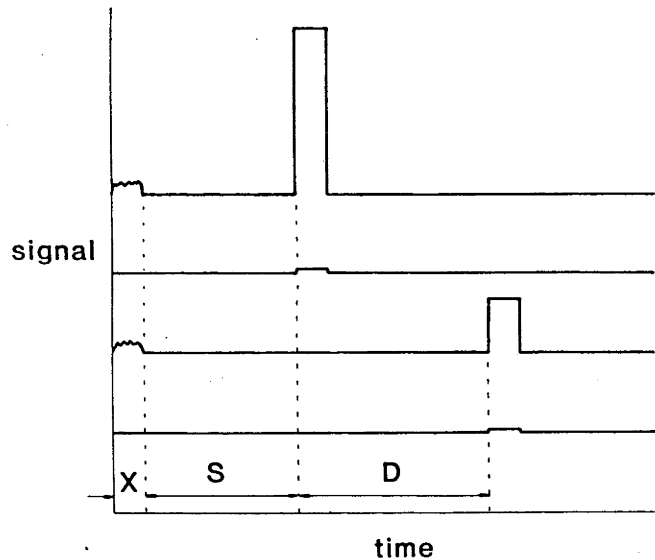


Figure 4.3 Waveforms corresponding to one shot. The small pulse coincident with the X-ray pulse comes from fluorescence of the glass. The signal coming from the cell during the sampling is shaped by a "sample and hold" circuit in order to enable the AD conversion, and therefore its level corresponds to the maximum of the light output.

The waveforms as observed by the cathode-ray-oscilloscope are shown in Fig. 4.3. At this point it is convenient to define the following nomenclature:

- a) a pulse - a single waveform that includes the signal resulting from one X-ray pulse and a sampling pulse either at time S or $S + D$;
- b) a noise pulse - a pulse in the absence of the X-ray pulse;
- c) a shot - a set of two pulses and two noise pulses with sampling at both S and $S + D$ which can therefore be used to determine a single value of the time constant;

- d) an experiment - a series of shots, normally 1000 - 4000;
- e) a series - a series of 1-20 experiments all performed with identical conditions (S, D, R, X, ...);
- f) an experimental run - a group of 1 - 5 series, each with different operating conditions.

After every shot the corresponding noise is subtracted from the signal and the remaining signal is summed in the appropriate memory location. After every experiment the time constant is calculated. After every series the average value of the time constant is calculated from the values for experiments for that series, and the mean standard deviation is also determined.

The number of electrons produced by a given X-ray pulse is subject to fluctuations. Therefore it is necessary to repeat the shots many times in order to average out the fluctuations. It is hoped that a reasonably good averaging can be achieved over the period of one experiment, and then comparison of results for various experiments can provide a measure of the statistical quality of the results.

When one has metal electrodes inside the cell it is possible to apply a sweeping field. The repetition rate of such an experiment is therefore much faster than for the "all glass" cell. In the "all glass" cell the optimum repetition rate can be easily determined as a rate close to the point where the results become independent of R.

Assuming a single exponential decay $N_e(t) = N_e(0)\exp(-t/\tau)$ of the number of electrons in the cell, the ratio of light intensities and consequently number of electrons can be expressed in the following form relating it to the time constant of the decay of the total number of electrons:

$$\tau = \frac{D}{\ln \left| \frac{I(S)}{I(S+D)} \right|} = \frac{D}{\ln \left| \frac{N_e(S)}{N_e(S+D)} \right|} \quad (4.1)$$

Normally the results are presented as time constants rather than ratios of intensities. The quality of the results depends on the choice of the times X and R and especially on S and D. It is optimal to choose D in such a way that the ratio of the measured photomultiplier signals (i.e. electron densities) is 3:1. Then D is approximately equal to the electron density decay time constant τ . Choosing D to be much less than τ would lead to a situation where both signals (at S and at S+D) are of almost identical amplitude, and therefore it is much more difficult to determine τ accurately. From equation (4.1) it can be shown that if the signals can be measured with equal accuracy regardless of amplitude, then $\Delta\tau/\tau \rightarrow 0$ as $D \rightarrow \infty$. On the other hand if D were to be chosen much greater than τ , the second pulse would be very small as compared to the first one, and its amplitude would be less accurately known than that of the first one. The results can be improved in both cases by choosing a much larger number of shots per experiment (C), but there is a practical limit at which the duration of the experiment becomes unacceptably long.

The value of S is limited at the lower end by the time necessary for electrons to thermalize (see Appendix 2) and for higher order diffusion modes to decay (see the next section), while at the higher end the limiting factor is an insufficient number of electrons left in the cell.

To summarize, we apply sampling pulses to the cell at times S or S+D following the X-ray pulse that produces the initial ionization. The intensity of radiation from the cell following the sampling pulse is proportional to the number of electrons in the cell and thus we obtain a measure of the loss of electrons during the time D that can be related to

the time constant of a single exponential. A sequence of measurements of the light intensity at times S and D and also of the level of the noise at the same times is repeated until a satisfactory statistical quality of the results is achieved.

Advantages of the CDE over some experiments that compete with it are the following:

1) Very low electron densities ($n \leq 10^2$), and thus it is possible to measure free diffusion.

2) The simplicity of the cell itself. There are no moving parts, no gas flow and no differential pumping. Electrodes are outside the cell, and their configuration is very simple.

3) The pressures of the order 0.5-10kPa that are normally used can be measured to an accuracy better than 0.1%.

4) Very simple analysis and interpretation of the results as compared to other methods in terms of both the transport coefficients and cross sections since the electron energy distribution function is a known Maxwellian.

5) The relatively simple diagnostics that can be used to discover anomalous experimental results and to assist in their interpretation.

Disadvantages are the following:

1) The relatively limited number of swarm parameters that can be investigated.

2) In some measurements (i.e. Penning ionization) the duration of experiments becomes unacceptably long. Therefore the "productivity" as compared to the FALP technique is very low.

3) It is difficult to vary the energy of the electron swarm. The gas temperature range that can be covered is limited and it has proved

difficult to apply the heating RF field. Therefore very limited information about the energy dependence of the momentum transfer cross section can be obtained, although in conjunction with other data the results provide a valuable source of absolute cross section data (see Chutjian 1981).

4.3: Processes Governing the Electron Density Decay

As already mentioned the population of electrons in the cell will decay through diffusion to the walls and subsequent neutralization, attachment, and decay of metastable levels coupled with Penning ionization. In Chapter 2 we have seen that the appropriate equation governing the behaviour of the electron swarm in much more general conditions is:

$$-\frac{\partial n}{\partial t} + (v_i - v_{att})n + D_T \left(\frac{\partial^2 n}{\partial x^2} + \frac{\partial^2 n}{\partial y^2} \right) + D_L \frac{\partial^2 n}{\partial z^2} - v_{dr} \frac{\partial n}{\partial z} = -S(x,y,z,t) \quad (4.2)$$

The notation is standard with the addition of the source $S(x,y,z,t)$ that can represent Penning ionization. First we shall outline the solution of equation (4.2) and then analyse a simplified form relevant to the CDE with the source term representing Penning ionization.

a) The time constant of the decay of electron number including the effects of diffusion and of an electric field.

Substituting $S=0$ and

$$n = U(x',y',z) e^{\{(v_i - v_{att}) - \beta^2 D_L\}t + \lambda_L z} \quad (4.3)$$

into equation (4.2) (see Huxley and Crompton 1974; Rhymes 1976) with

$$x' = \left(\frac{D_L}{D}\right)^{1/2} x, \quad y' = \left(\frac{D_L}{D}\right)^{1/2} y, \quad \lambda_L = \frac{v_{dr}}{2D_L} \quad (4.4)$$

(β remains to be determined) we obtain the equation for U:

$$\left(\frac{\partial^2}{\partial x'^2} + \frac{\partial^2}{\partial y'^2} + \frac{\partial^2}{\partial z^2}\right)U = -k^2U \quad (4.5)$$

where $k^2 = \beta^2 - \lambda_L^2$.

For the cylindrical geometry of the CDE cell it is appropriate to choose the cylindrical coordinate system and to separate $U(x',y',z)$ into $Z(z)R(\rho')$ with $\rho' = (D_L/D_T)^{1/2}(x^2+y^2)^{1/2}$. This step also assumes axial symmetry in order to be able to neglect the derivatives with the respect to the angle θ in the cylindrical coordinate system. Therefore we obtain the following system of equations to solve:

$$\frac{d^2Z}{dz^2} = -\gamma^2Z \quad (4.6)$$

and

$$\frac{d^2R}{d\rho'^2} + \frac{1}{\rho'} \frac{dR}{d\rho'} + (k^2 - \gamma^2)R = 0 \quad (4.7)$$

where γ^2 is the constant of separation. Boundary conditions are

$$Z(0) = Z(d) = 0 \quad \text{and} \quad R(a') = 0, \quad (4.8)$$

and finally we have the following solutions:

$$Z = \sum_{m=1}^{\infty} B_m \sin \gamma z = \sum_{m=1}^{\infty} B_m \sin\left(\frac{m\pi}{h}z\right) \quad (4.9)$$

and

$$R = \sum_{\ell=1}^{\infty} C_n J_0\left(\frac{c_{\ell} \rho'}{a'}\right) \quad (4.10)$$

where

$$k^2 = \left(\frac{m\pi}{h}\right)^2 + \left(\frac{c_{\ell}}{a'}\right)^2 \quad (4.11)$$

and c_{ℓ} is the ℓ^{th} zero of the zeroth order Bessel function J_0 . We can therefore construct the solution of equation (4.2):

$$n(\rho', z, t) = e^{\{\lambda_L z + (v_i - v_{att})t\}} \sum_{m=1}^{\infty} \sum_{\ell=1}^{\infty} A_{m\ell} J_0\left(\frac{c_{\ell} \rho'}{a'}\right) \sin\left(\frac{m\pi z}{h}\right) \exp\{-D_L [(\frac{m\pi}{h})^2 + \lambda_L^2 + (\frac{c_{\ell}}{a'})^2] t\}, \quad (4.12)$$

where $A_{m\ell} = B_m C_{\ell}$.

In the CDE we measure the total number of electrons in the cell and not the local density. It is therefore desirable to obtain the formula for the total number of electrons as a function of time, $N_e(t)$:

$$N_e(t) = e^{(v_i - v_{att})t} \sum_{m=1}^{\infty} \sum_{\ell=1}^{\infty} A_{m\ell} \exp\{-D_L [(\frac{m\pi}{h})^2 + \lambda_L^2 + (\frac{c_{\ell}}{a'})^2] t\} \quad (4.13)$$

where

$$A_{m\ell} = A_{m\ell}' \int_0^a e^{\lambda_L z} J_0\left(\frac{c_{\ell} \rho'}{a'}\right) \sin\left(\frac{m\pi z}{h}\right) 2\pi \rho \, d\rho \, dz \quad (4.14)$$

b) Field free diffusion.

Initially the CDE with the all-glass cell was aimed at achieving field

free conditions and therefore this is the basic situation. Thus $\lambda_L=0$, $a'=a$, and $D_L=D_T=D^{th}$ in addition to $v_i=v_{att}=0$. Therefore we have the following form of the time dependence of the total number of electrons:

$$N_e(t) = \sum_{m=1}^{\infty} \sum_{l=1}^{\infty} A_{ml} e^{-D^{th} \left[\left(\frac{m\pi}{h} \right)^2 + \left(\frac{c_l}{a} \right)^2 \right] t} \quad (4.15)$$

The amplitudes of various modes (m, l) may be determined by expanding the initial electron distribution in the series given by (4.12) and calculating the constants A_{ml} . However, without getting into that much detail we may note that the narrow pencil of X-rays, as transmitted by the sphere with thin walls at the top of the cell, favours the lowest order mode in the z coordinate. We should also add that for m , only odd modes are present because of the integration in (4.14) (with $\lambda_L=0$).

The time constant of the lowest mode is:

$$\tau_{D11} = \{ D^{th} \left[\left(\frac{\pi}{h} \right)^2 + \left(\frac{2.405}{a} \right)^2 \right] \}^{-1} \cong \left\{ \frac{D^{th}}{\Lambda^2} \right\}^{-1} \quad (4.16)$$

The quantity Λ^2 is usually called the effective cell constant. The time constant of the next higher mode τ_{D31} is 7 times shorter than τ_{D11} for the geometry of our experiment (for infinite parallel plates it would be 9 times shorter). Thus at $t=\tau_{D11}$, $\exp(-t/\tau_{D31}) \cong 0.002 \exp(-t/\tau_{D11})$. Thus to be just able to notice the influence of the second mode at time $t=\tau_{D11}$ its amplitude would need to be at least five times the amplitude of the first mode. Higher order modes decay even faster, and therefore at time $t=\tau_{D11}$ practically only the first mode exists. This means that it is possible to represent the decay of electrons by a single exponential function:

$$N_e(t) = N_e(0) e^{-\frac{t}{\tau_{D11}}} = N_e(0) e^{-\frac{D^{th}}{\Lambda^2} t} \quad (4.17)$$

Here $N_e(0)$ is, strictly speaking, not the electron number at $t=0$ but A_{11} . We shall, however, use $N_e(0)$ instead of A_{11} in situations where we can neglect all the modes except the fundamental one.

It may be noticed that the boundary conditions $N_e(0)=N_e(h)=0$ (see 4.8) are usually modified (see Cavalleri 1969) so that h in (4.16) is corrected by the extrapolation distance 0.71λ (λ is the electron mean free path). Under the conditions of our experiment this term is negligible in comparison with h and boundary conditions (4.8) are quite adequate.

c) Field free diffusion and attachment

The expansion form given by (4.3) conveniently separates the effects of attachment and diffusion. This is a consequence of the proportionality to the electron density of the losses due to attachment. Consequently attachment does not influence the spatial distribution but simply reduces the number of electrons in proportion to the local density. The electron density decay is given by the following expression:

$$N_e(t) = N_e(0) e^{-\frac{t}{\tau}} = N_e(0) e^{-\left|\frac{D^{th}}{\Lambda^2} + v_{att}\right|t} \quad (4.18)$$

The time constant τ is

$$\tau = \left[\frac{D^{th}}{\Lambda^2} + v_{att}\right]^{-1} = \left[\frac{(ND)}{N\Lambda^2} + k_{att}N'\right]^{-1} = \left[\frac{1}{\tau_D} + \frac{1}{\tau_{att}}\right]^{-1} \quad (4.19)$$

where k_{att} is the attachment rate coefficient (assumed here to be

two-body), $N'=N$ for the pure gas, and $N'=fN$ for a gas mixture with the abundance f of the attaching gas. The different pressure dependence of the two terms in (4.19) enables us to determine both coefficients.

Equations (4.18) and (4.19) were derived with the assumption that only the fundamental diffusion mode is present in the cell. Sometimes attachment losses are so high that measurements have to be performed at very short times, before the higher order modes have decayed. This situation is very important and will be discussed in Chapter 6.

d) Field free diffusion and Penning ionization

Let us assume now that there is no attachment, but a source of electrons that is time dependent:

$$S(t) = S(0)e^{-\frac{t}{\tau_m}} \quad (4.20)$$

We shall write here only the equation for the total number of electrons, representing the term for the diffusion losses by D^{th}/Λ^2 . Then

$$\frac{dN_e(t)}{dt} = -\frac{D^{th}N_e(t)}{\Lambda^2} + S(0)e^{-\frac{t}{\tau_m}} \quad (4.21)$$

The solution of the homogeneous equation is given by (4.17) and the total solution by

$$N(t) = N(0)e^{-\frac{t}{\tau_D}} + \frac{S(0)}{\left[\frac{1}{\tau_D} - \frac{1}{\tau_m}\right]} e^{-\frac{t}{\tau_m}} \quad (4.22)$$

Here, τ_D will be used to denote the time constant for the diffusion losses

that can be obtained by approximating the electron decay with a single exponential (in the absence of all the other processes). For $t \geq \tau_{11}$ $\tau_D = \tau_{11}$ and such conditions will be assumed in this section.

If the source of electrons is Penning ionization then

$$S(0) = M(0) k_{\text{penn}} f N \quad (4.23)$$

where $M(0)$ is the number of metastable atoms (molecules) at $t=0$, k_{penn} is the ionization coefficient and f is the abundance of the ionizable impurity. Typically (for the conditions of our experiment) $\tau_m \gg \tau_D$, $N(0) = 0.3M(0)$, $k_{\text{penn}} = 10^{-11} \text{ cm}^3 \text{ s}^{-1}$ and $f = 1\text{-}10 \text{ ppm}$. In this case the constant multiplying the second exponential in (4.22) is much smaller than 1% of the one multiplying the first term. However the first term decays faster than the second one and Penning ionization becomes increasingly important at later times. Of course it is possible to adjust conditions to increase or reduce the effect of either of the terms.

4.4: Description of the Experiment and the Experimental Procedure

We have already presented the basic arrangement of the CDE in Fig. 4.2. In this work two experimental sets were used, one for room temperature only (RT) and one (HT) that can be operated at higher temperatures (up to 530 K). The glass cells were made of Pyrex glass following a special procedure (Gibson et al. 1973) that enabled the geometry of the cells to be determined very accurately. Internal radii are $a = 3.705 \text{ cm}$ (RT) and 3.764 cm (HT) and the internal heights $h = 2.984 \text{ cm}$ (RT) and 2.980 cm (HT). Thus the characteristic dimensions of the cells are $\Lambda^{-2} = 1.530 \text{ cm}^{-2}$ (RT)

and 1.520 cm^{-2} (HT). These dimensions were determined with an uncertainty of less than 0.3%, which includes all the possible inaccuracies in parallelness of the two flat surfaces and deviations from a perfect cylinder of the third surface.

The radiation from the X-ray tube passes first through a beryllium window in the envelope of the tube itself and then through a small glass sphere that is located at the top of the cell. The walls of this sphere are made to be very thin in order to minimize absorption. Finally the X-rays are absorbed by the gas inside the cell. The X-ray tube is positioned above the glass cell and it is important to achieve very good alignment to maximize electron production. The anode voltage of the X-ray tube was normally 20-25kV and the duration of the pulse from 1-19 μ s. Other operating conditions were adjusted to maximize the output but without producing X-rays when the tube is not being triggered.

The RF sampling pulses are produced by a circuit shown in Fig. 4.4. The ringing frequency of the LC circuit that was used is 27 MHz. The capacitor of the LC circuit is the cell itself. The hydrogen thyratron is pulsed by a DC pulse applied to its grid which causes it to conduct. A high voltage (0-15kV) is thereby suddenly connected to the LC circuit causing it to oscillate. The oscillations are damped and the effective duration of the sampling pulse is limited to 1 μ s. The frequency of the sampling pulses is chosen to be sufficiently high that electrons are localized and not swept to the walls. The amplitude is chosen so that the optimum light output is achieved.

The light intensity is measured by a photomultiplier tube PMT with a diameter of 50mm (S20 trialkali photocathode) that is sensitive to the visible and near ultraviolet radiation. The tube is operated in the

proportional regime. Its output first passes through a preamplifier in order to adjust the impedance of the PMT to that of the coaxial line. The signal is then fed to the main amplifier that has a variable gain between 1 and 1000 (normally between 50 and 200), then to the "sample and hold" circuit that holds the peak value of the signal for a time long enough to enable the digitization of the signal by the AD converter. The converter produces a 12 bit binary number that is stored by a computer that is controlling the experiment.

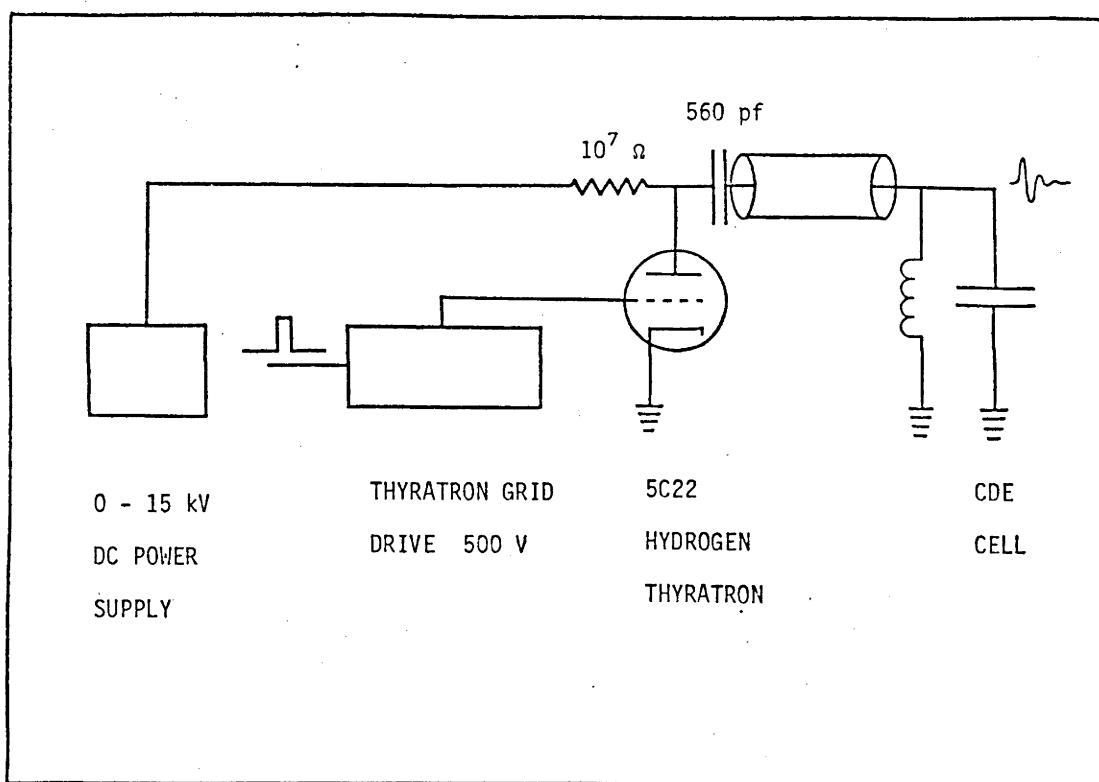


Figure 4.4 The circuit of the CDE.

Most of the measurements were performed using the PDP 8e computer and the interface system that was developed some time ago (see Rhymes 1976). The basic disadvantage of that system is its limited memory. A new computer-interface system was therefore designed that would provide more flexibility in writing programmes and a wider range of possible working

conditions which were previously limited by the interface (see Appendix 1). Since the number of the electrons produced initially is relatively small (10^4) measurements of light intensities must be repeated many times at times S and S+D (and also measurements of the noise) in order to achieve results of good statistical quality. The computer is programmed in such a way that it sums the light intensities at times S and S+D into two memory locations and does all the calculations following every shot or experiment or series. The interface system produces the appropriate pulses to trigger the X-ray tube and the thyratron at the appropriate times and it also controls the amplitude of the sampling voltage.

The linearity of the response of the detection chain is checked frequently. A pulse generator is connected to the system and the amplitude is changed over a wide range (1-10). The linearity of the response of the system is normally better than 0.3%.

The CDE cell is connected to a vacuum system that satisfies UHV standards. The system was occasionally baked at 200°C for 24-48 hours. After baking, a pressure of $2 \cdot 10^{-9}$ Torr was usually achieved. Normally the system was pumped down to $0.5-2 \cdot 10^{-7}$ Torr before introducing a new sample of gas.

The gases used were always of the highest available purity (Matheson Research Grade or equivalent). Hydrogen was purified from technical grade gas by osmosis through a heated silver-paladium tube.

Gas pressures were measured to within $\pm 0.1\%$. This was achieved by using a calibrated Texas Instrument quartz spiral manometer. The same instrument was used to determine the ratios of the two volumes in the specially made stainless steel mixing vessels that were used to produce the gas mixtures. One mixing chamber (see Crompton and Haddad 1983) has a

volume ratio of 1:938 and was used to produce mixtures with abundances of the order of 1-1000ppm with an uncertainty better than 0.75% either by a single or a two step process. The second mixing chamber has a volume ratio of 1:16.85 and was used to make mixtures of the order of 0.1-5%, with an accuracy better than 0.2% (Haddad 1983).

The temperature measurements were performed using three chromel-alumel thermocouples. One junction of each thermocouple was in a room temperature bath, the others attached to the cell and to the top and bottom of the oven (for HT-CDE). When the gas was admitted the temperature was measured to within ± 0.1 K in order to enable an accurate value of the gas number density N to be calculated. For the high temperature experiments a temperature control unit was used that is in principle capable of controlling the temperature to ± 0.1 K. Measurements were commenced only after 2-3 days of heating when the system was fully stabilized. The temperature was then measured at the top and bottom of the oven and the cell itself; normally the differences did not exceed 0.5 K. Temperature variations over 24 hours (which was the normal duration of a single measurement) was ± 0.2 K, probably due to changes in room temperature and the relatively small heat capacity of the oven, but this stability was considered to be satisfactory.

Other points specific to particular gases will be discussed in the appropriate chapters. The general experimental procedure, including the diagnostic measurements that are normally performed, will now be described.

1) Preliminary measurements are made to determine the optimum conditions (p, f, S, D, X, R, \dots) for the experiment, after which the diagnostic measurements described in 2, 3, and 4 below are performed.

2) To check whether the initial density of electrons and ions is too

high to inhibit free diffusion the duration of the X-ray pulse is varied. To check whether full thermalization is achieved and whether the decay of the total number of electrons is accurately described by a single exponential, S is varied. Variation of the repetition rate provides information about the possible build-up of charged particles from pulse to pulse.

3) A dependence of the results on pressure reveals the presence of the possible attaching impurities, lack of thermalization, "diffusion cooling",....

4) For mixtures a dependence of the results on the abundance is also an important diagnostic indicating adsorption or desorption of the attaching component, breakdown of Blanc's law (see Chapter 5), attachment cooling...etc. .

5) Final measurements are performed under optimal conditions. The number of pulses per experiment is changed until a satisfactory value is achieved for the mean standard deviation. The measurements are performed at different pressures (and abundances for the gas mixtures) and the results compared.

4.5: Mechanism of Field Compensation in an All-Glass Cell

In his 1969 paper Cavalleri presented a full account of the apparatus he used to measure diffusion coefficients in He. As mentioned in 4.1 the electrodes of this apparatus were within the glass envelope. The cylindrical wall between the electrodes was coated by a thin film of nickel. In this configuration special precautions were needed in order to eliminate the influence of inhomogeneous contact potentials and the stray

fields that are their consequence. Use of the all-glass cell and exterior electrodes (Gibson et al. 1973; Rhymes et al. 1975) enabled a more accurate determination of the geometry to be made and simplified the construction of the cell and its circuitry. However, above all, it enabled truly free diffusion to be studied through the compensation of stray fields. This compensation is achieved by differential accumulation of charge on areas initially having different surface potentials. The high resistivity of the glass enables these charges to remain on the surface for a long period. The disadvantages of this configuration are first that one has to wait for all the electrons and ions to diffuse to the walls rather than sweeping them with a DC field, which makes the experiment much slower, and second the difficulty in applying RF heating fields for non-thermal measurements.

The process of the stray field compensation was noticed to be different in various gases. To be specific, the compensation in the nitrogen was found to be much less efficient than in most of the other gases (e.g. hydrogen). For example, in nitrogen it was not possible to perform the measurements for some time after the cell was subjected to mechanical strain, presumably due to piezoelectric effects. Reliable measurements could be made only after the cell had not been disturbed for many days, whereas it was possible to use hydrogen without any delay. Furthermore, it was observed that when measurements in nitrogen were begun after a period when the experiment was not running, the first shots showed lack of compensation, and the first few values of the measured time constant were low by 1-2% as compared to the value averaged over a series of twenty experiments. In contrast, if a series was commenced immediately after the completion of the previous one, this reduction of the time constant was not observed.

The intention of this section is to analyse the processes that lead to field compensation in all-glass cells and to point out that important differences exist between the mechanism in hydrogen and nitrogen.

The inverse of the time constant for the electron density decay in the CDE in the presence of an external field E differs from the one for the field free situation by $v_{dr}^2/4D_L$ (see equation 4.12). The stray fields are very weak but nevertheless the $v_{dr}^2/4D_L$ term can be relatively large. With metal electrodes small local fields of the order of 10-100mV are always present superimposed on the overall contact potential difference. While it is possible (Cavalleri 1969) to compensate the overall contact potential differences, it is very difficult to reduce the effect of the local inhomogeneities (see Chapter 8).

In order to compare the process of compensation in nitrogen and hydrogen measurements were made with the addition of a DC potential to one of the electrodes. First, the entire electrode was put to 1.36 V DC corresponding to $E/N=8.6 \cdot 10^{-2}Td$ at 2kPa. If there were no compensation this would mean that the time constant in N_2 would be reduced from 33.5 μs to 0.7 μs and in H_2 from 80.8 μs to 1.4 μs .

In hydrogen the compensation was found to be extremely fast so that it was necessary to reduce the amplitude of the sampling pulses and the number of electron density samplings per experiment to be able to observe the time dependence of the time constant as presented in Fig. 4.5. However, the statistics with such a low number of pulses is not very good. Both sets of measurements show that the first experiment, and even the second, give time constants below the average value. On the same figure the results of 1500 shots per experiment are shown where one cannot observe the variation of the time constant with time (as measured by the number of shots). The same

is true if the amplitude of the sampling pulse is increased even for 120 shots per experiment. This indicates that the degree of the compensation depends on the number of electrons and ions generated per pulse.

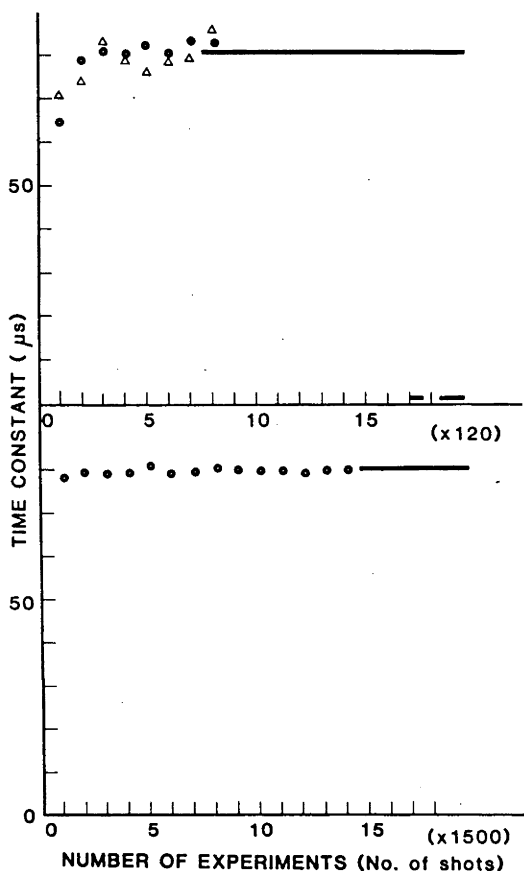


Figure 4.5 The variation of the measured time constant with the number of shots in hydrogen. The fully compensated value is drawn as a solid line —; the fully uncompensated as a dashed line - - -; and two successive experimental runs as circles and triangles (● ; Δ).

For nitrogen it was possible to use higher sampling pulse amplitudes and still observe the process of compensation (i.e. the time dependence of the results). Fig. 4.6 shows the time dependence of the time constant as observed in two different measurements with high sampling pulse amplitude. On the same figure is shown the long time behaviour of the results with experiments consisting of 1500 pulses. Full compensation is evidently not achieved even after 30000 pulses. With a lower amplitude of the sampling

pulses (PMT signal amplification increased by a factor of 5) it was possible to observe the time dependence of the results with 1500 pulses per experiment (Fig. 4.6) even more clearly. The saturated value is lower than with the sampling pulses of higher amplitude.

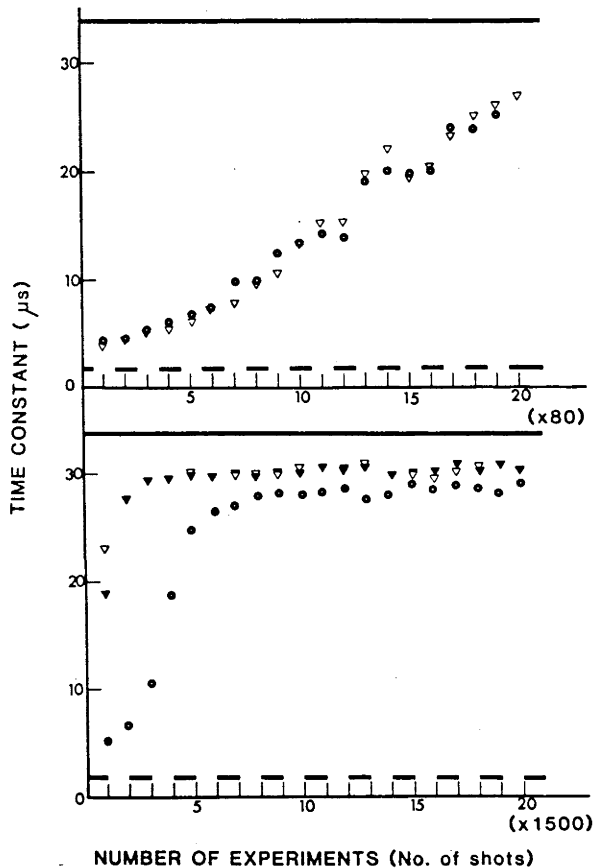


Figure 4.6 The variation of the measured time constant with number of shots in nitrogen. Fully compensated and fully uncompensated levels are shown using solid and dashed lines respectively. (a) Small number of shots per experiment, two successive experimental runs are shown as (●) and (▽). The sampling amplitude is V_1 . (b) Large number of shots per experiment, two successive experimental runs (▽) and (●). Sampling amplitude V_1 . Results obtained using a smaller sampling amplitude $V_2 < V_1$ are shown as (●).

On the basis of the above experiment one can conclude that the approach to the field free situation in the two gases is quite different. In H_2 it is fairly rapid and full compensation is achieved even with a relatively

low degree of ionization. In N_2 it is sufficiently slow that it is never possible to fully compensate the field generated by the applied voltage of 1.36 V.

It has been suggested that a difference in surface mobility of the charges could be one reason for the differences in compensation observed in H_2 and N_2 and an attempt was made to check this suggestion. In order to do so one of the sampling pulse electrodes was replaced by one having a small circular segment of 15mm diameter that was connected to a DC potential while the rest of the electrode was at ground potential. The procedure was to fully compensate the surfaces inside the cell (without the DC voltage) and then to switch the voltage on. The experiment would start after a certain delay from that time. If surface mobility plays any role in the compensation mechanism, the available charge would redistribute and partially compensate the voltage on the small circular patch during that delay time.

This is exactly what has been observed. Fig. 4.7 shows the time constants determined from individual experiments in N_2 . The experiments consisted of 40 pulses each and were performed after a certain time delay from the moment when the voltage was turned on. It can be seen that something of the order of a few hours is required to partially compensate the voltage, but that the losses eventually reduce the charge on the surface (and consequently the time constant) so that full compensation is never achieved.

For H_2 it was very difficult to perform the measurements. The reason is that full compensation was achieved after only one or two pulses even at the lowest possible sampling amplitude. It was therefore necessary to use the amplitude of the first pulse to estimate the degree of compensation.

When the compensation is small τ is reduced and the amplitude is significantly reduced. It was noticed that after only 15 minutes at least 90% of the compensation was achieved. This was still true after 1.5 hours, but after 15 hours the compensation was less, presumably due to charge leakage. This conclusion was also supported by a few measurements of the time constant with an extremely small number of shots of the smallest possible sampling amplitudes, but the "statistics" of these results was so bad that the observation of the first pulse amplitude was considered to be more reliable. From these observations it is possible to conclude that the surface mobility is much larger in H_2 than in N_2 which might explain the different compensation in the two gases.

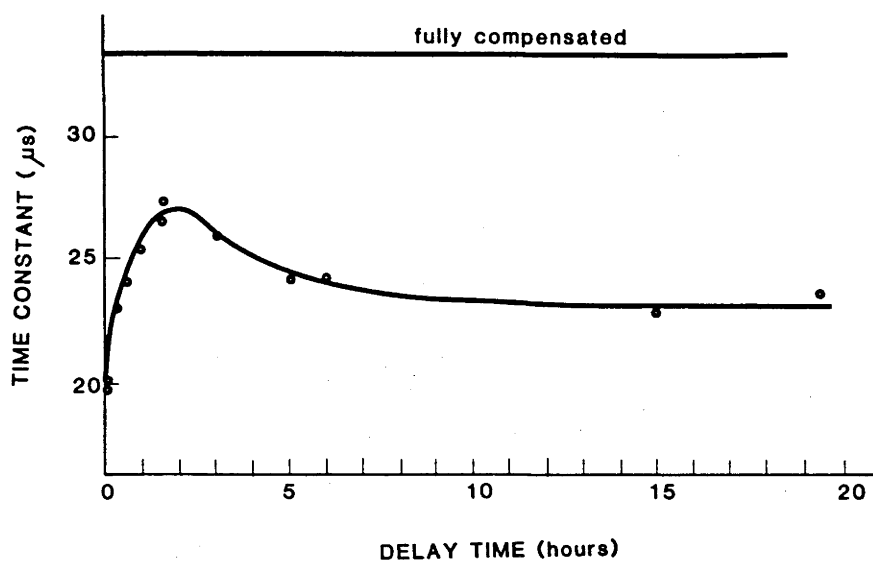


Figure 4.8 The dependence of the measured time constant in nitrogen on the delay time between the application of 1.36 V to the central disc of the pulsing electrode and the measurement of the time constant. The cell was quiescent during the delay time.

Finally it is possible to give a speculative picture of the process of the stray field compensation in the CDE. It is possible that the charged particles while approaching the surface are very little affected by the weak stray fields. When they reach the layers of gas adsorbed on the surface they become quasi-bound. If the mobility is small, the charges have a greater chance to recombine or leak through the glass before they reach the place of origin of the stray field. When the mobility is higher the time it takes to reach the source of the field is shorter and therefore the process of compensation is more efficient.

CHAPTER 5: APPLICATION OF BLANC'S LAW TO THE DETERMINATION OF
DIFFUSION COEFFICIENTS FOR THERMAL ELECTRONS: THE
CASE OF WATER VAPOUR

5.1: Introduction

Several recent applications of Cavalleri's (1969) electron density sampling technique for measuring electron diffusion coefficients have required the use of gas mixtures. In the work of Rhymes and Crompton (1975) (see also Rhymes 1976) a buffer gas was used to suppress the effect known as "diffusion cooling" observed in experiments with pure argon, while in the work of Hegerberg and Crompton (1983) the technique was used to suppress "attachment cooling". More recently measurements have been made with mixtures containing water vapour rather than with pure water vapour in order to overcome a technical problem in measuring excessively large time constants with existing equipment (see Section 5.3). In each case the simplest way of analyzing the data is through the application of Blanc's law, but in none of the cases cited were the conditions satisfied that make the application of the law strictly valid. In this chapter the errors that can arise from the application of the law in these and other circumstances will be examined and a method proposed for minimizing them in situations where the errors are significant.

In 1908, Blanc proposed a relationship between the mobilities of ions in gas mixtures and their mobilities in the separate components of the mixture. Since the law is strictly valid only for thermal ions for one special case, significant effort has been devoted to checking its applicability to nonthermal situations (see for instance McDaniel 1964;

McDaniel and Mason 1972; Hasted 1972). The theory of Milloy and Robson (1973) was particularly successful in giving very good qualitative (though not always quantitative) agreement with measured deviations from Blanc's law. These authors, whose work was based on an approximate form of momentum and energy transfer equations known as momentum transfer theory (see Chapter 3 for an example of the application of such equations), concluded that at zero field Blanc's law is always satisfied. A similar conclusion was reached by Robson (1973) and Whealton et al. (1974).

The necessary condition for the application of the law is that the ratio of the momentum transfer cross sections for the individual components of the mixture is constant in the relevant energy range. This condition is much better satisfied for ions than for electrons. Furthermore ions remain quasi-thermal over a much wider E/N range thus further increasing the range of applicability of Blanc's law.

For electrons the situation is more complicated since the momentum transfer cross sections may be very different in both magnitude and energy dependence. Nevertheless Blanc's law has been applied to electron transport coefficients in mixtures (Verbeek and Drop 1974; Hegerberg and Crompton 1980 and 1983; see also Long et al. 1976). In this chapter the name Blanc's law will be specifically used for the law as applied to diffusion coefficients for thermal electrons. However, the conclusions arrived at in this chapter for diffusion coefficients can be generalized to other transport coefficients.

The basic aim of this work is to examine the applicability of Blanc's law to the determination of the density normalized diffusion coefficient for thermal electrons in a gas A (defined as ND^A) from data for the diffusion coefficient, ND^M , in a binary mixture containing gases A and B

when the diffusion coefficient, ND^B , for component B is known.

As already noted, Blanc's law is only strictly valid when the ratio of the electron momentum transfer cross sections in the constituents of a mixture is independent of energy. It would be difficult to find examples that meet this rather stringent condition, but it has been argued (Hegerberg and Crompton 1980) that "for reasonably well behaved cross sections the deviation from Blanc's law is small even when this (identical energy dependence) condition is not fulfilled". In Section 5.2 simple models will be used to illustrate that there are indeed situations in which the errors arising from the application of Blanc's law are not large. More importantly, however, it is shown that very large errors can result from its application in some circumstances. In Section 5.3 the latter point will be illustrated by discussing an analysis, based on Blanc's law, of experimental data for the density normalized diffusion coefficient for thermal electrons in mixtures of H_2O and N_2 where the aim was to derive ND^{H_2O} from ND^M and ND^{N_2} . It is then shown how Blanc's law can still be applied without incurring large errors by the use of appropriate correction factors, thus retaining the simplicity of the analysis inherent in its use.

5.2: Analysis of the Application of Blanc's Law to Diffusion

Coefficients for Thermal Electrons

5.2.1: Basic considerations. The formula for the density normalized diffusion coefficient for thermal electrons in a gas derived on the basis of the two term approximation is (Huxley and Crompton 1974):

$$ND = (2/3)(2/\pi m)^{1/2} (kT)^{-3/2} \int_0^{\infty} \frac{\epsilon}{\sigma(\epsilon)} \exp(-\epsilon/kT) d\epsilon \quad (5.1)$$

where $\sigma(\epsilon)$ is the momentum transfer cross section, m the mass of the electron, ϵ the electron energy, T the gas temperature and k Boltzmann's constant. For a binary mixture M with components A and B the effective cross section is:

$$\sigma_M(\epsilon) = x \sigma_A(\epsilon) + (1-x) \sigma_B(\epsilon) , \quad (5.2)$$

where x is the fractional abundance of A , and the diffusion coefficient for the mixture is therefore:

$$ND^M = (2/3)(2/\pi m)^{1/2} (kT)^{-3/2} \int_0^{\infty} \frac{\epsilon \exp(-\epsilon/kT) d\epsilon}{x\sigma_A(\epsilon) + (1-x)\sigma_B(\epsilon)} . \quad (5.3)$$

If the ratio of the cross sections for the constituent gases is independent of energy such that $\sigma_A(\epsilon) = F\sigma_B(\epsilon)$ it follows that

$$ND^M = \frac{ND^B}{xF + (1-x)} , \quad (5.4)$$

and therefore that

$$\frac{1}{ND^M} = \frac{x}{ND^A} + \frac{(1-x)}{ND^B} , \quad (5.5)$$

which is Blanc's law for the diffusion coefficients. When ND^A is to be determined by an application of this law the more useful form is:

$$ND^A = \frac{x ND^M ND^B}{ND^B + (x-1) ND^M} . \quad (5.6)$$

In what follows the value of ND found from the application of Blanc's law in this way will be denoted by ND_{BL} .

Equation (5.6) is derived on the assumption that the distribution function is the thermal Maxwellian ($E/N = 0$). If $E/N \neq 0$ then to the original condition that $\sigma_A(\epsilon)/\sigma_B(\epsilon) = \text{const.}$ must be added the additional one that the form of the electron energy distribution functions must be identical in the mixture and each of its constituents (see Milloy and Robson 1973).

5.2.2: Deviations from Blanc's law. The formulae for ND for the mixture and its components (equations 5.3 and 5.1) are such that it is not possible to derive a relationship similar to Blanc's law under circumstances other than the special case $\sigma_A(\epsilon)/\sigma_B(\epsilon) = \text{const.}$ On the other hand, the simplicity of the law (5.5) is such that it is an advantage to retain it where possible even though this condition is not satisfied. Whether or not the application of the law is useful depends on the magnitude of the errors that result from its use. To examine this question we consider the asymptotic behaviour of equations (5.3) and (5.6).

From (5.3):

$$\lim_{x \rightarrow 0} ND^M = ND^B \quad \text{and} \quad \lim_{x \rightarrow 1} ND^M = ND^A ,$$

while from (5.6)

$$\lim_{x \rightarrow 1} ND_{BL}^A = ND^A ,$$

$$\text{and} \quad \lim_{x \rightarrow 0} ND_{BL}^A = \frac{(ND^B)^2}{\frac{2\sqrt{2}}{3\sqrt{\pi m}} (kT)^{-3/2} \int_0^{\infty} \frac{\sigma_A(\epsilon)}{\sigma_B^2(\epsilon)} \epsilon \exp(-\epsilon/kT) d\epsilon} . \quad (5.7)$$

The last equation was derived from equations (5.1), (5.3) and (5.6) using L'Hospital's rule. The first three limits are obvious but the last shows that ND_{BL}^A differs from ND^A unless $\sigma_A(\epsilon)/\sigma_B(\epsilon)=\text{const.}$ and therefore that, unless this condition is satisfied, this application of Blanc's law becomes less satisfactory as $x \rightarrow 0$. Moreover a comparison of the limiting value of ND_{BL}^A calculated from (5.7) with ND^A calculated from (5.1) for specified energy dependences of σ_A and σ_B enables the maximum error resulting from this application of the law to be calculated.

5.2.3: Model calculations. Several model cross sections were used in order to illustrate the limits of applicability of Blanc's law for determining ND^A to a required accuracy from mixture data. For each model equations (5.1) and (5.3) were first used to calculate the diffusion coefficients for gases A and B and for the mixture $x_A+(1-x)B$ at room temperature (293 K). Equation (5.6) was then used to calculate the Blanc's law prediction of ND^A (i.e. ND_{BL}^A) from ND^M and ND^B . From the values of ND^A and ND_{BL}^A the fractional error δ_{BL}^A defined as

$$\delta_{BL}^A = \frac{ND_{BL}^A - ND^A}{ND^A} \quad (5.8)$$

was calculated. Finally, using the same integration procedure, the value of ND_{BL} as the abundance of the gas A tends to zero was determined from equation (5.7). The limiting error determined in this way is denoted by δ_{BLO}^A , that is,

$$\delta_{BLO}^A = \lim_{x \rightarrow 0} \delta_{BL}^A. \quad (5.9)$$

δ_{BLO}^A may be large but Blanc's law still applicable provided x is not too small.

(a) The first model comprises cross sections of the form:

$$\sigma_A = A_0 \varepsilon^a; \quad \sigma_B = 20 \varepsilon^b \quad (5.10)$$

with $b=\pm 1$; σ is in 10^{-16} cm^2 when ε is given in eV.

We first examine the influence on the limiting error δ_{BLO}^A of different energy dependences for the cross sections, i.e. $a \neq b$. Since A_0 appears as a multiplicative factor in the expressions for $\lim ND_{\text{BL}}^A$ as $x \rightarrow 0$ (5.7) and ND^A (5.1) it follows from equations (5.9) and (5.8) that the limiting value of the error is not affected by the choice of A_0 . Thus we may put $A_0=20$ for this purpose. The results for $b=\pm 1$ and a range of values of a are shown in Table 5.1. It can be seen that limiting errors larger than 1% occur only when a differs from b by more than 10% when $b=1$, and by more than 20% when $b=-1$. This conclusion has application to mixtures of gases that have permanent dipole moments (Altshuler 1957; Gilardini 1972).

Table 5.1

b = 1	a	1.5	1.2	1.1	1.05	1.0
		0.5	0.8	0.9	0.95	1.0
	δ_{BLO}^A (%)	24	4.3	1.1	0.28	0.0
b = -1	a	-1.5	-1.2	-1.1	-1.05	-1.0
		-0.5	-0.8	-0.9	-0.95	-1.0
	δ_{BLO}^A (%)	9.3	1.5	0.39	0.09	0.0

While the limiting error is independent of the value of A_0 , the approach to the limit as the abundance x of gas A decreases does depend on its value. The approach to this limit can be examined by selecting several values of A_0 , b having been put equal to 1 and a_0 having been given the value $a=1.2$ which gives a significant difference ($>4\%$ -see Table 5.1) between ND_{BL}^A and ND^A as $x \rightarrow 0$. The results are shown in Fig. 5.1 from which it can be seen that when $A_0 \ll 20$ the maximum error is approached much more rapidly than when $A_0=20$, while the opposite is true for $A_0 \gg 20$ (compare the curves for $A_0=2$ and $A_0=40$ with that for $A_0=20$). This is because for a mixture of given composition the diffusion coefficient for the mixture contains progressively less information about component A as the collision frequency for that component decreases with respect to the collision frequency for the other, that is as $\langle \sigma^A(\epsilon) \rangle / \langle \sigma^B(\epsilon) \rangle$ decreases.

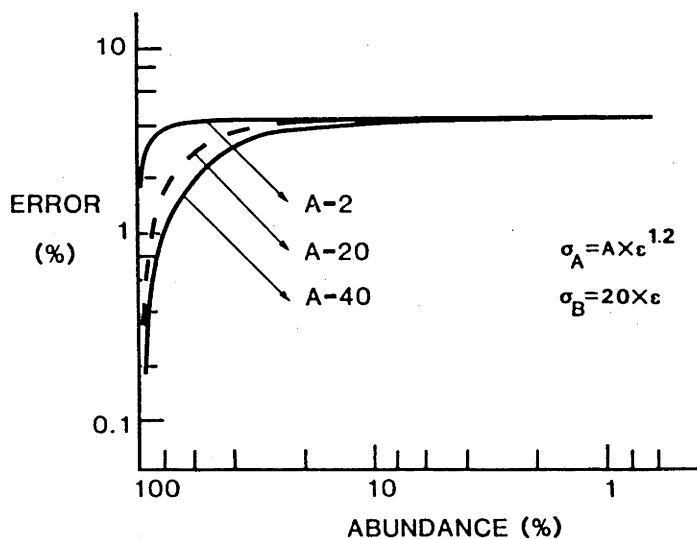


Figure 5.1 Errors (δ_{BL}^A) made when Blanc's law is used to determine the diffusion coefficient for gas A from values of coefficients for gas B and the mixture containing various abundances of gas A - model (a)

(b) The next model to be considered is one in which the two cross sections have the same energy dependent factor but one has an additional constant term:

$$\sigma_A = \sigma_{AO} + 20\varepsilon ; \quad \sigma_B = 20\varepsilon . \quad (5.11)$$

Such cross sections might loosely be described as having the same energy dependence. The results for several values of σ_{AO} are presented in Figure 5.2. When σ_{AO} is 0.01 the limiting error is only 0.43%, for $\sigma_{AO} = 0.1$ it is 11.6%, and for $\sigma_{AO} = 1$ it is 47%. The most important factor is not, of course, the absolute value of σ_{AO} but its relative contribution to σ_A in the thermal energy range.

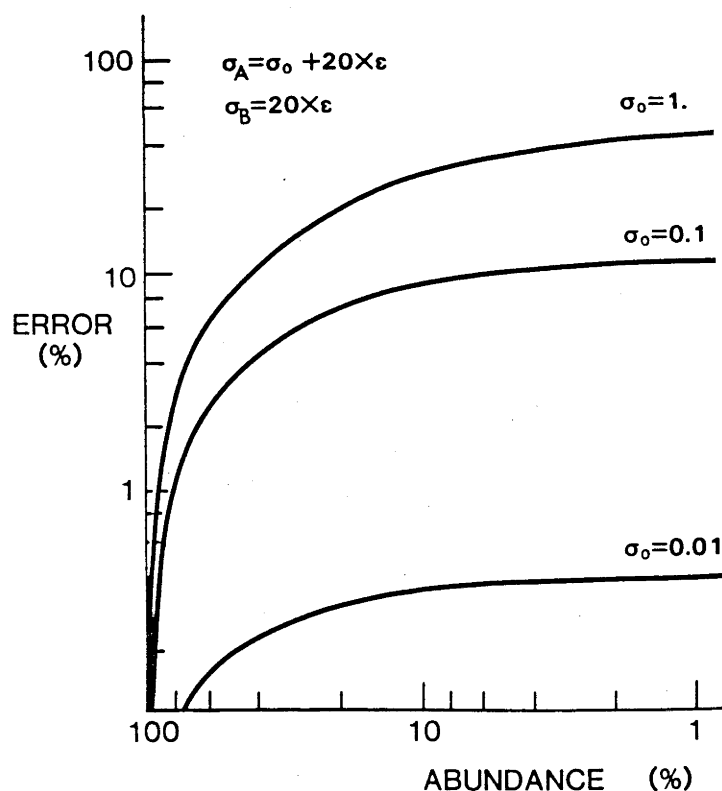


Figure 5.2 Errors (δ_{BL}^A) made when Blanc's law is used to determine the diffusion coefficient for gas A from values of coefficients for gas B and the mixture containing various abundances of gas A - model (b)

(c) A more general situation is described by the third cross section set:

$$\sigma_A = \sigma_{A0} + A_0 \epsilon^a ; \quad \sigma_B = 1 + 20\epsilon . \quad (5.12)$$

Table 5.2

	a = 1		A ₀ = 20				
σ_{A0}	0.2	0.5	0.8	1.0	1.1	1.5	2.0
δ_{BLO}^A (%)	7.3	1.4	0.14	0.0	0.02	0.41	1.1
	A ₀ = 20		$\sigma_{A0} = 1.0$				
a	0.5	0.8	0.9	1.0	1.1	1.2	1.5
δ_{BLO}^A (%)	0.56	0.27	0.08	0.0	0.10	0.41	2.2
	a = 1		$\sigma_{A0} = 1.0$				
A ₀	5.0	10	15	20	21	25	30
δ_{BLO}^A (%)	3.26	1.08	0.21	0.0	0.007	0.14	0.48

Parameters for σ_A (i.e. σ_{A0} , a and A_0) were varied in turn. The results for δ_{BLO}^A are shown in Table 5.2. While these data are useful in showing the maximum errors that can be incurred in deriving ND^A from the data for ND^M and ND^B they are necessarily incomplete since the variation of δ_{BL}^A with x is not recorded here.

There are two reasons why one cannot reach any general conclusions on

the basis of data presented for the three models. First, although it is clear that Blanc's law can be usefully applied for any value of x provided δ_{BL0} is small, this criterion cannot be readily applied because the integral forms of equations (5.1) and (5.7) make it difficult to evaluate δ_{BL0} for a given set of cross sections. One might be tempted to assess the applicability without calculating δ_{BL0} by comparing approximate analytical expressions for the cross sections for the components, or by inspecting plotted or tabulated data, the law being considered to be applicable when the ratio of the cross sections appears to be approximately constant at all energies. However our calculations for the models clearly indicate the need to check the applicability. Second, our examination of the dependence of δ_{BL} on x for models (a) and (b) shows that even though δ_{BL0} may be quite large, δ_{BL} may be acceptably small provided x is not too small.

5.2.4: "Real" gases. In this section the application of Blanc's law to the analysis of diffusion coefficient data for several gas mixtures will be discussed.

The case of H_2O-N_2 mixtures will be considered first. These mixtures were used in the work described in Section 5.3. Curves for $\delta_{BL}^{H_2O}$ as a function of the water vapour concentration were generated using the momentum transfer cross section for N_2 of Pitchford and Phelps (1982) and the cross section of Chrisophorou and Pittman (1970) for water vapour. This cross section was presented in the analytical form

$$\sigma_{H_2O}(\epsilon) = 23.84\epsilon^{-1.085}. \quad (5.13)$$

It and the cross section of Pack et al. (1962) led to practically identical results for the error curves even though the calculated values of the

diffusion coefficients differ slightly (2% - see Table 5.3b). The cross section of Pack et al. as tabulated by Kieffer (1975) was fitted by a curve

$$\sigma_{\text{H}_2\text{O}}(\epsilon) = 23.98 \epsilon^{-1.075} \quad (5.14)$$

that produced the least square deviation from the tabulated data. The diffusion coefficients calculated on the basis of the available cross sections are in good agreement with the values obtained from experimentally determined thermal mobilities (Pack et al. 1962; Lowke and Rees 1963; Wilson et al. 1975. See also Giraud and Krebs 1982).

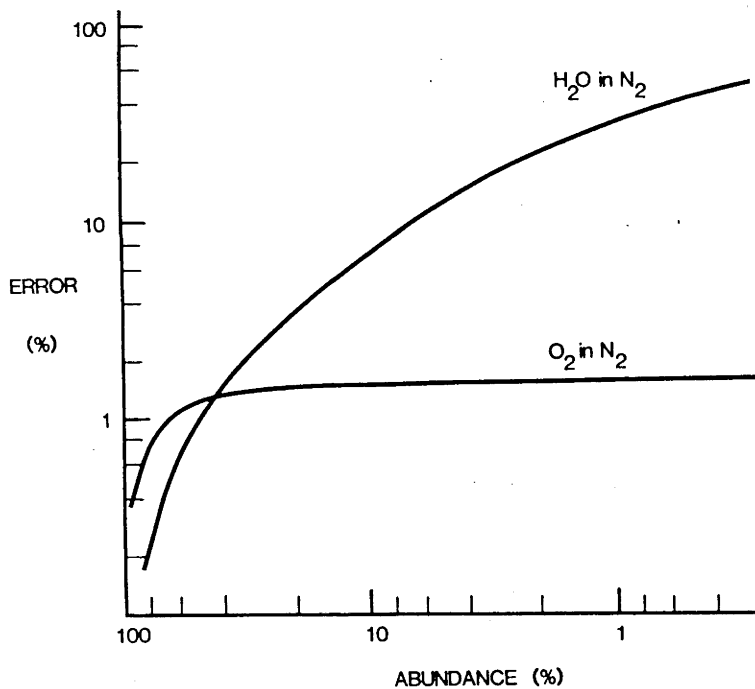


Figure 5.3 Errors (δ_{BL}^A) that are made when Blanc's law is used to determine diffusion coefficients for H_2O and O_2 from the appropriate mixture data and the data for pure N_2 .

The results for δ_{BL}^A are shown in Fig. 5.3. In order to check the sensitivity of $\delta_{\text{BL}}^{\text{H}_2\text{O}}$ to uncertainty in the water vapour cross section the multiplying constant in (5.13) was changed by 10%. In the case of the 10% H_2O - 90% N_2 mixture the 7% correction (see Fig. 5.3) was changed by less than 0.25%. Thus, when the uncertainty in the cross section is of this

order, negligible error in the derived value of ND results from the application of Blanc's law to the mixture data provided the calculated correction is applied. This example illustrates the point that, even in the case when the cross sections differ as much as those for N₂ and H₂O (see Fig. 5.4), an appropriate choice of the mixture composition enables the mixture data to be analyzed in this way without the necessity of a high order of accuracy in the cross sections.

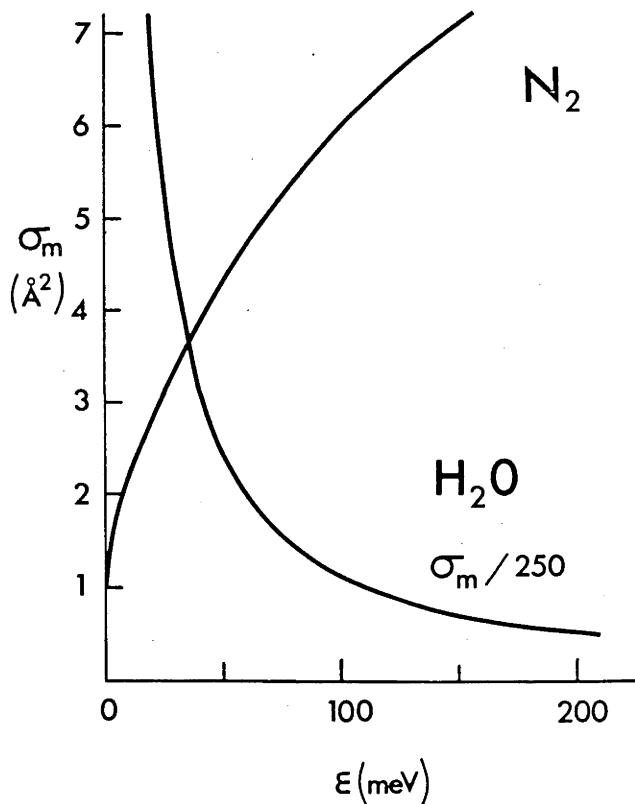


Figure 5.4 Momentum transfer cross sections for electrons in H₂O and N₂.

Fig. 5.3 also shows the results for O₂-N₂ mixtures, the motivation for these calculations being an examination of the validity of the procedure used by Hegerberg and Crompton (1983) to analyze their data for mixtures of these gases. The cross section for O₂ of Lawton and Phelps (1978) was used for the calculation of $\delta_{BL}^{O_2}$. As can be seen from the figure, the

calculated error is small enough (less than 1%) to justify the direct application of Blanc's law although even in this case one should be aware of the small systematic error that results.

Hegerberg and Crompton's work provides a good example of a situation where the use of mixtures is essential for the application of a particular experimental technique. In this case its use avoided significant errors from attachment cooling in experiments based on the Cavalleri electron density sampling method. A similar situation occurs when one wants to suppress diffusion cooling in experiments based on the same technique (see Rhymes and Crompton 1975 and Rhymes 1976).

In almost all realistic cases the application of Blanc's law can lead to unacceptable errors not only when the diffusion coefficient for a single gas is sought from the data for a mixture and its other constituent(s) but also when the diffusion coefficient for the mixture is calculated from the data for the pure gases. Fig. 5.5 illustrates some examples of this second point.

5.2.5: Discussion. Two points may be noted concerning the relation between this and other recently published work.

First, our conclusions based on model calculations are somewhat different from the conclusions reached by Milloy and Robson (1973) and Whealton et al. (1974). However the momentum transfer theory used by these authors breaks down at thermal energies since the momentum and energy balance equations upon which it is based are not strictly applicable when the influence of the electric field no longer dominates.

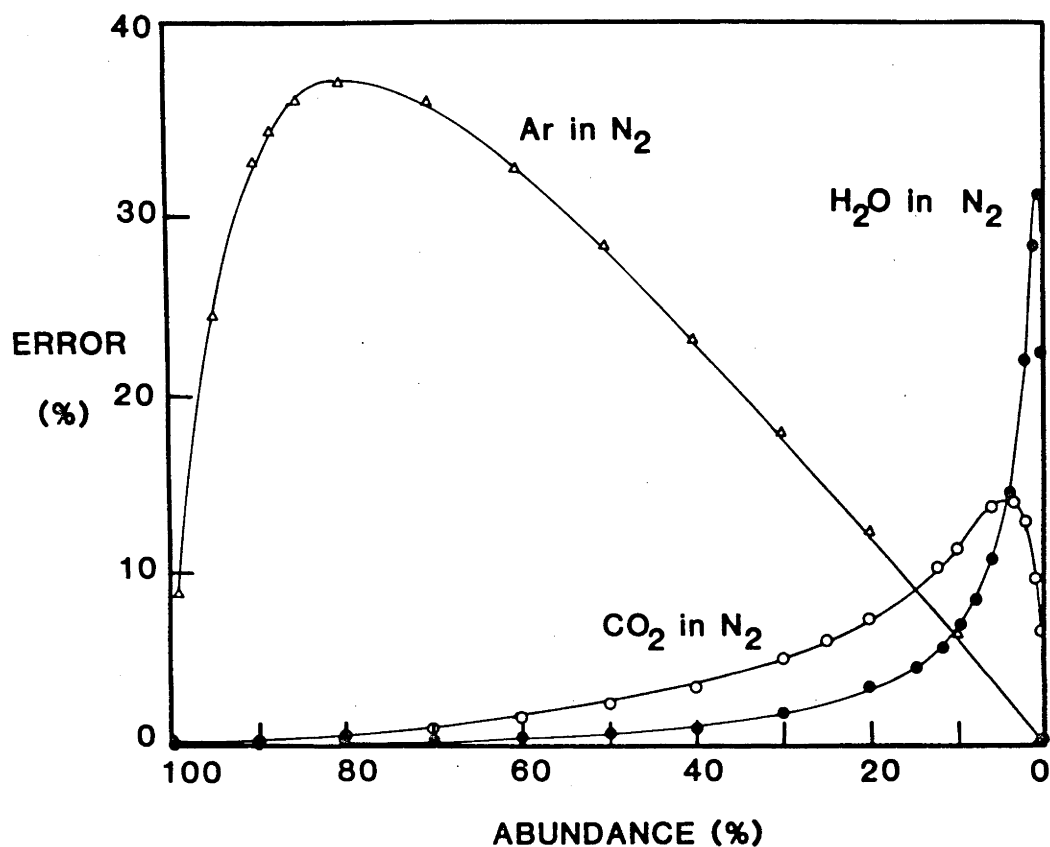


Figure 5.5 Errors that are made when diffusion coefficients for thermal electrons in H₂O-N₂, CO₂-N₂ and Ar-N₂ mixtures are calculated using Blanc's law and the data for the pure gases. Sources of data for the cross sections additional to those quoted in the text are: for CO₂, Kieffer (1975); for Ar, Haddad and O'Malley (1982).

Second, this work is relevant to the recent paper by Chen and Jones (1984). These authors discuss the application of Blanc's law for mobilities in gas discharges, in particular the case of discharges in argon-mercury mixtures. Relatively simple formulae for the temperature dependences of electron mobilities were derived by them on the basis of

simplified formulae for the momentum transfer cross sections. Subsequently, instead of using Blanc's law they derive a formula for the conductivity of an arbitrary mixture which is the sum of the conductivity of argon and a correction factor which includes the overall influence of the presence of mercury. Since their procedure necessarily depends on numerical integration, it would seem preferable to use Blanc's law and apply a correction. This procedure would also enable one to use experimental mobilities for pure gases, and thus obtain a very accurate result for the mixture even though the cross sections used to calculate the corrections were not as accurate as the mobilities. In contrast, the procedure suggested by Chen and Jones is restricted by the accuracy of the assumed analytical forms of the cross section which, for example, were unable to include the resonance in the vicinity of 2 eV (Elford 1980).

5.3.: Measurement of the Diffusion Coefficient for Thermal Electrons in Water Vapour

5.3.1: Introduction. Measurements of the diffusion coefficients for thermal electrons in mixtures of water vapour and nitrogen were made using Cavalleri's electron density sampling technique (Cavalleri 1969; Huxley and Crompton 1974). The apparatus and its operation have been described in Chapter 4.

The very large momentum transfer cross section for thermal electrons in H₂O results in a very small diffusion coefficient and time constants that are too large to be measured in our apparatus as presently configured. In principle the pressure could be reduced in order to reduce the time constant to a value that is within the measurement range, but this would

lead to unacceptable statistical errors due to inadequate initial ionization and insufficient avalanche development by the sampling pulses. The problem was overcome by using N_2 (with its very much smaller cross section) as a buffer gas in mixtures chosen to have suitable characteristics on the basis of the discussion in Section 5.2.4.

5.3.2: Experimental procedure. Matheson "Research Grade" nitrogen was used for the mixtures. Twice-distilled and deionized water was further purified by freezing and removing permanent gases by evacuating a reservoir containing the water. This procedure was repeated a number of times in order to release the frozen impurities and to monitor any dependence of the results on residual impurities. Final results were taken only after successive purification produced no further change. Pressures were measured by a calibrated Texas Instruments quartz spiral manometer.

The apparatus was baked at 210°C for three days prior to the measurements.

Mixtures of 5, 10 and 20% H_2O in N_2 were prepared in the following way. The system was first pumped down to $< 10^{-4}$ Pa. Water vapour was then introduced to a slightly higher pressure than desired and left for a short time to saturate the walls. The pressure drop due to adsorption was noted and the pressure finally adjusted to the desired value before nitrogen was slowly introduced. Mixing was monitored by measuring the time constants for electron density decay. Usually 12 to 48 hours mixing time was allowed before the final measurements were made.

All these measurements were performed in order to minimize adsorption and desorption effects. An alternative approach to making mixtures with H_2O , suggested by Pack and Phelps (1966), of freezing the desired quantity of

H₂O after saturating the walls was not used because it was not possible to locate the water reservoir close to the cell. The importance of the measures taken can be seen from Fig. 5.6 where data are presented for the diffusion coefficient for H₂O obtained using the corrections to Blanc's law as explained later. Filled square is the result obtained for a 2 kPa mixture of 10% H₂O in N₂ prepared with all the care. When the pressure is reduced after, to perform the measurements at 1 and 0.5 kPa, the results (open circles) correspond to an increased abundance of H₂O, while if the pressure is reduced by connecting a large evacuated stainless steel reservoir the values of ND are increased very much (full circles) corresponding to a significant loss of water vapour. The open triangles represent results of the measurements performed using the samples that were prepared at the desired pressure.

Results reported in the next section were shown to be free from measurable error due to space charge, non-thermalization of the electrons, and the presence of higher order diffusion modes. For each mixture composition the final results were an average of those taken with gas mixtures made from two different samples of water and at several pressures.

5.3.3: Results and discussion. Measurements with 10% and 20% mixtures of H₂O in N₂ were performed at pressures of 0.5, 1 and 2 kPa, and those with 5% at 2 kPa. Since the main interest was mainly an investigation of the application of Blanc's law the results taken at different pressures were averaged. These results are presented in Table 5.3a and Fig. 5.7.

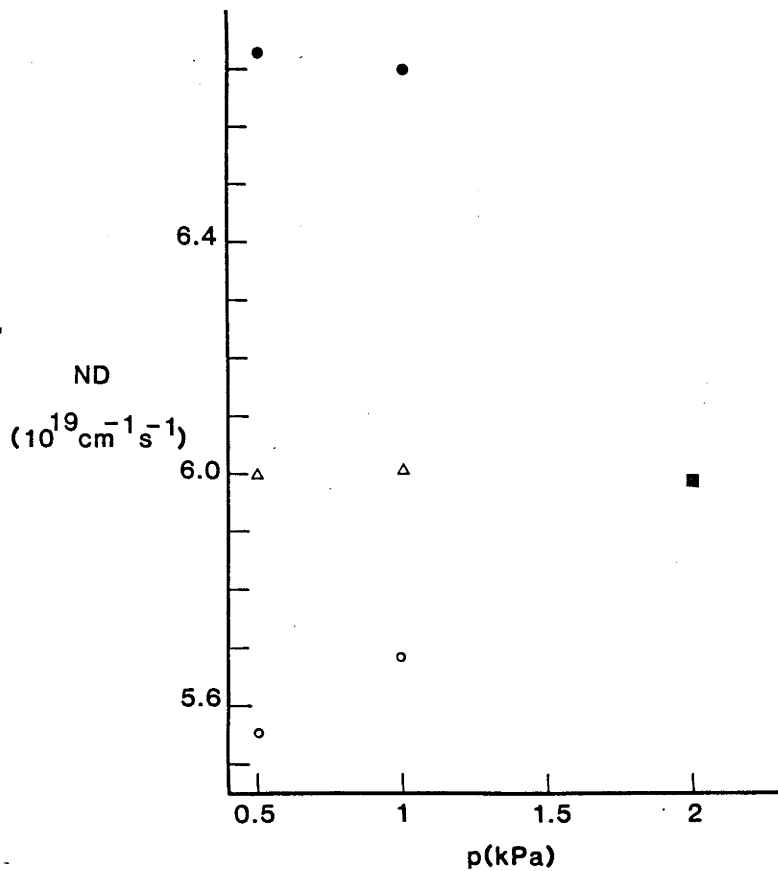


Figure 5.6 Influence of adsorption and desorption of H_2O on results for the density normalized diffusion coefficient in pure water vapour. All the symbols are explained in the text

Results for the diffusion coefficients for the mixtures are in very good agreement with the data calculated on the basis of the available cross sections (calculated values are presented in the brackets in Table 5.3). The results for $\text{ND}_{\text{BL}}^{\text{H}_2\text{O}}$ clearly show a systematic dependence on the mixture composition, revealing the expected breakdown of the law. It is therefore necessary to correct the data using equation (5.8) and the data for $\delta_{\text{BL}}^{\text{H}_2\text{O}}$ shown in Fig. 5.3. The corrected data are also shown in Table 5.3a and Fig. 5.7. The final result is $\text{ND}^{\text{H}_2\text{O}} = (5.98 \pm 0.20) 10^{19} \text{ cm}^{-1} \text{ s}^{-1}$ (using

the measured value for $ND^{N_2} = 9.65 \cdot 10^{21} \text{ cm}^{-1} \text{ s}^{-1}$). This value is the average of the results for different abundances (and pressures).

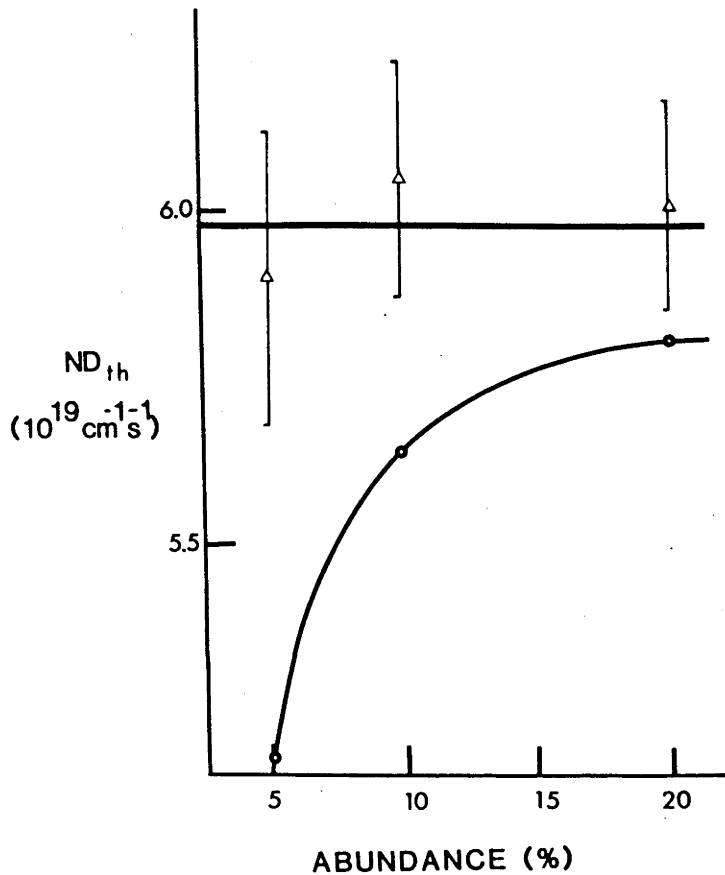


Figure 5.7 Experimental results for ND^{H_2O} obtained using Blanc's law. Uncorrected (i.e. $ND_{BL}^{H_2O}$) —○— ; corrected data Δ . The average value is represented by a horizontal straight line.

The uncertainty of the measured values of ND in this experiment is 2-3% (Gibson *et al.* 1973; Rhymes 1976; Crompton and Haddad 1983) but to this one should add 0.5 - 1% to account for the uncertainty in the mixture composition due to long term adsorption and desorption effects.

Present result for ND^{H_2O} is consistent with the available cross section data and the values obtained by the application of the Nernst-Townsend (Einstein) relation to the experimental thermal mobility data (see Table 5.3b).

Table BL.3 a)

x (%)	ND ^M (10 ²⁰ cm ⁻¹ s ⁻¹)	correction factor $\frac{1}{1 + \delta_{BL}^{H_2O}}$	ND ^{H₂O} _{BL} (10 ¹⁹ cm ⁻¹ s ⁻¹)	ND ^{H₂O} _{corr}
20	2.83 (2.86)	1.035	5.80	6.00
10	5.36 (5.36)	1.073	5.64	6.05
5	9.40 (9.64)	1.14	5.18	5.90
average value				5.98 ± 0.20

b)

Reference	ND ^{H₂O} (10 ¹⁹ cm ⁻¹ s ⁻¹)
Pack <u>et al.</u> (1962)	6.05 (300 K)
Christophorou and Pittman (1970)	5.93
Lowke and Rees (1963)	5.93 (293 K)
this work	5.98 (293 K)
see also Wilson <u>et al.</u> (1975) and Giraud and Krebs (1982)	

In addition to the measurements for water vapour mixtures similar experiments were performed using CO₂, but this time it was possible to perform measurement in pure CO₂. The errors caused by the application of Blanc's law exceed the experimental uncertainty for abundances of CO₂ below

25% in the CO₂-N₂ mixtures. However, as expected good agreement with the pure CO₂ value was achieved by using the calculated corrections.

5.3.4: A note on thermal electron attachment in water vapour.

Electrons are attached to water molecules via following processes (Crompton et al. 1965; Hasted 1972; see also Compton and Christophorou 1967; Belić et al. 1981):



with a threshold of about 5.6 eV and a maximum in the cross section at 6.4 eV ;



with a threshold of about 7.5 eV and a maximum in the cross section at 8.6 eV. It is therefore unlikely that a two body process could produce measurable attachment at thermal energies. However Bradbury and Tatel (1934) and Kuffel (1959) observed an increase of the attachment coefficient at very low E/N values. A number of papers followed proving that thermal electrons do not produce negative ions in water vapour (Takeda and Dougal 1960; Fox et al. 1961; Pack et al. 1962; Hurst et al. 1963; Chantry 1963). It is interesting to note that Hurst et al. observed a rather complicated attachment process in H₂O - CO₂ mixtures at thermal energies.

The present experimental results are consistent with finding that there is no attachment of thermal electrons in water vapour. Based on our experimental data an upper limit to a three body coefficient would be $2 \cdot 10^{-33} \text{ cm}^{-6} \text{ s}^{-1}$.

5.4: Conclusion

In this Chapter a discussion has been given of the application of Blanc's law to the determination of diffusion coefficients for thermal electrons in a gas from experimental data for a mixture containing that gas. A number of calculations for both model and real gases show that considerable errors may result from an application of the law, especially for low abundances of the gas. These errors are caused by different energy dependences of the momentum transfer cross sections for the constituents. However, it has been shown that it is possible to apply correction factors that are sufficiently accurate even when the cross sections are as dissimilar as those for H₂O and N₂. It has also been shown that the procedure of using Blanc's law with appropriate correction factors is remarkably accurate even though the available cross section data may not be highly accurate. Thus, for a gas for which the momentum transfer cross section in the thermal region has not been well established, the use of this procedure enables a value of the density normalized diffusion coefficient to be determined that is much more accurate than the value that could be calculated from the cross section.

CHAPTER 6: THERMAL ELECTRON ATTACHMENT TO SF₆ AT ROOM TEMPERATURE AND
AT 500 K

6.1: Introduction

The very large capture rate of SF₆ for low energy electrons, together with other desirable characteristics of the gas, have led to numerous applications (see, for example, Govinda Raju and Hackam 1982; Chantry 1982b; Christophorou et al. 1982b; Schoenbach et al. 1983; Christophorou and Hunter 1984). There have been many measurements of the attachment rate coefficient for thermal electrons (k_{att}^{th}) in the gas because the loss rate of thermal electrons from the partially ionized gas is often the electrical characteristic of prime interest. Moreover it is important to have an accurate value of the coefficient because it has been used to determine absolute values of the attachment cross section. Nevertheless, as can be seen from Table 6.1, there are serious differences between the various results for k_{att}^{th} , and in any case most of the available data have a statistical scatter of up to 10%. Normalizations of the cross section based on these data are therefore subject to rather large uncertainties. Crompton and Haddad (1983; see also Crompton et al. 1982) claimed to have succeeded in narrowing the error bounds to less than $\pm 3\%$, and their result of $2.27 \cdot 10^{-7} \text{ cm}^3\text{s}^{-1}$ was used by Chutjian (Ajello and Chutjian 1979; Chutjian 1981; Chutjian and Alajajian 1984) to normalize the cross section for the formation of SF₆⁻ which he obtained by the technique of photoelectron spectroscopy.

Table 6.1 Attachment rate coefficients for thermal electrons in SF₆ obtained at room temperature.

k_{att} ($10^{-7} \text{ cm}^3 \text{ s}^{-1}$)	uncertainty	buffer gas	reference	method
2.89	10^{-6}	Xe	Hasted and Beg (1965)	MW
0.385		C ₂ H ₄	Compton <u>et al.</u> (1966)	SW
3.1	± 0.8	He - NO	Mahan and Young (1966)	MW
2.7		He	Young (1966)	MW
2.41	± 0.51	10%CH ₄ +90%Ar	Chen <u>et al.</u> (1968)	PS
3.82	10^{-5}	C ₇ H ₁₄	Freeman (1968)	PR
2.13		various	Davis and Nelson (1970)	DDD
2.2		C ₃ H ₈	Fessenden and Bansal (1970)	MW
2.2	± 0.9	He, Ar	Fehsenfeld (1970)	FALP
2.7		N ₂	Christophorou <u>et al.</u> (1971a)	SW
2.8		C ₂ H ₄	Christophorou <u>et al.</u> (1971a)	SW
2.6		Ar	Mothes and Schindler (1971) and Mothes <u>et al.</u> (1972)	ECR
4.3	± 0.9 ($\epsilon=8-20\text{meV}$)		West <u>et al.</u> (1976) and Foltz <u>et al.</u> (1977)	RB
2.64*			Klots (1976)	TH
2.20	± 0.1	neo-C ₅ H ₁₂	Shimamori and Fessenden (1979)	MW
2.8	± 0.3 (? 0.7)**	10%CH ₄ -90%Ar	Ayala <u>et al.</u> (1981)	PS
2.49***			Christophorou <u>et al.</u> (1981)	SW
2.27	± 0.07	N ₂	Crompton and Haddad (1983)	CDE
3.1	± 0.47	He, Ar	Smith <u>et al.</u> (1984)	FALP
2.35	± 0.16	N ₂	Hunter (1984)	SW
2.27	± 0.09	N ₂ , H ₂ , CO ₂	this work	CDE
2.24	± 0.15	He	this work	CDE

MW microwave diagnostics of a static afterglow

SW swarm method

PS pulse sampling
 PR pulse radiolysis
 DDD drift dwell drift
 FALP flowing afterglow Langmuir probe
 ECR electron cyclotron resonance
 RB Rydberg atom beams
 TH theory
 CDE Cavalleri diffusion experiment

- * Accuracy of the theoretical value was not stated, but the author considers his result to be in very good agreement with the data of Fehsenfeld (1970)
- ** These authors state that the accuracy of their result is $\pm 25\%$ which disagrees with the stated value of ± 0.3 . Also they state that the result of Chen et al. (1968) should be 3.5.
- *** This is a reanalysis of the data of Christophorou et al. (1971) and therefore all the conditions are identical.

Smith et al. (1984) have recently published results for k_{att}^{th} measured in various gases using the Flowing Afterglow Langmuir Probe technique (FALP). While their value for k_{att}^{th} in $CFCl_3$ is consistent with the measurement by Crompton and Haddad (1983), who used CDE (see Table 6.2), their result of $3.1 \cdot 10^{-7} \text{ cm}^3\text{s}^{-1} (\pm 15\%)$ in SF_6 is outside the combined error bounds of the results from the two experiments. It is also worth noting that the ratios of the values of k_{att}^{th} for $CFCl_3$ and SF_6 obtained by the two experimental techniques (see Table 6.2) are quite different, which makes the probability of a systematic error in one of them less likely.

The importance of the value of k_{att}^{th} for SF_6 prompted a reinvestigation of possible sources of error in the technique used by Crompton and Haddad. Despite extensive, and as far as is known successful, applications of the technique used by Crompton and Haddad (see Section 4.1), some reasons for its possible failure when applied to the measurement

of k_{att}^{th} for SF₆ have been suggested (Smith 1983) in order to explain the differences between the results obtained by the electron density sampling and FALP techniques.

Table 6.2 Comparison of recently measured attachment rate coefficients at room temperature for electrons in CFC1₃ and SF₆.

	CFC1 ₃	SF ₆	Experimental	Ratio
	k_1	k_2	Error	k_1/k_2
	(10 ⁻⁷ cm ³ s ⁻¹)		(%)	
Smith <u>et al.</u>	2.7	3.1	15	0.87
Crompton and Haddad	2.37	2.27	3	1.04
Difference (%)	14	37		

The first suggestion is that there may have been a build-up of vibrationally excited molecules of the nitrogen buffer gas used by Crompton and Haddad (1983) in their experiments using the CDE technique, and that such a build-up of excited molecules could cause detachment and thus a lower effective attachment rate.

The second suggestion is related to the fact that the introduction of the attaching gas into the buffer gas reduces the free-electron lifetime dramatically, making it necessary to measure electron densities at much shorter times after the initial X-ray pulse. At such times higher-order diffusion modes might still be present, and the electron density decay

could then no longer be represented by a single exponential. This could possibly lead to spurious results (see Section 6.3.1), an effect that would be exacerbated if the viewing angle of the photomultiplier were limited.

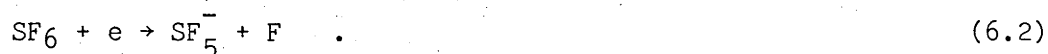
In this Chapter those two suggestions are analysed both experimentally and by calculations. In addition results for k_{att}^{th} in SF₆ at 500 K are presented, thus providing an additional comparison with the work of Smith et al. (1984).

6.2: Electron Attachment to SF₆

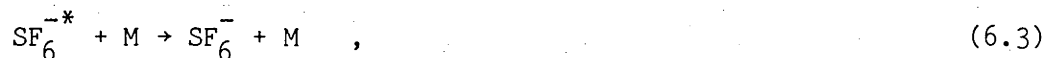
There are two possible processes that lead to attachment of electrons at thermal energies:



and



The excited negative ion SF₆^{-*} will be either stabilized in collision with some third body M:



or decay through autodetachment



If the characteristic lifetime for the process (6.4) greatly exceeds the mean lifetime between the collisions with third bodies it becomes irrelevant which particle M acts as the third body and therefore process

(6.1-6.3) and (6.4) can be represented using a two-body rate coefficient (that is a saturated three-body coefficient). That SF₆ falls into this category can be seen from the following argument:

- 1) The shortest reported lifetimes for autodetachment for SF₆^{-*} are of the order of 10 μs (Massey 1976; Christophorou 1978).
- 2) Collision frequencies of molecules at pressures normally used in swarm experiments correspond to a time between collisions of 10 ns (at 1 kPa of N₂ at room temperature).

Therefore swarm experiments are suited to analyse the attachment of electrons to SF₆ since at the pressures that are normally used practically every occurrence of the process (6.1) is followed by (6.3) rather than (6.4) and the results are independent on the choice of M (see Massey 1976).

The published results for the autodetachment lifetime τ_{ad} are quite different depending on the condition of the experiment (Massey 1976). It has even been noticed that autodetachment sometimes cannot be represented by a single exponential decay i.e. by a single time constant. It is therefore believed (Odom et al. 1975; see also Hansen et al. 1983) that attachment proceeds through a series of excited states (whose lifetimes could be a function of the gas density and of the electric field (Hansen et al. 1983)).

The electron affinity of SF₆ appears to be 1.0 eV (Strait 1982). Also it is of interest to note that Hay (1982) has recently published calculated potential energy curves for SF₆.

Attempts to apply electron beam methods to study low energy electron attachment are not as numerous as the studies using other methods. Some of the earlier work has been summarized by Massey (1976). It was aimed at establishing the energy profile of the cross sections and the peak values.

The later task proved to be much more difficult using available experimental techniques (and even nowadays the results of beam experiments are often absolutely calibrated using swarm data).

The paper of Spence and Schulz (1973) is especially interesting. They measured the temperature dependence of the attachment cross section for various gases. For SF₆ they found no variation over a very wide temperature range (300-1200 K). This is, however, for the total attachment, and is not in disagreement with the strong temperature dependence of the dissociative process that has been reported many times. To investigate this point Chen and Chantry (1978,1979) used infra-red laser radiation to increase the vibrational population of SF₆. They have shown that the process of dissociative attachment from higher vibrational levels is much faster than from the ground state, a conclusion that is quite important for SF₆ since vibrational energies are low (43-118 meV - see Chutjian 1982) and major changes of populations can occur over a fairly narrow temperature range. The same authors have also measured cross sections for production of various negative ions as a result of electron attachment to SF₆ (Kline et al. 1979). They have also used their data to calculate electron transport coefficients for various mixtures containing SF₆.

However, this and all previous attempts to obtain a very detailed and accurate profile of the peak of the attachment cross section failed, and its width had always been instrument-limited. The reason is, of course, that the cross section peaks at subthermal energies that are too low for beam methods. In an attempt to analyse attachment processes at very low energies (a few millivolts) another approach that is strictly speaking not a beam technique was developed. It is a technique known as Threshold

Photoelectron Spectroscopy by Electron Attachment (TPSEA). Low energy electrons are produced by photoionization of a buffer gas by a beam of light of controllable wavelength. These electrons attach and negative ions are created. Using a very low electric field, ions are extracted from the chamber and analysed by a quadrupole mass analyser (Ajello and Chutjian 1979 and Chutjian 1981). However, only the energy dependence of the relative cross section can be produced and the results have to be scaled using the rate coefficient values obtained by swarm experiments. On the other hand, a very high energy resolution down to practically zero energy can be achieved (see Chutjian and Alajajian 1984). In another approach beams of atoms (Xe) excited to high Rydberg states are used to mimic very low energy electron beams (West et al. 1976; Foltz et al. 1976, see also Zollars et al. 1984). In these experiments a beam of Rydberg atoms collides with the attaching gas in an interaction chamber. The binding energies of the electrons are very low and therefore they behave as free electrons. The attachment rates calculated from the rate of creation of negative ions are found to be somewhat higher than those obtained by swarm experiments (see Table 6.1). The probable explanation for this is that the relative energies between the electrons and the molecules may be lower than the thermal energy and therefore the rate coefficient corresponds to a lower mean energy. If the cross section for electron attachment has a sharp peak close to a threshold at or near zero energy an attachment rate as high as that measured using the Rydberg beam method may be compatible with the results obtained by other methods.

If the rate of loss of Rydberg states is monitored rather than the rate of production of ions the total cross section can be produced (Kellert et al. 1980). A more direct measurement of the total cross section was made

by Ferch et al. (1982) by a standard time-of-flight technique.

Theoretical investigations of the electron attachment to SF₆ include the work of Klots (1976) (Table 6.1-TH), Chutjian (1982) and Gauyacq and Herzenberg (1984). An important discussion of the threshold behaviour of the cross section can be found in a paper by Chutjian and Alajajian (1985).

Attempts to measure the rate coefficient (and eventually derive the cross section) were more numerous. The measurements for nonthermal swarms will not be discussed here (unless as a result the cross section for very low energy electrons was produced). These results have been thoroughly reviewed and discussed by the JILA Information Center Group (Gallagher et al. 1982) and various other authors (Christophorou 1971; Christophorou et al. 1982b). Here, a critical analysis of some of the published results will be presented in an attempt to clarify the rather confusing situation presented in Table 6.1 where a large number of results are presented but the differences between some of them are unacceptably large.

One might be tempted to label most of the methods that produce attachment rate coefficients as "swarm" methods. However many of these are performed under "plasma" conditions, when collective effects become important or even dominant. The term "swarm" will be reserved for situations in which collective effects are negligible, but the exclusion of the other class of experiments from this category is not intended to question the validity of results obtained from them.

Table 6.1 presents all the results that were available at the time of writing. These include flowing-afterglow (FA and FALP - flowing afterglow Langmuir probe), microwave diagnostics of static afterglows (MW) and pulse sampling (PS) techniques. Some of these results will be discussed in this section in order to point out some weak and some strong points of the

techniques that were used since it appears that the quality of the results and their presentation were not uniform and a false picture could be created if all the results were given the same weight.

Generally the results are grouped around two values, one "high" around $2.8 \cdot 10^{-7} \text{ cm}^3\text{s}^{-1}$, and the other "low" around $2.2 \cdot 10^{-7} \text{ cm}^3\text{s}^{-1}$.

From the first group the earliest are the results of Mahan and Young (1966). They used a microwave cavity technique to measure k_{att} (for SF_6 and also for C_7F_{14}) and produced a value of $3.1 \cdot 10^{-7} \text{ cm}^3\text{s}^{-1}$ ($\pm 25\%$). When the energy of the microwaves used for measuring the electron density was increased the temperature of the background gas increased and a small decrease of the attachment coefficient was observed. This observation was not illustrated by any quantitative data.

It seems that the treatment of diffusion losses in this paper may not have been as careful as it should have been. In fact a careful reading of Mahan and Young's paper reveals that diffusion losses were only roughly estimated, while some contradictory statements make a reanalysis of their data difficult for anyone not associated with the measurements. It is therefore no surprise that one of the authors has presented a different value for k_{att} (2.7 instead of 3.1) as a result of a reanalysis of the same set of measurements (Young 1966).

The work of Ayala et al. (1981) is also rather difficult to assess. Various modes of operation of the same system (i.e. the use of different radioactive sources to ionize the gas being studied) yielded quite different values (from 0.54 to $3.9 \cdot 10^{-7} \text{ cm}^3\text{s}^{-1}$; see also Chen et al. 1968) and the choice of the value accepted as the final result seems to have been mainly dictated by the agreement with the available experimental data from other sources. These authors have chosen MW and ECR (see Table 6.1)

results for comparison and have formed an average value that has helped them to decide which of their three values to choose as final. However, they failed to take into account all the MW (Fessenden and Bansal 1970) results which they quoted as well as omitting others altogether, e.g. Shimamori and Fessenden (1979). If these results are taken into account the results of Ayala et al. disagree with the average of those obtained by the experimental technique which they themselves believed provided the most reliable data. At some point in their paper the authors present $\pm 25\%$ as their experimental uncertainty but later on they quote 2.8 ± 0.3 as their final result. These estimates of uncertainty are inconsistent. Moreover the three different experimental results obtained using their experimental apparatus disagree by more than either of the estimates of experimental uncertainty. On the other hand these authors have not presented any explanation of why the three modes of operation of the apparatus yield three different results. Even though recently published, these results do not represent an improvement on any of the available data and should be treated with caution. On the other hand the results for the relative temperature dependence of the attachment rate coefficients and the derived activation energies should be reliable because no absolute measurements were involved.

Another result from the group of "high" values is the result of the swarm technique used by Christophorou et al. (1971a; and 1971b). In this technique dilute mixtures of an attaching gas with a buffer gas are used, and the attachment coefficients are measured for various field strengths. The results are then extrapolated to zero field. This technique relies on an accurate knowledge of transport coefficients and average energies in the pure buffer gases, and it is assumed that the electron distribution

function is not perturbed by a small amount of the attaching gas.

There are many problems in applying this swarm technique developed by Christophorou and coworkers. These include: the adequacy of the two-term approximation, the influence of attachment on the transport coefficients, the need for accurate data for the cross sections for the buffer gas (N_2 is normally used to study low energy attachment) and non-uniqueness of the derived cross sections due to the complexity of the processes involved. It is not surprising that reanalysis of the same data with a more reliable set of cross sections yielded a different value for the thermal attachment coefficient (namely $2.49 \cdot 10^{-7} \text{ cm}^3\text{s}^{-1}$ instead of $2.7 \cdot 10^{-7} \text{ cm}^3\text{s}^{-1}$ -see Table 6.1). Moreover, when values of attachment coefficients measured at even lower E/N values are used for the extrapolation, the value of $2.35 \cdot 10^{-7} \text{ cm}^3\text{s}^{-1}$ is obtained (Hunter 1984). This result is expected to be more reliable than the previous ones because the degree of extrapolation to thermal energy is significantly reduced (the lowest measured value is 2.4 - Hunter 1984). Therefore it may be concluded that swarm results can no longer be regarded as supporting the "higher" value of the attachment coefficient.

Of the "low" results, those of Fehsenfeld (1970), even though producing an average value that agrees with the result of Crompton and Haddad, are not inconsistent with the value of Smith et al. (1984). His results could also be regarded as not conflicting with Smith et al.'s observation of the temperature dependence since the scatter of the raw experimental data is large.

Of all the available data it appears that the results of Shimamori and Fessenden (1979) (which confirm the earlier results of Fessenden and Bansal 1970 who used the same technique) appear to be the most reliable.

Shimamori and Fessenden measured the attachment rate coefficient over a very wide range of pressures. The reproducibility of their results and the small degree of scatter are impressive and only surpassed by the work of Crompton and Haddad (1983).

In some cases the difference between the "low" and "high" values for the attachment rate coefficient for SF₆ is within the experimental error bars, but where the results have been obtained with high accuracy experiments the two groups of results cannot be reconciled. However, there appears to be more evidence in support of the lower value. One can criticize at least two papers supporting the "high" value, namely those of Mahan and Young (1966) and Ayala et al. (1981). The paper of Mothes et al. (1972) does not contain a detailed error assesment apart from the statement about the statistical scatter of the results which is 5%. On the other hand FALP is certainly a powerful technique for measuring thermal coefficients for a variety of processes and it is difficult to find any explanation for the high value for SF₆ that was obtained with it. Possibly the ambipolar field is not strong enough to keep the electrons in the centre of the plasma since they are repelled by the abundant negative ions. The overall breakdown of the ambipolar field can be observed at the end of the tube when the concentration of the charged particle becomes exceedingly small. However, the very different masses of the ions and electrons could lead to a redistribution of negative particles even before the end of the tube. Measurements should be made with the Langmuir probe positioned off axis to show that this is not the case.

6.3: Experimental

The principle of Cavalleri's electron-density sampling technique that was used to perform the measurements has been described in Chapter 4. For measurements of the attachment coefficients it is important to note that the time constants that are being measured with the attaching gas are normally much shorter than in most non-attaching gases. It is possible to choose conditions so that the time constants for the attaching gas (or mixtures of the attaching gas with some buffer gas) are fairly large, but in that case diffusion losses become increasingly important, or even dominant, and the accuracy of the attachment coefficient obtained under those circumstances is reduced. On the other hand if attachment is the dominant loss mechanism one has to take care of the following:

1. that the possible presence of higher order diffusion modes is accounted for,
2. that the measurements are made after thermalization of the electrons is complete,
3. that a sufficient number of electrons remains in the cell at the time of the measurement in order to achieve a reasonable statistical quality of the results.

The usual choice of operating conditions is such that the ratio of diffusion to attachment time constants (or the inverse of the losses) is 10:1.

Details of the experimental arrangement for the measurements at high temperatures were presented by Hegerberg and Crompton (1980) and will not be discussed here in great detail (see also Chapter 4). We simply note that the light-tight chamber housing the CDE was housed in an oven. The

temperature was held stable to within ± 0.3 K at 500 K during each individual run, while the maximum deviation of the temperature between the different runs of a set of measurements was 2 K. This temperature stability proved to be satisfactory since k_{att}^{th} was found to be relatively independent of the temperature in the range studied. At the time at which the gas was introduced into the cell the temperature was determined to within ± 0.2 K to enable the gas number density N in the cell to be determined to within ± 0.2 %. The cell was then isolated.

The diffusion coefficient in pure H_2 was also measured in order to check the performance of the cell at high temperatures (see Hegerberg and Crompton 1980), since it was possible that charge compensation would not be efficient under these conditions.

6.4: Measurement of Attachment Coefficients

6.4.1: Introduction. As mentioned in the section 4.3 the time constant for the decay of the electron population is determined from the ratio of light intensities. The formula that is used assumes a single exponential decay (see 4.1):

$$\tau = \frac{D}{\ln \left| \frac{N_e(S)}{N_e(S+D)} \right|} = \frac{D}{\ln \left| \frac{I(S)}{I(S+D)} \right|} \quad (6.5)$$

where $N_e(t)$ is the electron population in the cell at time t and $N_e(t) \propto I(t)$ as discussed above.

In this section the application of the CDE will be analysed in situations where attachment losses are significantly greater than diffusion losses and consequently the conclusions of Section 4.3 are inapplicable.

The continuity equation which describes the time dependence of the electron density $n(x,y,z,t)$ is (see equation 2.60):

$$-\frac{\partial n}{\partial t} + (v_i - v_{att})n + D_T \left(\frac{\partial^2 n}{\partial x^2} + \frac{\partial^2 n}{\partial y^2} \right) + D_L \frac{\partial^2 n}{\partial z^2} - v_{dr} \frac{\partial n}{\partial z} = 0 \quad (6.6)$$

where v_i and v_{att} are the ionization and attachment collision frequencies, D_T and D_L are the transverse and longitudinal diffusion coefficients, and v_{dr} is the drift velocity. This equation is relevant only to the situation where the electron population is fully thermalized (or in equilibrium with the field if present) and there are no nonequilibrium effects present such as diffusion or attachment cooling (see Rhymes and Crompton 1975; McMahon and Crompton 1983; Hegerberg and Crompton 1983; Skullerud 1983).

In the CDE the following conditions apply :

1) There is no applied field and stray fields are fully compensated in the all-glass cell (for a discussion of the compensation effects see Section 4.5). Therefore $v_{dr} = 0$, and $D_T = D_L = D^{th}$.

2) There is no ionization, i.e. $v_i = 0$.

Under these two conditions the solution of equation (6.6) is

$$n(\rho, z, t) = e^{-t/\tau_{att}} \sum_{m=1}^{\infty} \sum_{l=1}^{\infty} A_{ml} e^{-t/\tau_{Dml}} J_0\left(\frac{c_l \rho}{a}\right) \sin\left(\frac{m\pi z}{d}\right) \quad (6.7)$$

where a is the radius of the cell and d is its width,

$$\rho = (x^2 + y^2)^{1/2},$$

$$\tau_{att} = 1/v_{att} = 1/(k_{att} N_{att}), \quad (6.8)$$

$$\text{and } \tau_{Dml} = \{ND^{th} \left\{ \left(\frac{m\pi}{d}\right)^2 + \left(\frac{c_l}{a}\right)^2 \right\} / N\}^{-1}. \quad (6.9)$$

Here m and l are integers and c_l is the l^{th} zero of the zero-order Bessel

function $J_0(x)$. The coefficients A_{m0} are chosen so that the series expansion of the electron density distribution at $t = 0$ matches the real distribution. $N_{att} = Nf$ (where f is the abundance of attaching gas) is the number density of the attaching gas, and it is assumed that $N_{att} \ll N$.

It can be seen immediately from equation (6.7) that attachment is "decoupled" from the mode structure. This means that electrons that are lost by attachment are evenly distributed throughout the cell in proportion to the local electron density. Therefore whatever the mode composition the loss rate due to attachment is the same, although the loss rate due to diffusion depends on the mode composition and will vary until the fundamental mode alone remains. The presence of the higher order modes at early times presents a potential difficulty when calculating τ_{att} from the experimental measurements and therefore requires examination in some detail.

6.4.2: The effect of higher-order diffusion modes on the determination of the attachment time constant. A fundamental characteristic of the CDE limits the measurements to determinations of the ratio of the electron populations at two times separated by the delay time D rather than their absolute magnitudes. Fig. 6.1 shows typical time decay curves for the total number of electrons in the CDE cell. Curve A is for a non-attaching buffer gas, and curve B for a mixture of the buffer gas with an attaching gas. The decay in the mixture (characterized by the time constant τ) is faster than in the pure gas and therefore shorter starting times S must be used if the electron populations are to remain sufficiently large for a statistically reliable result. This is because it is not possible to vary the initial electron density by a large factor. The decay of the electron

number in the pure buffer gas at such short times is not necessarily exponential. Therefore one has to be careful to ensure that one calculates the diffusion losses accurately. If one were to overlook the fact that the electron number decay is not strictly exponential, one would use the time constant characteristic of the fundamental mode in the pure buffer gas τ_{D11} (labelled τ_{11} in Fig. 6.1). Alternatively, one could measure the time constant in the pure buffer gas using the same starting time S as was used for the measurement with the attaching gas mixture and optimize D to obtain the best possible statistics. To do this one would choose the value of D such that $I(S) = 3I(S+D)$. Figure 6.1 clearly indicates that, in this case, the measured time constant τ_{D2} would be dependent on the choice of D .

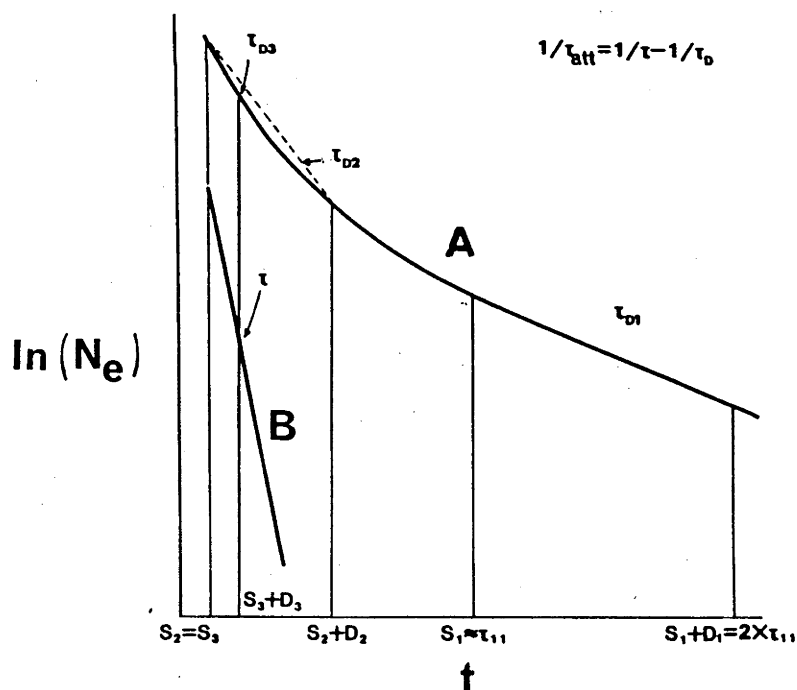


Figure 6.1 Typical decay of the total number of electrons in the CDE. See text for explanations and notation.

The third choice (yielding τ_{D3} in Fig. 6.1) would be to perform measurements using values of S and D that are identical to those used for the attaching mixture. In this case, however, the ratio of the amplitudes of the pulses in the pure buffer gas would be close to unity due to the delay time D being small compared to the time constant. The measured diffusion time constant obtained in such an experiment would therefore have a large uncertainty.

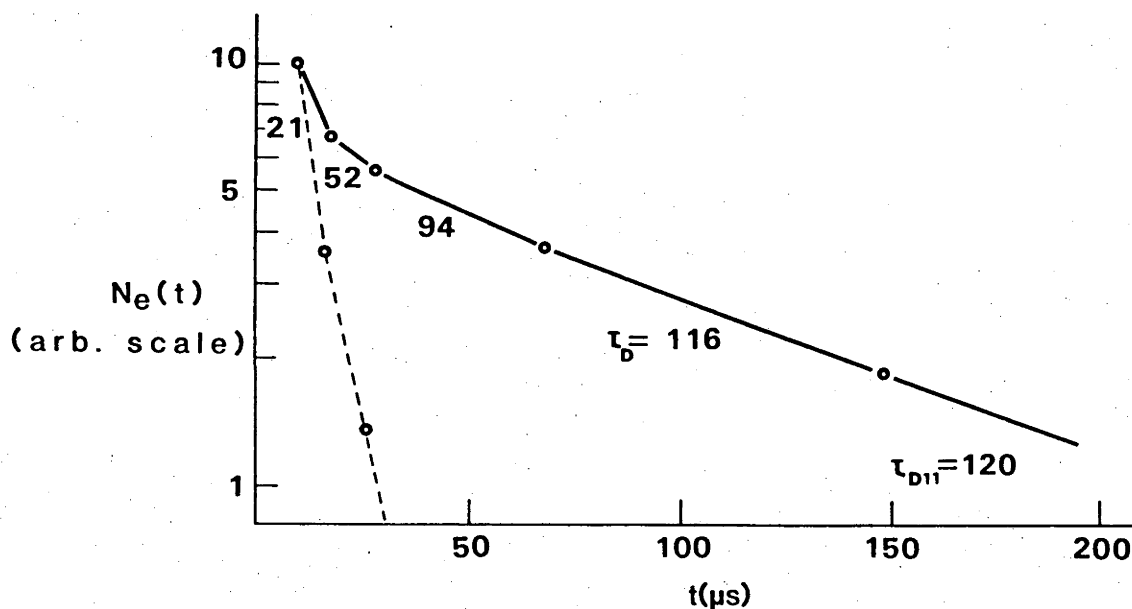


Figure 6.2 Measured electron population time dependence in pure H_2 (solid line) and in an SF_6 - H_2 mixture (dashed line). The time constants calculated on the basis of pairs of experimental points (-o-) are also shown.

An actual set of experimental results is shown in Fig. 6.2. Here the relative populations measured in pure H_2 and in a mixture with 0.568 ppm of SF_6 are shown. The initial value of $N_e(t)$ has been given the arbitrary value of 10, and renormalization of successive measurements has been made to generate the curves. Renormalization is necessary because the sampling

pulse amplitude must be progressively increased as the value of the starting time S is increased in order to maintain the photomultiplier signals within the range which gives maximum accuracy of the measured ratios.

This example clearly shows the necessity for making the measurements in the attaching mixture at times before the higher order diffusion modes have decayed. We must therefore discuss how to determine the diffusion losses with sufficient accuracy under such circumstances.

If it were possible to measure τ for the mixture at delay times which would ensure that the fundamental mode were the sole survivor, τ would be related to the attachment and diffusion time constants through the simple relation (see equation (4.19)):

$$\frac{1}{\tau} = \frac{1}{\tau_{\text{att}}} + \frac{1}{\tau_D} \quad (6.10)$$

where in this case $\tau_D = \tau_{D11}$. When this condition is not satisfied, however, the following argument shows that it is still possible to use equation (6.10) to calculate τ_{att} from τ provided the value of τ_D used is an effective diffusion time constant calculated from a measurement of the ratio $I(S)/I(S+D)$ in the pure buffer gas for values of S and D which match those for the measurement in the mixture, i.e. if τ_{D3} is used to represent the diffusion time constant.

Let us assume that several modes with time constants $\tau_{Dm\ell}$ are necessary to describe the electron density distribution. Then the time dependence of the number of electrons within the volume viewed by the photomultiplier (which may be part or all of the cell) is given by

$$N_e(t) = e^{-t/\tau_{att}} \sum_{m=1}^{\infty} \sum_{\ell=1}^{\infty} N_{em\ell} e^{-t/\tau_{m\ell}}, \quad (6.11)$$

where $N_{em\ell}$ is the result of integrating $A_{m\ell} J_0(c_{\ell} \rho/a) \sin(m\pi z/d)$ over the volume at time $t = 0$ (see equation (6.7)).

Let us assume that the measurements in the attaching mixture are made at times S and D , and those to determine the diffusion time constant for the pure buffer gas at times s and d . Then if equation (6.5) is used to relate the time constants to the populations, which are given in each case by equation (6.11) (but without the first exponential term in the case of the pure buffer gas), it follows from equation (6.10) that the apparent attachment time constant τ'_{att} is given by:

$$\frac{D}{\tau'_{att}} = \frac{D}{\tau} - \frac{D}{\tau_D} = \ln \left[\frac{e^{-S/\tau_{att}} \sum_{m=1}^{\infty} \sum_{\ell=1}^{\infty} N_{em\ell} e^{-S/\tau_{m\ell}}}{e^{-(S+D)/\tau_{att}} \sum_{m=1}^{\infty} \sum_{\ell=1}^{\infty} N_{me\ell} e^{-(S+D)/\tau_{m\ell}}} \right] - \ln \left[\frac{\sum_{\mu=1}^{\infty} \sum_{\lambda=1}^{\infty} N_{e\mu\lambda} e^{-s/\tau_{\mu\lambda}}}{\sum_{\mu=1}^{\infty} \sum_{\lambda=1}^{\infty} N_{e\mu\lambda} e^{-(s+d)/\tau_{\mu\lambda}}} \right] D/d. \quad (6.12a)$$

The first term on the R.H.S. of the equation (6.12a) reduces to:

$$\frac{D}{\tau_{att}} + \ln \left[\frac{\sum_{m=1}^{\infty} \sum_{\ell=1}^{\infty} N_{em\ell} e^{-S/\tau_{m\ell}}}{\sum_{m=1}^{\infty} \sum_{\ell=1}^{\infty} N_{me\ell} e^{-(S+D)/\tau_{m\ell}}} \right]. \quad (6.12b)$$

Equation (6.12) gives an apparent attachment time constant τ'_{att} derived by applying equation (6.10) to the general case, that is, when different

starting and delay times are used for the measurements in the mixture and in the pure buffer gas. The difference between the real attachment time constant τ_{att} and τ'_{att} becomes zero only when $s=S$ and $d=D$. In this case, since the two logarithmic terms in equation (6.12) may then be combined into a single term, the equation can be rewritten as:

$$\frac{D}{\tau'_{att}} - \frac{D}{\tau_{att}} = \ln \left[\frac{\sum_{m=1}^{\infty} \sum_{\ell=1}^{\infty} N_{em\ell} e^{-S/\tau_{m\ell}}}{\sum_{m=1}^{\infty} \sum_{\ell=1}^{\infty} N_{em\ell} e^{-(S+D)/\tau_{m\ell}}} \frac{\sum_{\mu=1}^{\infty} \sum_{\lambda=1}^{\infty} N_{e\mu\lambda} e^{-(S+D)/\tau_{\mu\lambda}}}{\sum_{\mu=1}^{\infty} \sum_{\lambda=1}^{\infty} N_{e\mu\lambda} e^{-S/\tau_{\mu\lambda}}} \right], \quad (6.13)$$

and it follows that the R.H.S is zero because it is always possible to cancel a term in the numerator with an identical term in the denominator.

This result partly rests on the fact that the presence of attachment does not influence the mode structure. Thus the experiment should be performed as a difference using the same sampling times S and $S+D$ for the measurements with and without attaching gas. In principle the imposition of this constraint on the measurement of τ_D presents no problem. In practice, however, it results in the accuracy of the measured value of τ_D being rather low. In order to optimize the accuracy of the measurement of τ in the mixture, the time D is chosen to be approximately equal to τ . In the pure buffer gas, therefore, $D \ll \tau_D$ and the accuracy with which τ_D can be measured is very much less than the accuracy of τ . (Note that even if $I(S)/I(S+D)$ could be measured with the same relative accuracy for all D the uncertainty in τ would approach infinity as $D \rightarrow 0$ - see section 4.2.) Fortunately the problem is not as serious as it may seem since the uncertainty in τ_D is not a large contributor to the uncertainty in τ_{att} because $\tau_D \gg \tau_{att}$ (see 6.10).

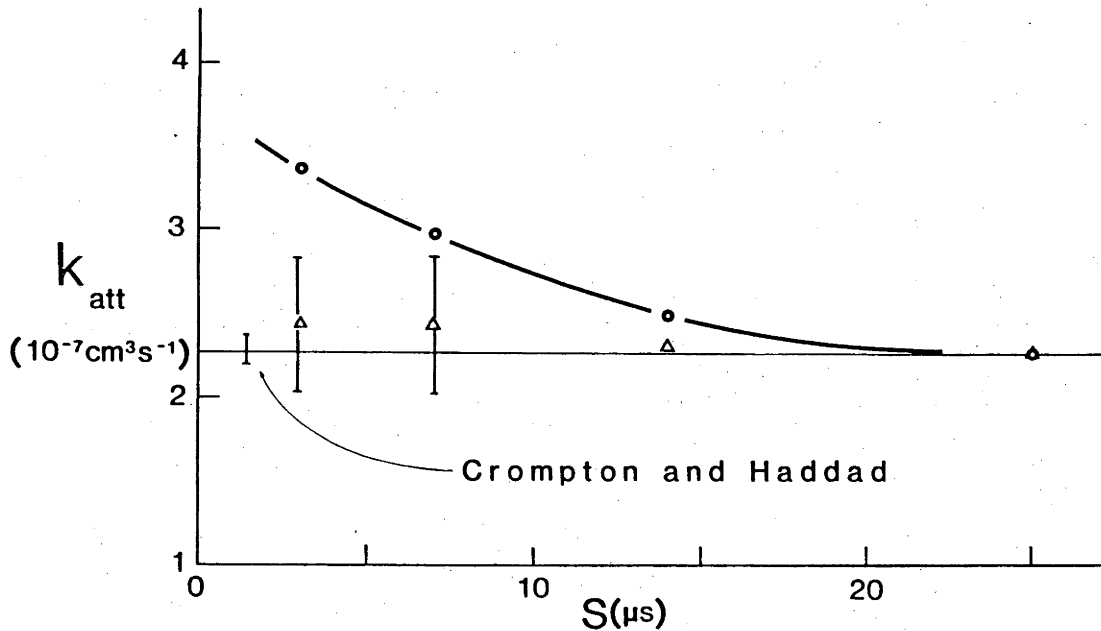


Figure 6.3 Anomalous dependence of results for $k_{\text{att}}^{\text{th}}$ on the starting time S when τ_{D11} was used instead of τ_{D} (—○—). Corrected results are shown as triangles with the corresponding error bars. These are only preliminary results that were used to determine the conditions for the final measurements. Crompton and Haddad's result is presented as a straight line with its error bar.

In the work of Crompton and Haddad (1983) the effect of using τ_{D11} rather than τ_{D} was not significant. Had it been so, there would have been a dependence of τ_{att} on S but this was not observed. In preliminary measurements in hydrogen, however, there was a significant dependence on S , the difference in behaviour being due in part to the fact that $\tau_{\text{D11}}^{\text{H}_2} \gg \tau_{\text{D11}}^{\text{N}_2}$. The results in hydrogen are shown in Fig. 6.3 where the full curve is drawn through values of k_{att} that were calculated from data recorded at various values of S on the assumption that $\tau_{\text{D}} = \tau_{\text{D11}}$. As expected k_{att} approaches an asymptotic limit as S increases. When the results were recalculated using values of τ_{D} that were measured subsequently in separate experiments no significant dependence on S was

found. Similar effects were observed with CO_2 as the buffer gas. From both sets of data the importance of correctly allowing for the presence of higher order diffusion modes was clearly evident.

6.4.3: Results for the attachment rate coefficient obtained using different buffer gases. The measurements of the attachment rate coefficient k_{att} using H_2 and CO_2 as buffer gases were made to supplement the earlier measurements of Crompton and Haddad. Results for both gases were obtained for $f = 0.568$ ppm. Pressures of 2 and 3 kPa were used for H_2 and 1 and 2 kPa for CO_2 . In all cases τ_D was determined in a separate measurement in the pure buffer gas with the appropriate S and D values. The purity of the buffer gas sample was checked by taking a measurement with $S = D = \tau_{D11}$. The expected value of the time constant was obtained in all cases, indicating that adsorption and desorption of SF_6 on the walls was negligible and that contamination of the vacuum system by SF_6 did not affect the composition of the mixture during the admission of the gas to the cell.

The average value of k_{att} with both buffer gases was found to be $2.27 \cdot 10^{-7} \text{ cm}^3\text{s}^{-1}$. All the results were within 1.5% of the average value, and no systematic pressure dependence was observed.

Possible sources of experimental error are: pressure and temperature (0.3%), nonlinearity of the detection chain (<0.5%), statistics (0.3 - 0.5%), mixture composition (<1%). For the reasons already described the time constant τ_D was determined under rather unfavourable conditions i.e. small S and D in comparison to τ_D . However the larger the value of τ_D the smaller is its contribution to τ in the mixture, and an increased uncertainty of τ_D in such a case has a small effect on the determination of

τ_{att} . An upper limit to the error due to the uncertainty of τ_D (which was between 2-10%) can be determined by calculating τ_{att} from equation 6.10 using the extreme values of τ_D . The contribution to the error was always less than 2%, and the overall uncertainty can therefore be estimated as less than 4%. This is an increase of 1% compared to the error quoted by Crompton and Haddad (1983). It does not mean that their error bounds on k_{att}^{th} for SF₆ need relaxing but rather that the use of H₂ and CO₂ as buffer gases introduces some additional difficulties compared with the use of N₂. On the other hand the accuracy of the measurements in H₂ and CO₂ is sufficient to fulfill the aim of the investigation.

6.4.4: The possible effect of a non-Boltzmann vibrational population on the attachment rate. It has been suggested (Smith 1984) that the difference between the results obtained by the FALP and CDE techniques might be a consequence of a possibly enhanced population of higher vibrational states of the molecular buffer gas (N₂) used in the latter experiments due to the "heating" action of the applied RF sampling pulses.

A non-Boltzmann distribution of vibrational states could have two effects. First, such a distribution might produce a quasi-stationary, non-thermal electron energy distribution through superelastic collisions (Capitelli et al. 1981; 1982; 1983). Whether or not this would significantly alter the attachment rate would depend on the extent to which the vibrational populations, and hence the distribution function, were changed, and the dependence of the attachment rate on the "electron temperature". However, the attachment rate is only weakly dependent on the electron temperature (Christophorou et al. 1971a) so that a significant error due to this effect seems unlikely. In any case, since a non-thermal

electron temperature produced in this way would depend on the composition of the buffer gas and since, as has now been found, the results for all buffer gases are consistent the effect, if present, is not significant.

A second possibility related to the build-up of an abnormal distribution of vibrational populations is that detachment might occur during the first step of the two-step attachment process (see, for example, Hansen et al. 1983) through collisions with vibrationally excited molecules of the buffer gas. After stabilization, detachment is unlikely to occur since the electron affinity of SF₆ appears to be of the order of 1 eV (Strait 1982). A necessary condition for the validity of this explanation of the difference between the CDE and FALP results is a significant build-up of the population of more highly excited molecules due to successive RF sampling pulses in the experiments. To check the likelihood of this calculations were made of the lifetimes of $v = 1$ states of N₂, H₂ and CO₂ against V-T relaxation through collisions with the parent gas molecules for typical experimental conditions ($T = 293$ K and $p = 1.33$ kPa) using the data from Lambert (1977 - see also Margottin-Maclou et al. 1971; Audibert et al. 1974; Yardley 1980). The results in Table 6.3 show that while abnormal vibrational populations in both H₂ and CO₂ are expected to decay through V-T relaxation in times that are short compared with the repetition times used in the experiments (1-4 s), the relaxation time constant for N₂ is large compared with any reasonable repetition time. Therefore it can be concluded either that N₂($v = 1$) states decay by collisions with the walls of the cell or that they cannot affect attachment to SF₆ since the results for all three buffer gases are the same. Note that higher vibrational states will decay faster than the $v = 1$ state (Yardley 1980).

The time necessary for excited states to diffuse from the centre of the tube to the walls (see Table 6.3) has been estimated using values of self-diffusion coefficients (Lambert 1977). Theoretical and experimental investigations (Kovacs et al. 1968; Ahtye 1972; Fujimoto et al. 1976) indicate that the effective diffusion coefficients for excited molecules differ from the self-diffusion coefficients by no more than a factor of two. This uncertainty in the diffusion coefficient is unimportant for our purpose. Once the excited molecules reach the walls they should make enough collisions with the walls to relax (see Doyennette et al. 1974; Black et al. 1974; Hiskes et al. 1982).

Table 6.3 Estimated times for vibrational relaxation (see text).

p=1.33kPa T=293K Gas	V-T relaxation*	Molecule Wall Collisions**
H ₂	25ms	20ms
N ₂	40s	110ms
CO ₂	600μs	150ms

* Data and references from Lambert (1977).

** This time is estimated as the time necessary for excited states to diffuse from the centre of the CDE tube to the walls.

The experiments with different molecular buffer gases provide strong circumstantial evidence that abnormal vibrational populations produced by the RF sampling pulses (or less probably by the initial X-ray ionization) do not affect the results. Nevertheless the most direct test is by the use of an atomic buffer gas. Unfortunately, the thermalization of electrons produced by the X-ray pulse in such gases is slow and the presence of an

attaching gas such as SF₆ is likely to diminish the electron population to an unacceptably low level before thermalization is achieved. An analysis of thermalization time constants and the problems caused by "diffusion cooling" (Rhymes and Crompton 1975; Mozumder 1980; Shizgal and McMahon 1984), shows that the only candidate for such a test would be helium (see Appendix 2), but the interpretation of experiments in which helium is used as a buffer gas is complicated by Penning ionization. The fast electrons produced by the X-ray pulse create a significant population of metastable He atoms before they are thermalized. These atoms may ionize SF₆ molecules, or impurity molecules present in the helium at levels that would not otherwise affect the results (Gibson et al. 1973). Electrons so released result in an anomalously slow rate of decrease of the electron population which is interpreted as an anomalously low attachment coefficient if the electron populations are sampled only at two times. If, on the other hand, measurements are made at a series of delay times the attachment coefficient appears to depend on these times since the electron population decay is no longer represented by a single exponential.

When Penning ionization involving a single metastable level and one molecular species occurs, the double exponential decay curve may be represented by the equation (see equation (4.22)):

$$N_e(t) = N_e(0) e^{-t/\tau} + f N_m(0) k_{\text{PENN}} T_{\tau} e^{-t/\tau_m}, \quad (6.14)$$

where f is the abundance of the molecular gas, $N_m(0)$ is the initial population of the metastable levels (the ratio $N_e(0)/N_m(0)$ can be determined in an independent experiment), k_{PENN} is the Penning ionization coefficient, $T_{\tau} = (1/\tau - 1/\tau_m)^{-1}$, and τ_m is the time constant for the decay of the metastable population. The time constant τ_m is mainly

determined by the losses through Penning ionization and collisional quenching in collisions with helium atoms (Bartell et al. 1973; Hurst 1974; Payne et al. 1975; West et al. 1975; Golde 1976; Muller III and Phelps 1980; Pouvesle et al. 1982).

In principle it is possible to analyse data obtained from the CDE for pure helium and for the He-SF₆ mixtures to derive the value of the attachment coefficient. However, this would be a rather involved procedure and would produce a result of no better accuracy than the result which can be obtained more easily by adopting the following approach. First, with the known value of k_{Penn} it can be shown that the coefficient of the second exponential term in equation 6.14 is less than $10^{-4}N_e(0)$, since τ_m is of the order of 0.3 to 2 ms (for the conditions of these experiments) and the measured value of $N_e(0)/N_m(0)$ is ≈ 0.3 . Thus for small values of S the second term in equation 6.14 can be neglected, whereas at larger times the first term decays rapidly due to attachment causing the second to become increasingly important. Therefore, as has been observed in the experiments, the measured time constant increases with S , and the apparent attachment coefficient obtained from equations (6.4), (6.5) and (6.6) (i.e. by neglecting Penning ionization) gradually decreases (see Fig. 6.4). However, the dependence of the coefficient on S is represented by a smooth curve, and it is possible to extrapolate the curve to zero time to obtain the true value of $k_{\text{att}}^{\text{th}}$.

For the measurements with helium it was necessary to reduce the number of electron-density samplings in the individual experiments because of the larger number of experiments associated with varying S . Consequently the statistical uncertainty of the results is increased to between 2% at $S = 10\mu\text{s}$ and 5% at $S = 49\mu\text{s}$. A simple extrapolation to zero S using a third-

order polynomial fit yields a value of k_{att}^{th} of $2.24 \cdot 10^{-7} \text{ cm}^3\text{s}^{-1}$. The uncertainty in this value can be estimated from the curves that correspond to the worst possible situation, that is, the dashed curves in Fig. 6.4. Note that the error bounds through which these curves are drawn allow for both the statistical and the maximum possible systematic errors. The uncertainty estimated in this way is $\pm 7\%$. Given this uncertainty the result for k_{att}^{th} obtained with helium as the buffer gas is in remarkably good agreement with that obtained with the molecular buffer gases and supports the earlier conclusion that the results in these gases are not falsified by possible effects from abnormal vibrational populations.

The conclusions from the discussion in this section may be summarized as follows:

- 1) It is questionable whether vibrationally excited N_2 molecules can influence SF_6^- ions at all.
- 2) Even if they could it seems doubtful that the vibrational populations are sufficiently changed in our experiments to have a significant effect because of the rate of vibrational energy relaxation either through V-T processes or through collisions with the walls.
- 3) The new experimental results with other molecular buffer gases and with helium show no dependence on the composition of the buffer gas and confirm the results obtained using N_2 .

It may be concluded therefore that the original results were not influenced by the presence of abnormal populations of vibrationally excited molecules.

Finally it may be noted that the investigation of the influence of buffer gases on measurements of k_{att}^{th} for SF_6 was carried out specifically to examine the possibility that the measurements using the Cavalleri

electron-density sampling technique were influenced by the buffer gas. On the other hand, the work of Davis and Nelson (1970) was aimed at proving that the attachment of electrons to SF_6 is a saturated three-body reaction at the low pressures used in their experiments and ours. Their conclusions have been accepted in this investigation.

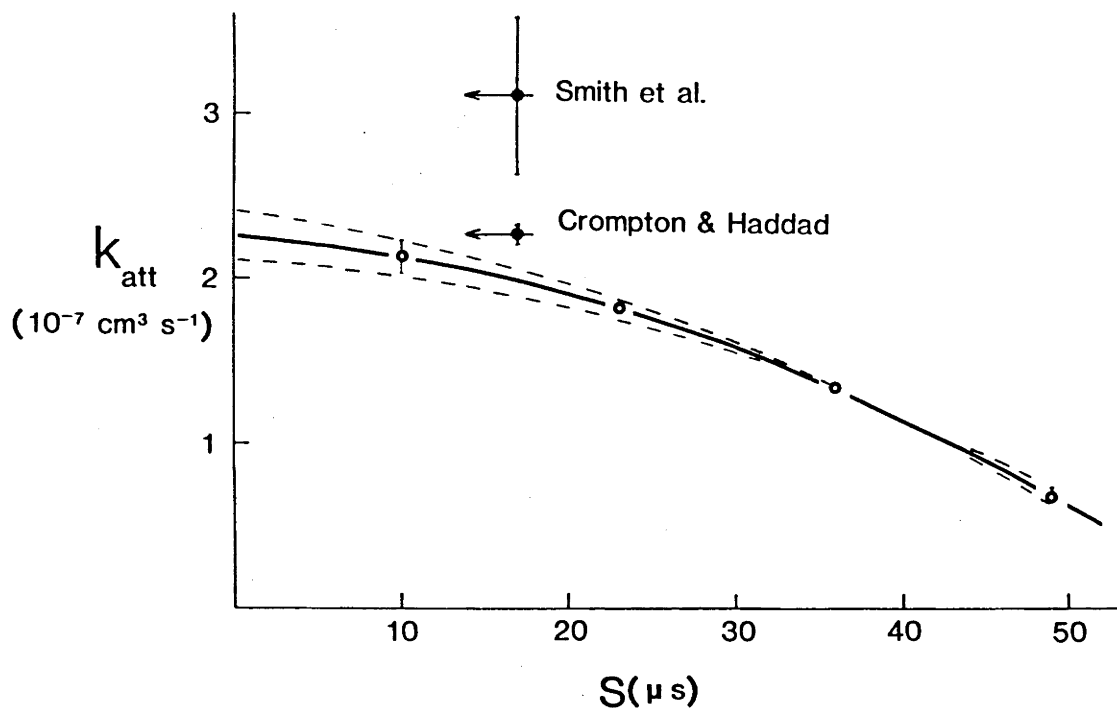


Figure 6.4 The dependence of the effective attachment coefficient in He- SF_6 mixtures which is caused by Penning ionization. The influence of this process at S close to zero should be negligible, and the curve is extrapolated to $S=0$. The dashed curves represents the fits to the data in the worst possible cases and correspond to the experimental uncertainty of $\pm 7\%$. Results of Crompton and Haddad (1983) and Smith *et al.* (1984) are shown as arrows with their corresponding experimental uncertainties.

6.5: The Temperature Dependence of k_{att}^{th} for SF₆

As mentioned above, values of k_{att}^{th} can be used to normalize experimental or theoretical cross section data. In addition, the variation of k_{att}^{th} with gas temperature provides an important check on the shape of the cross section and on the role of vibrationally excited levels.

As mentioned above Fehnsenfeld (1970) measured k_{att}^{th} for SF₆ in the temperature range 300 to 500 K and observed no temperature dependence. Similar results were obtained by Compton et al. (1966), Mahan and Young (1966) and Spence and Schulz (1973). On the other hand, Smith et al. (1984) observed a significant increase in the attachment rate with a peak of $4.5 \cdot 10^{-7} \text{ cm}^3 \text{ s}^{-1}$ at 450 K, that is, 45% above their 300 K value, and suggested that such a temperature dependence could be a manifestation of a cross section that peaks at energies less than kT (McCorkle et al. 1980).

Measurements of k_{att}^{th} were made at 500 K where Smith et al. obtained the value of $4.0 \cdot 10^{-7} \text{ cm}^3 \text{ s}^{-1}$, a value that is still 30% above their 300 K value. Results were obtained using numerous samples of mixtures containing 0.568 and 1.134 ppm of SF₆, and pressures of 4 and 6.613 kPa. The average value is $2.20 \cdot 10^{-7} \text{ cm}^3 \text{ s}^{-1}$ ($\pm 4\%$). The scatter of the data is less than 1.5%. No systematic dependence on pressure or SF₆ abundance was observed. Hydrogen was used as a buffer gas since its behaviour at high temperatures in the CDE has already been well established (Hegerberg and Crompton 1980). Again measurements were performed both with the mixture and with the pure gas. Measurements were made with the pure gas both with S and D values that matched those in the mixture, and with larger values of S ($S = \tau_{D1.1}$) to check the purity of the sample (see Section 6.4.1).

A time dependence of the results was observed in this set of measurements. A small time dependence was also observed at room temperature when CO_2 was used as a buffer gas. In both cases it was established experimentally that this was caused by the dissociation of SF_6 by the sampling pulses. It is possible to vary the amplitude of the sampling pulse and to compensate for the resulting change in the amplification of the electron avalanches by changing the gain of the photomultiplier amplifier. By reducing the amplitude it was possible to eliminate the time dependence of the results completely at 294 K, and to minimize it at 500 K. The reason for the failure to eliminate it entirely at 500 K is the large increase in population of more highly vibrationally excited states of SF_6 at that temperature. These states can be dissociated more easily during the sampling pulse. Products of the dissociation, or those which result eventually from reactions with the buffer gas, either do not attach at these energies or have a much smaller attachment rate coefficient (Sauers et al. 1980). It was established that the time dependence (which causes $k_{\text{att}}^{\text{th}}$ to decrease, corresponding to a depletion of SF_6) is close to linear and therefore some results at 500 K could be obtained by extrapolation to zero time. The time dependence was not very strong and normally 5-10 points were within the error bounds of the value obtained by extrapolation. Most of the data were taken by replacing each gas sample after a very short time (and therefore after exposure to a relatively small number of sampling pulses) and combining the results of several such experiments in order to produce the average value and the statistical uncertainty. It is believed that these two procedures when carefully implemented did not introduce any additional errors.

The present value of $k_{\text{att}}^{\text{th}}$ for SF_6 at 500 K is within the error bounds

of the room-temperature result. However, the decrease of approximately 3% is considered to be real since the reproducibility of the data is better than 3% and most of the systematic errors would affect both experiments in the same way. The result is in agreement with the result obtained by Fehsenfeld (1970) and is consistent with findings of Mahan and Young (1966) and Spence and Schulz (1973) who observed no temperature dependence. On the other hand, the result is in disagreement with the significant temperature dependence observed by Smith et al. (1984).

The experimentally determined cross sections of Chutjian (1981) and McCorkle et al. 1980 are consistent with a rate coefficient that is independent of the temperature, or even with one that slightly decreases; Chutjian's cross section predicts that k_{att} should decrease by 10% over this temperature range. The insensitivity of k_{att}^{th} to temperature calculated on the basis of these cross sections is due to the fact that the energy dependence of the cross section can be well approximated by $\epsilon^{-1/2}$, and hence the attachment collision frequency is almost constant. At higher energies the dependence becomes ϵ^{-1} which leads to a slow decrease of k_{att}^{th} with temperature (see Klots 1976 and also Chutjian 1982). The above mentioned decrease of 10% found using Chutjian's cross section was obtained using the exponential forms of the cross section suggested by the author. (Over the temperature range of the present experiments, dissociative attachment of SF_6 - see Fehsenfeld 1970; Kline et al. 1979; McCorkle et al. 1980; Smith et al. 1984 - does not play an important role.)

Chutjian and Alajajian (1985) have remeasured the cross section for electron attachment to SF_6 and reached lower energies than were achieved in the original experiments of Ajello and Chutjian. These authors found a sharp peak at very low energies and noted that the best fit to their data

could be achieved by using the Wigner threshold law which they applied in the form $\sigma_{att} = A\{a(\epsilon^{-1/2} - \epsilon_c^{-1/2}) + e^{-\epsilon/\gamma}\}$ where ϵ is the electron energy and ϵ_c was chosen to be 12 meV. The parameter a was varied to obtain the best fit to the energy dependence of the cross section, while A was used to normalise the value of k_{att}^{th} calculated from the cross section to the value measured by Crompton and Haddad (1984). However, Chutjian and Alajajian's cross section leads to a much larger decrease of k_{att}^{th} with increasing temperature, namely 35%. It is too early to say whether this is in disagreement with the present results because the temperature dependence of the cross section itself has not been determined. Also there is an indication that there was a numerical error in the fit to the experimental data (Chutjian 1984-personal communication to R. W. Crompton) and that the peak is not as sharp as initially indicated. Therefore one would expect a decrease of between 35 and 10% for the temperature dependence of k_{att} in the temperature range 300 to 500 K using the new cross section of Chutjian and Alajajian. As already stated, at 500 K higher vibrational levels become highly populated (for example the energy of one of the vibrational modes is 43 meV which is very close to the value of kT at 500 K). Apart from being more readily subject to dissociative attachment (see Chen and Chantry 1979), higher vibrational states of SF_6 could also have quite different cross sections for non-dissociative attachment from the ground state (see Gauyacq and Herzenberg 1984). The change in the effective cross section (that is, the cross section averaged over the vibrational populations at a given temperature) with temperature is therefore uncertain. This could explain the fact that there is still a disagreement between the decrease of 3% observed here and the calculated decrease of between 10 and 35%. However, a much larger dependence of the effective

attachment cross section on temperature would be required to produce an increase as large as that observed by Smith and coworkers.

Gauyacq and Herzenberg have produced two model cross sections for SF₆ that give an the independence of k_{att}^{th} with temperature. One of these has a sharp peak at low energies and could be consistent with the observation of Chutjian and Alajajian (1984). The presence of a sharp peak close to zero energy could also explain the relatively high values obtained by Foltz et al. (1977).

As a final comment we may examine the possibility that attachment cooling might be the source of the discrepancy between the results of the CDE and FALP techniques. It is true that a sharp attachment cross section can induce a "hole burning" effect on the electron energy distribution function as discussed by Crompton et al. (1980 - see also Hegerberg and Crompton 1983; Skullerud 1983; McMahon and Crompton 1983). However, this effect would be revealed when the abundance of the attaching gas is changed, and in neither the present experiments nor those of Crompton and Haddad (1983) was this observed. Changing the buffer gas would also make this effect evident since the various gases that were used have very different energy exchange rates in the relevant energy region, extending from the low rate due to the highly inefficient elastic exchange in He to the high rate associated with the very efficient energy exchange process of rotational and vibrational excitation of numerous levels of H₂ and CO₂. It may be concluded therefore that the results were not subject to attachment cooling. This conclusion is consistent with expectations based on the energy dependence of the cross section. Except perhaps at energies very near zero, where there are very few electrons in the thermal swarms at the temperatures of these experiments, the attachment collision frequency is

nearly independent of energy. Attachment cooling effects should therefore be minimal.

6.6: Conclusion

In this chapter results have been presented for the attachment coefficient of electrons to SF₆ obtained at room temperature (294 K) using H₂, CO₂ and He as buffer gases ($2.27 \cdot 10^{-7} \text{ cm}^3 \text{ s}^{-1}$) and at 500 K using H₂ as the buffer gas ($2.20 \cdot 10^{-7} \text{ cm}^3 \text{ s}^{-1}$). The results were independent of the pressure and of the choice of the buffer gas. The results show that the application of the Cavalleri electron-density sampling technique to the measurement of $k_{\text{att}}^{\text{th}}$ for SF₆ (Crompton and Haddad 1983) was not subject to errors caused by the detachment of negative ions by vibrationally excited molecules or by the presence of higher-order diffusion modes in the cell. However, it has been shown that one has to guard against possible errors from these effects.

The work described here was motivated first by the apparent inconsistency between the results of Crompton and Haddad for the thermal attachment rate coefficient at room temperature and the very recent results of Smith et al. (1984), and second by the difference between the temperature dependence observed by Smith et al. and that reported by others earlier, especially since Smith et al.'s observation of a positive dependence up to 450 K is unexpected in the light of what is known of the energy dependence of the attachment cross section. Measurements with several buffer gases confirm the confidence limits placed on the earlier measurements using Cavalleri's electron-density sampling technique, while the high temperature measurement does not support the temperature

dependence observed by Smith et al (1984) but appears to be more consistent with what is known of the energy dependence of the attachment cross section and the possible effect of temperature on the cross section.

CHAPTER 7: ATTACHMENT OF THERMAL ELECTRONS TO METHYL BROMIDE7.1: Introduction

Previous measurements of attachment coefficients for methyl bromide (or values calculated using measured attachment cross sections) indicate a very sharp temperature dependence (Wentworth *et al.* 1969; Spence and Schulz 1973; Alge *et al.* 1984; see also Massey 1976; Christophorou 1980). For instance Alge *et al.* (1984) observed an increase of more than two orders of magnitude over the temperature range between 300 and 585 K. This property could lead to some special applications of CH₃Br in gaseous electronics. In the present work experiments were carried out to verify the temperature dependence mentioned above and also to test the performance of the CDE when there is an extremely strong temperature dependence of the attachment coefficient.

Our motivation for measuring k_{att}^{th} for this gas also came from the fact that there is a significant scatter of the data recorded at room temperature (see Table 7.1). Differences almost as large as three orders of magnitude have been recorded. One could disregard the results of Blaunstein and Christophorou (1968) and Christodoulides and Christophorou (1971) on the grounds that these results must be in error because they differ from the others by orders of magnitude, but even then the scatter of the remainder is large enough (3.6 to $10 \cdot 10^{-12} \text{ cm}^3\text{s}^{-1}$) to warrant an attempt to produce a more accurate result.

The process of electron attachment to CH₃Br at low energies is a dissociative one



Stockdale et al. (1974), using a beam technique, found that the cross section has a maximum at 0.35 eV. On the other hand Christodoulides and Christophorou (1971) used a cross section $\sigma_{att}(\epsilon)=A/\epsilon^Y$ that peaks at subthermal energies which is in contradiction with the findings of Stockdale et al. The present work, along with other published data (Alge et al. 1984) provides the means of testing which of the two cross sections is correct.

Table 7.1 Thermal electron attachment coefficients for CH₃Br
for temperatures in the range 293-300 K.

k_{att}^{th} (10^{-12} cm ³ s ⁻¹)	Accuracy	Buffer gas	Reference	Method
3300 ^a		N ₂	Blaunstein and Christophorou (1968)	SW ^b
4.9 ^c			Wentworth <u>et al.</u> (1969)	PS
10 ^c (120 C)			Johnson <u>et al.</u> (1969)	PR
10 ^d			Schlinder (1971)	ECR
1000		N ₂	Christodoulides and Christophorou (1971)	SW
3.6			Mothes <u>et al.</u> (1972)	ECR
7.0	± 0.4 ^e	pure CH ₃ Br	Bansal and Fessenden (1972)	MW
7.1	± 0.7	C ₃ H ₈	" "	
6.0	± 3.0	Ar, He	Alge <u>et al.</u> (1984)	FALP
6.7(8)	± 0.2(7)	H ₂	present work	CDE

^a Obtained on the basis of the data published by Lee (1963)

^b Symbols have the same meaning as for the Table 6.1

^c Obtained by Bansal and Fessenden (1972) on the basis of the data from the paper by Wentworth et al. and Johnson et al.

^d Quoted by Mothes et al.

^e Error bars shown here are basically the scatter of the data for the pure gas. For the mixture with C₃H₈ these authors observed a pressure dependence of the results within the quoted error bars

7.2: Room Temperature Results

Matheson research grade CH_3Br (nominal purity 99.5%) was used in the present work. Contrary to claims in the manufacturer's catalogue and on the cylinder itself, the gas above the pressurized liquid CH_3Br was mainly N_2 and not CH_3Br . Even when this buffer gas was removed the impurity level exceeded the stated figure. An analysis by CIG, Sydney, showed a total impurity level of 1.83% (comprising 1.2% of N_2 and 0.58% of O_2 and Ar). Fortunately it was possible to reduce the level of impurities significantly by numerous fractional distillations at liquid nitrogen temperature. The results were found to be stable after the first and subsequent distillations. Therefore it was estimated that the influence of those impurities was much less than 0.5% in reducing the attachment coefficient by dilution of the pure CH_3Br . The presence of impurities that would increase $k_{\text{att}}^{\text{th}}$ was not detected (note that at the pressure of 2 kPa the effective two body attachment coefficient of O_2 - see Hegerberg and Crompton 1983 - is still almost an order of magnitude smaller than that for the pure methyl bromide). Any contamination could not have come from the apparatus itself since measurements performed in the pure buffer gas (H_2 in this case) yielded correct results.

No time dependence of the results was observed during a span of 4-5 days - i.e. 5-6 complete runs. After 5 days a reduction of 1% in $k_{\text{att}}^{\text{th}}$ was observed, presumably due to a loss of CH_3Br caused by dissociation during the sampling pulses. Surprisingly no effects of adsorption and desorption were observed. Many direct checks were performed similar to those for H_2O (see Section 5.3.2). For example in one of these checks measurements were performed either by using a fresh sample of the mixture

at a given pressure p or by reducing the pressure to p from a higher value. No difference between the results was observed. The absence of detectable adsorption effects was unexpected since adsorption of H_2O , which has a similar dipole moment, is very pronounced.

Initially attempts were made to perform the measurements at room temperature in the same way as those for SF_6 i.e. using mixtures of CH_3Br in H_2 whose compositions were such that it was necessary to make the measurements at times much shorter than the time constant for the fundamental diffusion mode (τ_{D11}). The abundances for these mixtures were chosen such that $\tau_{att} \approx \tau_D/10$. Since the thermal attachment coefficient for CH_3Br is much smaller than for SF_6 the abundances were several percent ($f=1.15$ and 2.30%) rather than the few ppm used for the SF_6 measurements. However, the results from these initial experiments (see Table 7.2) showed an unexpected pressure dependence.

Table 7.2 Pressure dependence of the apparent attachment coefficients in CH_3Br

p (kPa)	k_{att}	k_{att}^{corr} ($10^{-12} \text{ cm}^3 \text{ s}^{-1}$)
1	2.57	6.30
2	5.59	6.60
4	6.25	6.80
5.06	6.27	6.90
7.30	6.29	7.04

At higher pressures the values tended to saturate at 6.30 but at lower pressures the change of k_{att} was quite dramatic. This could not be explained by any experimental error. It was therefore decided to examine

the possibility that the explanation lay in the breakdown of the assumption that diffusion losses in the pure buffer gas and in the mixture containing 1 or 2% of CH_3Br are identical. As a first approximation it was assumed that the value of k_{att} at the highest pressure (7.30 kPa) is not significantly in error as a result of assuming that the diffusion time constant for the mixture (τ_D') is equal to the diffusion time constant for pure hydrogen. Using this value of k_{att} the value of τ_D' was calculated from the measured time constant at the lowest pressure where diffusion losses are a maximum. This value was found to be very different from τ_D for H_2 . Using the value of $N\tau_D'$ corresponding to this value of τ_D' , the values of k_{att} were recalculated to give the data shown as $k_{\text{att}}^{\text{corr}}$ in Table 7.2. This step removed much of the pressure dependence but some still remained.

The value of τ_D' was calculated on the assumption that the influence of higher order diffusion modes was negligible. However at the highest pressures this assumption is definitely incorrect. At 7.30 kPa, where the results were used to calculate τ_D' , $\tau_D=54 \mu\text{s}$ whereas the measured time constant was $6.71 \mu\text{s}$.

The preceding discussion shows that it is necessary to determine τ_D' for the mixture as well as $k_{\text{att}}^{\text{th}}$, which requires measurements at two or more pressures and their subsequent analysis. However, it is clearly necessary to choose mixture compositions and pressures that avoid the necessity of measuring electron populations at times significantly shorter than the time constant for the first diffusion mode. (Note that the extremely dilute mixtures used in the SF_6 measurements made it unnecessary to measure τ_D' , and that the "difference" technique described in Section 6.4.2 is not applicable to the CH_3Br measurements because it is not

possible to determine an effective τ_D (which is necessary when the measurements are made with the starting time much shorter than the time constant for the fundamental diffusion mode) because of the influence of the CH_3Br on the diffusion losses.).

The value of τ_D' calculated from the first-order analysis of the data described above was used to estimate the diffusion coefficient of the mixture and to choose the experimental conditions such that $S > \tau_D'$. In order to meet this requirement the mixtures were diluted and lower pressures were used. The final measurements were made with $f = 1.149\%$ and 0.574% with $p = 0.5, 1, 1.5$ and 2 kPa in the first case and $p = 1, 2$ and 3 kPa in the second. Results at both abundances and for all the combinations of pressures agreed very well. The average value of $k_{\text{att}}^{\text{th}}(\text{CH}_3\text{Br})$ is $6.78 \cdot 10^{-12} \text{ cm}^3\text{s}^{-1}$ with a scatter of ± 0.11 ($< 1.7\%$). This relatively large scatter is due to the results derived from pairs of time constants measured at pressures that were close to each other, for example, the data obtained at 0.5 and 1 kPa gave a value of $6.69 \cdot 10^{-12} \text{ cm}^3\text{s}^{-1}$. On the other hand the results derived from more widely spaced pressures agree very well with the average value, for example, the pair of measurements at 0.5 and 2.0 kPa gave the value $6.76 \cdot 10^{-12} \text{ cm}^3\text{s}^{-1}$. The overall uncertainty is estimated to be ± 0.27 . This includes all the possible sources of error as in the case of SF_6 but here the uncertainty in τ_D is removed, and the abundance could be determined much more accurately (to within $\pm 0.2\%$) in the mixing volume with the ratio $\approx 1:17$. On the other hand, the statistical scatter of the results as given above is somewhat larger due to the need to combine two results in the formula (4.19). The final result for $k_{\text{att}}^{\text{th}}$ is compared to other available results in Table 7.1.

7.3: Diffusion Coefficient for Thermal Electrons in CH₃Br

The additional benefit of the procedure described in the previous section is the possibility to determine the diffusion coefficient for the mixture and eventually for pure CH₃Br. The results are: for the f=1.149% mixture $ND_{\text{mix}}^{\text{th}}=1.95 \cdot 10^{21} \text{ cm}^{-1}\text{s}^{-1}$ and for the f=0.574% mixture $ND_{\text{mix}}^{\text{th}}=2.50 \cdot 10^{21} \text{ cm}^{-1}\text{s}^{-1}$. The overall uncertainty of these results is ± 0.10 ($\pm 5\%$). This uncertainty is larger than it might be, due to the choice of conditions for the experiment which were selected to favour the determination of $k_{\text{att}}^{\text{th}}$ rather than τ_D (the delay time D was $\approx \tau \approx \tau_D/2$). Consequently the scatter of the data was $\pm 2.5\%$. Again agreement with the average value was much better than this figure for the results derived from the pairs of time constants measured at the more widely spaced pressures.

The large difference between τ_D' obtained from these measurements and τ_D for H₂ proved that the explanation of the pressure dependence was correct and that one could not neglect the influence of CH₃Br on the diffusion loss even at the 0.5% level of that gas. The result for τ_D' also showed that the values that were chosen for S in the final measurements satisfy the condition that $S > \tau_D$ and that the influence of the higher order modes could therefore be neglected.

Having determined the diffusion coefficients in the mixture Blanc's law (see Chapter 5) was used to calculate $ND_{\text{CH}_3\text{Br}}^{\text{th}}$. The value of $3.98 \cdot 10^{22} \text{ cm}^{-1}\text{s}^{-1}$ was used for $ND_{\text{H}_2}^{\text{th}}$ (see Huxley and Crompton 1974). This value was confirmed by measurements in pure H₂, and is in very good agreement with the value calculated from the hydrogen momentum transfer cross section given in Chapter 9. The results for $ND_{\text{CH}_3\text{Br}}^{\text{th}}$ derived in this way from the 1.149% and 0.5745% mixtures were $4.3(4) \cdot 10^{19}$ and $3.8(2)$

$10^{19} \text{ cm}^{-1} \text{ s}^{-1}$ respectively.

The dependence of the diffusion coefficient on the abundance suggested that Blanc's law was not applicable in this case without modification (see Chapter 5), and that the results required correction. In order to apply corrections one must know something about the shape of the cross section, but to our knowledge data for CH_3Br are not available in the literature. However, it was noted that the dipole moment for CH_3Br is 1.81 Debyes (for H_2O it is 1.85; see West 1982) which is moderately high. For molecules with such dipole moments electron scattering at low energies is dominated by the electron-dipole interaction (Altshuler 1957; Itikawa 1978; Fabrikant 1980; and 1983; and Norcross and Collins 1982). Hence it is possible to approximate the energy dependence of the cross section (see 5.2.4) with:

$$\sigma_m = A \epsilon^{-\alpha} \quad (7.2)$$

(Altshuler 1957; Christophorou and Pittman 1970) or :

$$\sigma_m = A \epsilon^{-1} \psi(\epsilon) \quad (7.3)$$

where $\psi(\epsilon)$ is a very slowly varying function of the electron energy ϵ (Fabrikant 1977a and 1977b). In the present analysis the same exponent in (7.2) was adopted as was quoted in Chapter 5 for H_2O , namely $\alpha=1.075$. It is well known that cross sections for polar molecules are approximately proportional to the dipole moment (Norcross and Collins 1982), and the fact that the values of the dipole moment for H_2O and CH_3Br are very close seemed to justify the choice of the energy dependence. This is nevertheless a somewhat arbitrary choice and some other value of α would lead to a slightly different result for A and for ND .

The same type of calculation as described in Chapter 5 was carried out

but this time A was varied, keeping α fixed, until agreement was reached between the values of ND_{mix} for the two abundances. A was found to be 23 (for energy in eV and the cross section in 10^{-16} cm^2). It is difficult to assign error bars to A as the value of A would vary if one were to change α , but with α fixed, A was determined to within less than $\pm 10\%$. With these values of A and α the value of the diffusion coefficient for pure CH_3Br is $ND^{\text{th}} = 6.3 \pm 0.5 \cdot 10^{19} \text{ cm}^{-1} \text{ s}^{-1}$. The corrections to the results from the direct application Blanc's law are 13.9 and 15.6% at the two abundances, but the zero abundance limit of the correction (see Chapter 5) is quite large, i.e 60%.

If one forms the ratio of $(ND^{\text{th}})^{-1}$ for H_2O and CH_3Br one gets 1.05 which is quite close to the ratio of the dipole moments which is 1.02. The ratio is also consistent with the fact that the energy-averaged cross section is proportional to the dipole moment (ND is not strictly speaking proportional to $\langle \sigma \rangle^{-1}$).

It should be added that if one chooses $\alpha=1$ the result for ND is slightly different but still within the quoted error bounds. In addition, it is not possible to achieve a satisfactory fit to the data for the two abundances if α varies by more than 10-15%.

7.4: The Temperature Dependence of $k_{\text{att}}^{\text{th}}$

Measurements at two additional temperatures were made using a technique similar to that used for SF_6 . Since $k_{\text{att}}^{\text{th}}$ was reported to be strongly temperature dependent (Wentworth et al. 1969; Alge et al. 1983) it was necessary to use much lower abundances thus enabling the difference technique (see Section 6.4.2) to be used for these measurements.

At the temperature of $T=498.8\text{K}$ an abundance of CH_3Br of 206 ppm and pressures of 3 and 5.37 kPa were chosen. The result at this temperature is $k_{\text{att}}^{\text{th}}=4.40 \cdot 10^{-10} \text{ cm}^3\text{s}^{-1}$. The scatter of results is less than $\pm 2\%$ and the overall uncertainty $\pm 0.18 \cdot 10^{-10} \text{ cm}^3\text{s}^{-1}$ ($\pm 4\%$). The same relative uncertainty applies to the result at 445.3 K which is $k_{\text{att}}^{\text{th}}=1.83 \cdot 10^{-10} \text{ cm}^3\text{s}^{-1}$. This result was obtained using $f=0.1067\%$ and pressures of 2 and 3 kPa. Only at the highest temperature was a time dependence of the time constants observed. The final results were obtained as a linear interpolation to zero time and were highly reproducible.

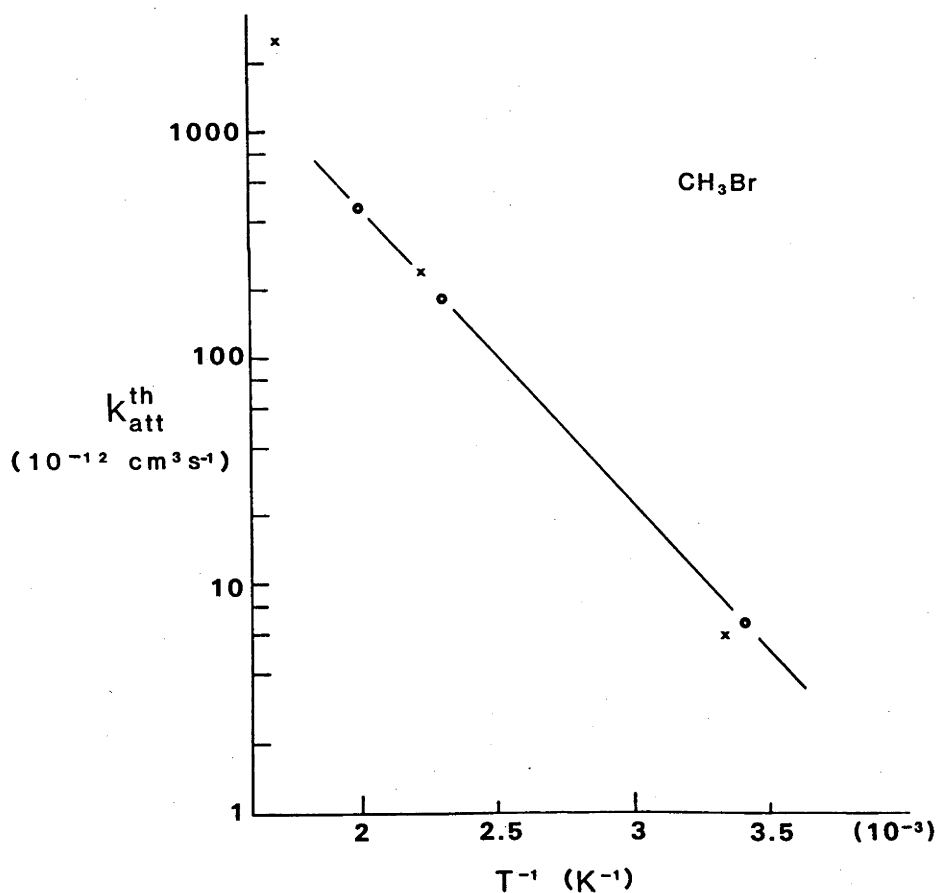


Figure 7.1 Arrhenius plot for CH_3Br . Present data are shown using (o) and the data of Alge et al. (1984) using (x).

The present data at various temperatures are shown in Fig. 7.1. At room temperature the present result agrees extremely well with the results of Bansal and Fessenden (1972) and Alge et al. (1984). The latter result has a rather large uncertainty ($\pm 50\%$). The present results are consistent with an electron attachment cross section that has a peak and a threshold at some energy higher than thermal and is therefore inconsistent with the cross section that was used in the analysis of the swarm data by Blaunstein and Christophorou (1968) and Christodoulides and Christophorou (1971). It also seems that the results used in the analysis of these authors were subject to some error, possibly caused by the influence of CH_3Br on electron transport even at low abundances (although the large σ_m for CH_3Br would improve the thermalization and it is therefore difficult to see an explanation for the failure of the swarm technique as implemented by these authors in the case of CH_3Br). Data for similar molecules obtained by authors from the same group indicate that the the threshold for CH_3Br should be larger than the thermal energy (Goans and Christophorou 1975). Another possible cause for the disagreement is that Lee (1963) and Christodoulides and Christophorou (1971) may have used an incorrectly labelled gas cylinder (Hunter 1984 - personal communication).

The present results at different temperatures lie on a very well defined straight line in an Arrhenius plot of $\ln(k_{\text{att}})$ vs. $(1/T)$ (Fig. 7.1). The activation energy for CH_3Br derived from this plot is 260 ± 15 mV. This value is in excellent agreement with the result of Wentworth et al. (1969), which is 247 mV, and the result of Alge et al. of 300 mV. However the interpretation of Arrhenius plots is questionable since plots of data for processes having cross section of an arbitrary shape (rather

than a constant cross section) would not yield a straight line. These plots are however still widely used and the "activation energy", if positive, is usually a fair approximation of the threshold energy of the process (it is actually defined as the energy required to excite the molecule to a vibrational level in the vicinity of the crossing of the potential energy curves for the negative ion and the neutral molecule).

CHAPTER 8: MEASUREMENTS OF DRIFT VELOCITIES AND D_T/μ VALUES FOR NON-THERMAL ELECTRONS

8.1: Introduction

Specific features of the Cavalleri diffusion experiment that was used for the experiments with thermal electrons have already been discussed (see Chapter 4). For measurements with non-thermal electrons standard apparatuses were used, without any major modifications. Consequently, the presentation of these experimental techniques will be brief. A more detailed description of them can be found in numerous references (Crompton and Jory 1962; Crompton et al. 1965; McIntosh 1967; Elford 1969; Robertson 1970; Huxley and Crompton 1974).

8.2: Measurements of Drift Velocities

8.2.1: Principle of the operation and the description of the apparatus.

The Bradbury-Nielsen method as described by Crompton et al. (1970) was used to measure drift velocities. The apparatus is shown in Fig. 8.1.

Basically the apparatus consists of two shutters that are separated by a certain drift distance h . The shutters are a set of very thin parallel wires, and the odd and the even wires are inter-connected. A sinusoidal voltage is applied to one group of wires and a voltage of the same amplitude and frequency but with an additional phase shift of π to the other group. Thus at any time the DC potential on the shutters resulting from the application of two sinusoidal voltages is zero. During the periods when the AC signal is non-zero electrons cannot pass through, since

they are attracted to one or the other half of the shutter wires. Electrons can enter the drift region only during the interval when the sinusoidal signal passes through zero (the so called "open time"). In performing the experiment the frequency is adjusted until maximum current is transmitted by the second shutter. This occurs when electrons transmitted by the first shutter arrive at the second during its open time and can therefore pass through it to the collecting electrode. There is therefore a simple relation between this frequency and the transit time of the electrons which enables the drift velocity to be determined.

The geometrical length of the drift region is approximately 10 cm and is known to within ± 0.04 mm (i.e. 0.04%). The positions of the guard rings must also be known accurately in order to achieve a homogeneous electric field when appropriate potentials are applied to them. The geometrical distance between the shutters was taken as the effective drift length (Elford and Robertson 1973).

The gas number density N was determined from accurate pressure and temperature measurements. A calibrated quartz spiral manometer (Texas Instruments) was used for pressures from 1.0 to 100 kPa and/or a capacitance manometer (MKS Baratron) for pressures below 1.34 kPa. The corresponding accuracy of the pressure measurements is better than $\pm 0.1\%$ (including the error in calibration) (see Gascoigne 1970). Corrections for the second virial coefficient were not made since very high pressures and low temperatures were not used in the present work (see Elford 1972). The temperature of the water bath, in which the experimental tube was immersed, was measured to better than $\pm 0.1\%$ at the moment when the tube was filled and sealed. The overall temperature was kept stable (to within 0.3 K) during the course of the experiment. The level of the water in the bath

was well above the highest electrode thereby minimizing temperature gradients in the drift tube.

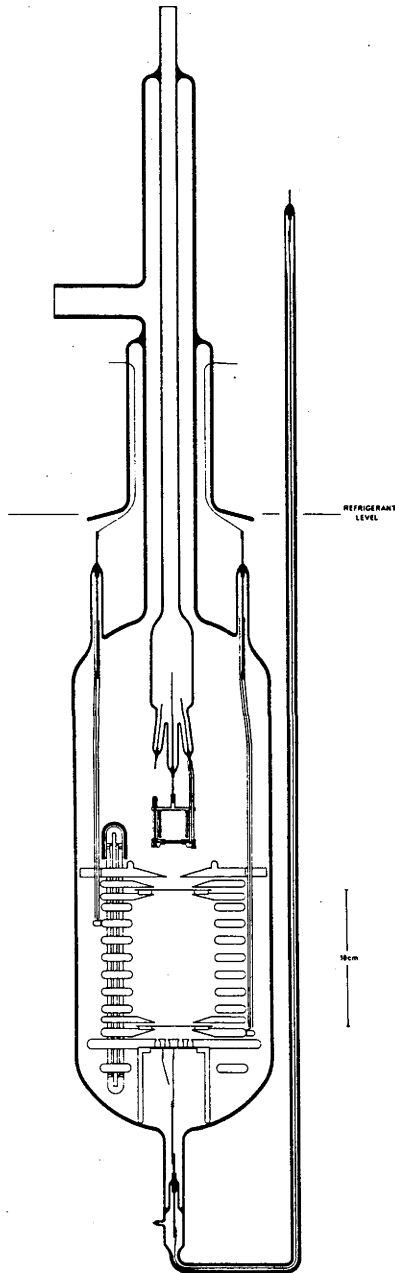


Figure 8.1 The Bradbury-Nielsen type apparatus for measuring drift velocities that was used for the present measurements.

The voltage between the shutters was supplied from a stable DC source and set to the correct value by using a differential voltmeter. The uncertainty of the potential difference between the shutters leads to an

error in v_{dr} of less than $\pm 0.05\%$ (Elford 1972). The potential of all the electrodes was known to better than 0.1%. The use of gilded shutters and guard rings resulted in a very homogeneous field (i.e. small scale variations due to inhomogeneous contact potential differences were negligible).

Adequate gas purity was achieved by the use of research grade gases, or in the case of H_2 and D_2 by purification through a heated palladium osmosis thimble that is known to produce gas of very high purity (Crompton and Elford 1962; Crompton et al. 1968). In the case of the measurements in pure helium no extra purification was needed since the results for this gas are not affected significantly by the presence of small amounts of impurity ($\ll 200$ ppm of N_2 or H_2 , see Crompton et al. 1970). In the case of the Ar- H_2 mixtures, the argon was not further purified as the quantity of hydrogen in the mixture was sufficient to screen the effect of any other impurities.

Before all the measurements the UHV system was evacuated to below 2×10^{-5} Pa (10^{-7} Torr).

8.2.2: Determination of the frequency corresponding to the peak of the transmitted current. The Bradbury-Nielsen type shutters were supplied with a high frequency sinusoidal signal from a frequency synthesiser and a pair of amplifiers each delivering output voltages of identical amplitude but shifted in phase by π . The stability and the amplitude of the shutter voltages was monitored using an oscilloscope. It was relatively easy to ensure that there was negligible distortion of the field due to unequal amplitudes of the shutter voltages by adding them and checking that the signal was zero.

Under favourable conditions it was possible to vary the amplitude of the shutter voltage and prove that the results were not affected by the change. However in some situations when relatively high values of E/N were used (e.g. for the measurements in pure He and pure D₂) it was necessary to use the maximum available voltage in order to stop the high energy electrons. Sometimes in such cases the results for the first peak in the electron arrival time spectrum were systematically different from those for other peaks by 0.1-0.3%. This was an indication that the shutter voltage was insufficient (i.e. open time too long). In those cases this additional uncertainty was added to the statistical scatter of the results. The results for the first peak were usually disregarded if it was possible to derive reliable results from the higher order peaks. This problem only occurred for a limited number of values of E/N (usually the highest) and the majority of the results were not subject to this uncertainty.

In situations when high E/N values and consequently low pressures were used, the resolving power which determines the "sharpness" of the current maxima and hence the accuracy with which the peak frequency can be determined (see Elford 1972 and the references therein), was not satisfactory in all cases. This parameter is defined as the ratio of the frequency at the maximum of the peak to its half-width, and it can be shown that for a drift tube of length d the resolving power (R.P.) is given by (see Elford 1972):

$$\text{R.P.} = N^{1/2} \left[\frac{E/N}{D_L/\mu} \frac{d}{2\ln 2} \right]^{1/2} \quad (8.1)$$

An increase of pressure therefore improves the resolving power, but when high E/N values were used there was a limit to the maximum pressure that could be used because of the onset of electrical breakdown.

It has been found (Elford 1972) that a value of 5 for the resolving power is sufficient to achieve 0.1% accuracy in the determination of the peak frequency. Sometimes it was not possible to satisfy this condition in the present experiments although this occurred only for the two or three highest values of E/N for the measurements in He, CO and D₂. However, good agreement between the values obtained from the peaks of different order in the arrival time spectrum and the overall agreement of the results of numerous experiments ensured that the effect mentioned above did not exceed 0.2%.

Measurements of the frequency that corresponds to the maximum transmitted current were not performed at the maximum since the variation of transmitted current with frequency is small at the maximum (see Fig. 8.2) and consequently it is difficult to determine the frequency accurately. Normally a current level was chosen (a certain percentage of the maximum current) and then two frequencies were determined, each corresponding to that level on either side of the peak. The frequency was then determined as the half of the sum of these two measured frequencies. The measurements were performed at 4 to 6 levels on each peak from 0.4 to 0.95 of the peak height, but usually above 0.7. Results at different peak levels were extrapolated to the peak value to allow for any systematic trends due to skewness, but usually this was unnecessary. Also, measurements were performed using different order peaks (normally the first four). The agreement between the peak frequencies obtained from various levels was to within 0.1% in all but exceptional circumstances, as was the agreement between the drift velocities calculated from the different peaks.

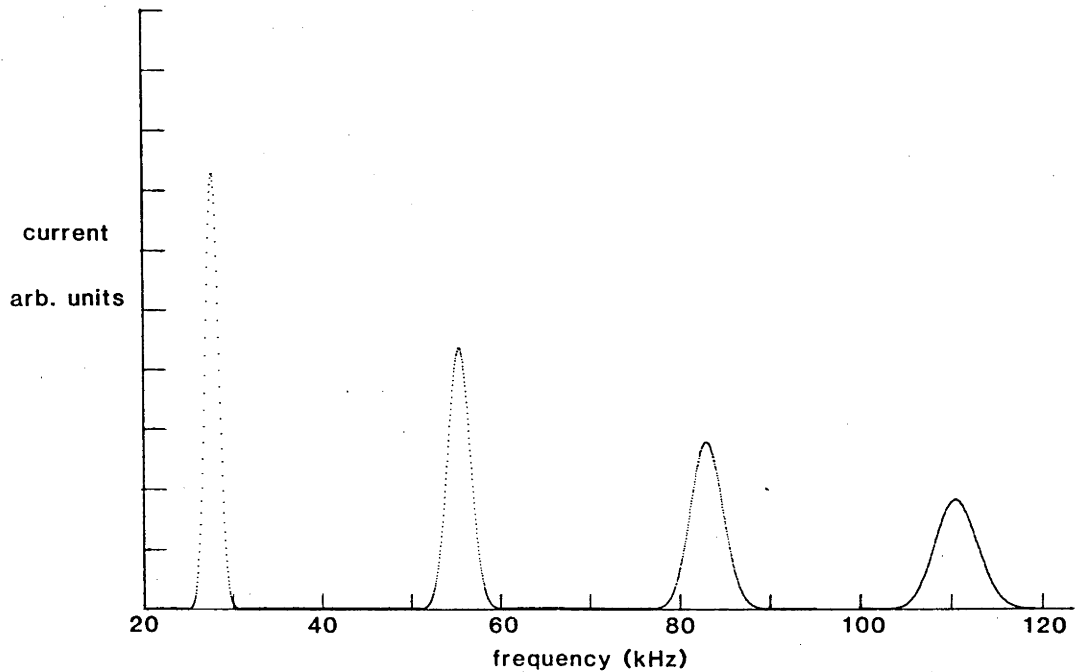


Figure 8.2 One example of the measured dependence of the transmitted current on frequency in the Bradbury-Nielsen experiment.

As can be seen from the previous paragraph it is necessary to make numerous measurements of transmitted current versus frequency for each E/N value, and the procedure is both tedious and time consuming when performed manually. The computer controlled system developed by Haddad (1983) was introduced to overcome this problem and was used for measurements of drift velocities in the present work. It was possible to use the system in two modes: to measure the drift velocities by concentrating the sampling densely around the peak or to measure arrival time spectra by stepping the frequency through equal increments over a wide frequency range. In the first mode, between 10 and 60 samplings were normally taken at each

frequency in order to average out the short time oscillations of the electrometer due to signal noise. Arrival time spectra were usually taken with 2 samples per frequency point. Some examples are shown in Fig. 8.2.

8.2.3: Sources of systematic errors. The pressures used in all the measurements were sufficiently low that it was possible to attribute the entire observed pressure dependence of the drift velocities to diffusion effects and not to multiple collision effects.

The statistical scatter of the data, the influence of any ionic background, and the diffusion correction will be discussed with every set of measurements. A summary of the systematic errors for the present experiments is given in Table 8.1

Table 8.1 Systematic Errors in the Drift Velocity Experiment

a	geometrical accuracy	<0.1 %
b	pressure measurement and calibration	0.1 %
c	temperature	0.1 %
d	voltage between the shutters	0.05 %
e	gas purity	0.01 %
f	determination of the peak frequency	<0.1 - 0.3 %
total		<0.6 - 0.8 %
g	mixture composition	<0.2 %
	total (for measurements in mixtures)	<0.8 - 1.0 %

8.2.4: Preparation of mixtures. Drift velocities were measured in various gas mixtures. In order to achieve accurate composition of the mixtures the following procedure was used:

1) A stainless steel vessel containing an inner vessel that can be isolated (approximate ratio of the two volumes: 1/17) was used (see Haddad 1983 and Fig. 8.3).

2) The volume ratio was accurately determined by taking advantage of the very wide dynamic range of the quartz spiral gauge. The small volume was filled to a high pressure just within the range of the gauge, then isolated from the larger volume which was then evacuated. The isolating valve was then opened and the resulting pressure measured. Proper account was taken of the volume of the gauge and the tubes connecting the gauge to the mixing vessel.

3) The mixture was made by first filling the small volume to a certain pressure and then isolating it. After evacuating the bigger volume it was filled with the buffer gas and the mixing vessel was then isolated from the vacuum system. The valve between the two volumes was then opened. Normally identical pressures were used for both gases or, if this was not possible, pressures corresponding to gauge calibration points were used in order to reduce errors due to interpolation between the calibrated points.

4) The mixing vessel was immersed in a water bath, thus keeping the temperature stable during the filling procedure. Sufficient time was allowed at each stage for the gas to reach thermal equilibrium with its surroundings.

5) A sufficient time was allowed for the gases to mix properly. The geometry of the mixing vessel (Fig. 8.3) is such that it favours fast mixing, but nevertheless the mixing cylinder was normally taken off the system and rolled so that the vanes that were built into the cylinder would hasten the mixing.

Using this procedure it was possible to determine the mixture

composition to better than 0.2%.

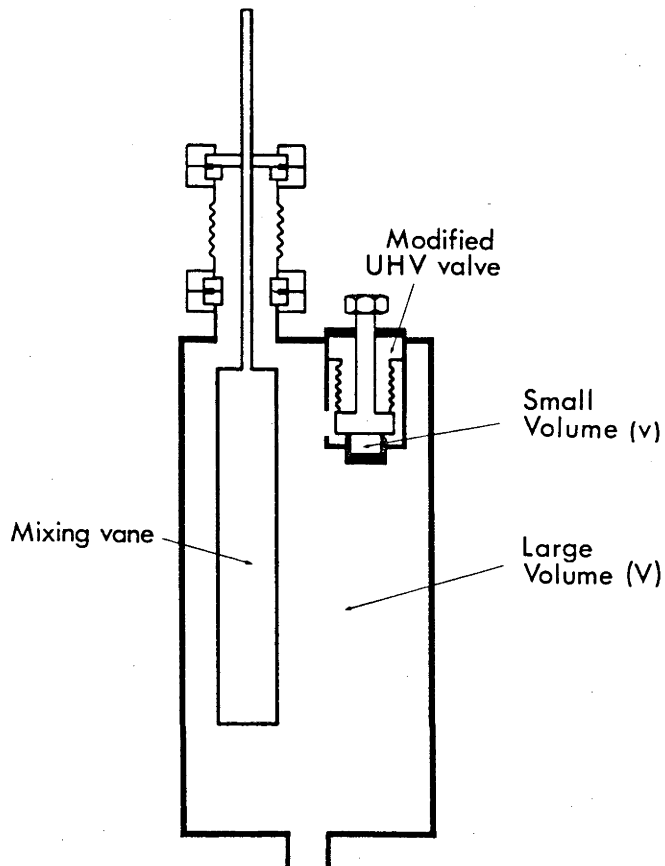


Figure 8.3 The geometry of the mixing cylinder.

8.3: Measurements of the D_T/μ values

8.3.1: Geometrical and structural considerations. The Townsend-Huxley method was used for the measurements of D_T/μ . In an apparatus that is based on this method a point source of electrons is used. The solution of the diffusion equation used to relate the measured current ratios to the

values of D_T/μ assumes a point source, but in order to have a reasonable current of electrons a hole of 1 mm in diameter was used in this experiment. A bigger hole would have increased the current and made the measurements less difficult but in that case the accuracy of the solution would have been questionable. Electrons that pass through the hole (see Fig. 8.4) drift and diffuse through the region between cathode and anode in a constant electric field. The ratio D_T/v_{dr} determines the ratio R of the number of electrons that are collected by the central disc (the anode is divided into a central disc and outer annulus) to the total number falling on the anode. The success of this technique in measuring accurately D_T/μ values is a result of a number of considerations that will be briefly presented in this section.

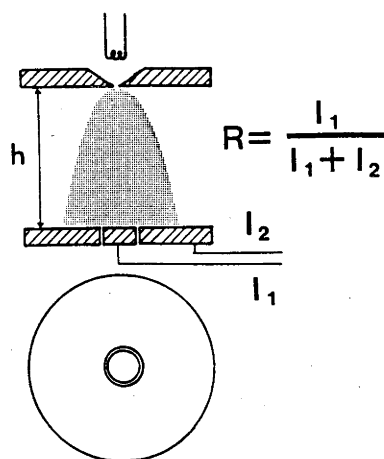


Figure 8.4 A diagram illustrating the principle of the Townsend-Huxley experiment.

The apparatus is constructed in such a way that any inaccuracy of the solution of the diffusion equation is minimized. Therefore the length of the drift region (h) is considerably larger than the radius of the central disc (b) which in turn should be much larger than the radius of the source hole (see Crompton and Jory 1962, see also Crompton 1972).

The electric field has to be highly homogeneous. There are two possible choices for guard electrodes. If thin electrodes are chosen, the field is in principle much more homogeneous than with thick electrodes but such a structure has much less mechanical rigidity and consequently the initial advantage may be lost. The thick electrode system (Crompton et al. 1965) is much more mechanically stable, and it can be shown that it is not difficult to ensure that field distortion in the central region of the drift space due to the thickness of the rings is negligible. In this work the apparatus with a variable drift length (Crompton and Jory 1962 - see Fig. 8.5) was generally used. The apparatus had thin guard rings but some tests and measurements in CO (and tests in H₂) were also performed for comparative purposes using the apparatus with a fixed drift length and thick guard rings (see Crompton et al. 1965 and Milloy and Crompton 1977b).

High geometrical precision must be achieved both in the manufacture of various parts, especially the collecting electrode, and in the assembly of the apparatus. The alignment of the source hole and the parallelness of the source and the collecting electrodes are of prime importance.

8.3.2: Effect of nonuniform surface potentials. A high degree of uniformity of the potentials over all surfaces, especially that of the collecting electrode, must be achieved. Overall contact potential differences (eg between cathode and anode, or between these electrodes and the guard rings) can be easily compensated by an additional shift of the DC levels (Crompton et al. 1965; Crompton and Huxley 1974). This is performed in such a way that the results become independent of the pressure. However, in the present work this measure was only applied to some test measurements in H₂ and was completely unnecessary for the measurements

described here. This is because relatively high fields (always exceeding 3 Vcm^{-1} and normally exceeding 6 Vcm^{-1}) were used.

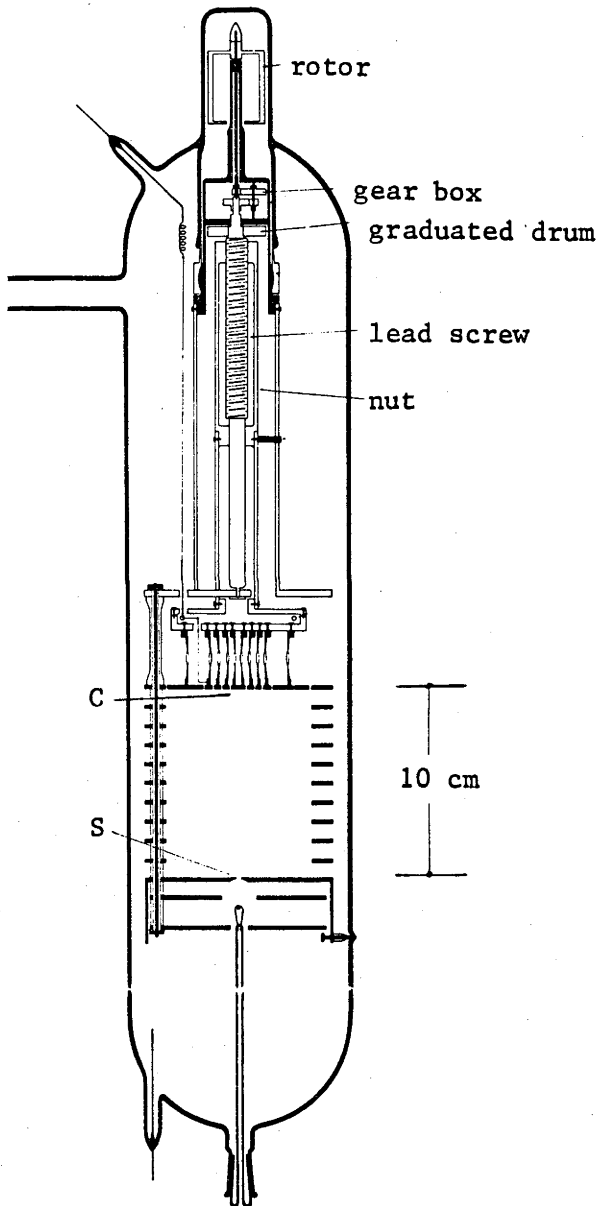


Figure 8.5 Experimental apparatus for measuring D_T/μ ratios using the Townsend-Huxley method. The drift length can be varied.

If the contact potential is not uniform over the surface of the collecting electrode, a much more serious problems can occur. This is especially so if there is a non-uniform contact potential in the vicinity of the gap between the central disc and the annulus (see Elford 1972). The reason is that electrons are easily swept from disc to annulus or vice versa, even by very small local fields. On the other hand the influence of non-uniform potentials on the surface of the annulus away from the gap is small. In this case the distribution of electrons is affected in an area where it cannot alter the current ratio.

Using a modified version of the apparatus that was proposed by Crompton et al. (1965) measurements of the contact potentials over various surfaces were performed since there were suggestions that some techniques, different to those that are standardly used at IDU, could provide surfaces with more homogeneous potentials. The basic modification to the apparatus from the form used by Crompton et al. is the addition of a coil that induces small oscillations of the probe (3.5 mm in diameter) thereby modulating the capacitance between the probe and the surface being investigated (see Fig. 8.6). Maximum sensitivity of the apparatus is achieved when the frequency of the coil is adjusted to the resonant frequency of the probe. If the potential between the probe and the surface is non-zero an AC signal consisting of several harmonics of the basic frequency is produced. Only when the DC level of the surface is adjusted to compensate for the existing potential difference is the signal zero.

Using this apparatus, variations of the contact potential over three types of surfaces were measured: polished copper, polished copper with a vacuum evaporated gold layer, and stainless steel surfaces coated with layers of silica of different thicknesses. The third type of surface was

suggested as a possible surface for application in low energy electron beam experiments with chemically active gases (Ehrhardt 1982).

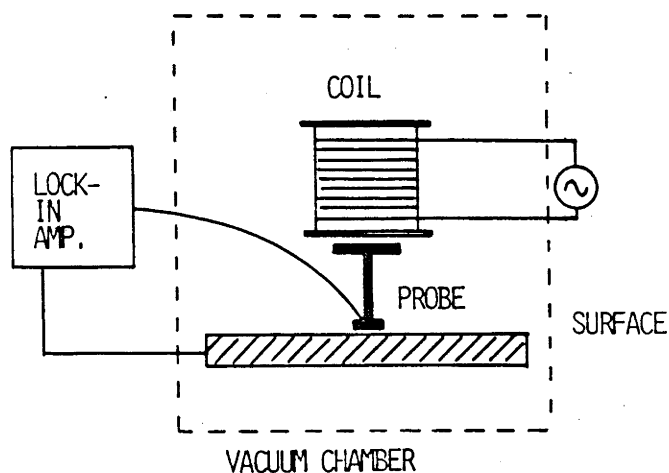


Figure 8.6 A block diagram of the apparatus used to measure the contact potential differences on surfaces.

Measurements were performed in a vacuum of 10^{-5} Pa (10^{-7} Torr). The copper surface showed a maximum contact potential variation of 19 mV and numerous irregularities. The sample of copper when gilded showed an overall variation of the contact potential of 15 mV but this was monotonically distributed from one edge to another of a disc 5 cm in diameter. Variations over small areas similar to that of the central disc of the collecting electrode in the Townsend-Huxley apparatus were less than two millivolts.

Surfaces coated with silica were prepared in Professor Ehrhardt's laboratory and came in three thicknesses of the silica layer, namely 30, 60 and 100 nm. Again, as for the copper surface, very sharp local structure

was observed and differences from 30 mV (for the 100 nm sample) to 110 mV (for the 30 nm sample) were seen over distances of 1 cm.

The conclusion from the work on this problem is that vacuum evaporation of gold is still superior to other techniques in producing surfaces with homogeneous contact potential, although it should be noted that none of the surfaces were rigorously outgassed by baking. This is in agreement with the conclusion of Crompton et al. (1965). These authors examined the collecting electrodes prepared for the Townsend-Huxley experiment. The surface preparation of these electrodes was superior to the preparation of the gilded surface used in the tests described above and therefore these authors observed variations that were smaller than those reported here (less than 7 mV over the entire surface). Most importantly, small-scale variations of the contact potential are effectively removed, by gilding, to an acceptable level of 2-3 mV/cm.

8.3.3: Measurement of current ratios. Apart from the above mentioned problems one of the major difficulties is an accurate determination of the current ratio. Fig. 8.5 shows the schematic diagram of the circuitry (see Huxley and Crompton 1974) used to achieve this goal. Using this system it is possible to accurately integrate currents falling on the two parts of the anode during a period of one minute without changing the potential of the electrode (the anode is maintained at earth potential) (see Huxley and Crompton 1974 and the references therein).

It is important to prove that space charge effects (due to the presence of negative ions) are negligible. This was done by varying the total current and checking whether the measured current ratios were affected.

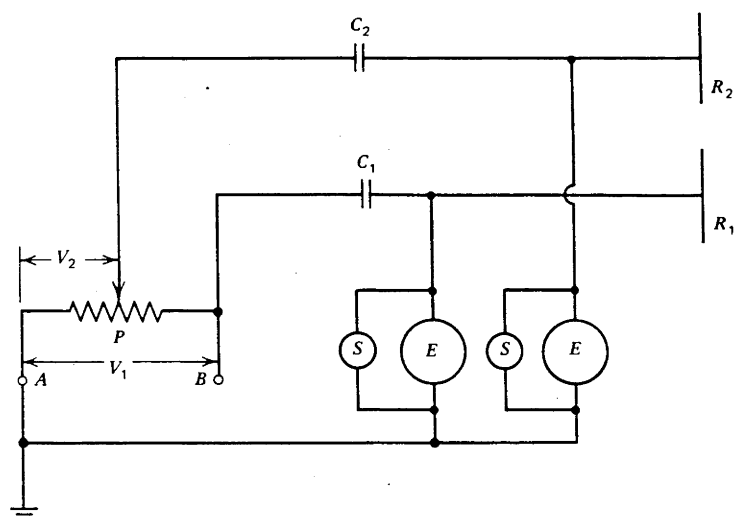


Figure 8.7 Schematic diagram of the system used for measuring the current ratios in the Townsend-Huxley experiment.

8.3.4: Electron sources. Finally it is necessary to address the question of an appropriate electron source. Although the radioactive sources developed for these experiments were suitable for most gases, carbon monoxide presented a particular problem. Carbon monoxide is a gas that has a pronounced dissociative attachment cross section. The energy required for this process is relatively large and therefore the number of negative ions produced by an electron swarm in the energy range of interest in the present work is very small. However, the secondary electrons produced by the radioactive source are sufficiently energetic to cause dissociative attachment. Therefore an alternative source of electrons had to be found that would not involve high energy electrons at any stage.

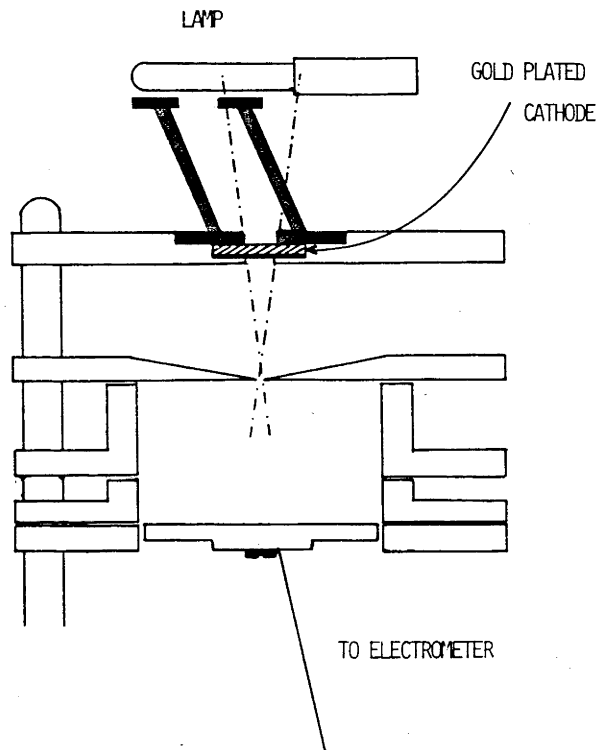


Fig. 8.8 Experimental apparatus used to test the application of the back-illuminated electron source in the Townsend-Huxley experiment. Radiation that can enter the drift region without reflection would have to come through the cone shown by dot-dashed lines.

A logical first choice would be a back illuminated photoelectric source (Moruzzi 1967) which has proved to be very successful in various swarm experiments. A series of tests was made of the performance of such a source of electrons for the geometrical conditions that are normally found in Townsend-Huxley experiments (see Fig. 8.8). Unfortunately the amount of scattered light was large enough to produce a significant current originating from areas outside the source hole. This current was sometimes as big as 30% of the current passing through the source hole. It was proved that a significant portion of that current originated from the region on the cathode that is distant from the source hole. This was done by placing a small metal cup on the axis of the drift region whose diameter

was large enough to ensure that all the electrons passing through the source hole or generated at it were collected. In addition there was significant emission from the anode, but it is believed that unless such a current originates from the region of the gap between the central disc and the outer annulus, it would not affect the results.

In performing these tests numerous precautionary measures were taken, such as ensuring oblique incidence of the UV light (see Fig.8.8), in order to prevent photons from entering the drift region directly. The reflectivity of most of the surfaces between the lamp and the source plate was reduced as much as possible. It is possible that the choice of geometry was not appropriate and that one could still build a Townsend-Huxley experiment using a back-illuminated source of electrons without any unwanted currents being produced by scattered light. A recently published paper by Koizumi et al. (1984) contains a description of such an attempt. However these authors too were not able to reduce the unwanted currents to a negligible level. The currents were measured by reversing the field between the source plate and the photocathode thus preventing electrons from entering the drift region through the source hole.

Following the failure of these experiments it was decided to return to a thermionic source (made of platinum wire 0.1 mm in diameter) as used previously in the variable length Townsend-Huxley apparatus. Heating of the gas was monitored by constantly measuring the pressure and the experiment was stopped when the observed change exceeded 0.1%. As the final check it was established that experiments performed using hydrogen were in excellent agreement (better than 0.4%) with those obtained using the radioactive source (Huxley and Crompton 1974 and the references

therein). The additional uncertainty in the results caused by thermal effect from the thermionic source probably does not exceed 0.1%.

8.3.5: Summary of sources of error. Some other possible sources of systematic error have already been mentioned in relation to the drift velocity measurements. These include: gas number density, temperature, voltage, gas purity.

A summary of all the significant sources of systematic errors in measurements of D_T/μ is given in Table 8.2.

Table 8.2 Systematic Errors in D_T/μ measurements

a	geometrical accuracy	0.1-0.3%
b	pressure measurement and calibration	0.1%
c	temperature	0.1%
d	voltage between the electrodes	0.05%
e	solution of the diffusion equation	0.1%
f	uniformity of the electric field	<0.1%
g	current ratio measurement	0.1-0.4%
h	inhomogeneous contact potential	<0.05%
j	additional heating by the filament	0.1%
total		0.8-1.3%

At this point it should be noted that the upper limit of all the possible sources of error were taken and summed. It is therefore considered that the resulting error estimates are rather conservative upper limits.

CHAPTER 9: ROTATIONAL AND VIBRATIONAL EXCITATION OF HYDROGEN

9.1: Introduction

The importance of hydrogen in gas discharges was one of the reasons for the present and numerous other studies of its low energy cross sections for electron scattering. The applications that require knowledge of cross sections include: modelling of hydrogen thyratrons (Kunc and Gunderson 1982; Gunderson and Guha 1982), analysis of the appropriate conditions for negative ion production for fusion research (Bacal 1982; Hiskes et al. 1982; Prelec 1984), modelling of gas lasers (Hodgson 1970; Hodgson and Dreyfus 1972) and other gas discharges (Erwin and Kunc 1983; Haas 1973).

An equally important reason for interest in H_2 is its importance for testing the theory of electron-molecule collisions. If a theory is shown to give satisfactory results for hydrogen it is at least an indication that the theory can be used to calculate data for other gases for which data are difficult to obtain experimentally.

Hydrogen is usually chosen to test scattering theory because it is the simplest molecule and theoretical treatment at a given level of sophistication normally requires less calculation than for other gases. Another characteristic of H_2 is its low mass which in turn means that the thresholds for rotational excitation are higher than for any other molecule. The number of channels that need to be included in theoretical calculations is therefore smaller, while at room temperature the populations of excited rotational levels are smaller than those for other molecules. The latter is an advantage for experimental physics. In swarm experiments the analysis benefits from low populations of the higher order

rotational levels because the number of the cross sections that have to be taken into account is smaller, while beam experiments also benefit from the fact that the rotational excitation thresholds are relatively high since it is much easier to resolve various rotational transitions.

It is therefore important to achieve good agreement between the results for H_2 obtained from theory and from the alternative experimental methods. This chapter describes a reanalysis of the data from swarm experiments in hydrogen and hydrogen mixtures, with particular reference to the impact of the new theoretical results on the analysis, and new measurements in He- H_2 mixtures to confirm its conclusions.

9.2: Low Energy Cross Sections for Hydrogen

9.2.1: Results based on swarm experiments. Work on the determination of electron scattering cross sections for H_2 from swarm data has been reviewed in numerous publications (Phelps 1968; Kieffer 1973; Huxley and Crompton 1974). The early attempts of Frost and Phelps (1962) and Engelhardt and Phelps (1963) resulted in cross sections of limited accuracy because the swarm data that were used had relatively large uncertainty. The development of high precision methods for measurements of drift velocities and characteristic energies provided a basis for a much more accurate determination of cross sections. The work on this problem at IDU will be briefly reviewed next.

Crompton et al. (1969) took advantage of the fact that at 77 K 99.5% of molecules in pure parahydrogen ($p-H_2$) are in the ground rotational state. Therefore, only two cross sections are significant for low E/N values, the momentum transfer cross section (σ_m) and the rotational excitation cross

section (σ_{rot}) for the J=0-2 transition. Using the accurately measured v_{dr} and D_{T}/μ values these authors determined both cross sections very accurately (to within 5% up to 0.35 eV). The agreement of the results based on the swarm data ($\sigma_{\text{rot}}^{\text{SW}}$) with the theoretical cross section of Henry and Lane (1969) was very good in the region where $\sigma_{\text{rot}}^{\text{SW}}$ was determined uniquely (below 0.35 eV). Therefore it was possible to extrapolate the cross section to higher energies where vibrational excitation is also present and the two transport coefficients are not sufficient to determine three cross sections uniquely (see Section 2.3). Using the σ_{rot} of Henry and Lane, Crompton et al. (1969; 1970b) determined the vibrational excitation cross section $\sigma_{\text{vib}}^{\text{SW}}$ to within 10% close to the threshold.

Subsequently Gibson (1970) analysed the data for normal hydrogen (n-H₂) at 77 K. Using the previously derived cross sections for rotational and vibrational excitation and momentum transfer he determined the cross section for rotational excitation for J=1-3. Since the analysis in this case is more complex than for p-H₂ the cross section was determined only to within $\pm 15\%$.

Further progress followed the introduction of multi-term theory (see Haddad et al. 1981). Haddad and Crompton (1980) used the data for p-H₂ at 77 K, n-H₂ at 77 and 293 K and their data for drift velocities and ratios of transverse diffusion coefficient to mobility in two mixtures of argon and hydrogen (see Section 9.3 and Appendix 3). They concluded that the transport coefficients calculated on the basis of the available cross sections are in very good agreement with the whole range of experimental data. By introducing the data for the mixtures they improved the uniqueness of the cross sections derived from the swarm data.

Two important points should be made here. The first is that the shape of the rotational excitation cross section derived on the basis of the swarm data is quite different from the shape for quadrupole transitions that can be determined using the Born approximation (Gerjoy and Stein 1955). The second is that the cross section σ_{vib} of Ehrhardt *et al.* (1968) (see 9.2.2) is incompatible with the swarm-derived cross section even though $\sigma_{\text{vib}}^{\text{sw}}$ could not be determined uniquely. This can be clearly seen from Fig. 9.1 where Crompton *et al.* (1969) have presented the adjusted σ_{rot} which should be used with the vibrational excitation cross section of Ehrhardt *et al.* in order to bring the calculated transport coefficients and the experimental data into agreement.

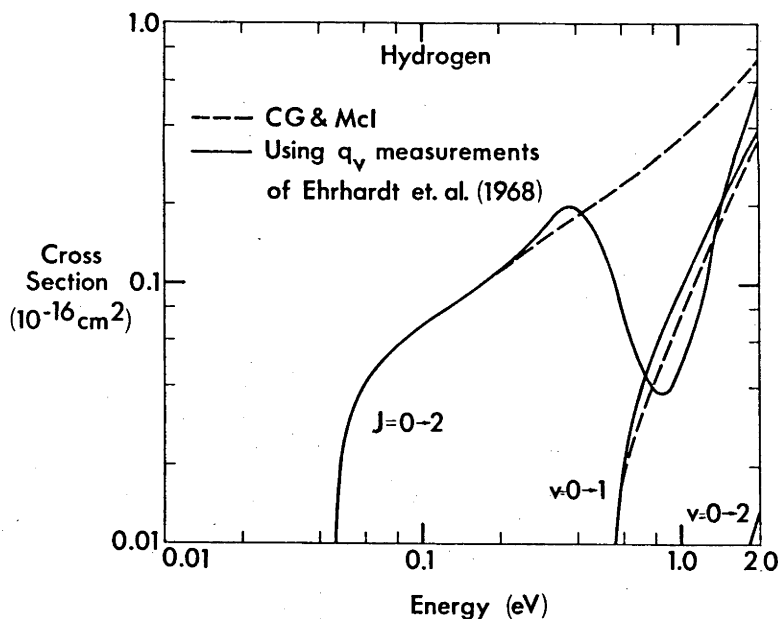


Figure 9.1 The modified rotational cross section (dashed line) that when used with the vibrational excitation cross section of Ehrhardt *et al.* (dashed line) gives good agreement with the experimental transport data. The results of Crompton, Gibson and McIntosh (1969) are shown by solid lines.

Buckman and Phelps (1985) have recently measured the excitation coefficient for the $v=0-1$ transition in H_2 using a tracer technique (see Section 2.3). The accuracy of their experimental data is not sufficient to make it possible to reach any general conclusions about the differences

(see Section 9.4.5) between the beam and swarm vibrational excitation cross sections.

It is also worth noting that Wada and Freeman (1981), who measured thermal mobilities at high pressures, reported the existence of a Ramsauer-Townsend minimum in hydrogen. However, their findings were challenged by Crompton and Morrison (1982) from both the theoretical and experimental standpoints. Therefore, no attempts were made in the present work to check their results.

9.2.2: The beam data. The number of beam experiments performed in the energy range of interest to the present work is relatively small. A comprehensive review of the available data for H₂ from both beam and swarm methods was published by Trajmar et al. (1983). Therefore only selected results will be mentioned here.

The most extensive measurements of the total cross section in the region below 2 eV were reported by Ferch et al. (1980). Linder and Schmidt (1971), Shyn and Sharp (1981), Furst et al. (1984) and some other authors have reported the differential cross sections for elastic scattering. Their work indicated that the elastic scattering of electrons is not markedly anisotropic, but that there is somewhat larger back-scattering than forward-scattering. The consequences of such anisotropy on electron transport were discussed by Haddad et al. (1981).

The cross section for the J=1-3 transition was measured by Linder and Schmidt (1971; see also Linder 1974). The cross section was found to be in satisfactory agreement with the swarm derived cross section.

Extensive measurements of the vibrational excitation cross sections ($v=0-1, 0-2$ and $0-3$) were performed by Ehrhardt et al. (1968). The primary

purpose of the work described in this paper was to study resonances in electron molecule scattering; the absolute accuracy of the data, especially near threshold, is therefore uncertain (Linder 1984 - personal communication). More accurate results were obtained by Linder and Schmidt (1971) for the $v=0-1$ transition. However, the energy range of their data did not extend to sufficiently low energies to provide the possibility of a meaningful comparison with the swarm data.

The present analysis of swarm data extend only to energies where the influence of electronic excitation and ionization is negligible. Therefore papers presenting results obtained under conditions when excitation and ionization become appreciable will not be discussed here (see Buckman and Phelps 1985 for a detailed review).

There are various problems associated with the application of beam techniques at low energies. First, it is very difficult to produce low energy electron beams that have sufficient intensity and spatial and energy resolution. Second, it is hard to make absolute measurements. In absorption-type (e.g. Ramsauer or time-of-flight) experiments to measure total cross sections it is difficult to measure with sufficient accuracy the low pressures that must be used, while the crossed beam experiments that are used to measure inelastic cross sections have to be normalized to some accurately measured scattering cross section (see Trajmar et al. 1983). There is also the problem related to the determination of integrated cross sections from the differential cross section data. Usually the range of experimentally accessible angles is limited and the results have therefore to be extrapolated to zero and high angles. The adequacy of such extrapolations is questionable in some cases. Finally, it is very difficult to make reliable beam measurements of inelastic processes

with very small cross sections whereas such processes may be easily detected by the swarm technique (see Section 11.3.3).

Nevertheless, low energy beam experiments have benefited greatly from technological advances in the last ten years (while the technology essential for high precision swarm experiments has been available from the 1960s) and it has now become possible to perform meaningful comparisons between results from the two techniques in the low energy range. Also, as pointed out by Crompton (1983; 1984a; and 1984b), one should not view these two methods as competing but as complementary.

9.2.3: Theoretical results. As mentioned above, hydrogen is usually the most favourable choice for testing any new theoretical developments. Numerous detailed reviews of the theoretical work on H_2 exist (e.g. Lane 1980; Thompson 1983; Morrison 1983). Therefore, the discussion in this section will be brief and will concentrate on the latest theoretical results.

As mentioned in Section 9.2.1, the predictions of Gerjov and Stein (1955) were found to be inadequate for hydrogen (Frost and Phelps 1962; Crompton et al. 1969). Henry and Lane (1969) achieved a considerable improvement of the theoretical results by including exchange and polarization effects. The results of their close-coupling calculations are in very good agreement with the cross sections derived from swarm data.

A different approach to the theory of electron-molecule scattering was adopted by Klonoover and Kaldor (1979). These authors carried out the most detailed calculations within the so called adiabatic nuclei approximation. Since their theory was free from any adjustable parameters it was the first *ab initio* calculation of vibrational excitation of molecules by electrons.

An important feature of their paper is an indication of the importance of polarization effects.

More recent theoretical developments for electron-hydrogen scattering include: a semi-empirical analysis based on the resonant model (Bardsley and Wadehra 1979); an application of the R-matrix method (Nesbet et al. 1984); ab initio calculations of polarization effects (Gibson et al. 1984); optical potential calculations (Schneider and Collins 1983); an analysis of the applicability of adiabatic nuclei theory (Varracchio and Lamanna 1984), and an extensive analysis of scattering at low energies (below the threshold for electronic excitation) performed by Morrison and coworkers at Oklahoma University (OU).

The first step in the analysis carried out at OU was to derive accurate parameter-free potentials for exchange and polarization for electron (and positron) scattering on H_2 (Gibson and Morrison 1981; 1984; Morrison et al. 1984a). Next, laboratory-frame close-coupling (LFCC) and adiabatic nuclei (AN) calculations were performed for their model potentials. It was shown (Morrison et al. 1984b; 1984c) that large errors may arise when AN theory is used. These errors are especially large when the electron energy is close to threshold or near the resonance; in the case of vibrational excitation the ratio of the LFCC to AN results may be as large as 1000%.

An important question arose from this study, that is, whether the breakdown of the AN approximation for other gases is as serious as for hydrogen. The answer to this question may be different for different inelastic processes. For instance there are indications that the large discrepancies between the AN and LFCC results for rotational excitation are unique to hydrogen, and a procedure was developed to overcome the inadequacy for other gases (Feldt and Morrison 1984).

However, for vibrational excitation the application of the AN approximation is more difficult. First, the discrepancies observed by Morrison et al. are much larger than for rotational excitation, and second, it is not possible to perform full LFCC calculations for any gas other than hydrogen (even when the most powerful available computers are used). Therefore, it is not possible to check the validity of the AN approximation for other gases in the same way as for hydrogen. A new method was developed at OU to improve upon the results from AN theory. It is the so-called body-frame vibrational close-coupling theory (BFVCC) and the basic idea is to treat rotational excitation as in AN theory (with appropriate corrections) but to perform full close-coupling calculations for vibrational excitation. Even though this approach is more difficult to implement than AN theory it is believed that it will be possible to apply it to gases other than hydrogen.

As the final result of their analysis, Morrison and coworkers made detailed LFCC calculations using realistic calculated potentials. The improvement in respect to the work of Henry and Lane (1969) comes from the more flexible polarization potentials that were used. The cross sections derived in this way have a much firmer theoretical foundation than the results of Henry and Lane and therefore provide a better basis for the swarm analysis. The results of the work of Morrison and coworkers will be compared to the swarm results in this Chapter.

As a general comment about theoretical methods it should be pointed out that the treatment of electron-molecule scattering in general necessarily involves numerous approximations. It is especially important to use very accurate potentials (Klonover and Kaldor 1979).

Ab initio calculations are the ultimate achievement of electron

molecule scattering theory but are very difficult to carry out. In some cases one would benefit from theoretical results that involve adjustable parameters chosen to give agreement between certain quantities calculated on the basis of the cross section and the corresponding experimental data. As an example one may mention very useful analytical relations for the momentum transfer and total scattering cross sections. These relations were obtained for molecules by Chang (1981) and by Fabrikant (1981; 1984) using modified effective range theory (MERT) (see Chapter 12). Unfortunately when applied to electron-molecule scattering MERT has a very narrow range of validity ($\epsilon < 0.2$ eV) but nevertheless this range was sufficient to compare the total cross section of Ferch et al. (1980) with the momentum transfer cross section of Crompton et al. (1969) and to conclude that there is very good agreement between the two sets of data (i.e. the MERT parameters obtained from both sets agree very well).

9.3: The Swarm Data Used in the Present Analysis

9.3.1: Experimental transport coefficients - reliability and accuracy.

Since the swarm cross section analysis used in the present work relies on transport data (drift velocities v_{dr} and lateral diffusion coefficient to mobility ratios D_T/μ) of high accuracy a comment will be made on the reliability of the experimental technique. This section is a recapitulation and an extension of the relevant discussion presented in Section 2.3. The following should be stressed:

1. Swarm experiments are performed at much higher pressures than beam experiments (1 Torr - 10 atm.). Therefore it is possible to achieve a much better determination of the gas number density through very

accurately measured pressures. It is normal to expect an error limit of $\pm 0.1\%$ and better for pressure measurements in the pressure range used in swarm experiments.

2. Experiments are designed in such a way that the results rely only on quantities that can be measured with great accuracy. Examples are frequency (for v_{dr}) and current ratios rather than individual currents (for D_T/μ). Additional quantities necessary for the evaluation of the experimental results are the geometrical dimensions of the apparatus and the applied voltages. It is possible to measure both to a very high degree of accuracy.

3. Relatively simple electron transport theory can be used to derive the transport coefficients from measurable quantities. The experiments are designed so as to take advantage of this simplified theory. Various corrections that are made (e.g. the D_L correction to the current ratio formula in the D_T/μ experiment, the diffusion correction in drift velocity experiments, etc. - see Section 2.4) are normally kept at a very low ($< 1\%$) level by the appropriate choice of experimental conditions. The experimental data that were used in the present analysis were obtained at E/N values that are too low for any appreciable ionization (and/or attachment) and thus complications caused by longitudinal density gradients introduced by attachment or ionization were avoided. The influence of the presence of radial gradients on the definition of the transverse diffusion coefficient was negligible (see Section 2.5).

4. Results were obtained in different apparatuses with different geometries. The reproducibility was extremely good; results repeated many times over a very long period of time agreed to within 0.5% for D_T/μ and 0.2% for v_{dr} .

Results obtained at different pressures are usually presented in order to show the adequacy of applied corrections or the validity of neglecting others, and that the purity of gas was such that no negative ions were formed.

5. Nonequilibrium effects, which may influence swarm experiments under certain conditions, can be detected easily through a dependence of the results on pressure and/or geometry of the apparatus. Normally measurements are performed under conditions where these effects are negligible.

9.3.2: Sources of data. The tables of the transport data for pure H₂ and Ar-H₂ mixtures are given in Appendix 3. The data were compiled by Huxley and Crompton (1974) but it should be noted that there are some differences between the values presented in Appendix 3 and in Huxley and Crompton (1974) due to interpolation errors in the latter. The error estimates presented in this section were taken from Huxley and Crompton (1974).

For p-H₂ at 77 K the drift velocities of Robertson (1971) that are accurate to within $\pm 1\%$ were used together with the D_T/μ values of Crompton and McIntosh (1967; 1968). The uncertainty of the D_T/μ data is $\pm 3\%$ below 0.4 Td and $\pm 2\%$ between 0.5 and 6 Td.

For normal hydrogen at 77 K the drift velocities measured by Robertson (1971) (again to within $\pm 1\%$) were used along with the D_T/μ values of Crompton et al. (1968). These data were determined to within $\pm 2\%$ in the entire E/N range.

Room temperature data for drift velocities were taken from Lowke (1963) up to 1 Td and from Robertson (1971) up to 30 Td. The uncertainty of these

data is less than 1%. D_T/μ values determined to within $\pm 1\%$ by Crompton et al. (1968) were used up to 6 Td and the unpublished data by the same authors (Crompton et al. 1966) up to 30 Td. The estimated error bars for the latter data are $\pm 2\%$ but the results were not published because relatively low current ratios were used and it was suspected that the results could be subject to some small systematic error. Some of the values obtained by Crompton et al. were checked in the present work. The newly measured values were always in very good agreement with the old data, though systematically lower by between 0.1 and 0.3%. These measurements were not sufficiently comprehensive for presentation (i.e. the measurements were made only for a limited number of E/N values, pressures and drift lengths) but it can be concluded that the recent measurements obtained under somewhat better conditions than the data of Crompton et al. (1966) confirm that the results of these authors are reliable.

The data for Ar-H₂ mixtures were taken from Haddad and Crompton (1980); their drift velocities are accurate to within $\pm 1.5\%$ and the D_T/μ data to within $\pm 2.5\%$.

The stated uncertainties of $\pm 1\%$ for v_{dr} and $\pm 2\%$ for D_T/μ data for pure H₂ (and the appropriate uncertainties for the mixture data) are thought to be conservative since the errors from all sources were summed and the maximum error was taken for each. The much smaller spread of the data (than the figures quoted above) of 0.2% for v_{dr} and 0.5% (and better) for D_T/μ indicates that the random errors are smaller than assumed in obtaining those figures. This is especially so for D_T/μ values below 6 Td, and the drift velocities in the entire range (up to 30 Td). Therefore it seems that the measured transport coefficients should be the most accurate test yet available of any cross section set for hydrogen provided adequate

transport theory is applied in the analysis.

9.3.3: Scaling of D_T/μ data for parahydrogen. As can be seen from Table A.3.1 some of the required data for D_T/μ ratios in parahydrogen at 77 K are lacking. Since parahydrogen is the easiest gas to interpret it has been used for the basic analysis. Table A.3.1 shows that reliable D_T/μ data for p-H₂ between 6 and 30 Td are missing. Such data can be obtained from those for n-H₂ by the procedure described below.

First, by comparing the data for $E/N < 6$ Td in Tables A.3.1 and A.3.2 it can be seen that the difference between the p-H₂ and the n-H₂ data becomes progressively smaller as one approaches 6 Td. This means that the influence of different rotational populations, and consequently different energy losses in rotational excitation, becomes less and less important (a consequence of the decreasing fraction of the total power being dissipated in rotational excitation). At 6 Td the results differ by less than 1%, and bearing the experimental inaccuracy in mind one might choose to use the n-H₂ data without modification above this point. However a correction to the n-H₂ data has been applied to obtain the required p-H₂ data, the correction being calculated on the basis of the best currently available cross section set for H₂ (Haddad and Crompton 1981). These values are listed in Table 9.1. The justification for this procedure is the fact that the corrections are very small.

Data for D_T/μ in n-H₂ at 77 K extend only to 12 Td. In a similar way, the n-H₂ data at 293 K were adjusted to obtain p-H₂ data at 77 K. The necessary correction factors are also small (below 1%) but it is better to use them rather than the n-H₂ (293 K) data without modification, though

both choices could be justified by the experimental error bars. The fact that one can use the n-H₂ (293 K) data in this way simply means that the gas temperature does not influence electron transport very much in this range of E/N, that is, that it is dominated by vibrational excitation, with energy transfer through rotational excitation and de-excitation being almost negligible.

Table 9.1 Comparison of calculated D_T/μ values for p-H₂ (at 77K) and n-H₂ (at 77K and 293K). Calculations were based on the best available set of cross sections (Haddad and Crompton 1980).

E/N (Td)	p-H ₂ 77K	n-H ₂ 77K	n-H ₂ 293K	[p-H ₂ (77K) n-H ₂ (77K)]	[p-H ₂ (77K) p-H ₂ (293K)]	[n-H ₂ (77K) n-H ₂ (293K)]
	D_T/μ (eV)	D_T/μ (eV)	D_T/μ (eV)	Δ (%)	Δ (%)	Δ (%)
30	1.051	1.050	1.055	0.009	0.27*	0.17
27.3	0.9710	0.970	0.9741	0.10	0.32*	0.22
25	0.9088	0.9079	0.9117	0.10	0.32*	0.22
20	0.7807	0.7802	0.7837	0.06	0.38*	0.32
17	0.7032	0.7030	0.7065	0.03	0.47*	0.44
14	0.6220	0.6222	0.6258	0.03	0.61*	0.58
12	0.5646	0.5651	0.5689	0.11*	0.76	0.65
10	0.5032	0.5042	0.5082	0.20*	0.99	0.79
8	0.4006	0.4025	0.4069	0.37*	1.57	1.10
7	0.4006	0.4025	0.4069	0.47*	1.57	1.10
6	0.3622*	0.3645	0.3691	0.64	1.91	1.27
5	0.3204*	0.3232	0.3283	0.87	2.47	1.60
4	0.2737*	0.2772	0.2829	1.28	3.36	2.08
3.5	0.2476*	0.2517	0.2578	1.66	4.12	2.46

Δ denotes the difference between the calculated values of D_T/μ for the gases and temperatures as nominated (in brackets). These differences were used to derive the p-H₂ data from the available experimental data in

normal hydrogen at 77 and 293K.

The values marked * represent the differences that were actually used to derive the final set for p-H₂, or the calculated values of D_T/μ at E/N values where the experimental data for p-H₂ exist (see text).

The data marked with an asterisk in Table 9.1 indicate either calculated values of D_T/μ where experimental data are available (p-H₂ 77 K) (to enable the validity of the correction procedure to be verified - see next paragraph) or the magnitude of the correction applied to n-H₂ data at 77 and 293 K to produce the data used in the analysis.

As an example of the validity of this procedure let us take the data at E/N=3.5 Td where the experimental p-H₂ 77 K result for D_T/μ exists and is 0.250 V (see Table A.3.1). The calculated correction factor of 4.12% (for 293 K) (see Table 9.1) brings the corresponding experimental result for n-H₂ at 293 K (which is 0.259 V - see Table A.3.3) to 0.249 V. Therefore even when the corrections are as high as 4% the corrected results are sufficiently accurate. In the E/N region where those corrections were actually used, their magnitude was well within the experimental uncertainty.

9.4: Analysis

9.4.1: Introduction. As already stated, the basic set of data for the analysis was that for p-H₂ at 77 K because it is the least complicated system. However, since at high values of E/N the D_T/μ values for p-H₂ were scaled from n-H₂ 77 and 293 K data, the D_T/μ data for p-H₂ (77 K), n-H₂ (77 K), and n-H₂ (293 K) at high E/N should not be regarded as three independent sets of data. The scaling was performed mainly because it was

more convenient to carry out the basic analysis using p-H₂.

The experimental data for p-H₂ were divided into two groups: low E/N values (below 2 Td) and high E/N values (above 2 Td). The theoretical and the swarm derived rotational excitation cross sections for the J=0-2 transition and the momentum transfer cross section were first used in calculations for the low energy range. The next step was to test the vibrational cross sections in the high E/N range using an extrapolation of rotational cross sections to energies higher than 0.35 eV (see Section 9.2.1). The maximum value of E/N used in the analysis was chosen so that the transport coefficients at this value were not affected by inelastic processes with high thresholds (electronic excitation and ionization). At 30 Td the difference between the transport coefficients calculated with and without realistic cross sections for these processes is less than 0.2%.

If the vibrational excitation processes v=0-2 and v=0-3 are not included the effects on v_{dr} and D_T/μ at 30 Td are 1% and 3.5% respectively. These effects decrease rapidly as E/N decreases and are negligible below 12 Td. Nevertheless v=0-2 and v=0-3 processes have to be included (Haddad and Crompton 1980) even though high accuracy for the cross sections for these processes was not required.

The next step following the p-H₂ analysis was a comparison with the n-H₂ data at 77 K and then with the n-H₂ data at 293 K. The calculations of the transport coefficients for these gases require cross sections for higher rotational transitions. Initially the rotational excitation cross sections for the J=2-4 and J=3-5 transitions were scaled from $\sigma_{rot}(J=0-2)$ using results from the AN theory (see Appendix 5) and were checked by scaling from $\sigma_{rot}(J=1-3)$. However, as pointed out previously the AN theory used to carry out the scaling breaks down close to the threshold.

Therefore Morrison's (1984) theoretical results for these cross sections were used for the final calculations.

Finally, the transport coefficients for the two mixtures of hydrogen with argon were calculated and compared with experimental data.

9.4.2: Multiterm transport theory for hydrogen. In the range of E/N values relevant to this work the two-term approximation in general provides sufficiently accurate results for the calculated transport coefficients. However, as pointed out by Haddad and Crompton (1980), a small difference between the results of the two-term and the multiterm theories still exists. It is less than 1.4% for D_T/μ and is negligible for v_{dr} . In Table 9.2 the results of multiterm corrections (i.e. corrections to the two-term results) are listed for $n\text{-H}_2$ (77 K) with both isotropic and anisotropic scattering, $p\text{-H}_2$ (77 K) with isotropic scattering, and $n\text{-H}_2$ (77 K) with the theoretical cross section for vibrational excitation σ_{vib}^{th} ($v=0-1$) replacing that of Haddad and Crompton (1980) (again assuming isotropic scattering).

First, it should be noted that the difference between the corrections for normal and parahydrogen is negligible. Also the inclusion of anisotropy makes very little difference ($< 0.3\%$). However, the corrections are not negligible even at very low E/N values. Corrections were applied in the present analysis over the entire range of E/N .

When the theoretical vibrational cross section is used the correction factors differ from those obtained using the swarm cross section, but again not greatly ($< 0.2\%$). This gives a measure of the sensitivity of the corrections to the vibrational cross sections (the average energy at 28 Td is in the region where the theoretical and swarm cross sections differ the

most).

Table 9.2 Multiterm corrections for hydrogen

E/N	Correction for D_T/μ
n-H ₂ (77 K) Isotropic Scattering Assumed	
33.70	1.18
28.91	1.18
26.13	1.18
23.14	1.16
19.96	1.14
16.54	1.08
13.01	0.98
9.491	0.88
3.360	0.64
1.332	0.63
0.7140	0.60
0.4166	0.48
0.3431	0.45
0.1995	0.34
0.0734	0.14
n-H ₂ (77 K) Anisotropic (Realistic) Scattering	
28.50	1.37
16.39	1.26
9.46	1.05
3.42	0.81
0.564	0.64
p-H ₂ (77 K) Isotropic Scattering	
26.48	1.17
13.24	1.03
6.317	0.80
1.4226	0.63
0.0260	0.07

n-H₂ (293 K) Isotopic Scattering

25.81	1.15
16.31	1.05
9.281	0.84
1.180	0.54

n-H₂ (77 K) Isotropic Scattering $\sigma_{\text{vib}}^{\text{th}}$ ($v = 0-1$)

28.51	1.37
-------	------

The values of E/N were chosen to optimize the convergence of the LRM code for a given temperature T_b . The corrections to D_T/μ at the values of E/N required for the calculations were found by interpolation.

9.4.3: Momentum transfer and total cross sections. In the next three sections the conclusions that were reached on the basis of the analysis will be described. Comparison of the swarm-derived and theoretical cross sections will be given first starting with the momentum transfer (and total) cross section.

The theoretical momentum transfer cross section of Morrison and co-workers was available only for a limited number of energies. The agreement with the swarm result (the momentum transfer cross section of Crompton et al. was used in this work) is very good (see Table 9.3 and Fig. 9.2) up to 2.5 eV, i.e. the differences between the two cross sections do not exceed 5% which is the uncertainty of σ_m^{sw} (except for one point where the difference is 5.3%). However, the relatively limited number of data would lead to large interpolation errors if σ_m^{th} were used in the calculations of the transport coefficients. Also the application of σ_m^{th} would lead to somewhat larger discrepancies of the calculated drift velocities and this would make the comparison of the inelastic cross sections more difficult. Therefore it was decided to use the best available set of σ_m values (that is σ_m^{sw}) for all the subsequent

calculations (i.e. even for those with the theoretical inelastic cross sections) but if necessary to adjust σ_m to achieve the best agreement with the experimental transport coefficients.

An analysis using MERT (see section 9.2) indicated that the experimental beam results for the total cross section σ_T^{exp} (Ferch *et al.* 1978) is consistent with σ_m^{SW} below 0.2 eV. The theoretical analysis of Morrison and coworkers provided a means of extending the consistency check of σ_T^{exp} and σ_m^{SW} beyond 0.2 eV. Using theoretical ratios of σ_T to σ_m (Morrison 1984) a total cross section based on σ_m^{SW} was calculated and compared with the corresponding experimental data (Fig. 9.2 and Table 9.3). Agreement with the experimental results for σ_T is very good up to 4 eV. Beyond that energy σ_m^{SW} becomes less accurate and any comparison is difficult to justify.

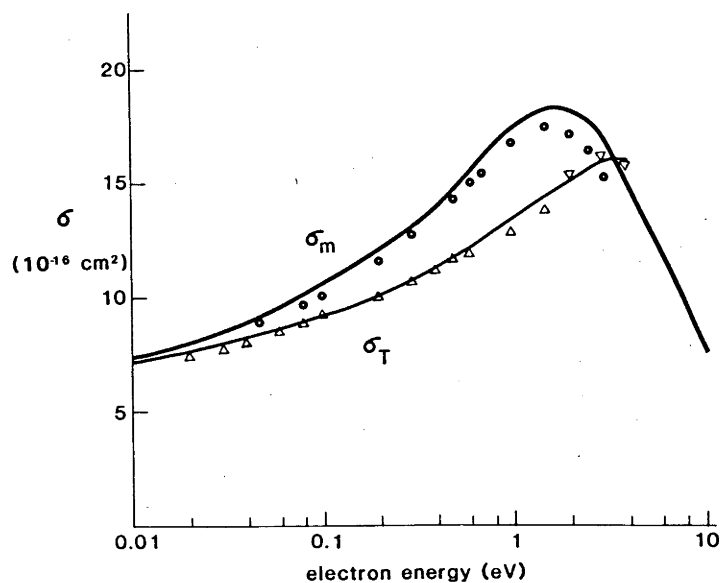


Figure 9.2 The momentum transfer cross section used in the present work (thick line) and the total cross section that is derived from it (thin line). Theoretical results for σ_m^{th} are shown as (o). The experimental data for the total cross section of Ferch *et al.* (1978) are shown as (Δ) while the data of Jones and Bonham (see Trajmar *et al.* 1983) are shown as (∇).

Table 9.3 Comparison of the momentum transfer and total cross sections

ϵ	σ_m^{sw} (10^{-16} cm 2)	σ_m^{th}	Δ^a (%)	$\sigma_T^{th}/\sigma_m^{th}$	σ_T^{sw} (10^{-16} cm 2)	σ_T^{exp}	Δ^b (%)
0.0	6.40			1	6.40		
0.01	7.30				7.17		
0.02	8.0				7.71	7.41	4
0.03	8.5				8.05	7.77	3.6
0.04	8.96				8.33	8.05	3.5
0.047	9.10	8.81	3.3	0.92	8.37		
0.05	9.28				8.50		
0.06	9.56				8.68	8.52	1.9
0.07	9.85				8.87		
0.08	10.1	9.67	4.4	0.892	9.01	8.79	2.5
0.09	10.3				9.14		
0.10	10.5	10.09	4.1	0.882	9.26	9.19	0.8
0.13	11.0				9.40		
0.15	11.40				9.59		
0.20	12.0	11.65	3.0	0.845	10.14	10.05	0.9
0.30	13.0	12.76	2.6	0.821	10.77	10.71	-0.3
0.40	13.9				11.2	11.21	0
0.50	14.7	14.37	2.3	0.700	11.61	11.62	0
0.60	15.6	14.96	4.3		12.20	(11.90)	2.5
0.70	16.3	15.48	5.3	0.773	12.6		
0.90	17.1				13.2		
1.0	17.4	16.62	4.7	0.766	13.3	(12.8)	4.1
1.1	17.7						
1.4	18.2						
1.5	18.25	17.38	5.0	0.785	14.3	(13.7)	4.6
1.6	18.3						
1.8	18.2						
2.0	18.0	17.15	5.0	0.826	14.9	15.4	-3.3
2.5	17.8	16.34	8.9				
3.0	17.0	15.24	11.5	0.9411	16.0	16.2	-1.2
4.0	14.8	12.92	14.5	1.069	15.8	15.7	0.6
5.0	13.0						
6.0	12.0	9.11	32	1.33	15.9	13.9	14
10.0	7.65	4.93	55	1.81	13.8	10.3	34

a difference between σ_m^{th} and σ_m^{sw}

b difference between σ_T^{sw} and σ_T^{exp} (Ferch et al. 1978 up to 1.5 eV and Jones and Bonham above 1.5 eV-see Trajmar et al. 1983)

9.4.4: Rotational cross sections. The agreement between the theoretical cross sections (from this point on the term theoretical will imply the data of Morrison and coworkers) and the swarm cross sections for the rotational excitation ($J=0-2$) is satisfactory. The maximum disagreement is 9.5% at 250 meV. Although the theoretical result lies outside the error bounds of the swarm result at some energies the combined error bounds are always larger than the disagreement. The cross sections for rotational excitation are shown in Fig. 10.3 (see also Table 10.4).

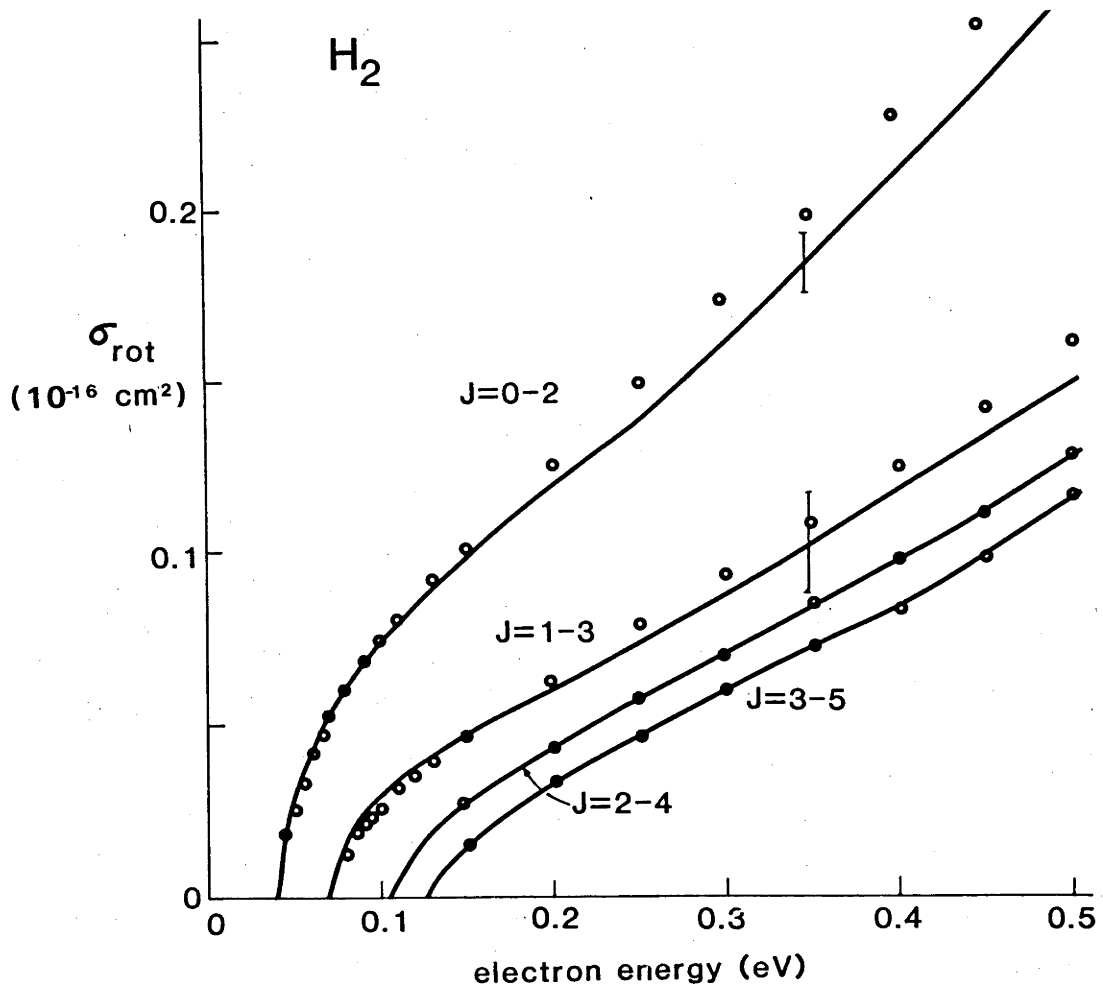


Figure 9.3 Rotational excitation cross sections. Results based on the swarm data are shown as the curve and the theoretical results as (o).

Table 9.4 Rotational excitation cross sections for the transition
J=0-2.

(all cross sections are in 10^{-16}cm^2)

ϵ (eV)	$\sigma_{\text{rot}}^{\text{th}}$	σ_{rot}^*	$\frac{\Delta\sigma_{\text{rot}}}{\sigma_{\text{th}}}$ (%)	$\sigma_{\text{rot}}^{\text{SW}}$
0.047	0.0182	0.0185	1.6	0.0185
0.050	0.0255	0.0270	5.9	0.0270
0.055	0.0342	0.035	2.3	0.035
0.060	0.0411	0.042	2.2	0.042
0.065	0.0468	0.048	2.6	0.048
0.07	0.0518	0.053	2.3	0.053
0.08	0.0603	0.060	-0.5	0.060
0.09	0.0676	0.068	+0.6	0.068
0.10	0.0740	0.074	0.0	0.074
0.11	0.0801	0.079	-1.4	0.079
0.13	0.0910	0.089	-2.2	0.089
0.15	0.1012	0.0999	-2.2	0.0999
0.20	0.1258	0.120	-4.8	0.120
0.25	0.150	0.137	-9.5	0.137
0.30	0.175	0.160	-9.4	0.160
0.35	0.2013	0.185	-8.8	0.185
0.40	0.2288	0.210	-8.9	0.215**
0.45	0.255	0.236	-8.1	0.245**
0.50	0.282	0.263	-7.1	0.278**
0.60	0.349	0.321		0.349
0.70	0.4235	0.385		0.4235
6.80	0.4986	0.452		0.4986
0.90	0.5777	0.520		0.5777
1.00	0.6599	0.592		0.6599
1.20	0.8301	0.781		0.8301
1.50	1.082	0.965		1.082
2.0	1.432	1.302		1.432
2.5	1.657	1.566		1.657
3.0	1.781	1.780		1.781
3.5	1.833	1.819		1.833
4.0	1.835	1.770		1.835
5.0	1.758	1.547		1.758
6.0	1.639	1.370		1.639
7.0	1.513	1.237		1.513
8.0	1.394	1.118		1.394
10.0	1.190	0.902		1.190

*Haddad and Crompton (1980)

**merged values

The disagreement between the two cross sections is nevertheless significant for the calculation of the transport coefficients. As can be seen from Fig. 9.4 the results of the calculations for both sets of cross sections agree very well with the experimental results up to 1.2 Td. Above that value the predictions based on σ_{rot}^{th} are outside the experimental error bounds. The electron energies corresponding to the range between 1 and 2 Td are such (see dot-dash line in Fig. 9.4) that the differences between the vibrational excitation cross sections (see next Section) cannot significantly affect the transport coefficients at these E/N values. Therefore the fact that the deviations of the calculated data from the experimental data in the range 1.2 to 2 Td are larger when the theoretical rather than the swarm-derived cross sections are used can only be attributed to the difference between the rotational cross sections.

Identical momentum transfer cross sections were used in both sets (see Section 9.4.3) but an attempt was made to optimize the fit by adjusting σ_m . An overall increase to σ_m^{sw} of between 3 and 5% (note that the theoretical cross section σ_m^{th} is already smaller than σ_m^{sw}) led to the situation where the calculated v_{dr} values were within the experimental error bounds but the calculated D_T/μ values were even further from the experimental data. It was not possible to achieve simultaneous agreement between calculated and experimental values of both v_{dr} and D_T/μ by adjusting σ_m . Therefore it must be concluded that the difference between the theoretical and swarm rotational excitation cross sections for the J=0-2 transition is significant and that the theoretical result is incompatible with the transport data. In fact if the σ_{rot}^{sw} of Haddad and Crompton (1980) is used up to 0.5 eV even better agreement is achieved. However, it was considered that any scaling of $\sigma_{rot}^{th}(J=0-2)$ at energies higher than 0.5

eV, where it was used to extrapolate $\sigma_{rot}^{sw}(J=0-2)$ (see Section 9.4.1), was not justified because the results obtained by using it were still in satisfactory agreement with the transport data.

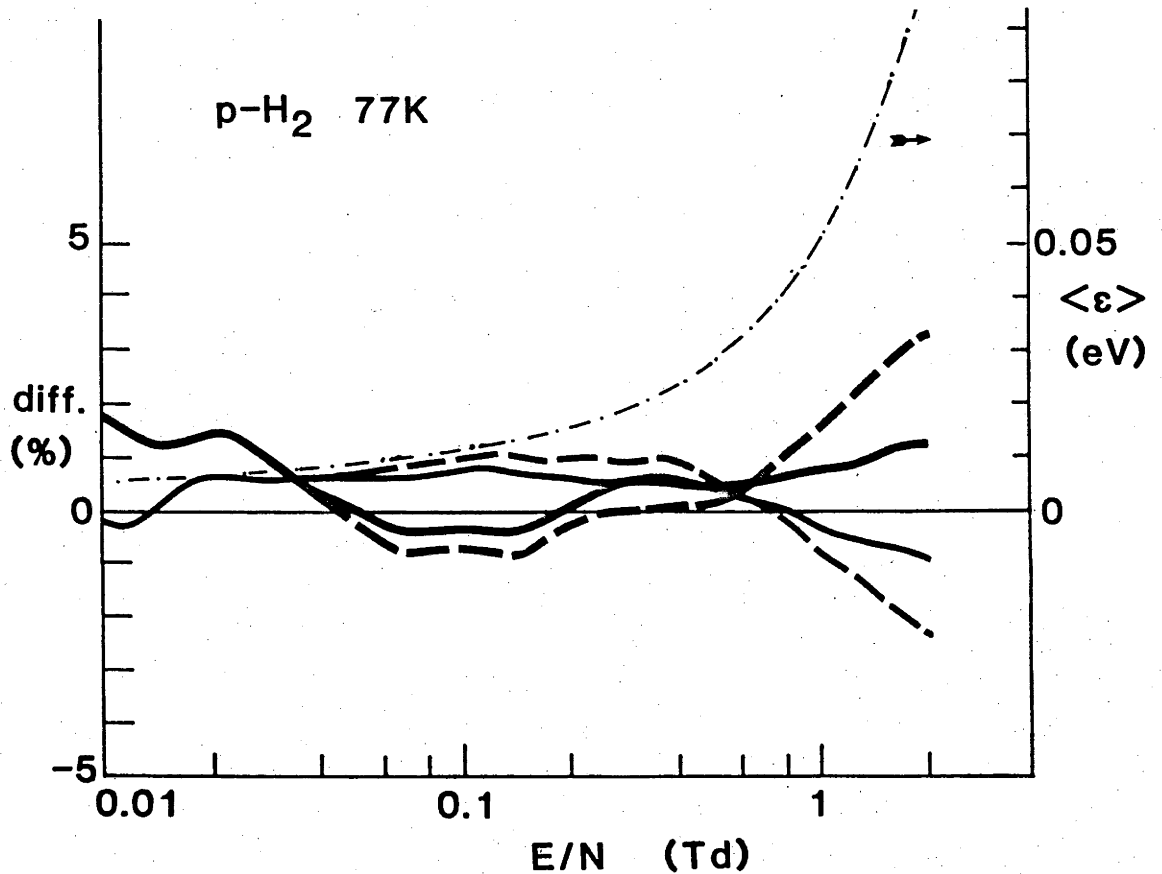


Figure 9.4 The differences between the calculated transport coefficients and the experimental values for low values of E/N . In all the figures in this chapter the differences between D_T/μ values will be shown using a thick line (solid and dashed for those calculated using the swarm-derived and theoretical cross sections respectively) and the differences between drift velocities will be shown using a thin line. The dot-dash line shows the values of average energies for the corresponding E/N values. The experimental error bounds are also shown.

A comparison between the cross sections for the $J=1-3$ transition (see Table 9.5 and Fig. 9.3) reveals that the agreement between these two cross sections is somewhat worse than in the case of $J=0-2$ transition. Nevertheless, all but the values at the two lowest energies at which $\sigma_{\text{rot}}^{\text{th}(J=1-3)}$ is tabulated are within the rather wide error bounds of the swarm cross section. Therefore the agreement between the experimental transport data and the data calculated using the theoretical cross section for $n\text{-H}_2$ at 77 K (Fig. 9.5) and $n\text{-H}_2$ at 293 K (Fig. 9.6) is still good for the low values of E/N . Again, as for $p\text{-H}_2$, the results based on the theoretical cross section are outside the experimental error bounds around 2 Td. This indicates that $\sigma_{\text{rot}}^{\text{th}(J=1-3)}$ is also too high at energies between 0.2 and 0.5 eV. However, when the swarm cross section is used up to 0.35 eV and then merged to the theoretical cross section the calculated values of the transport coefficients are in good agreement with the experimental data.

Theoretical cross sections for the $J=2-4$ and $J=3-5$ processes were used in the calculations (see Table 9.6 and Fig. 9.3). Since the populations of the $J=2$ and $J=3$ levels are relatively low (see Appendix 6) the accuracy of the representation of the corresponding cross sections is not critical. Thus, when the cross sections scaled from the $J=0-2$ cross section (see Section 9.4.1) were replaced by the theoretical results, which differed by up to 30% below 0.5 eV, only small changes of the calculated transport coefficients were observed.

It may be concluded that the theoretical rotational excitation cross sections are essentially in agreement with those obtained from the swarm data, although better agreement between experimental and calculated transport data can be obtained by reducing the theoretical cross sections

by up to 10% above 0.2 eV. Finally it should be noted that the error bounds on the present rotational excitation cross sections at low energies are the same as those previously claimed, namely 5% for J=0-2 transition (Crompton et al. 1969) and 15% for J=1-3 transition (Gibson 1970). However, the error bounds of the swarm-derived cross sections increase rapidly above 0.35 eV; for the J=0-2 transition the uncertainty of the cross section at 0.5 eV is 10%, while above that energy the cross section cannot be determined uniquely.

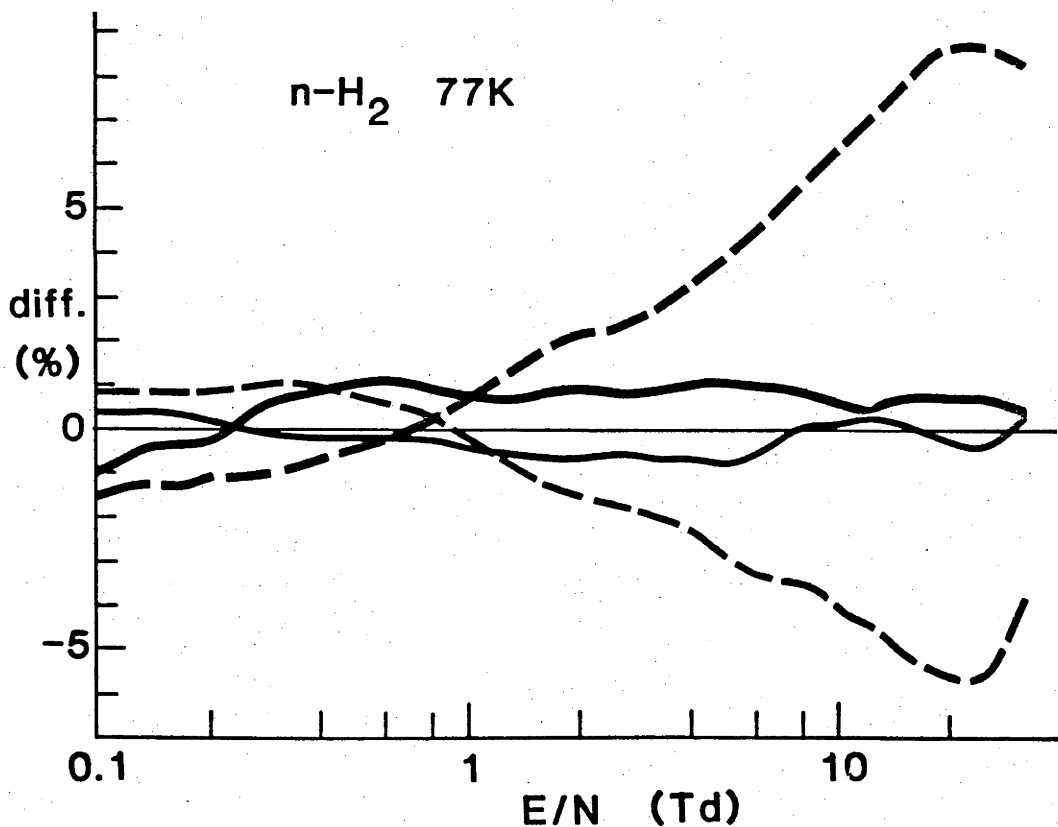


Figure 9.5 Comparison of the results for the transport coefficients calculated using the two sets of cross sections with experimental data for n-H₂ at 77 K.

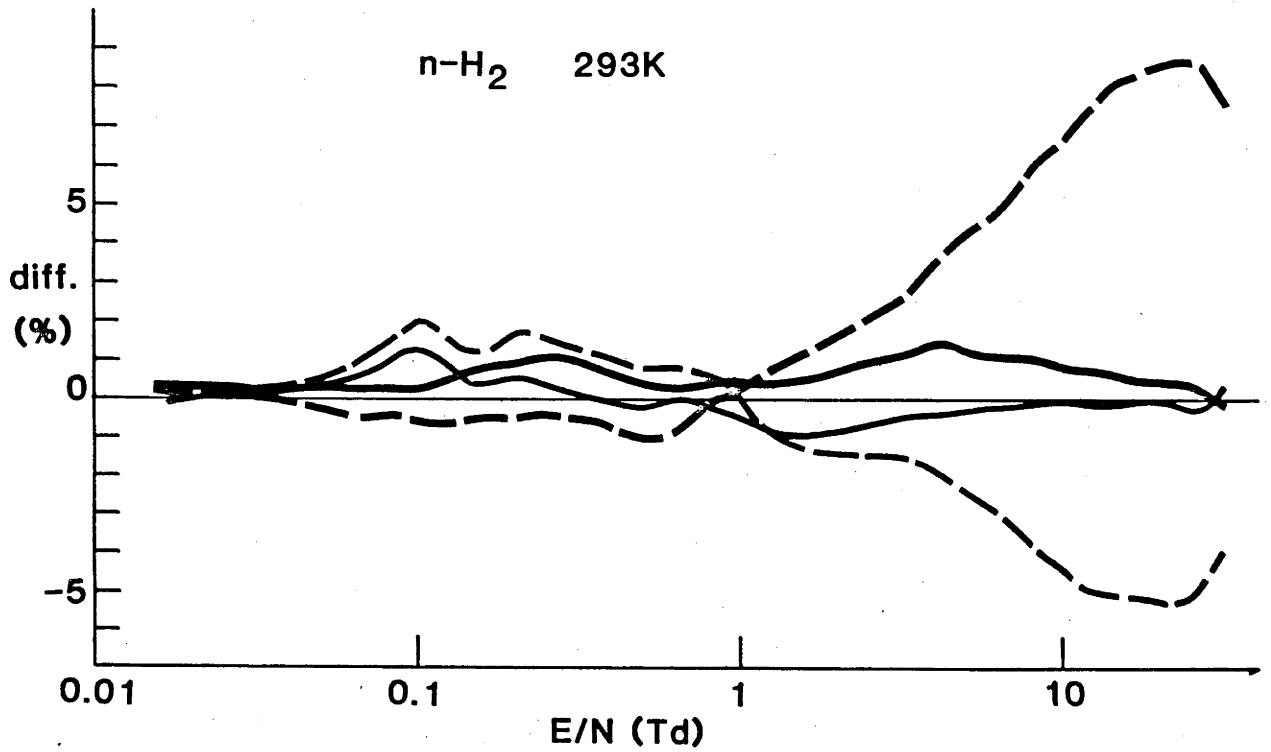


Figure 9.6 Comparison of the results for the transport coefficients calculated using the two sets of cross sections with experimental data for n-H₂ at 293 K.

Table 9.5 Rotational excitation cross sections for the J=1-3 transition

ϵ (eV)	$\sigma_{\text{rot}}^{\text{th}}$	σ_{rot}^*	$\Delta\sigma_{\text{rot}}$	$\sigma_{\text{rot}}^{\text{sw}}$
			$\frac{\Delta\sigma_{\text{rot}}}{\sigma_{\text{rot}}^{\text{th}}}$	
			(%)	
0.08	0.0131	0.0170	23	0.0170
0.085	0.0180	0.0215	16	0.0215
0.090	0.0207	0.0250	17	0.0250
0.095	0.0235	0.0275	14	0.0275
0.100	0.0264	0.0295	10	0.0295
0.11	0.0310	0.0335	7.5	0.0335
0.12	0.0357	0.0380	6.0	0.0380
0.13	0.0395	0.0410	3.6	0.0410
0.15	0.0469	0.0470	0.2	0.0470
0.20	0.0630	0.060	5.0	0.060
0.25	0.0779	0.0740	5.3	0.074
0.30	0.0935	0.088	6.3	0.088
0.35	0.1092	0.1025	6.5	0.1035**
0.40	0.1257	0.1175	7.0	0.120**
0.45	0.1422	0.1330	6.9	0.0139**
0.50	0.1607	0.149	7.9	0.1600**
0.55	0.1772	0.165		0.1772
0.60	0.1977	0.181		0.1977
0.65	0.2197	0.200		0.2197
0.70	0.2409	0.220		0.2409
0.80	0.2854	0.270		0.2854
0.90	0.3324	0.316		0.3324
1.0	0.3811	0.364		0.3811
1.5	0.6338	0.590		0.6338
2.0	0.8455	0.810		0.8455
2.5	0.9832	0.980		0.9832
3.0	1.060	1.066		1.060
3.5	1.093	1.092		1.093
4.0	1.096	1.078		1.096
4.5	1.079	1.048		1.079
5.0	1.052	6.992		1.052
6.0	0.9815	0.883		0.9815
7.0	0.9065	0.779		0.9065
8.0	0.8354	0.693		0.8354
10.0	0.7134	0.558		0.7134

*Haddad and Crompton (1980)

**merged values

Table 9.6 Cross sections for the rotational excitation (J=2-4 and J=3-5) used in the present work.

ϵ (eV)	$\sigma_{\text{rot}} \quad J = 2-4$	$\sigma_{\text{rot}} \quad J = 3-5$
0.15	0.0278	0.0153
0.20	0.0433	0.0329
0.25	0.0579	0.0458
0.30	0.0704	0.0587
0.35	0.0855	0.0717
0.40	0.0984	0.0821
0.45	0.1124	0.0983
0.50	0.1277	0.1116
0.60	0.1602	0.1408
0.70	0.1969	0.1745
0.80	0.2340	0.2090
0.90	0.2730	0.2460
1.00	0.3110	0.2860
1.50	0.5290	0.4816
2.00	0.6840	0.6540
2.50	0.8320	0.7685
3.0	0.9190	0.8350
3.5	0.9290	0.8620
4.0	0.9350	0.8640
4.5	0.9200	0.8530
5.0	0.870	0.8300
5.5	0.844	0.8040
6.0	0.819	0.7750
7.0	0.763	0.7160
8.0	0.704	0.6610
10.0	0.605	0.5650

9.4.5: Vibrational excitation: splitting of the cross section into rotationally elastic and inelastic parts. Since the rotational excitation cross sections ($\sigma_{\text{rot}}^{\text{sw}}$) used in the earlier swarm data analysis (Crompton et al. 1969; Henry and Lane 1969; Haddad and Crompton 1980) were not much different from the new cross sections (the modifications arising from the new theoretical results at higher energies) one cannot expect major changes in the swarm-derived vibrational cross section σ_{vib} as compared to the data of Haddad and Crompton (1980) when $\sigma_{\text{rot}}^{\text{th}}$ is used to extrapolate the J=0-2 rotational excitation cross section instead of the previously used cross section of Henry and Lane. A potentially important difference from previous analyses is the inclusion of rotationally inelastic vibrational excitation "splitting" in the present work.

The theoretical calculations were used to divide the v=0-1 vibrational excitation cross section into its rotationally elastic and inelastic components. The theoretical results for the ratio between the two components agree very well with the experimental results of Linder and Schmidt (1971). The energy losses (see Appendix 4) for the $\Delta J=0$ and $\Delta J=2$ processes differ by about 10%. Figure 9.7 shows the importance of the inclusion of this effect for p-H₂; the differences are always less than 1%. The differences are small but nevertheless significant for H₂, but would be of less importance for other molecular gases because of the very much smaller energy losses in rotational excitation.

No attempt was made to split the v = 0-2 and v = 0-3 cross sections into rotationally elastic and inelastic components. The overall contribution of these two processes is small while their energy losses are higher so that the importance of the additional energy loss due to $\Delta J=2$ transition is smaller.

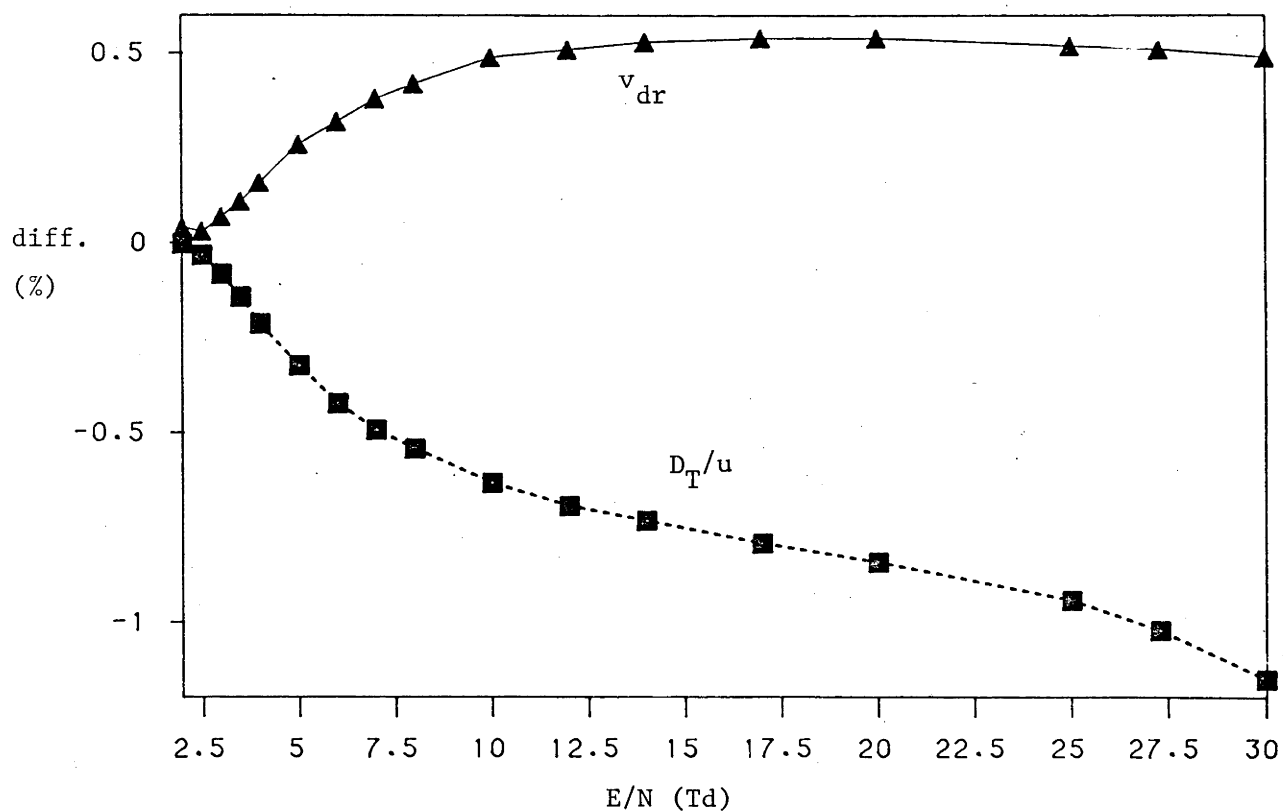


Figure 9.7 Influence of splitting of the vibrational excitation cross section. The differences between the transport data calculated with and without splitting are shown for p-H₂ at 77 K.

For n-H₂ it is necessary to use four cross sections for vibrational excitation ($v=0-1$) because of the significant $J=1$ rotational state population. This is because the energy losses for $J=1-3$ and $J=0-2$ transitions differ significantly (Appendix 4) and there is even a small difference (0.7 meV) between the losses for the rotationally elastic transitions. However, for hydrogen the difference in the ratio of the cross sections for rotationally elastic and inelastic transitions is such that it compensates very well for the different energy losses (i.e. for $J=0-2$ or $J=1+3$) except close to threshold. Therefore it proved possible to

analyse the data for n-H₂ (at 77 and 293 K) by using only the cross sections for J=0-0 and J=0-2 transitions. When the full set of v=0-1 vibrational cross sections is used for n-H₂ at 77 K (a set that also includes appropriately scaled and weighted cross sections $\sigma_{\text{vib}}(J=1-1)$ and $\sigma_{\text{vib}}(J=1-3)$) the calculated transport coefficients are not more than 0.13% different from those calculated using the cross sections for 0-0 and 0-2 transitions only. For the room temperature calculations the vibrational cross section should be split into at least eight different cross sections. The data were not available to enable such a set to be constructed, but calculations were made using the set of vibrational excitation cross sections for n-H₂ and p-H₂. The agreement was similar to the one reported above even for Ar-H₂ mixtures where one would expect the largest sensitivity to the energy losses (see Section 9.4.7).

It may therefore be concluded that in the analysis of the transport data for H₂ the cross section for v=0-1 vibrational transition should be split into its rotationally elastic and inelastic components and that the splitting appropriate for p-H₂ at 77 K is adequate for n-H₂ at both temperatures.

9.4.6: Vibrational excitation: comparison of cross sections. As expected, when the cross sections of Haddad and Crompton (1980) are used the calculated transport data are in very good agreement with the experimental transport data. However, when the vibrational excitation cross section (v=0-1) is split into its rotationally elastic and inelastic parts the disagreement with the experimental data exceeds 2% both for drift velocities and characteristic energies. Improvement (leading to agreement to within 1% for D_T/μ and v_{dr}) was achieved when σ_{vib} (v=0-1) was scaled by

0.85 and reduced slightly more (by up to 3%) close to the threshold. The theoretical results of Morrison et al. for the cross sections for the $v=0-1$ transition and the corresponding splitting factors (SF) are shown in Table 9.7 along with some other experimental or theoretical data. The results of the present analysis are also shown.

On the other hand if the theoretical vibrational cross sections are used the calculated transport coefficients are in serious disagreement with the experimental results (Figure 9.8; see also Fig. 9.5 and Fig. 9.6). The disagreement is well beyond the experimental uncertainty.

The momentum transfer cross section was modified in an attempt to achieve better agreement with the transport coefficients. As expected the modifications that led to a better fit for one of the transport coefficients meant worse agreement for the other. It is especially difficult to fit D_T/μ values by modifying only σ_m . For example, if the values of D_T/μ are brought into agreement with the transport data to within 2% the differences between the experimental and calculated drift velocities exceed 17%. If the drift velocities are brought into agreement, there is an additional 1% difference between calculated and experimental values of D_T/μ bringing the disagreement to 9.5% at some values of E/N .

Since σ_{vib}^{th} ($v=0-1$) is considerably larger than $\sigma_{vib}^{sw}(v=0-1)$ (Table 9.7) the use of σ_{vib}^{th} results in calculated energy losses that are too large, and clearly, the addition of a hypothetical inelastic process could not reconcile σ_{vib}^{th} with the experimental electron transport data. However, one might argue that a reduction of $\sigma_{vib}(v=0-2)$ and other higher-order inelastic cross sections could compensate for this. Present calculations show that this is not possible. If one uses the final set for $p-H_2$, and reduces to zero the cross sections for all inelastic processes

apart from $\sigma_{rot}(J=0-2)$ and $\sigma_{vib}(v=0-1)$ the maximum deviation of the transport coefficients from those calculated with the full set is 1.0% for v_{dr} and 3.5% for D_T/μ . This is insufficient to compensate the 5.8% and 8.8% differences that result from using σ_{vib}^{th} for p-H₂ (see Fig. 9.8).

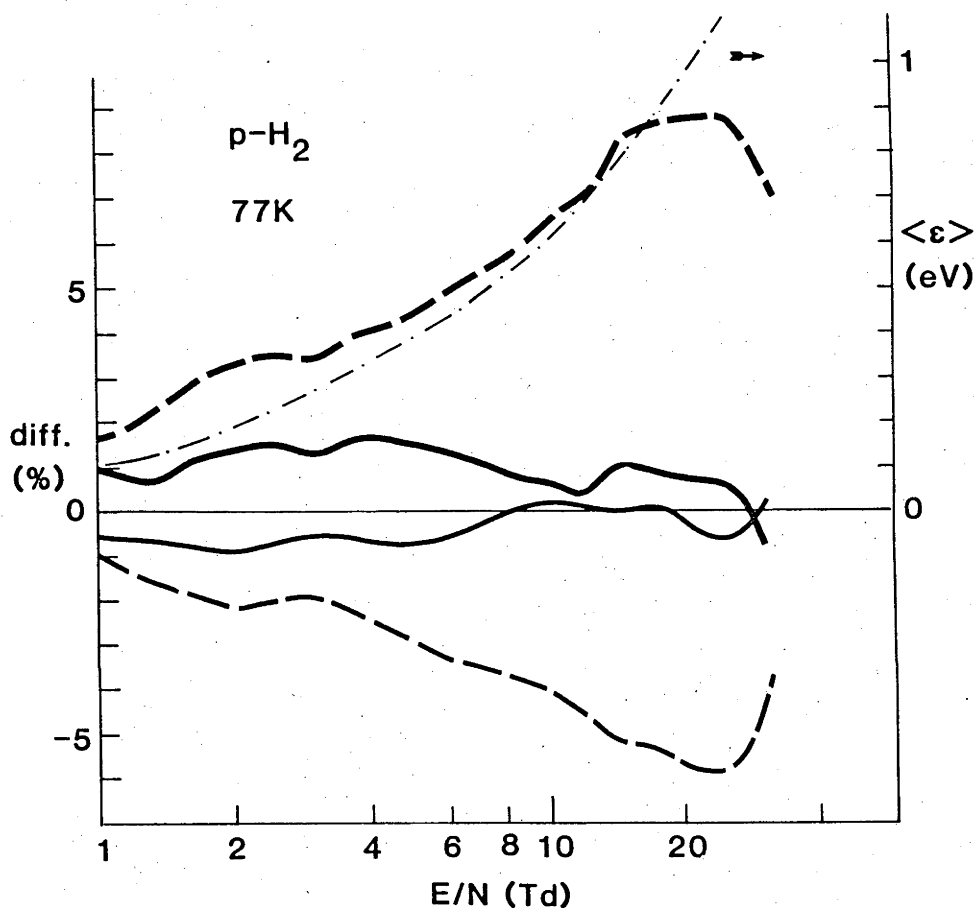


Figure 9.8 Comparison of the results for the transport coefficients in p-H₂ at high values of E/N based on the two sets of cross sections.

To conclude, it should be noted that the disagreement between σ_{vib}^{th} and σ_{vib}^{sw} lies outside the combined uncertainties claimed for each. The maximum difference is 81% (of σ_{vib}^{sw}) or 45% (of σ_{vib}^{th}) (Table 9.7 and Fig. 9.9). However one should note also that the theoretical data agree well with the data of Ehrhardt *et al.* (1968) in the low energy range, while for energies higher than 5 eV the disagreement is quite significant (65% at

10 eV) (see Fig. 9.10). Note that in Fig. 9.10 the total vibrational excitation cross section of Haddad and Crompton (1980) is plotted in order to make the comparison with Ehrhardt *et al.*'s cross section in which the rotationally elastic and inelastic components are unresolved. Haddad and Crompton's cross section is the one that leads to the best fit with the transport data when the splitting is not accounted for.

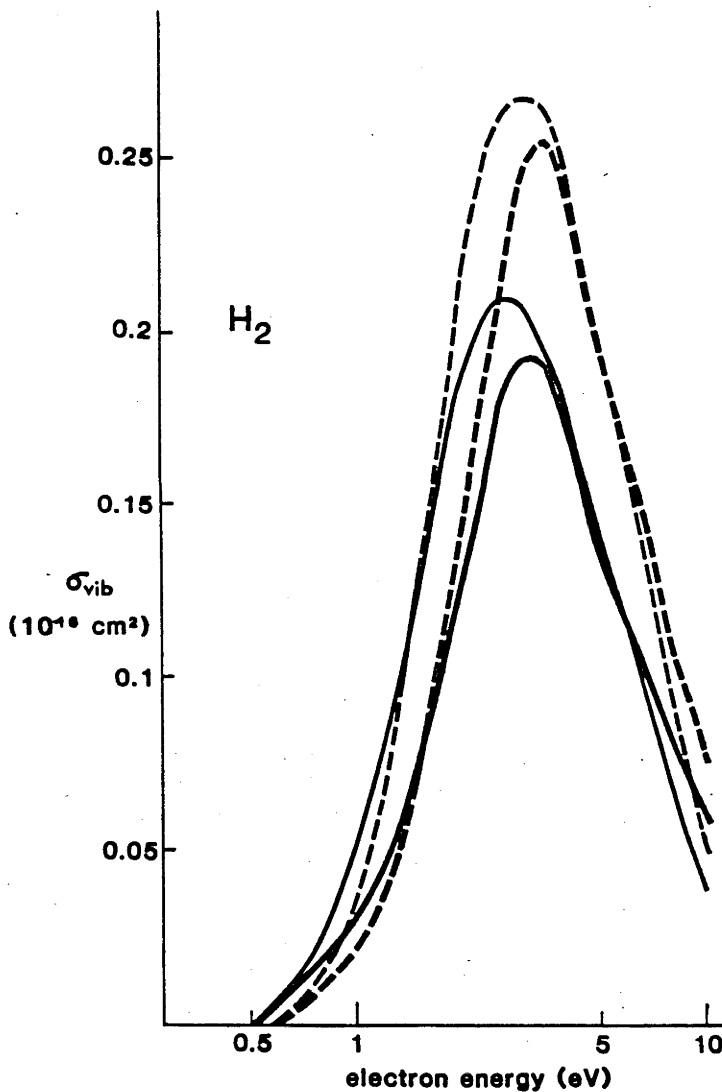


Figure 9.9 Vibrational excitation cross sections for hydrogen. The theoretical results are shown using thin lines and the swarm result using thick lines. Rotationally inelastic cross sections are shown with dashed lines and rotationally elastic cross sections are shown with solid lines.

Table 9.7 Vibrational cross sections (10^{-16} cm^2) for hydrogen.

ϵ (eV)	$\sigma_{\text{vib}}^{\text{th}}$ J=0-0	SF	$\sigma_{\text{vib}}^{\text{th}}$ J=0-2	$\sigma_{\text{vib}}^{\text{th}}$ J=1-1	SF	$\sigma_{\text{vib}}^{\text{th}}$ J=1-3	$\sigma_{\text{vib}}^{\text{th}}$ TOTAL
0.525	0.0012						
0.575	0.0046		0.0006				0.0052
0.60	0.0069	0.81	0.00157	0.0084	0.96	0.00034	0.00847
0.65	0.0110	0.72	0.004	0.0137	0.90	0.0015	0.0150
0.7	0.0156	0.68	0.0071	0.0197	0.85	0.0032	0.0227
0.8	0.0257	0.62	0.0151	0.0337	0.82	0.0076	0.0408
0.9	0.0377	0.59	0.0253	0.0500	0.79	0.0134	0.0630
1.0	0.0507	0.57	0.0376	0.068	0.77	0.0205	0.0883
1.1	0.0651	0.55	0.0522	0.0887	0.75	0.0289	0.1173
1.2	0.0800	0.54	0.0684	0.1103	0.74	0.0384	0.1484
1.4	0.1109	0.51	0.1049	0.1562	0.72	0.0600	0.2158
1.5	0.1262	0.50	0.1245	0.180	0.71	0.0715	0.2507
1.6	0.1410	0.49	0.1442				0.2852
2.0	0.1874	0.47	0.2138	0.276	0.69	0.125	0.4012
2.5	0.2095	0.45	0.2589	0.315	0.67	0.153	0.4684
3.0	0.2069	0.44	0.2681	0.316	0.66	0.160	0.4750
3.5	0.1944	0.43	0.2608	0.300	0.66	0.156	0.4552
4.0	0.1785	0.42	0.2447	0.277	0.66	0.146	0.4232
4.5	0.1449	0.42	0.2034	0.227	0.65	0.122	0.4083
6.0	0.1169	0.41	0.1647	0.183	0.65	0.099	0.2816
7.0	0.0954	0.41	0.1332	0.149	0.65	0.082	0.229
8.0	0.0793	0.42	0.1088	0.123	0.65	0.065	0.1881
10.0	0.0577	0.43	0.0753	0.0880	0.66	0.045	0.1330

ϵ (eV)	Ehrhardt et al. TOTAL	Linder and Schmidt				Klonover and Kaldor		
		J=1-1	SF	J=1-3	TOTAL	$\Delta J=0$	$\Delta J=2$	TOTAL
0.60	0.0172							
0.80	0.0471							
0.85	0.0586							
1.0	0.0945					(0.07)	(0.035)	(0.105)
1.1	0.123							
1.4	0.213							
1.5		(0.1975)	0.69	(0.0848)	(0.2873)	0.14	0.08	0.22
1.6	0.274							
1.7	0.308							
2.0	0.403							
2.5		0.272	0.09	0.120	0.392	0.24	0.13	0.37
2.6	0.495							
3.0	0.512							
3.5		0.285	0.68	0.136	0.422	0.25	0.14	0.39
4.0	0.441							
4.5	0.391	0.237	0.66	0.122	0.359	0.22	0.12	0.34
5.0	0.3427							
6.0	0.278	0.187	0.65	0.101	0.288	0.15	0.09	0.24
7.0	0.213							
8.0	0.1516	0.1155	0.62	0.0699	0.1854	0.11	0.07	0.18
10.0	0.0874	0.761	0.66	0.0388	0.115			

ϵ (eV)	Haddad & Crompton TOTAL	PRESENT		$\frac{\Delta\sigma_{\text{vib}}}{\sigma^{\text{th}}}$	$\frac{\Delta\sigma_{\text{vib}}}{\sigma^{\text{SW}}}$
		J=0-0	J=0-2	(%)	(%)
0.56	0.0045	0.0036			
0.60	0.009	0.0059	0.0014		
0.65	0.0145	0.0086	0.0033		
0.75	0.027	0.0747	0.0080		
0.85	0.040	0.0206	0.0134		
0.95	0.055	0.0270	0.0197		
1.00	0.0635	0.0305	0.0235	40	66
1.05	0.0720	0.0342	0.0270		
1.10	0.080	0.0374	0.0306	43	74
1.15	0.094	0.0433	0.0366		
1.20	0.100	0.0453	0.0397	44	76
1.30	0.122	0.541	0.0500		
1.40	0.140	0.0611	0.0589	45	81
1.60	0.203	0.0863	0.0891	39	63
1.80	0.258	0.1072	0.1176		
2.20	0.343	0.140	0.164		
2.40	0.400	0.162	0.195		
2.60	0.44	0.177	0.219		
3.0	0.48	0.191	0.248		
3.5	0.48	0.192	0.255		
4.0	0.44	0.177	0.241		
4.5	0.39	0.158	0.219		
5.0	0.35	0.144	0.201		
6.0	0.28	0.118	0.167		
7.0	0.21	0.0894	0.125		
8.0	0.152	0.0650	0.0897		
9.0	0.119	0.0516	0.0698		
10.0	0.0874	0.0384	0.0508		

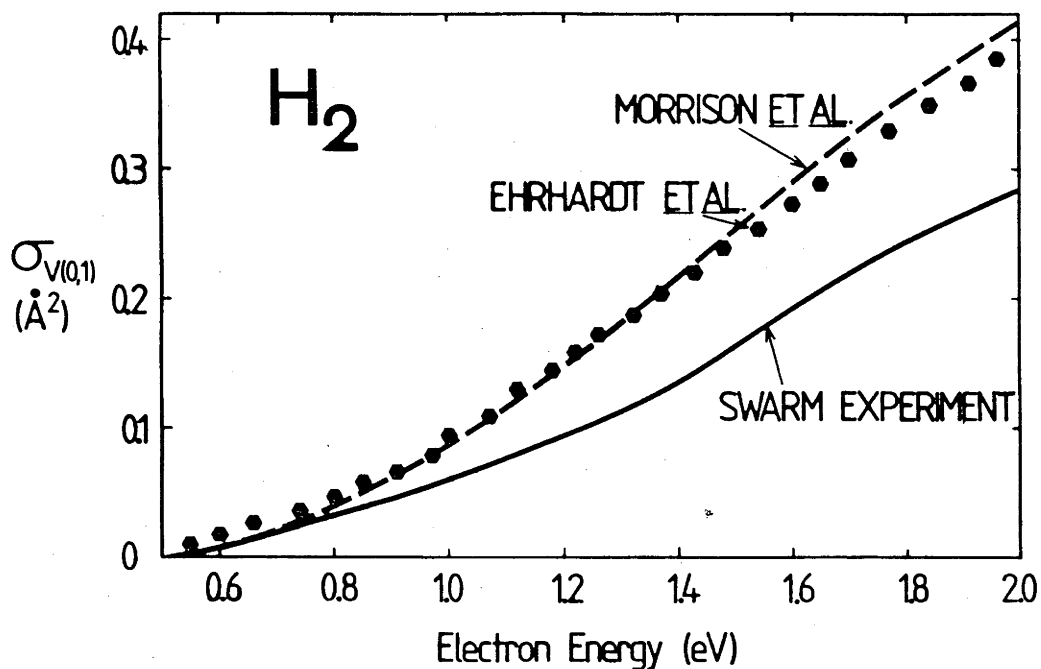


Figure 9.10 Vibrational excitation cross sections for hydrogen $v=0-1$ (total). The data of Ehrhardt et al. (1968) are presented as points, the theoretical results as a dashed line and the cross section of Haddad and Crompton (1980) as a solid line.

The theoretical results of Klonover and Kaldor (1979) lead to somewhat better agreement with the swarm data than those of Morrison and coworkers (1984) but the agreement is still far from satisfactory. The results of Linder and Schmidt (1971) are generally slightly lower than those of Ehrhardt et al. (1968) but are not sufficiently numerous in the energy range 1-2 eV, the most important energy range for this discussion, to draw a definitive conclusion.

9.4.7: Sensitivity of the transport data to local perturbations of $\sigma_{vib}(v = 0-1)$: analysis of the accuracy of the swarm cross section.

The fact that swarms are not monoenergetic tends to obscure the relationship between the cross sections and the transport coefficients at specific values of E/N . An illustration of this fact in the case of $\sigma_{vib}(v = 0-1)$ will be given here. As a result of the following analysis the error bounds of the vibrational excitation cross sections will be determined. The procedure to be described is a more detailed study of the accuracy of a swarm-derived cross section than the usual procedure of multiplying the cross section by a constant over the entire energy range. It could be argued that the cross section has a sharp feature that might be undetectable in the swarm analysis, or that by increasing the cross section at some energy one could compensate for values that are too low at some other energy, and therefore that the swarm-derived cross section could have a completely unrealistic energy dependence. The application of a multiplying constant to check the accuracy of the swarm-derived cross section does not reveal such inaccuracies whereas the present procedure does.

First, a "local" perturbation to the cross section will be defined. To produce a perturbation the cross section is reduced by a certain percentage ("depth") starting from a certain energy ("threshold") and extending for a certain range ("width"). Widths are normalized in such a way that the ratio of the width of the perturbation to the halfwidth of the energy distribution function at the value of E/N where the local perturbation has the largest influence is kept approximately the same. When investigating the effect of such a perturbation on the transport coefficients only the threshold energy of the perturbation is initially varied. First, a

perturbation of width W_1 and threshold T_1 is applied. The value of E/N is found at which the influence of this perturbation is the largest, and the corresponding value of eD_T/μ ($\approx \epsilon_{k1}$) is used as a measure of the width of the distribution function. The next step is to change the threshold to T_2 , keeping the same width (W_1). The E/N value that now corresponds to the maximum deviation is different and so is the corresponding characteristic energy ϵ_{k2} . For the final calculation at this threshold (T_2) the width W_2 is chosen such that $W_2 = W_1(\epsilon_{k2}/\epsilon_{k1})$. This means that the ratio of the width of the perturbation to the width of the electron energy distribution function is approximately constant, differing only as a result of changes in the shape of the electron energy distribution function. In this way the influence of the perturbation is kept at an approximately constant level while the value of E/N where the effect is a maximum is changed.

The results are shown on Fig. 9.11 (a-d). The width of the local perturbation is chosen to have a significant effect on the transport coefficients, that is, an effect which could not pass unnoticed in the swarm analysis. As can be seen, the chosen widths, starting from 0.25 eV at the lowest energy, have an influence over a wide range of E/N .

From the results presented one can conclude that the transport data are sensitive to local perturbations of 25% for values of T up to 2 eV. Of course they are very responsive to perturbations around the threshold energy for this process (0.516 eV) and up to perhaps 1.6 eV.

Above 2 eV perturbations extending from the threshold upwards had to be used in order to have a significant effect on the transport coefficients. Results are presented for two different depths, 25 and 50%, in Fig. 9.12 (a and b). They indicate that the overall accuracy of the cross section σ_{vib} ($v=0-1$) from 2 to 4 eV should be better than 25% while above 4 eV it

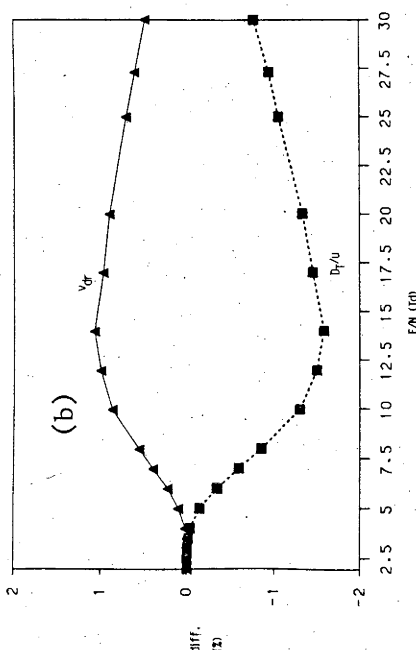
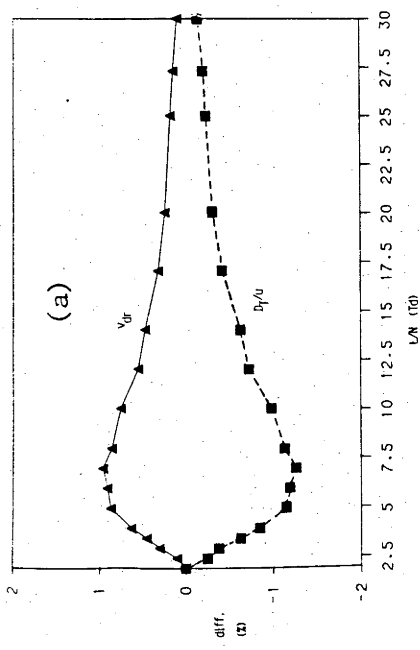
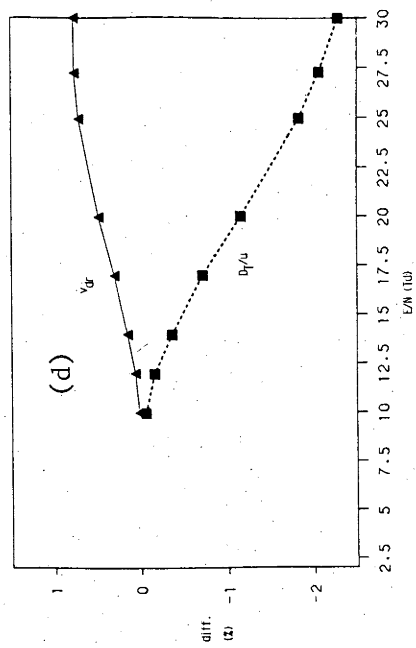
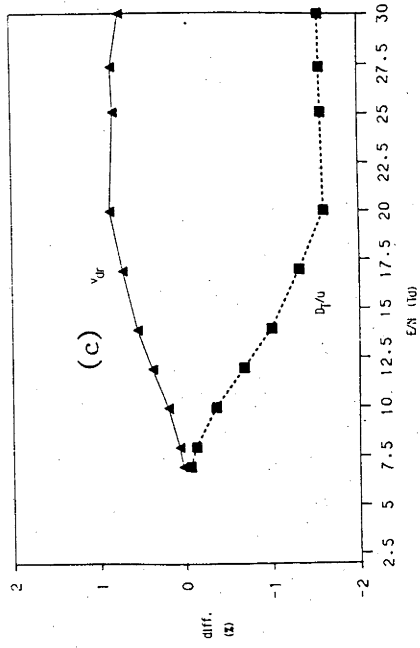


Figure 9.11 The influence of the perturbations on the transport data for p-H₂. a) T=0.6, W=0.25, 25% deep; b) T=1.0, W=0.39, 25% deep; c) T=1.4, W=0.5, 25% deep; d) T=1.8, W=0.85, 25% deep.

should be better than 50%. This narrows the energy range of the cross section based on the available electron transport data in parahydrogen to the energy range between threshold and 2 eV.

If the vibrational cross section is increased by 10% over the entire energy range the differences between the experimental and calculated transport coefficients become significantly larger than the error bound. Therefore it may be concluded that the vibrational excitation cross section is known to within 10% in the energy region up to 2 eV. The tests described above show that the cross section could vary locally by 25% in a narrow energy range of between 0.25 eV close to the threshold and 0.6 eV around 2 eV. It is, however, hard to accept that such a local inaccuracy would pass unnoticed since the shape of the cross section would not be smooth. Above 2 eV the overall accuracy of the swarm cross section obtained from the presently used data is $\pm 25\%$ and above 4 eV it is $\pm 50\%$.

9.4.8: Electron transport coefficients in argon-hydrogen mixtures.

Measurements and analysis of transport coefficients in mixtures were used by Engelhardt and Phelps (1964) and Haddad and Crompton (1980) to determine the cross sections in hydrogen. As will be seen the advantage of this technique is that it is possible to have a sensitivity to a particular process that is greater than in the pure gas. Another advantage is that it provides a wide range of independent data and therefore the uniqueness of the derived cross sections may be improved.

The experimental data obtained by Haddad and Crompton were compared with the predictions based on the cross sections presently derived and the theoretical cross sections. There was no need to make corrections to the two-term results for either transport coefficient at any of the values of

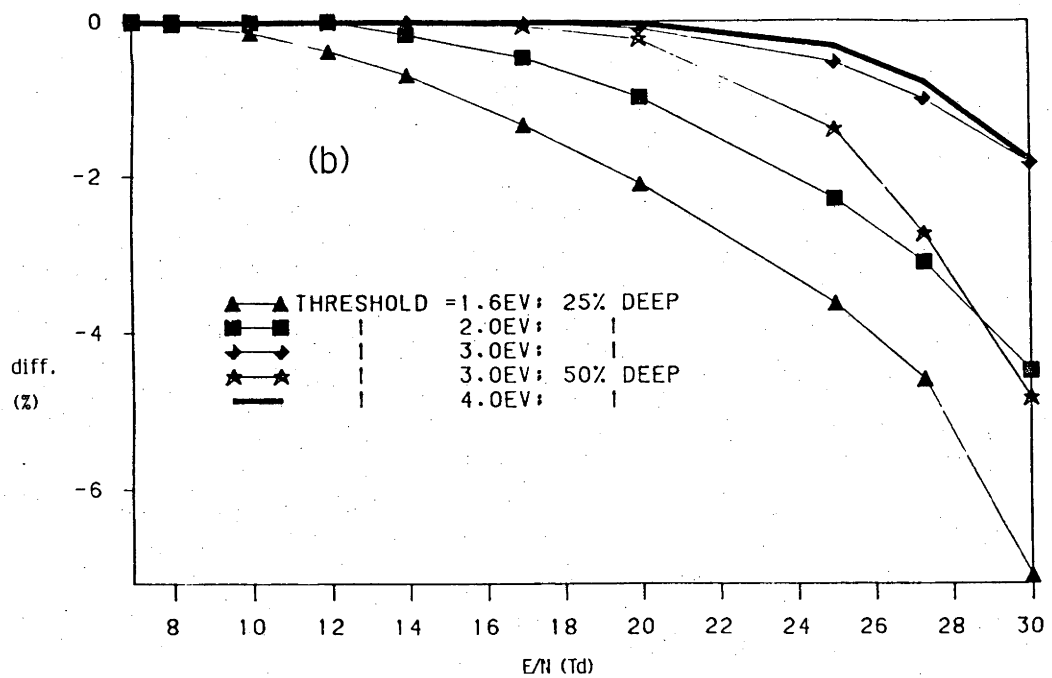
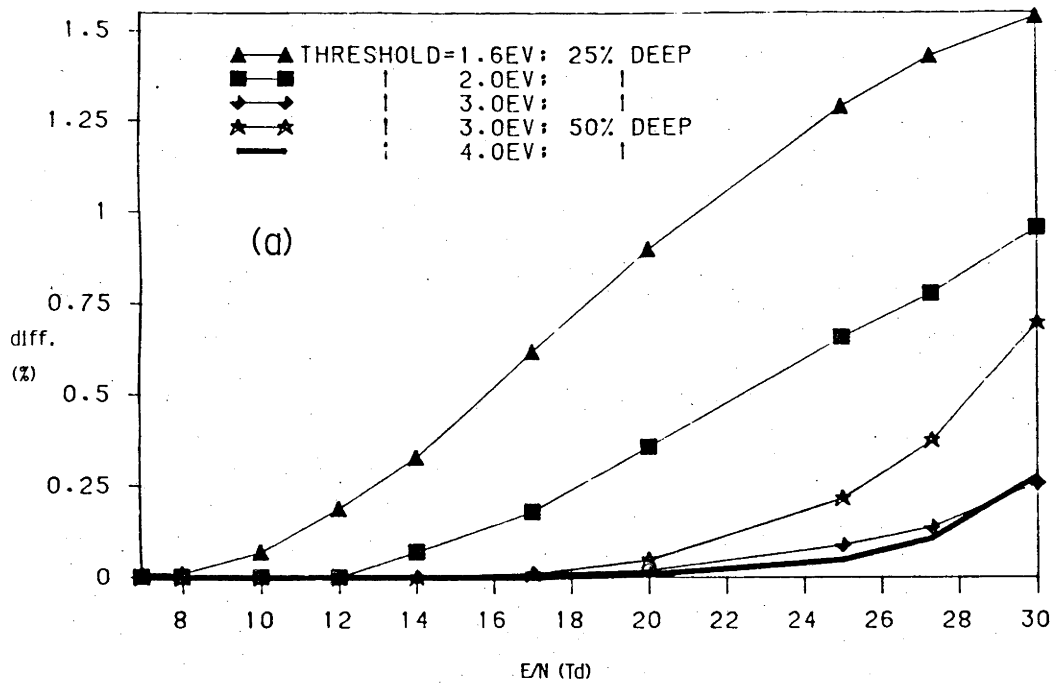


Figure 9.12 a) Influence of wide perturbations on calculated drift velocities for p-H₂ at 77 K; b) Influence of wide perturbations on calculated values of D_T/μ for p-H₂ at 77 K.

E/N used. This was shown by carrying out multiterm calculations with appropriate differential cross sections. The results of these calculations confirmed the conclusion of Haddad and Crompton (1980) that the multiterm corrections do not exceed 0.3% for D_T/μ and 0.1% for v_{dr} .

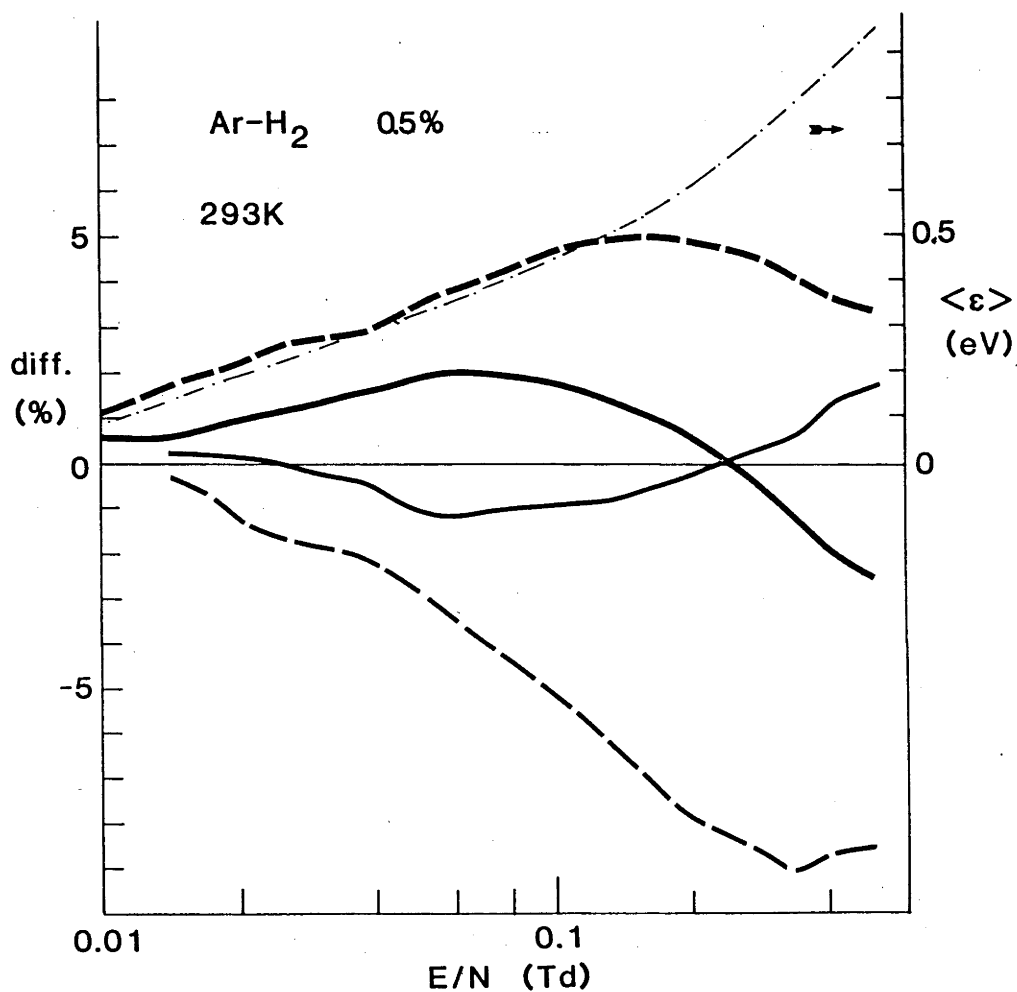


Figure 9.13 Comparison of the transport coefficients for the 0.5% Ar-H₂ mixture calculated using the theoretical (thin line) and the swarm-derived (thick line) cross sections. The values of D_T/μ and v_{dr} are shown as dashed and solid curves respectively.

The results are presented in Fig. 9.13 and Fig. 9.14. Haddad and Crompton found differences between the predicted and experimental values of

up to 3.5% for D_T/μ and 2.5% for v_{dr} . Using the present cross sections the calculated values differ from the experimental data by less than 2.5% for D_T/μ and 1% for v_{dr} and therefore do not exceed the experimental error bounds. However, if the theoretical vibrational cross section is used in the calculations the differences are as large as 5% for D_T/μ and 8% for v_{dr} . The average energies in the E/N region used (see Fig 9.13) are such that the difference may be attributed to the differences in the vibrational cross sections. In all the calculations the momentum transfer cross section for argon derived by Haddad and O'Malley (1982) was used.

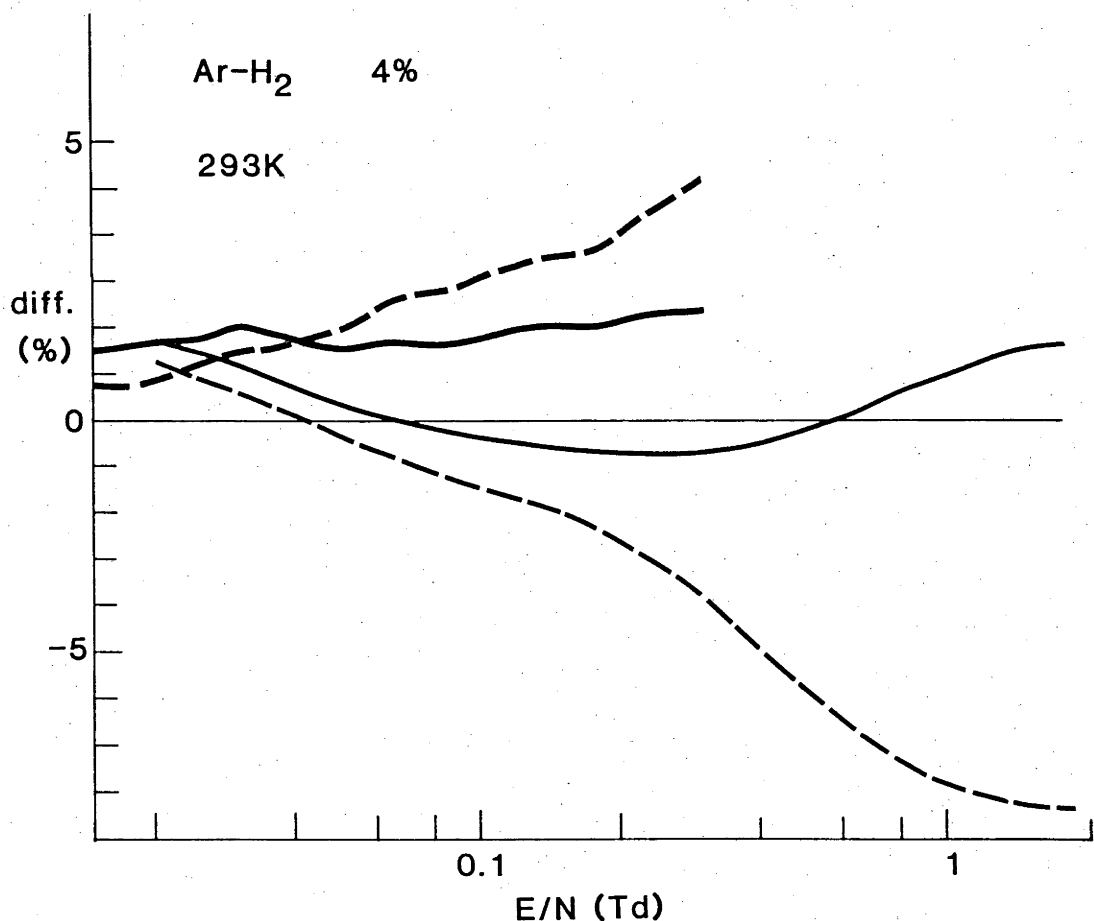


Figure 9.14 Comparison of the transport coefficients for the 4% Ar-H₂ mixture calculated using the theoretical (thin line) and the swarm-derived (thick line) cross sections.

One could perhaps ask the following question: if in pure hydrogen the discrepancies for the D_T/μ values exceed 8% why in the mixtures are they never more than 5%? A qualitative explanation can be given based on an approximate form of the energy balance equation neglecting elastic energy losses (see Chapter 3):

$$e E v_{dr} = \epsilon_i \langle v_i \rangle = N \epsilon_i \langle \sigma_i c \rangle \quad . \quad (9.1)$$

In the ranges of E/N used in the analyses, the energy balance, both in pure H_2 and in the mixtures, is determined mainly by the vibrational excitation cross section. In the case of the mixtures, the argon momentum transfer cross section increases sharply with energy in the range corresponding to the range of the most probable swarm energies. Further, it is important to note that the momentum transfer cross section in the mixture is dominated by the argon momentum transfer cross section (because of the low hydrogen concentration) but that the inelastic losses are solely due to the hydrogen and entirely dominate the elastic losses. If we now assume that the swarm vibrational cross section gives the correct energy and momentum balance both in pure H_2 and in the mixtures, then its replacement by the higher theoretical cross section would increase the vibrational energy loss and tend to suppress the mean energy and $\langle c \rangle$. Since the drift velocity is given approximately by $v_{dr} = eE/mN\langle \sigma_m c \rangle$ a reduction in $\langle c \rangle$ leads to an increase in v_{dr} . Because of the very rapidly increasing σ_m in the mixture compared with the very weak energy dependence in pure H_2 , only a small change in the swarm energy and hence D_T/μ is required to restore the balance between the power input from the field and the energy loss rate in the case of the mixture (i.e. restore equality between the two sides of

equation 9.1), whereas a larger change is required for pure H₂. Nevertheless the smaller change in the swarm energy in the mixture leads to a larger change in v_{dr} than in the pure gas, again because of the rapidly increasing σ_m with energy in the mixture. (Note that if $v_m = \text{const}$, a condition that is approached in H₂ but is strongly violated in the mixture, the energy balance would be restored entirely by a change in the swarm energy since the power input from the field would then be constant.)

The enhanced sensitivity of v_{dr} in the mixture to the vibrational excitation cross section is one of the major advantages of the mixture technique using Ar. Use of the technique also enables one to base the analysis on drift velocity data alone, enabling one to use the two-term theory with negligible error and experimental data having the highest intrinsic accuracy. There are fewer problems in interpreting the raw experimental data from drift tubes in terms of the drift velocity than in deriving D_T/μ data from the Townsend-Huxley experiment, and thus the accuracy of the experimental data for v_{dr} is normally higher than for D_T/μ data. Nevertheless, the D_T/μ data available for the Ar-H₂ mixtures fully confirm the conclusions that follow from an analysis of the v_{dr} data alone.

9.5: Electron Transport Coefficients in a Helium-Hydrogen Mixture

9.5.1: Introduction. One of the necessary conditions for the application of the mixture technique is that the cross sections for the buffer gas must be known very accurately. It could be argued that, since there are still some discrepancies between recent determinations of the momentum transfer cross sections for argon, the results obtained from Ar-H₂ transport data are not a conclusive proof that the swarm-derived cross

sections for H_2 are superior to the theoretical cross sections. Because this objection could be made to the results obtained in the previous section and by Haddad and Crompton (1980) it was decided to perform measurements in helium-hydrogen mixtures. The momentum transfer cross section for helium is known very accurately (to within $\pm 2\%$ see Crompton et al. 1967; O'Malley et al. 1979; Nesbet 1979) and therefore helium is a good candidate for the application of the mixture technique. A major disadvantage is that the momentum transfer cross section is only weakly dependent on the electron energy in the range of interest and therefore the sensitivity to the inelastic processes is reduced when helium rather than argon is used. The fact that the sensitivity is reduced could make it difficult to differentiate between the two cross section sets if the differences in drift velocities predicted on the basis of these two sets were comparable to the experimental uncertainty.

In order to compensate for the reduced sensitivity a different approach to the mixture technique was adopted. First, drift velocities in pure helium and in a mixture of helium with hydrogen were measured. The differences between the drift velocities measured under identical conditions with and without hydrogen were then determined. Calculations were then performed for pure helium and for the helium-hydrogen mixture and the differences calculated. In this way predictions based on different H_2 cross section sets could be compared with experimental data that were free from subject to most systematic errors. The residual systematic errors are those arising from the determination of the mixture composition, and due to a possible change of the temperature between the two measurements.

Table 9.8 Drift velocities (10^5 cm s^{-1}) in pure helium.

E/N (Td)	Previous Experiments		p(kPa)			Final
	Milloy & Crompton (1977)	Huxley & Crompton (1974)	13.423	8.0581	6.61	
0.25		2.41	2.414			2.414
0.3		2.65	2.652			2.652
0.35		2.87	2.872			2.872
0.4		3.08	3.074	3.072		3.073
0.5		3.44	3.436	3.436		3.436
0.6		3.77	3.764	3.768		3.766
0.7		4.07	4.062	4.067		4.065
0.8		4.35	4.336	4.338		4.337
1.0		4.85	4.843	4.839		4.841
1.2		5.30	5.297	5.305		5.301
1.4		5.73	5.721	5.723		5.722
1.7		6.33		6.310		6.310
2.0		6.86		6.858	6.852	6.856
2.5	7.68	7.69		7.711	7.705	7.708
3.0	8.49	8.52			8.516	8.516
3.5	9.26	9.27				
4.0	10.01					
5.0	11.52					
6.0	13.13					
7.0	15.03					

Table 9.9 Drift velocities (10^5 cm s^{-1}) in 10.69% H_2 -He mixture.

E/N (Td)	p (kPa)					FINAL RESULT
	13.423	8.0581	6.611	5.3719	2.686	
0.25	2.910					2.910
0.3	3.212					3.212
0.35	3.482					3.482
0.40	3.725					3.725
0.5	4.156					4.156
0.6	4.543					4.543
0.7	4.904	4.899		4.904		4.903
0.8	5.245	5.242		5.248		5.245
1.0	5.894	5.893		5.897		5.895
1.2	6.509	6.509		6.508		6.509
1.4	7.097	7.096	7.098	7.096		7.097
1.7		7.931	7.939	7.931		7.934
2.0		8.718	8.724	8.718	(8.727)	8.722
2.5		9.955	9.963	9.949	(9.968)	9.956
3.0			11.115	11.10	11.11	11.11
3.5				12.19	12.18	12.19
4.0					13.21	13.21
5.0					15.16	15.16
6.0					16.95	16.95
7.0					18.61	18.61

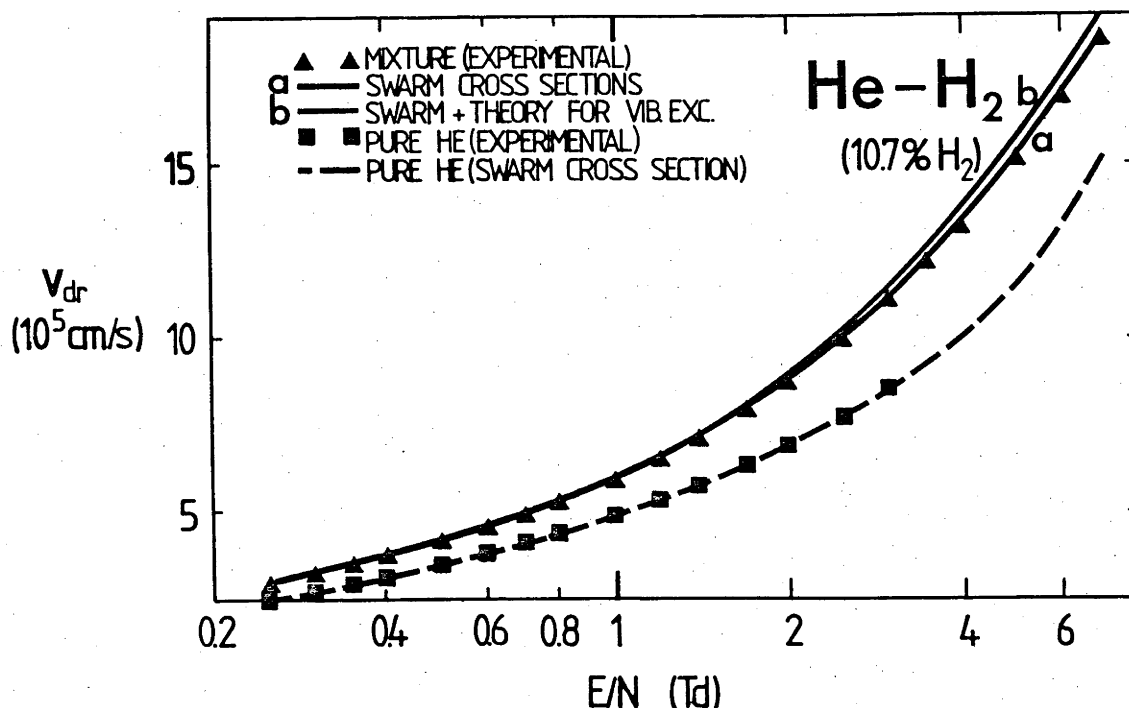


Figure 9.15 Drift velocities in pure He and He-H₂ mixture.

9.5.2: Results and analysis. Measurements were made in pure helium up to 3 Td. The results are in very good agreement (see Table 9.8) with the data of Crompton et al. (1967) and Milloy and Crompton (1977a). A background of high energy electrons prevented measurements at higher E/N values.

A mixture of 10.69% of hydrogen in helium was made in a mixing vessel. The choice of the abundance of 10.69% was determined by the available calibrated pressures for the gauge that was used and the volume ratio of the mixing vessel. The results for drift velocities are presented in Table 9.9 and in Fig. 9.15, proper account having been taken of the diffusion corrections.

Table 9.9 and Fig. 9.15 also contain the drift velocities calculated

using either the swarm-determined H₂ cross sections described in Sections 9.4.3 to 9.4.5 or the theoretical cross sections. It is important to note that multiterm calculations for the mixture indicate that, between 0.25 and 7 Td, the two-term theory gives drift velocities that are accurate to within 0.1%. It can be seen that the values of v_{dr} measured for the mixture agree to within 1% with values predicted on the basis of the swarm cross sections while using the theoretical cross sections for H₂ the results for the mixture are well outside the error bars.

As discussed in the previous section, the disagreement between the experimental results and the predictions based on the theoretical cross sections becomes more significant if one makes a comparison between the calculated and experimental values of the relative change of v_{dr} when H₂ is added to He. The relative change Δ is defined as

$$\Delta = \frac{|v_{dr}^{He} - v_{dr}^{mix}|}{v_{dr}^{He}} \quad (9.2)$$

Fig. 9.16a shows three sets of values for Δ : the experimental values (Δ^{exp}) and those based on calculations using theoretical (Δ^{th}) and using swarm-derived (Δ^{sw}) cross sections. (σ_m for He for both sets of calculations was that of Crompton et al. 1967; negligible difference was observed when σ_m of Nesbet 1979 was used). The values for v_{dr}^{He} above 3 Td were taken from Milloy and Crompton (1977a).

A more effective comparison can be made by forming the relative "double difference" defined as

$$\text{diff.} = \frac{|\Delta - \Delta^{exp}|}{\Delta^{exp}} \quad (9.3)$$

because, as already stated, only the mixture composition (and possibly the

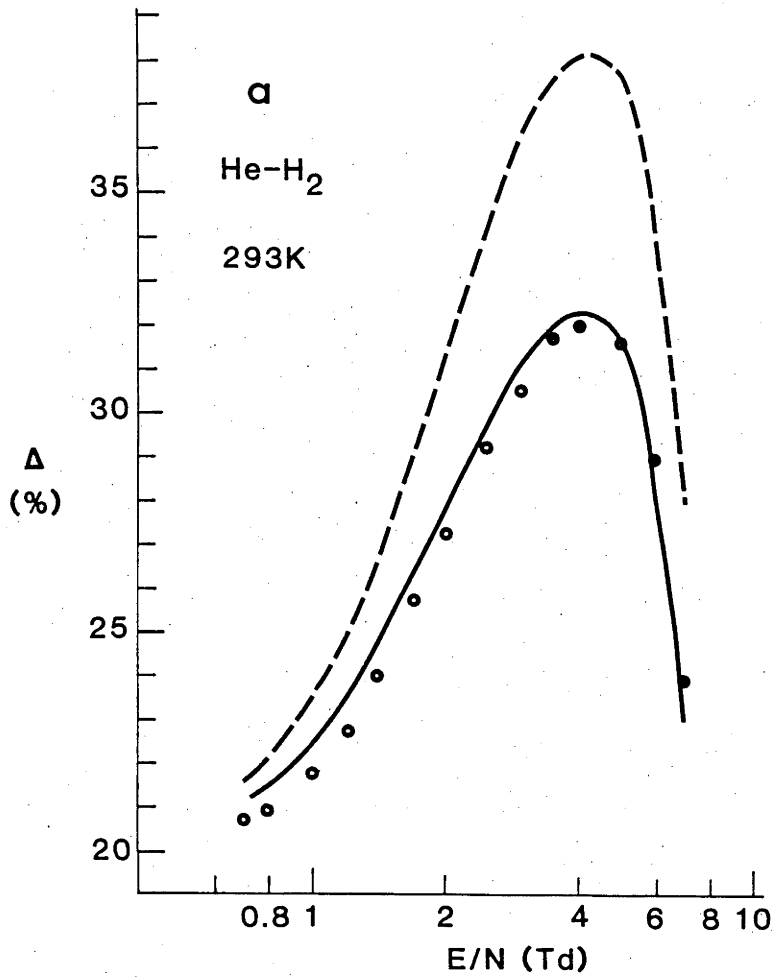
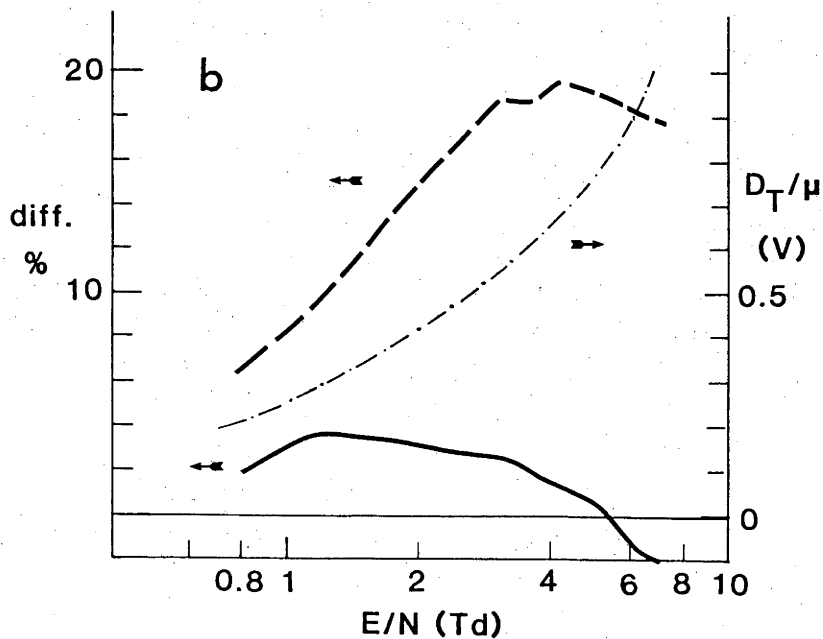


Figure 9.16 a) Differences between drift velocities in pure He and in the He-H₂ mixture: experimental data (circles) predictions based on swarm-derived (solid line) and theoretical (dashed line) cross sections. b) Double differences as described in the text. Calculated D_T/μ values are also shown.



variation of the temperature) contribute to the systematic error in Δ^{exp} when the difference measurements are made consecutively, that is below $E/N=3T_d$. Combining statistical scatter with the error in the mixture composition one obtains $\pm 0.5\%$ for the absolute error which translates into less than $\pm 2.5\%$ in Δ^{exp} . Above $3 T_d$, where the earlier data of Milloy and Crompton in pure He were combined with the new mixture data, the error bounds are increased to somewhat less than $\pm 4\%$.

A comparison of differences between the calculated values of Δ and the experimental value is shown in Fig. 9.16b. Predictions based on the swarm-derived cross sections are up to 3.7% different from the experimental results, a difference which is somewhat larger than the estimated error bounds. Small adjustments of the momentum transfer cross sections (within the error bars for the cross section sets for H_2 and He) bring the calculated values of Δ^{sw} to within 2.5% of the experimental data (i.e. $\text{diff.} < 2.5\%$ - see Fig. 9.16.b). However, the predictions based on the theoretical cross sections result in Δ^{th} that are up to 19% larger than Δ^{exp} . Such a difference exceeds the experimental error bounds by as much as eight times the relative uncertainty. The adjustments to σ_m (for He and H_2) required to obtain good agreement with the experimental data would therefore be considerably larger than the uncertainties in the cross sections.

It can therefore be concluded that the present results for He- H_2 mixture are inconsistent with the theoretical results for the vibrational cross section. On the other hand the results are in very good agreement with the cross section obtained using the swarm data.

9.6: Conclusion

The significance of the results presented in Section 9.5 is that a buffer gas was used whose cross section is known better than any other cross section, that the use of a difference technique reduced the uncertainty due to systematic errors, that the raw data from drift velocity measurements are the most straightforward to interpret, and that the multiterm corrections are negligible. When combined with conclusions based on a wide range of data in pure H₂ and Ar-H₂ mixtures, the results from these experiments give a high degree of confidence in the swarm-derived cross section and certainly suggest that, in order to test the validity of the theoretical predictions, accurate low energy beam experiments should be performed. If results from these experiments support the swarm cross section the conclusion would be that the theory that has been applied (even though the most sophisticated so far) included some approximations that were not adequate. If, on the other hand, the beam experiments support the theoretical results and produce results that are incompatible with the swarm results, the situation would be difficult to understand. The swarm method as applied to H₂, and therefore to any molecular gas, would be under serious doubt even though its application to atomic gases has been outstandingly successful. It is not possible at the present time to single out any step in the procedure which might be suspect as all the steps have been thoroughly checked. The interpretation of the current ratios observed in the Townsend-Huxley experiment in terms of the ratio D_T/μ calls for further investigation and a Monte Carlo analysis for the conditions appropriate to H₂ is presently being carried out by Braglia and coworkers.

However, even if the standard procedure normally used to analyse the Townsend-Huxley experiment is shown to be incorrect (which is very unlikely because of the success of that technique in cases such as helium and hydrogen at lower energies) all the drift velocity results would have to be explained, especially those for the Ar-H₂ and He-H₂ mixtures, since it is most unlikely that there is any problem in the interpretation of the experiments used to obtain these data.

CHAPTER 10: VIBRATIONAL EXCITATION OF DEUTERIUM BY LOW ENERGY ELECTRONS10.1: Introduction

Deuterium shares with hydrogen advantages (see Section 9.1) for both experiment and theory. Also, the practical applications of the two gases are similar. Buckman and Phelps (1985) recently performed a detailed analysis of the transport and cross section data for D₂. These authors pointed out the need for more accurate transport data in the intermediate E/N range which are required in order to derive a more accurate vibrational excitation cross section close to the threshold. Following their suggestions the measurements and subsequent analysis reported in this chapter were performed.

First, a short review of the available cross section data for D₂ will be given. Some low energy processes are expected to have identical cross sections for both hydrogen and deuterium. Among these are the total scattering (Golden et al 1966) and electronic excitation cross sections (de Heer 1981; Buckman and Phelps 1985). However, modified effective range theory (Chang 1974) predicted that the scattering length for H₂ and D₂ should be slightly different. On the other hand Gibson (1970) found σ_m for zero energy in H₂ and D₂ to be identical although he found it necessary to use a cross section that increases slightly less rapidly with increasing energy than the hydrogen cross section in order to obtain the best agreement between the calculated and measured transport coefficient for D₂. Chang's prediction was also found to be incorrect by Rhymes (1976) who measured diffusion coefficients for thermal electrons in D₂ and H₂ and found them to be the same to within the experimental error. The momentum

transfer cross section for the two gases are therefore expected to be similar, the only difference occurring in the region where inelastic processes differ significantly. Some difference may also occur due to the slightly different polarizabilities.

Although the rotational excitation cross sections near threshold differ because of their different threshold energies, they are expected to merge at higher energies (Chang and Wong 1977; see also Buckman and Phelps 1985).

Vibrational excitation is expected to show strong isotope effects (Chang and Wong 1977; Bardsley and Wadehra 1979). Moreover these effects are different for rotationally elastic and inelastic transitions. Significant isotope effects are also observed for dissociative processes (Carnahan and Zipf 1977; Bardsley and Wadehra 1979; de Heer 1981).

The differences between the relevant cross section for H_2 and D_2 are sufficient to produce observable differences of the transport coefficients in a range of E/N values (see Crompton et al. 1968). Previous investigations using swarm techniques include measurements of drift velocities (Pack et al. 1962; McIntosh 1966; Crompton et al. 1968; Robertson 1971; Crompton and Robertson 1971), D_T/μ values (Hall 1955; Warren and Parker 1962; McIntosh 1966; Crompton et al. 1968), magnetic deflection coefficients (Creaser 1967), and the most recent detailed study of excitation coefficients in mixtures of D_2 with various tracer gases (Buckman and Phelps 1985).

On the basis of the available data for the transport coefficients several sets of cross sections for deuterium have been derived (Engelhardt and Phelps 1963; Gibson 1970; Buckman and Phelps 1985). The present work was motivated by the need for highly accurate data for drift velocities and D_T/μ values in the region of energies where vibrational excitation is the

most important inelastic process. The room temperature results presented by McIntosh (1966) overlap with this region since his drift velocity data extend up to 15 Td and D_T/μ data up to 6 Td. However, at 6 Td the power input into rotational excitation is approximately one half of the input into vibrational excitation, and even at 15 Td there is a considerable contribution. The present work is an attempt to increase as much as possible the range of the available transport data and to check their consistency with the cross sections of Buckman and Phelps (1985).

10.2: Experimental Details and Results

10.2.1: Drift velocities. Drift velocities for electrons in D_2 were measured using the Bradbury-Nielsen technique as described in section 8.2. Samples of gas were prepared from the highest available purity gas using the silver palladium osmosis tube (see Chapter 9). Deuterium passes through the palladium foil much more slowly than hydrogen. In order to avoid enhancement of the hydrogen present in the deuterium as a trace impurity (<0.5%) a high flow of the gas at close to atmospheric pressure was used rather than a low flow rate at higher pressure.

Some measurements of v_{dr} were made with a somewhat lower pressure (0.413 kPa) than the lowest pressure (0.667 kPa) used by McIntosh (1966). Therefore it was possible to make measurements up to 30 Td. Above this value of E/N at this pressure electrical breakdown occurred. If the pressure was lowered still further in an attempt to reach higher values of E/N the efficiency of the electrical shutters was reduced and this prevented any reliable measurements even at 25 and 30 Td.

The results for drift velocities in D_2 are presented in Table 10.1 and

Figure 10.1. Diffusion corrections with $C=2$ were found to be adequate for all the data obtained at more than one pressure. Diffusion corrections based on this value of C were therefore applied to the values of V_{dr} measured at 25 and 30 Td where only one pressure could be used. The maximum diffusion correction was 0.8%, and the maximum scatter of the data was $\pm 0.2\%$. Therefore it is possible to estimate the total uncertainty as $\pm 1\%$ up to 14 Td and $\pm 1.5\%$ between 17 and 30 Td.

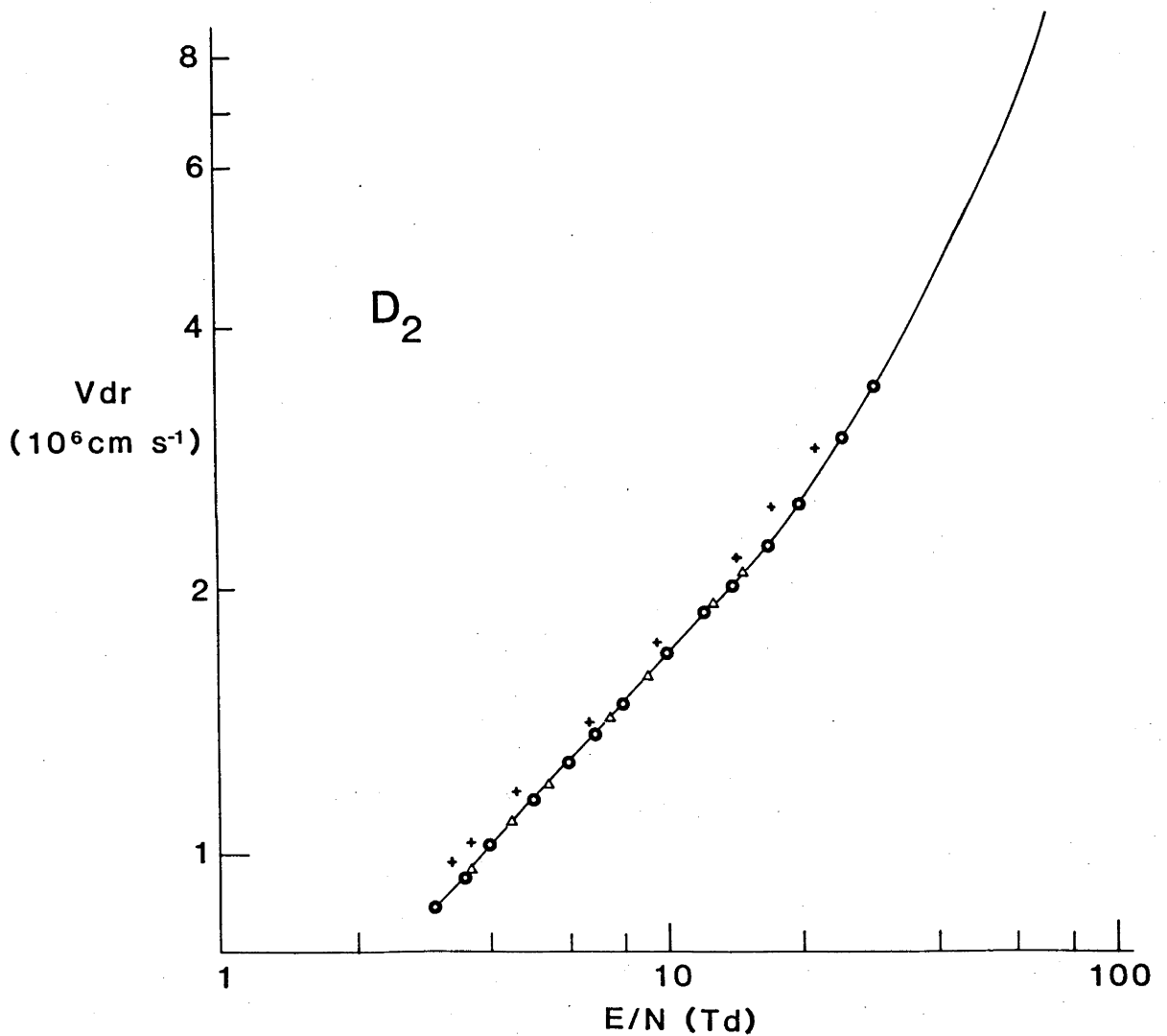


Figure 10.1 Drift velocities in deuterium. The present data: (o); McIntosh (1966): (Δ); Pack et al. (1962): (+). The continuous curve passing through the data represents the results of the calculations based on the cross section derived in this chapter.

Table 10.1 Measured drift velocities in deuterium.

E/N (Td)	v_{dr} (10^6 cm/s)				
	McIntosh (interpolated)	P (kPa)			Best Estimate*
		1.343	0.723	0.413	
3	0.888	0.888			0.888
3.5	0.961	0.961			0.961
4	1.028	1.029			1.029
5	1.154	1.155			1.155
6	1.270	1.271	1.270		1.270
7	1.378	1.379	1.377		1.378
8	1.480	1.480	1.479		1.480
10	1.669	1.671	1.668		1.669
12	1.847	1.846	1.846	1.846	1.846
14	2.02	2.01	2.01	2.01	2.01
17	(2.25)**		2.25	2.25	2.25
20			2.49	2.48	2.49
25			2.89	2.89	2.89
30				3.37	3.37

* Diffusion correction $1 + 2 \frac{D_T/\mu}{V}$

** Extrapolated.

10.2.2: D_T/μ values Prior to the measurements the experimental apparatus with a variable drift length had to be rebuilt. It was then noticed that the resistivity between the outer collecting annulus of the anode and ground was unacceptably low. This problem would not result in errors in the experimental results but it made the process of measurement rather difficult. Therefore it was decided to continue the measurements without the outer annulus, that is, with an effective radius of the collecting electrode of 2 cm. However, in some cases the current falling outside the effective collective electrode was not zero as is necessary for the application of the Huxley formula. In these cases the current of electrons to the outer annulus was estimated using the Huxley formula, making it possible to adjust the experimentally determined current ratio to obtain the current ratio for the infinite collecting electrode.

The procedure for determining D_T/μ was as follows. First, the Huxley formula was applied to the measured current ratio and the first estimate of D_T/μ was obtained. Second, this value of D_T/μ was used to determine the current falling outside the effective collecting electrode enabling a modified current ratio (corresponding to an infinite-diameter outer annulus) to be calculated. Third, the Huxley formula was applied to the modified current ratio and the new value of D_T/μ was obtained. Normally, after only one (or in the worst case three) iteration the values of D_T/μ became stable in consequent iterations. For high current ratios (above 0.3) there was no need to make the corrections because the current falling outside the effective collecting electrode was negligible.

Initially it was intended that any data obtained when the current to the outer annulus exceeded 1% of the total current should be discarded (only results with the current ratios below 0.2 would fall in this

category). However, it was found that, using the iterative technique, the results obtained with as much as 11% of the current going to the outer annulus were in excellent agreement with the data obtained under more favourable conditions, and these data were therefore included in the final set.

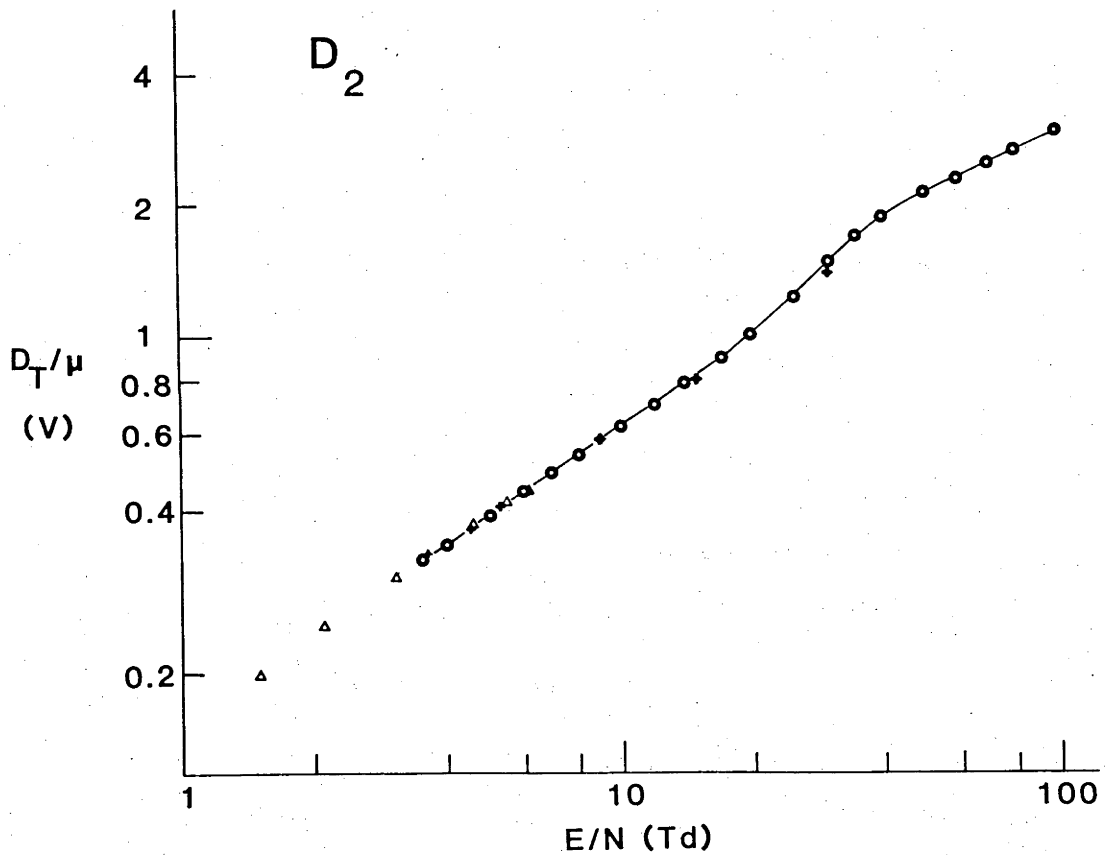


Figure 10.2 D_T/μ values for electrons in deuterium. Present results: (o); McIntosh (1966): (Δ); Hall (1955): (+).

E/N McIntosh(1966) (Td) (interpolated)		D_T/μ (V)									
pressure(kPa)		2.066	1.343	1.033	0.7231	2.066	1.033	0.7231	0.4133	0.3306	Average
Range of current ratios		0.3-0.4	0.25-0.3	0.20-0.25	0.15-0.25	0.5-0.7	0.4-0.5	0.3-0.4	0.25-0.3	0.2-0.3	
length (cms)		10	10	10	10	5	5	5	5	5	
	100								2.90	2.90	2.90
	80								2.63	2.63	2.63
	70								2.49	2.49	2.49
	60								2.33	2.33	2.33
	50							2.14	2.14	2.14	2.14
	40							1.878	1.872	1.877	1.876
	35							1.696	1.695	1.697	1.697
	30							1.476	1.474	1.474	1.474
	25				1.229			1.229	1.228	1.231	1.230
	20				1.006			1.006	1.007	1.006	1.006
	17			0.886	0.887	0.889		0.887	0.887	0.887	0.887
	14			0.770	0.774	0.774		0.774	0.772	0.773	0.773
	12		0.695	0.695	0.697	0.697		0.696	0.696	0.696	0.696
	10		0.615	0.614	0.615	0.616		0.616	0.614	0.615	0.615
	8		0.530	0.529	0.530	0.531		0.530	0.530	0.530	0.530
	7		0.485	0.485	0.484	0.486		0.485	0.485	0.485	0.485
	6	0.437	0.436	0.436	0.438	0.438		0.438	0.438	0.437	0.437
	5	0.388	0.388	0.387	0.388	0.388		0.388	0.388	0.388	0.388
	4	0.334	0.334		0.334	0.334		0.334	0.334	0.334	0.334
	3.5	0.305	0.305		0.305	0.306		0.306	0.306	0.305	0.305
	3.0	0.275	0.274		0.274						0.305

Table 10.2 Measured D_T/μ values for electrons in deuterium. The results obtained with current ratios lower than 0.2 are shown in brackets. The values of the current ratios are also given. Note that this table does not include the ionization and D_L/D_T corrections.

The results were obtained for a number of pressures and for two drift lengths (5 and 10cm), and they are presented in Fig. 10.2 and in Table 10.3. Because some of the measurements were performed under difficult conditions (low current ratio or high correction for the current falling outside the collecting electrode) the range of current ratios is also shown. Conditions were regarded as difficult when $R < 0.3$; when $R < 0.2$ the data were expected to be unreliable with respect to the level of accuracy of 1 to 2% normally expected from these experiments. The good agreement between "good", "difficult" and "unreliable" results observed in the case of D_2 suggests that this criterion is somewhat conservative and the measurements with $R < 0.2$ (see values in brackets in Table 10.2) were made to prove this point.

10.2.3: Corrections for longitudinal diffusion and for ionization. As can be seen from equation (2.65), if the ratio of the longitudinal to transverse diffusion coefficients is not 0.5 the experimental conditions may be such that the Huxley formula (2.63) is not exactly applicable. In this case the correction calculated using the formula (2.65) is pressure dependent, even though it is not apparent from (2.65), because the current ratios are different at different pressures. Therefore formula (2.65) has to be used in each case to calculate D_T/μ from the measured current ratio instead of using (2.63) and applying a correction.

The ratios of D_L/D_T required to apply the Lowke formula (2.65) were determined using the LRM code and the cross sections for deuterium that were subsequently derived (see section 10.3). Also a comparison was made with predictions based on the generalized Einstein relations (see Robson 1972; 1976; 1984) which is given by

$$\frac{D_L}{D_T} = 1 + (1 + \Delta_L) \frac{\partial \ln \mu}{\partial \ln(E/N)} = 1 + (1 + \Delta) \hat{\mu} \quad (10.1)$$

where

$$\Delta_L = \frac{Q}{2kTv_{dr}} \quad , \quad (10.2)$$

μ is the mobility of electrons and Q is the heat flux per particle. It was assumed that Δ_L is zero which should be adequate for high fields when inelastic collisions are not dominant in the energy balance (Robson 1984). The two techniques employed to determine D_L/D_T ratios gave results that are in good agreement and indicated that above 40 Td the ratio becomes greater or equal to 1 while below 40 Td it suddenly decreases to around 0.5.

Even though $D_L/D_T \neq 0.5$ and the conditions for some of the experiments were such that the use of the Huxley formula would be expected to lead to some errors in the values of D_T/μ determined using it, Table 10.2 shows that the results obtained using the formula are independent of pressure and that there is very good agreement between the measurements with two different drift lengths (5 cm and 10 cm). When equation (2.65) is used the values of D_T/μ between 40 and 100 Td increase by up to 2%, but a small pressure dependence (<1%) is introduced which suggests that the data calculated in this way may be less accurate than those calculated using the Huxley formula. The pressure dependence is not induced by the corrections for the current falling on the outer annulus since these corrections were small and did not significantly change when equation (2.65) was used for the analysis. Therefore it was decided to use the results calculated using the Huxley formula but to increase the upper error bound by 2%.

A possible explanation of the superiority of (2.63) over (2.65) for analysing the data is that the boundary conditions that were used to derive equation (2.65) are not satisfied in the present case. Certain boundary conditions lead to the applicability of the Huxley formula (2.63) regardless of the D_L/D_T ratio. This is so when the Townsend-Huxley experiment can be modelled by a point source above the anode, in which case the boundary condition $n(0)=0$ at the cathode is not satisfied (Crompton 1972; Huxley and Crompton 1974).

Table 10.3 Corrections to D_T/μ values due to ionization and the final values.

E/N	$\frac{\alpha_T}{\lambda_L}$ (%)	The final value of D_T/μ
50	0.09	2.14*
60	0.20	2.33*
70	0.60	2.48
80	0.80	2.61
100	1.40	2.86

* to three figures these values are not affected.

At the higher values of E/N it is necessary to apply a correction for ionization as given by equation (2.66). The correction is pressure independent as can be seen from

$$c_{ion} = \left(1 - \frac{\alpha_T}{\lambda_L} \right) = \left(1 - 2 \frac{\alpha_T D_L}{v_{dr}} \right) = \left(1 - 2 \frac{\alpha_T}{N} \frac{D_T}{\mu} \frac{1}{E/N} \frac{D_L}{D_T} \right) \quad (10.3)$$

and should be applied to the value D'_T/μ which is calculated using (2.63). The corrected value of D_T/μ is then $(D'_T/\mu) \times c_{ion}$. In equation (10.3) α_T is

the Townsend ionization coefficient. Values of α_T were taken from Buckman and Phelps (1985). The calculated corrections are presented in Table 10.3 together with the final values of the results for D_T/μ that were affected by this correction.

The reproducibility of the data was to within $\pm 0.2\%$ and therefore the error bars can be estimated (see section 8.3) as $\pm 1\%$ from 3.5 to 25 Td; $\pm 1.5\%$ from 25 to 35 Td; and $+3.5$ to -1.5% from 40 to 100 Td.

10.2.4: Discussion. In the range of overlap the present results for drift velocities are in excellent agreement with the results of McIntosh (1966). The data of Crompton et al. (1968) that were taken at 77 K are also in agreement with the present results at the highest E/N values used by Crompton et al. The somewhat older results of Pack et al. (1962) are larger than present values. Similar discrepancies between the data of Pack et al. and the IDU data exist for hydrogen. It appears that there are no other high precision measurements of v_{dr} for D_2 in the E/N range that was used in the present work (see Beaty et al. 1979).

The present data for D_T/μ values agree very well in the range of overlap with the data of Hall (1955), McIntosh (1966) and Crompton et al. (1968). The results of Warren and Parker (1962) are different by 5 to 7% in the region of the overlap of E/N values (for an assessment of the data of Warren and Parker see Crompton et al. 1968).

10.3: Derivation of the Vibrational Excitation Cross Section

10.3.1: The basic set of cross sections. In this work only the presently measured values of the transport coefficients were used initially

to derive the cross sections. As a first step the "reference" cross section set of Buckman and Phelps (1985) (i.e. a set that fitted the previously available transport data) was chosen. The following cross sections comprise this set:

- a) The rotational excitation cross sections of Gibson (1970) up to 0.5 eV, and above 0.5 eV the values of Henry and Lane (1969) that were derived for H₂ (see also Henry and Lane 1971);
- b) The vibrational excitation cross sections of Gibson (1970) up to 0.5 eV merged to the cross sections for hydrogen (Ehrhardt et al. 1968) scaled by the factor of 0.76 derived by Chang and Wong (1977), (For $v=0-2$ and $0-3$ transitions the corresponding cross sections for hydrogen were scaled using the results of Bardsley and Wadehra 1979);
- c) Electronic excitation cross sections as compiled by Buckman and Phelps from numerous experimental and theoretical cross sections, in some cases using semi-empirical correlations between the different cross sections. (It should be pointed that these authors found that the total cross section for excitation of the triplet states determined by Corrigan (1965) is inconsistent with the measured ionization coefficients);
- d) The ionization cross section measured by Rapp and Englander-Golden (1965);
- e) The momentum transfer cross section for H₂ derived by Crompton et al. (1969) at low energies (< 2 eV), at intermediate energies the momentum transfer cross section that led to the best agreement with the then available experimental transport data, and at high energies (> 9 eV), the sum of the elastic momentum transfer cross

section recommended by Hayashi (1981) and the inelastic cross sections.

Buckman and Phelps (1985) found that the cross section set mentioned above was inconsistent with their measured vibrational excitation coefficients. Therefore they recommended an additional, "adjusted", set that gives improved agreement. In this set the vibrational cross sections were increased by a factor of approximately 1.6. As a consequence the agreement between the predicted and the experimental transport data was not good (see Fig. 10.3).

10.3.2: Low energy analysis. The range of E/N values can be separated into two regions, 30 Td being the boundary. At 5 Td the power input into vibrational excitation begins to exceed the power input to all other inelastic processes, and this continues to be so up to 50 Td. Since vibrational excitation of $v=2$ and $v=3$ levels influences the energy balance very little (they contribute only 10% of that due to $v=0-1$ excitation at 50 Td), the cross section for the $v=0-1$ transition can be accurately and uniquely determined from the transport data below 50 Td. However, the drift velocities above 30 Td are not available while above 40 Td there is an additional uncertainty in the measured D_T/μ values due to the D_L/D_T correction. Therefore the results based on the data below 30 Td are believed to be determined more accurately than the high energy cross sections that were determined mainly on the basis of the high E/N data.

Fig. 10.3 shows unacceptable differences between calculated and measured transport coefficients when the reference set is used, and still poorer agreement when the adjusted set is used. It should be noted that for the calculations presented in Fig. 10.3 the rotational cross sections

of Buckman and Phelps (1985) were supplemented by rotational cross sections for $J=2-4$, $J=3-5$ and $J=4-6$ processes using the scaling factors as explained in Appendix 4. The scaling procedure leads to some errors, especially close to the threshold, which can be of the order of 20% (see Chapter 9). However, since there is a lack of reliable cross section data in that energy range for deuterium, the scaling procedure was adopted as the best available choice.

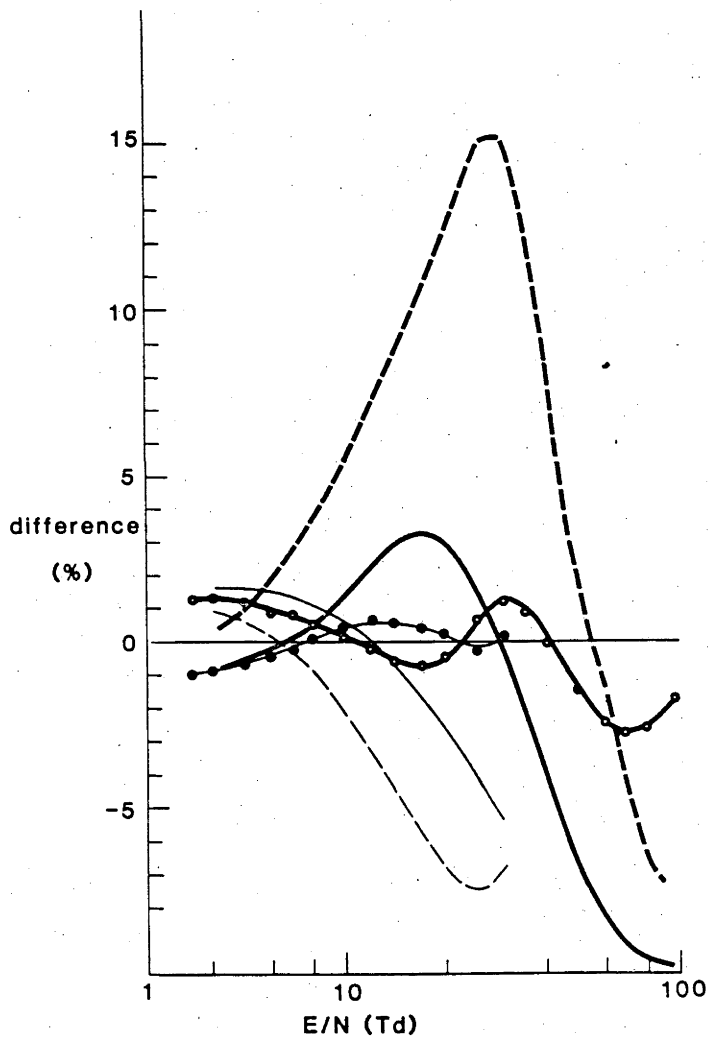


Figure 10.3 The agreement between the measured transport coefficients and the coefficients calculated using: presently derived cross sections (curves with the points marked by open (D_T/μ) or full (v_{dr}) circles), the reference set (full lines) and the adjusted set (dashed lines). The results for D_T/μ values are shown using thick lines while the results for the drift velocities are shown using thin lines in all cases.

As mentioned above Buckman and Phelps (1985) used the theoretical results of Henry and Lane (1969; 1971) for H_2 to extrapolate the rotational cross sections to high energies. The present analysis was performed both with their cross sections and with the theoretical cross sections of Morrison and coworkers as presented in the Chapter 9. There are small differences between the results obtained using the two sets but these are not larger than 0.7%.

The reference vibrational excitation cross section was multiplied by different scaling factors at different energies to obtain the final cross section. The choice of these factors was arbitrary but made to achieve the best agreement with the transport data. Similarly the momentum transfer cross section was slightly modified.

The final vibrational excitation cross section that was derived is shown in Fig. 10.4. As can be seen from the figure, below 1 eV the reference cross section was increased by up to 20%, while between 1.5 and 3 eV it was reduced by 30%. This reduction could be an independent confirmation that the cross section $\sigma_{vib}(v=0-1)$ of Ehrhardt et al. (1968) is too high in this energy range (see Chapter 9). The amount of reduction of the vibrational cross section for D_2 is similar to the reduction needed to bring the electron beam and the electron swarm results for H_2 into agreement.

Also, it can be seen from the Fig. 10.4 that the peak of the present cross section occurs at a somewhat higher energy than the peak of the cross section of Buckman and Phelps (1985). The present cross section is therefore in better agreement with the shape of the theoretical cross section of Bardsley and Wadehra (1979).

The momentum transfer cross section (see Fig.10.4) is somewhat reduced

for energies below 1.5 eV, while for energies above that value it is larger, although the difference is less than 10%.

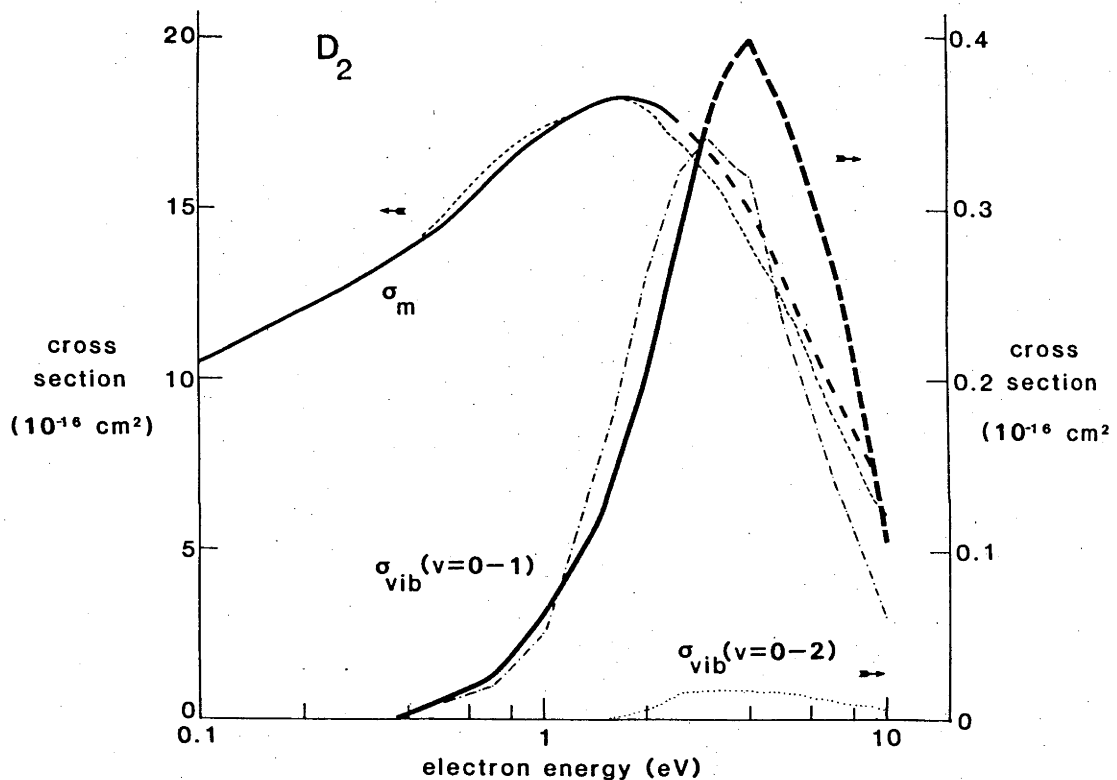


Figure 10.4 The presently derived cross sections (full lines) compared to the "reference" set of Buckman and Phelps (1985). In the region of energies where the present cross sections are determined with a reduced uniqueness the thick dashed lines are used. The momentum transfer cross section of the reference set is shown as the thin dashed line while the vibrational excitation cross section of the same set is shown by the curve of alternate dashes and dots.

In order to achieve agreement between the calculated and experimental transport coefficients for high values of E/N , it was necessary to increase the excitation cross sections by 1.7 for $b^3\Sigma$ and by 1.5 for all other cross sections.

The agreement of the transport data calculated on the basis of the present cross sections is shown in Fig. 10.3. If the cross sections of Morrison and coworkers are used to extrapolate the rotational excitation cross sections to high energies the maximum disagreement between the calculated and the measured D_T/μ values is 1.3% in the low E/N range (the maximum disagreement for v_{dr} values is not more than 1%), and 2% in the high E/N range. If the cross sections of Henry and Lane are used (as tabulated by Buckman and Phelps) the maximum disagreement in the low E/N range is 1% (not shown in Fig. 10.3).

Fig. 10.3 shows that the agreement between calculated and measured transport coefficients using the cross sections of Buckman and Phelps (1985) is considerably worse than that obtained with the revised set.

The transport coefficients for D_2 at 77 K were also calculated and compared to the available data (Crompton *et al.* 1968). There is excellent agreement in the entire E/N range indicating the adequacy of $J=0-2$ and $J=1-3$ rotational cross sections and that the modification to σ_{vib} ($v=0-1$) close to the threshold did not affect the quality of the fit.

10.3.3: Multiterm corrections for deuterium. In all the calculations presented above the multiterm corrections to the transport coefficients calculated with the two-term (Gibson) code were incorporated. Initially the "reference" set of Buckman and Phelps (1985) was used to calculate the

corrections, but finally the presently derived set was used. All the cross sections were assumed to be isotropic. Inclusion of anisotropy is expected to result in corrections of not more than 0.3% to the presently calculated values (see Chapter 9). The multiterm corrections for the range of E/N values used in the present work are presented in the Table 10.4

Table 10.4 The multi-term corrections for D_T/μ calculated using the presently derived cross sections and assuming isotropic scattering. The corrections to v_{dr} are negligible (<0.02%).

E/N (Td)	correction (%)	E/N (Td)	correction (%)
2.525	0.40	41.560	0.70
6.909	0.55	60.42	1.10
16.408	0.63	83.68	1.70
20.472	0.65	109.0	2.60
29.352	0.65		

10.3.4: Analysis at higher energies. In the analysis described so far only the presently measured values of D_T/μ and v_{dr} were used. However, it is important to make a comparison of calculated vibrational excitation coefficients and ionization coefficients based on the present set of cross sections with the experimental data of Buckman and Phelps (1985).

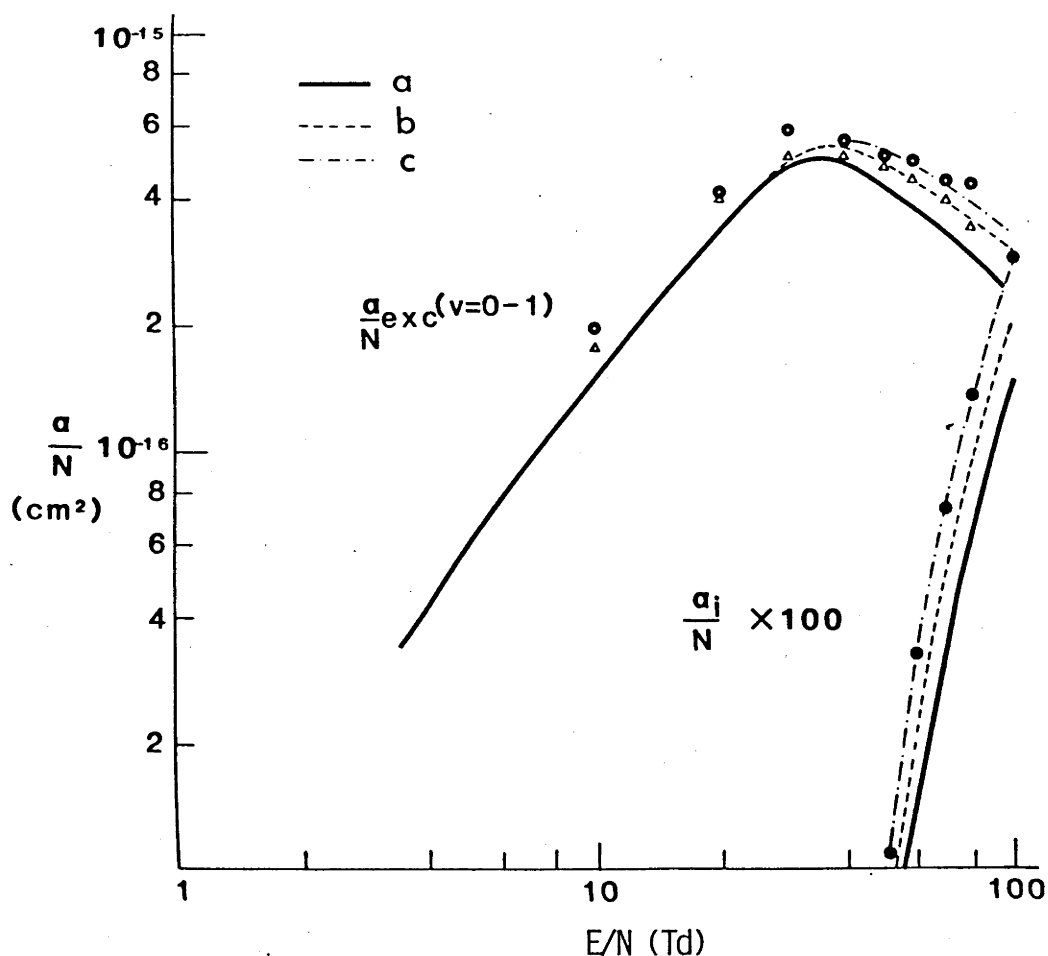


Figure 10.5 The agreement between the calculated ionization and vibrational excitation coefficients and the experimental data of Buckman and Phelps. The excitation coefficients were measured by these authors in mixtures of 2% of CO in D₂ (o) and 0.2% of CO in D₂ (Δ). The values calculated on the basis of the cross section derived from the transport data are denoted by (a) while the results of the calculations based on the modified vibrational excitation cross sections are denoted by (b) and (c) (see text). The results for the ionization coefficients are also shown.

Buckman and Phelps' result for excitation coefficients for D₂-CO mixtures should be compared with the results of calculations based on the cross sections for both gases scaled according to the composition of the mixtures. However, for the experimental conditions used by these authors

it is possible to compare the results with the results of calculations for pure D_2 because the contribution of the direct excitation of CO was small except for the lowest E/N values (see Buckman and Phelps 1985), while the electron distribution functions in the mixtures were not greatly affected by the presence of the CO tracer gas because its abundance was relatively small.

The experimental results for D_2 -CO mixtures are presented in Fig. 10.5. At low values of E/N the calculated values of $\alpha_{vib}(v=0-1)/N$ (for pure D_2) are lower than the experimental data (the difference still being smaller than the combined error bounds), presumably due to the contribution of direct excitation of CO by electron impact. The contribution of this process was estimated by Buckman and Phelps to be 30% at 20 Td. There is a good agreement around 40 Td, and at higher E/N values the calculated results decrease faster than the experimental (though still being within the experimental error bars). A similar E/N dependence of the calculated excitation coefficients was obtained by Buckman and Phelps (1985) with their cross section set.

Since the excitation cross sections were increased significantly, in order to achieve good agreement between calculated and experimental transport coefficients at higher values of E/N, the calculated ionization coefficients are 50% lower than the experimental values of Buckman and Phelps (1985). The experimental uncertainty of the ionization coefficients determined by Buckman and Phelps is significantly smaller than this.

In order to improve the agreement with the ionization coefficients it was necessary to reduce the scaling factors applied to the electronic excitation coefficients. When this was done, however, the agreement of the calculated transport data with the experimental values was not

satisfactory, but it could be improved by appropriate modifications of the vibrational cross section above 4 eV. As a first step all the electronic excitation cross sections were scaled by 1.3. The vibrational cross section that then gives the best agreement with the high E/N transport data is shown in Fig. 10.6(b). The vibrational, excitation, and ionization coefficients calculated using these modifications are shown in Fig. 10.5(b). The agreement of the ionization coefficient is still not satisfactory (there are still differences of up to 30%) but it is interesting to note that the E/N dependence of the vibrational excitation coefficient is more similar to the experimentally observed dependence than with the cross section set obtained in the previous section.

A further modification of the vibrational cross section would be necessary if the electronic excitation cross sections were not to be scaled. In that case the vibrational excitation cross section would have to be greatly modified (b in Fig. 10.6), and its shape would then be unacceptably different from the shape of the theoretical cross section (d in Fig. 10.6) that was derived by Bardsley and Wadehra (1979). If this were done the best fit to the measured transport coefficients would still leave discrepancies of $\pm 6\%$, but good agreement with the measured excitation and ionization coefficients would be achieved (Fig. 10.5 - curves c). Other shapes of the vibrational cross section above 4 eV would give similar agreement with the swarm data used in this analysis because the vibrational excitation is not the dominant inelastic process in that energy range and therefore cannot be determined uniquely.

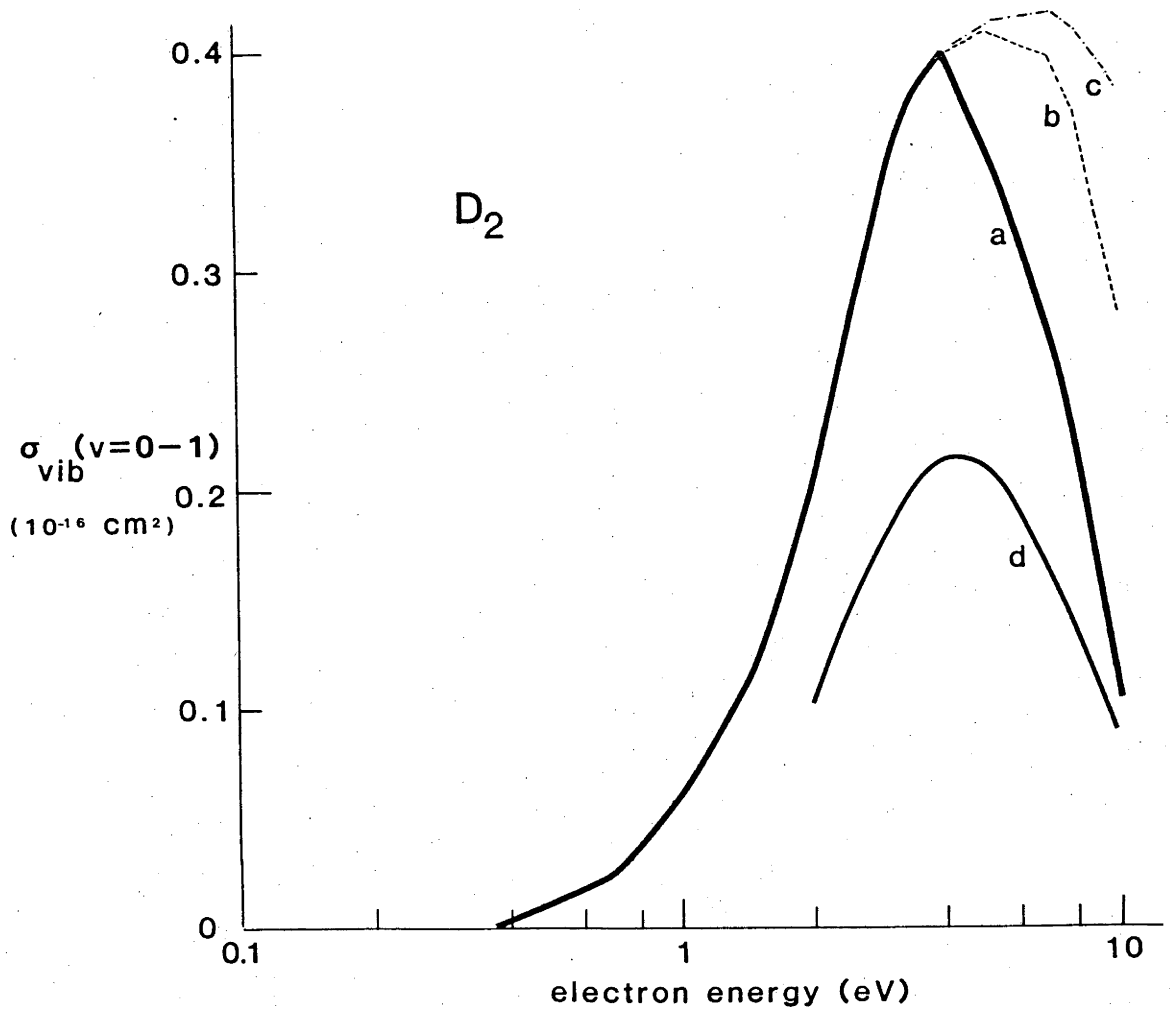


Figure 10.6 The modifications of the vibrational excitation cross section: (a) the final set derived from the transport data; (b) the modification of $\sigma_{vib}(v=0-1)$ when the scaling of 1.3 is applied to all the electronic excitation cross sections (σ_{exc}); (c) modification of σ_{vib} when σ_{exc} are not modified; (d) σ_{vib} calculated by Bardsley and Wadehra (1979).

10.4: Conclusion

Experimentally determined values of v_{dr} and D_T/μ , over a wider E/N range than previously available, were used to derive the low energy

electron cross sections for deuterium.

For energies below 2.5 eV (full lines in Figure 10.4) the vibrational excitation cross section was determined to within $\pm 15\%$, and between 2.5 and 3 eV to within $\pm 25\%$. These error limits are conservative. The agreement of the calculated transport coefficients with the measured values is very good, but there is a significant disagreement between the calculated ionization coefficients and the values measured by Buckman and Phelps (1985). The agreement of the calculated vibrational excitation coefficients with the values measured by Buckman and Phelps is satisfactory, since the differences are smaller than the experimental uncertainty, but there is a somewhat different E/N dependence at higher values of E/N.

An attempt was made to achieve overall agreement with all the available swarm data, but the shape of the vibrational excitation cross section so obtained is very different from the shape that was predicted theoretically by Bardsley and Wadehra (1979) or from the shape that can be expected on the basis of the corresponding cross section for hydrogen (see Cheng and Wong 1977).

In order to resolve the problems that exist in the determination of the vibrational excitation cross section for deuterium for electron energies above 4 eV the following should be done:

- a) The present D_T/μ values for the high E/N range (Section 10.2) should be confirmed;
- b) The ionization coefficients measured by Buckman and Phelps (1985) should also be confirmed (though the data of Morgan et al. 1967; and Haydon 1985 are consistent with the values of Buckman and Phelps);
- c) A complete set of electronic excitation cross sections (for H₂ or

- D₂) from a single source (either theoretical or experimental) is required;
- d) The magnitude of the ionization cross section should be verified;
 - e) Finally, theoretical or experimental results for the vibrational cross section (and the rotational cross sections at energies above 0.5 eV), similar to the extensive set of cross sections for hydrogen obtained by Morrison and coworkers are also required.

At the moment it is not possible to recommend a single set of electron scattering cross sections for deuterium. Nevertheless, the $v=0-1$ vibrational excitation cross section up to 2.5 eV has been determined very accurately in the present work and any further investigation of electron scattering in deuterium at low energies should take it as a starting point. It is unlikely that any alternative shape of the cross section in the energy range up to 2.5 eV would be consistent with the transport data for E/N up to 30 Td because there is a wide range of E/N values where the values of D_T/μ are mainly determined by $\sigma_{vib}(v=0-1)$.

CHAPTER 11: VIBRATIONAL EXCITATION OF CARBON MONOXIDE11.1: Introduction

Even though important for various applications such as CO and CO₂ lasers (Nighan 1970; Yardley 1971; Nighan 1977; Morgan and Fisher 1977; Garscadden 1981; Braglia et al. 1983), open cycle MHD convertors (Norcross 1982), and gas discharges in general (Long et al. 1976; Kaufman and Kagan 1981; Gorse et al. 1984), transport coefficients for CO of satisfactory accuracy are still not available in the moderate and low E/N range. As a consequence there is still considerable work to be done in assembling a satisfactory set of low energy cross sections for this gas. Another reason for this situation is that the data for CO are some of the most difficult to analyse because the two-term theory becomes seriously inadequate, especially in the range of the 2Π shape resonance (1-5 eV) where vibrational excitation is the major inelastic process.

Some attempts were made by Land (1978) to include the effects of the breakdown of the TTT but Haddad and Milloy (1983) were the first to make a rigorous analysis. The latter authors applied the multiterm theory of Lin et al. (1979) to the analysis of drift velocities in pure CO and in Ar-CO and He-CO mixtures. At the time of their analysis high precision D_T/μ data were not available, and Haddad and Milloy concluded their work with a statement that it would be desirable to have such data as these would put an additional constraint on the swarm-derived cross sections. In the work described in this chapter experimental data for D_T/μ in the region between 1 and 100 Td were obtained and, in addition, the E/N range of the drift velocities for pure CO was extended from 10 Td down to 0.03 Td. The

consistency of the cross sections derived by Land and by Haddad and Milloy with the new data was then checked.

11.2: Measurement of the transport coefficients

11.2.1: Available transport data. Only a limited number of data for D_T/μ and v_{dr} exist in the literature. Values of D_T/μ were measured by Warren and Parker (1962) in the low E/N range and at 77 K. The room-temperature results of Skinker and White (1923) and Roznerski and Mechlinska-Drewko (1979) extend over the entire E/N range used in the present analysis, while the lower end of the E/N range investigated by Lakshminarasimha et al. (1974) overlaps with the range of present interest. Nelson and Davis (1969) measured the diffusion coefficient for thermal electrons, while Wagner et al. (1967) measured values of the longitudinal diffusion coefficient.

Drift velocities were measured by Paek et al. (1962) (at three different temperatures including room temperature), by Saelee et al. (1977; see also Saelee and Lucas 1977) at high values of E/N, and by Roznerski and Leja (1984) over a very wide range of E/N values. Haddad and Milloy measured drift velocities in pure CO between 10 and 100 Td and also in Ar-CO and He-CO mixtures. Their data, supplemented by the new measurements, were used in the present analysis. An interesting feature of their mixture results is the occurrence of negative differential conductivity (see Chapter 3), although the effect was not as pronounced as predicted by Long et al. (1976).

11.2.2: Measurements of D_T/μ . The measurements of D_T/μ were made using the two Townsend-Huxley apparatuses described in Chapter 8. The basic modification to the apparatuses used in recently published measurements of D_T/μ from these laboratories was the replacement of the radioactive sources by thermal sources of electrons. This was necessary in order to eliminate negative ions produced by dissociative attachment in the region of these sources (see Chapter 8). The measures taken to ensure that the results were not affected by heating from a thermal source were discussed in Chapter 8.

Gas samples of the highest available purity turned out to be slightly contaminated. The manifestation of this was the time dependence of the results after a new sample of gas was admitted to the apparatus. It was found that purification could be achieved either by the gettering action of the hot filament over a long period (24 hours typically) or by purifying the gas in a liquid nitrogen trap. Ultimate values obtained by both techniques turned out to be identical and the latter technique of purification was adopted for the final measurements.

The results shown in Fig. 11.1 and Table 11.1 and Table 11.2 were shown to be independent of the apparatus geometry, the current, and the pressure used in the measurements. In order to make a test of the dependence of the results on the geometry of the apparatus measurements were performed in the "expandable" apparatus with a variable length, where lengths of 5 and 10 cm were used, and in an apparatus with a fixed length of 10 cm having a very stable structure (due to the use of thick guard rings) and extremely well defined geometry (see section 8.3). The dependence of the results on the value of the current was tested by varying the current (which was of the order of 10^{-12} A) over a range 1:10. That the results were not dependent

on the pressure can be seen from Table 11.1 and Table 11.2. Each experimental value is an average of between 5 and 10 experimental results obtained with at least three different samples of gas.

Table 11.1 D_T/μ (in volts) in pure CO for $E/N > 10$ Td measured in the "expandable" apparatus

E/N (Td)	p (kPa)				Average
	0.1333	0.2667	0.6667	1.333	
120*	1.631	1.630			1.631
100	1.377	1.380			1.379
90	1.269	1.267			1.268
80	1.170	1.170			1.170
70	1.094	1.091			1.093
60	1.030	1.030	1.030		1.030
55		1.003	1.004		1.003
50	0.978	0.976	0.977		0.977
45		0.947	0.947		0.947
40		0.913	0.913		0.913
35		0.873	0.873	0.873	0.873
30		0.823	0.822	0.823	0.823
25		0.7587	0.7589	0.7597	0.7591
20		0.6802	0.6785	0.6785	0.6790
15		0.5738	0.5720	0.5716	0.5725
12			0.4860	0.4882	0.4871
10			0.4281	0.4274	0.4278

* correction due to longitudinal diffusion was not made and is uncertain

Table 11.2 D_T/μ (in volts) in pure CO for $E/N > 10$ Td measured in the apparatus with thick guard rings.

E/N (Td)	p (kPa)				Average	Final Average for both tubes
	0.1333	0.2667	0.6667	1.333		
120 *	1.628					1.631
100 *	1.387					1.380
90 *	1.273					1.270
80 *	1.174					1.171
70 *	1.096					1.094
60 *	1.032	1.032				1.030
55 *		1.003				1.003
50 *		0.977				0.977
45 *		0.949				0.9475
40 *		0.916				0.9135
35 *		0.874				0.8733
30 *		0.820				0.8225
25			0.7591		0.7591	0.7591
20			0.6800	0.6800	0.6800	0.6795
17			0.6204	0.6204	0.6204	0.6204
15			0.5728	0.5727	0.5728	0.5727
14			0.5479	0.5476	0.5478	0.5478
12			0.4910	0.4911	0.4910	0.4905
10			0.4276	0.4281	0.4279	0.4279

*Results obtained in unfavourable conditions - i.e. with low current ratios.

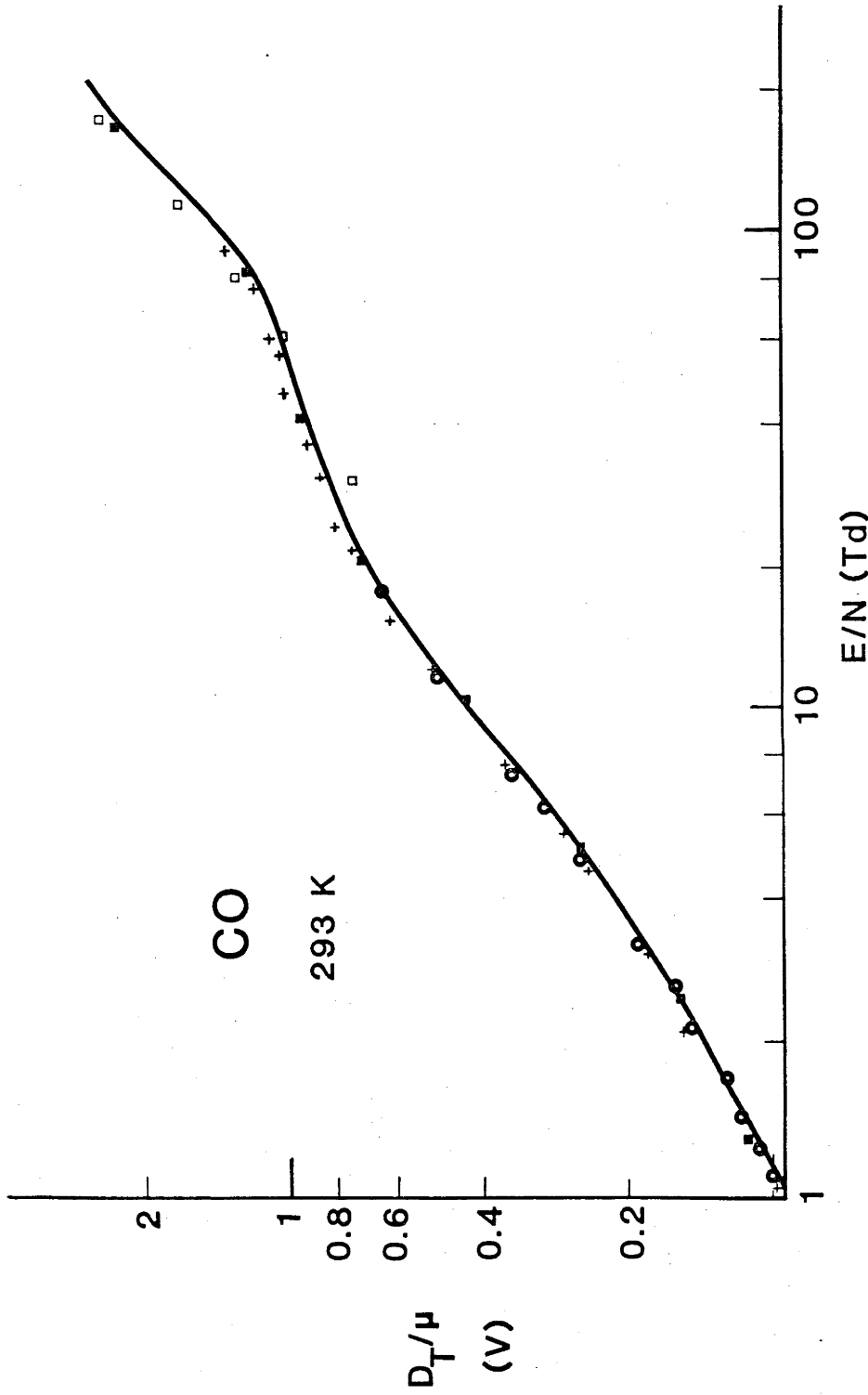


Figure 11.1 Values of D_T/μ . The present results are shown with a line, the results of Warren and Parker by circles, the results of Roznerski and Mechlinsk-Drewko by crosses, the results of Skinner and White by full squares, and the results of Lakshminarasimha *et al.* by open squares.

Table 11.3 D_T/μ (in volts) in pure CO for $E/N < 10$ Td.

E/N (Td)	p(kPa) h(cm)	expandable tube			tube with thick guard rings		Final
		1.333 10	1.333 5	0.667 5	1.333 10	0.667 10	
10		0.427	0.427	0.428	0.428	0.428	0.428
9			0.392		0.392	0.394	0.393
8		0.350	0.358	0.358	0.358	0.358	0.358
7		0.319					0.319
6		0.282			0.285		0.284
5		0.244	0.245	0.246	0.245	0.245	0.245
4		0.208			0.209		0.209
3.5		0.1902					0.1902
3.0		0.1730	0.1721		0.1728	0.1728	0.1728
2.5		0.1559					0.1559
2.0		0.1385			0.1380	0.1385	0.1384
1.7		0.1278					0.1278
1.4		0.1167					0.1167
1.2		0.1077					0.1077
1.0		0.0985			0.0983		0.0984

In table 11.3 the results obtained below 10 Td are presented. It was not possible to purify the gas samples adequately above 1.333 kPa and therefore these results were obtained only at the pressures shown.

The Huxley formula was used to derive D_T/μ values from the current ratios over the entire range of E/N . For $E/N = 100$ Td, which is the

highest value of E/N where the data for D_L derived by Lowke and Parker (1969) are available, the correction for longitudinal diffusion (calculated from equation 2.66) was found to be only 0.3%. In the subsequent analysis only the data up to 100 Td were used; the data above $E/N = 100$ Td shown in Fig. 11.1 do not incorporate corrections for either longitudinal diffusion or ionization (see Section 2.4).

The estimated uncertainty of the data is less than $\pm 2\%$. This value possibly overestimates the uncertainty due to the presence of impurities and thermal effects (for which 0.5% was assigned) and the statistical scatter of the data which was better than 0.5%. (To a certain degree the first uncertainty is also incorporated in the second.)

The present results are in good agreement with other experimental data below 20 Td (Skinker and White 1923; Warren and Parker 1962) but at moderate values of E/N there is a difference of up to 5% with the data of Roznerski and Mechlinska-Drewko; the older data of Skinker and White agree with the present data somewhat better. It is difficult to assess the quality of the results of Roznerski and Mechlinska-Drewko and to accept the claimed accuracy of $\pm 2\%$ (Roznerski 1983 - personal communication) for the following reasons:

- the experimental results at different pressures were not shown;
- it is uncertain whether the pressure and other experimental parameters were varied over a wide range;
- the accuracy of the method of pressure measurement and calibration is not stated;
- the geometrical accuracy of the apparatus is difficult to assess;

and finally • it seems that the authors sometimes used very low fields without taking into account the possibility of the presence of non-uniform contact potentials on the collecting electrode.

On the other hand the present results were verified by numerous diagnostic checks, and field strengths lower than 3 Vcm^{-1} were not used (normally the fields were larger than 10 Vcm^{-1}).

11.2.3: Measurement of drift velocities. Haddad and Milloy (1983) could not extend their measurements below 10 Td because of a large background of negative ions. The present work was undertaken in a further attempt to extend the E/N range.

Mass spectrometric analysis of the gas from the cylinder of pure CO used by Haddad and Milloy (1983) revealed that a small quantity of impurities was present. Therefore it seems that the large negative ion backgrounds reported by these authors were not ions created by dissociation of CO as they suggested. Two new cylinders were purchased which proved to have a much lower level of impurity. Gas from these cylinders was therefore used for all the drift velocity and D_T/μ measurements. The ionic background made the measurements difficult only when high pressures were used ($\geq 13 \text{ kPa}$). Using pressures up to this values it was possible to extend the measurements to 0.3 Td.

The results are shown in Fig. 11.2 and in Table 11.4. The estimated error bounds are $\pm 1.5\%$. These error limits are somewhat higher than in other drift velocity measurements due to the diffusion corrections being sometimes as large as 0.7% at the lowest pressures and due to the presence of the background at higher pressures. These effects somewhat degrade the

measurements at the highest and lowest values of E/N. However, most of the data were obtained under more favourable conditions and therefore the suggested error bounds are thought to be conservative.

The present results are in good agreement with the results of Pack et al. (1962) except at the two highest values of E/N where their data are up to 10% lower. On the other hand the results of Roznerski and Leja (1984) are, lower than the present data and the data of Pack et al. by up to 12% below 6 Td. The agreement of the present results with the data of Haddad and Milloy in the range of overlap is better than 0.3% except at 10 Td where the difference is 1% (still inside the error bars).

11.3: Swarm-Derived Cross sections

11.3.1: Available cross section data. Carbon monoxide is a polar molecule but its dipole moment is sufficiently small (Nelson et al. 1967) that, except at very low energies, its cross section resembles more the cross sections for some non-polar molecules (N₂ especially).

Several review articles on the theory of electron scattering by polar molecules have been published recently and some information about electron-CO scattering may be found in them (Itikawa 1978; Norcross and Collins 1982; for a review of recent theoretical results see also the paper by Salvini et al. 1984). A short review of the experimental data has been given by Trajmar et al. (1983).

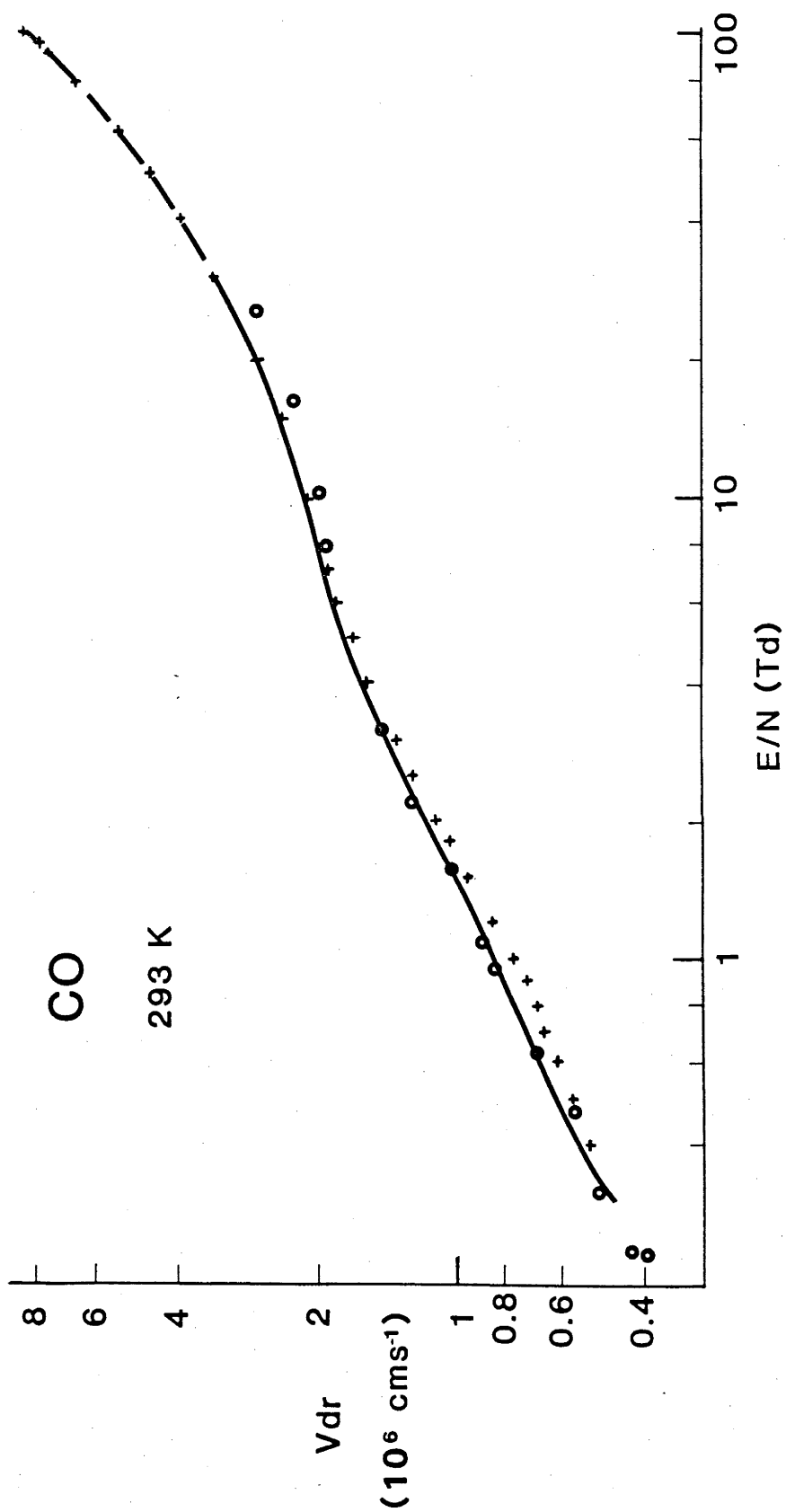


Figure 11.2 Drift velocities in pure CO. The present results are shown as a line, the results of Pack *et al.* as circles, the results of Haddad and Milloy as a dashed line, and the results of Roznerski and Leja as crosses.

Pressure (kPa) E/N (Td)	0.4133	0.7231	1.0334	2.066	4.	6.6128	8.059	13.425	Final
25	3.008								2.349
20	2.708								2.230
17	2.527								2.106
14	2.347	2.351							1.983
12	2.227	2.231	2.231						1.913
10	2.107	2.111	2.110						1.832
08	1.982	1.983	1.984						1.734
7	1.912	1.914	1.914						1.603
6	1.830	1.833	1.833						1.521
5		1.734	1.735	1.734					1.422
4		1.604	1.603	1.603					1.305
3.5		1.522	1.521	1.520					1.169
3			1.422	1.421					1.077
2.5			1.305 ₉	1.304 ₃	1.305 ₁				0.9767
2.0			(1.170)	1.168	1.169				0.9067
1.7			(1.078)	1.075	1.076	1.078	0.977 ₄		0.8338
1.4				0.975 ₁	0.9757	0.978 ₀	0.9070		0.7580
1.2				0.906 ₄	0.9062	0.9070	0.833 ₈		0.7178
1.0					(0.832)	0.834 ₄	0.757 ₈		0.6732
0.8						0.758 ₅	0.717 ₆		0.6196
0.7						0.717 ₉	0.673 ₁		0.5493
0.6						0.673 ₃	0.619 ₆		0.5044
0.5						0.619 ₁		(0.5498)*	(0.5047)*
0.4									(0.4527)*
0.35									(0.4524)
0.30									

Table 11.4 Drift velocities (10^6 cm s⁻¹) in pure CO at 293 K.

As vibrational excitation is of special interest for the present work the cross sections obtained by beam methods will be briefly mentioned here. Ehrhardt et al. (1968) measured cross sections for excitation of the first seven vibrational levels, and their work was supplemented by the results of Boness and Schulz (1973) for the excitation of levels from the seventh to the tenth. Chutjian and Tanaka (1980) measured absolute differential cross sections for $v=0-1$ vibrational excitation at energies above 3 eV. They also determined the integral vibrational excitation cross section for the same process which, at their lowest energy of 3 eV, they found to be 50% smaller than the cross section of Ehrhardt et al..

Derivations of the cross sections on the basis of swarm data were performed by Hake and Phelps (1967), Land (1978), and Haddad and Milloy (1983). The most interesting feature of the cross section derived by Hake and Phelps is the contribution from non-resonant vibrational excitation which they found to be non-negligible below the onset of the resonance. The existence, and the order of magnitude, of the cross section for this process were confirmed in the subsequent work of Land (1978) and Haddad and Milloy (1983) and in the beam experiment of Ehrhardt et al. (1968) (see Section 11.3.3).

Haddad and Milloy initially used the cross section of Hake and Phelps for non-resonant vibrational excitation and supplemented it by the cross sections of Ehrhardt et al. (1968) and Boness and Schulz (1973) in the resonance region. In their analysis the electronic excitation cross sections tabulated by Land (1978) were used with the addition of a resonance structure near the threshold for excitation of the $a^3\Pi$ state (see Swanson et al. 1975). The momentum transfer cross section was adjusted to give the best fit with the transport data for pure CO. Due to lack of

uniqueness when a large number of cross sections is being derived from the transport data for the pure gas (see Section 2.3) these authors performed measurements of drift velocities in Ar-CO and He-CO mixtures and used these results (mainly for Ar-CO mixtures) to scale appropriately the initial vibrational excitation cross sections while preserving their shape. They found that a scaling factor of 1.3, rather than 1.9 as suggested by Land (1978), gave the best agreement between the experimental and the calculated data. The disagreement between the scaling factors for the same initial set of vibrational excitation cross sections was attributed to the breakdown of the TTT that was used by Land. Land made some attempts to compensate for the breakdown by applying corrections that were based on the work of Kontoleon et al. (1973). These corrections were shown by Haddad and Milloy to be too small.

It is interesting to point out that Braglia et al (1983), in an analysis of their experimental data for drift velocities in CO₂ gas laser mixtures, found that when CO was added to the mixture the agreement of calculated and measured drift velocities was considerably worse than in the case when measurements and calculations were performed for the mixture without CO. These authors used the cross sections of Land (1978) in their analysis and it is possible that their findings are another indication that the cross sections derived by Land are in error.

11.3.2: Analysis. The standard two-term code was used to carry out the calculations in the present analysis. However, corrections for the breakdown of the TTT were always applied. The corrections were calculated using the cross sections obtained by Haddad and Milloy (1983) for the values of E/N below 10 Td, and were supplemented by the corrections already

calculated by Haddad and Milloy above 10 Td. The maximum correction to D_T/μ was less than 10%; in the region below 10 Td the corrections to the results from the TTT were found to vary from 1% at 1 Td to 2.5% at 10 Td. The multiterm corrections to drift velocities were negligible.

Initially the cross sections of Haddad and Milloy were used in the analysis. The calculated values of D_T/μ were found to differ from the experimental data by up to 6%. The maximum difference occurred at and about 20 Td (note that for this value of E/N there is good agreement between the present experimental results for D_T/μ and other sources of data - see Section 11.2.2). When the cross sections of Land (1978) were used, the calculated transport data are in good agreement with the experimental results between 5 and 50 Td. Above and below these limits a maximum difference of 6% is found for D_T/μ and 4% for v_{dr} . One could therefore argue that the cross sections of Land are not inferior to those of Haddad and Milloy, but such an argument is not supported by a comparison of calculated and measured drift velocities for the mixtures where large differences exist when Land's cross sections are used.

In order to improve the agreement of the calculated D_T/μ values with the new experimental data, but not spoil the agreement achieved by Haddad and Milloy for drift velocities in pure CO and the mixtures, some modifications to the cross sections were applied. The scaling factor for vibrational excitation was increased from 1.3 to 1.35, and the non-resonant part of the cross section was increased by up to 35%. (see Fig. 11.3). The momentum transfer cross section was also adjusted. Up to 1.5 eV it was increased by up to 9% and above 1.5 eV decreased by up to 8% (see Fig. 11.4). Also the electronic excitation cross section for the $a^3\pi$ state was increased by 5% in the region of the resonance. (Note that Haddad and

Milloy scaled the cross sections tabulated by Land by 0.7.) These modifications were all within the error bounds that might reasonably be assigned to the cross sections derived by Haddad and Milloy (1983).

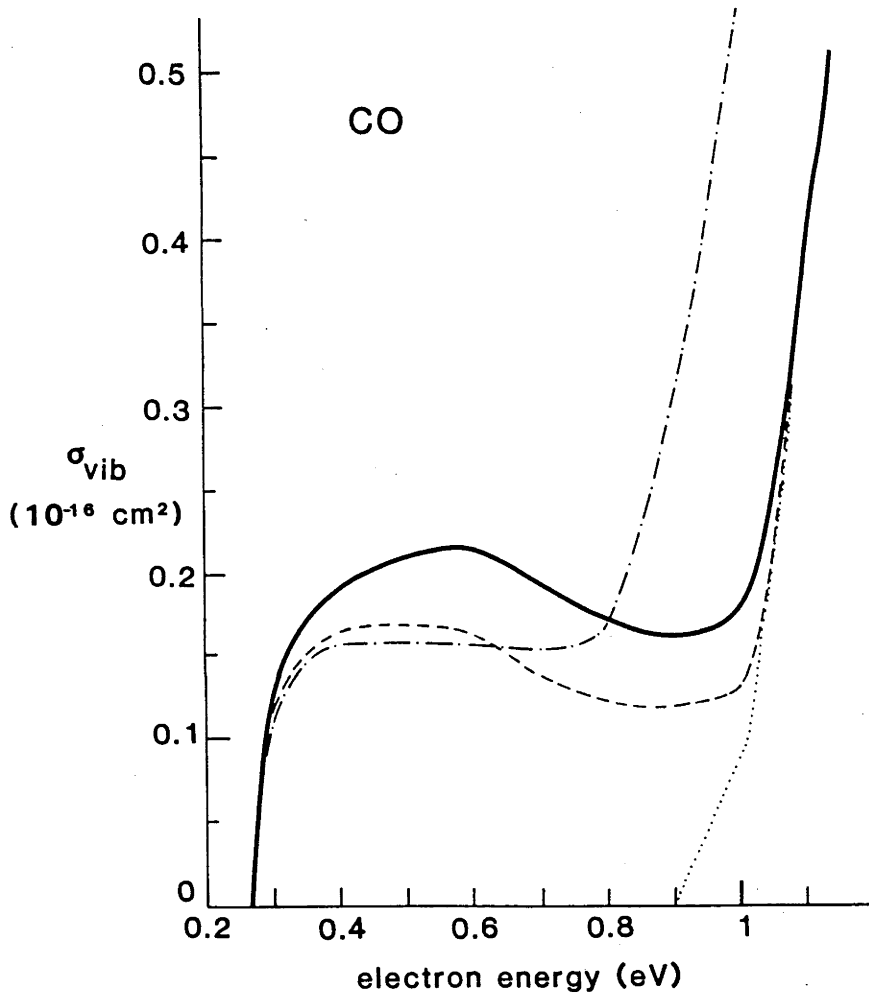


Figure 11.3 The cross section for non-resonant vibrational excitation of CO. The present result is shown as a solid line, the result of Haddad and Milloy as a dashed line, and the results of Land as a dot-dash line. The dotted line represents the cross section used in calculations aimed to show the sensitivity of the transport data to the cross section for non-resonant excitation (see Section 11.3.3).

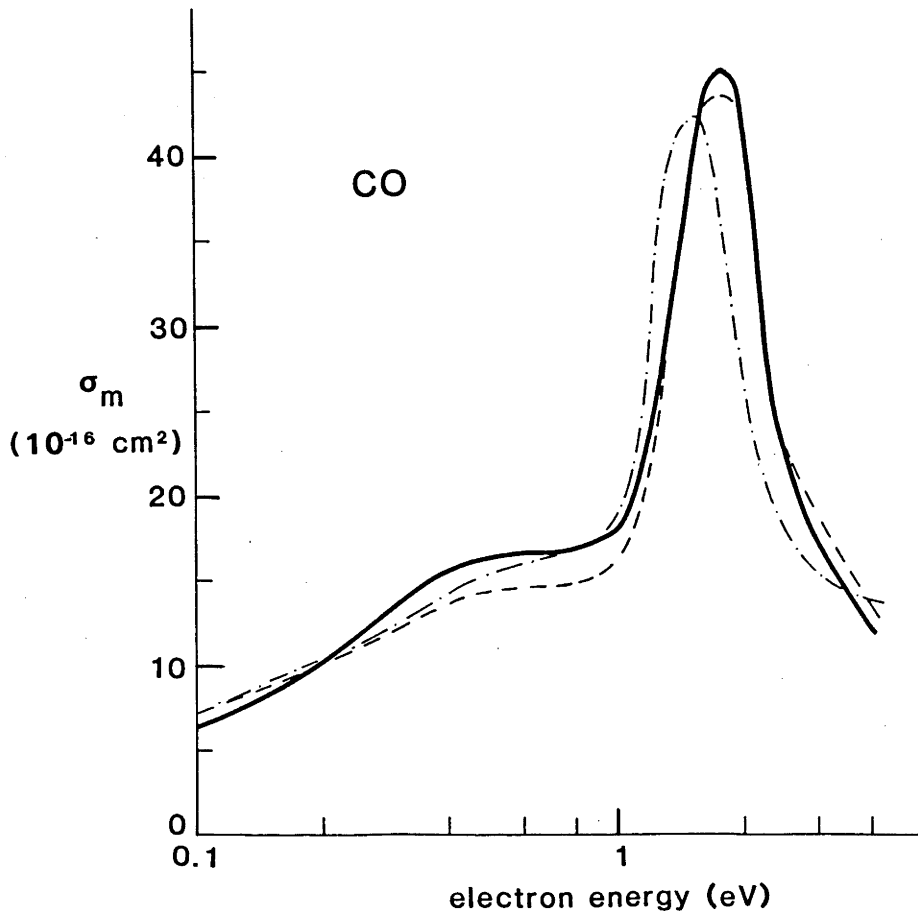


Figure 11.4 Momentum transfer cross section used in the present analysis (solid line) and the corresponding results derived by Haddad and Milloy (1983) (dashed line) and Land (1978) (dot-dashed line).

When the cross section set described above is used, the calculated values of the transport coefficients in the range between 4 and 100 Td are within the experimental error bounds of the data for pure CO. For the mixtures of 10 and 20% of CO in Ar the calculated drift velocities are within the claimed error bounds of $\pm 3\%$. However for the mixtures of 1, 2 and 5% of CO in Ar the calculated drift velocities are up to 4% different from the experimental data. This difference at some values of E/N is

somewhat larger than the claimed experimental uncertainty but it could not be reduced without significantly degrading the agreement in pure CO. Haddad and Milloy found similar differences between the calculated and experimental data for the mixtures, but when Land's cross sections are used the differences exceed 10%. It is possible that the error bounds on the data of Haddad and Milloy should be somewhat larger for the mixtures with low abundances because these authors did not use a specially built mixing vessel to make the mixtures. They made mixtures directly in the apparatus and it is possible that for low abundances insufficient time was allowed to achieve a homogeneous mixture. Another possible explanation for the differences between the calculated and experimental data is that, for the low abundances of CO, the measurements were made at values of E/N such that the average energy is considerably larger than in the pure gas or in the mixtures with larger abundances of CO. These results could therefore be affected by a possible inaccuracy of the momentum cross section for argon at higher energies (see Haddad 1984).

Haddad and Milloy (1983) showed that at 10 Td the influence of rotational excitation is negligible. However, the present analysis was extended below that point and therefore rotational excitation had to be taken into account (both in the two- and multi-term calculations). The analytical formula derived by Takayanagi (1966) for rotational excitation of polar molecules

$$\sigma_{\text{rot}}(J, J+1; \epsilon) = \frac{8\pi\mu^2 a_0^2 R_y}{3\epsilon} \frac{J+1}{2J+1} \ln \frac{\sqrt{\epsilon} + \sqrt{(\epsilon - \epsilon_J)}}{\sqrt{\epsilon} - \sqrt{(\epsilon - \epsilon_J)}} \quad (11.1)$$

was used, where μ is the dipole moment in atomic units, a_0 is the Bohr radius and R_y is one Rydberg, and ϵ_J is the threshold energy for excitation

from the rotational level J . Populations of the rotational levels at 293 K were calculated (see Appendix 6), and up to 24 levels were used in calculations of transport coefficients. It was shown that the quadrupole excitation cross sections (calculated using the formulae of Gerjoy and Stein 1955) become comparable to the dipole excitation cross sections only above 0.5 eV where vibrational excitation is the dominant inelastic process. Inclusion of quadrupole excitation leads to a change of the calculated transport coefficients of less than 0.2% (at 10 Td), and therefore it was not taken into account in the present analysis. Resonant rotational excitation was also neglected. In order to test the validity of omitting this process a cross section was included that had the shape of $\sigma_{\text{vib}}(v=0-1)$ above 1.2 eV but an energy loss of 3.8 meV, which is the energy loss associated with rotational excitation of the most populated rotational level ($J=7$) at 293 K. Changes of less than 0.05% were observed in the calculated transport coefficients. Even when the energy loss for this process was increased to 20 meV (Phelps - personal communication) the effects were still small.

The present analysis was extended down to 4 Td where rotational excitation becomes almost as important an energy loss process as vibrational excitation. However, the results for σ_{vib} and σ_m below 0.4 eV obtained on the basis of the transport data below 10 Td are subject to somewhat larger errors than the results obtained from the transport data for pure CO above 10 Td and from the data for the mixtures. The reason for this increased uncertainty is that rotational excitation cross sections are represented only approximately by equation (11.1) even though rotational excitation is a significant energy loss process in that range of E/N .

11.3.3: Non-resonant vibrational excitation. Engelhardt et al. (1964) and Hake and Phelps (1967) showed that direct (non-resonant) vibrational excitation plays a significant part in determining electron transport in N_2 and CO in certain ranges of E/N. The theoretical results of Takayanagi (1966) support the cross sections for this process unfolded from swarm experiments but it is very difficult to apply beam methods to obtain direct experimental data for the cross sections because of their small magnitudes. For CO, where the cross section is of the order of $0.1 \cdot 10^{-16} \text{ cm}^2$, some beam results are available but even then, not surprisingly, the accuracy of the results is low.

However, when swarm methods are used it is not difficult to derive accurate cross sections for this process. In order to show how sensitive the swarm data are to non-resonant excitation, calculations were made in which $\sigma_{\text{vib}}(v=0-1)$ was set to zero below 0.9 eV and then linearly connected to its value at 1.1 eV (Fig. 11.3 - dotted line). In the Ar-CO mixtures, changes in the calculated drift velocities of up to 32% were seen for the 10 and 20% mixtures (see Fig. 11.5). For the mixtures with a smaller abundance the effects were smaller as the average energy in those mixtures is higher and the results are more sensitive to the resonant portion of the vibrational excitation cross section. For the pure CO data at 10 Td the effects of the modification are a 33% decrease for v_{dr} and a 58% increase for D_T/μ (see Fig. 11.6), while below 10 Td these effects increase up to 50 and 150% respectively (at 4 Td).

The large effects of the modification of $\sigma_{\text{vib}}(0-1)$ on the calculated transport coefficients indicate that this cross section can be derived very accurately using the swarm method.

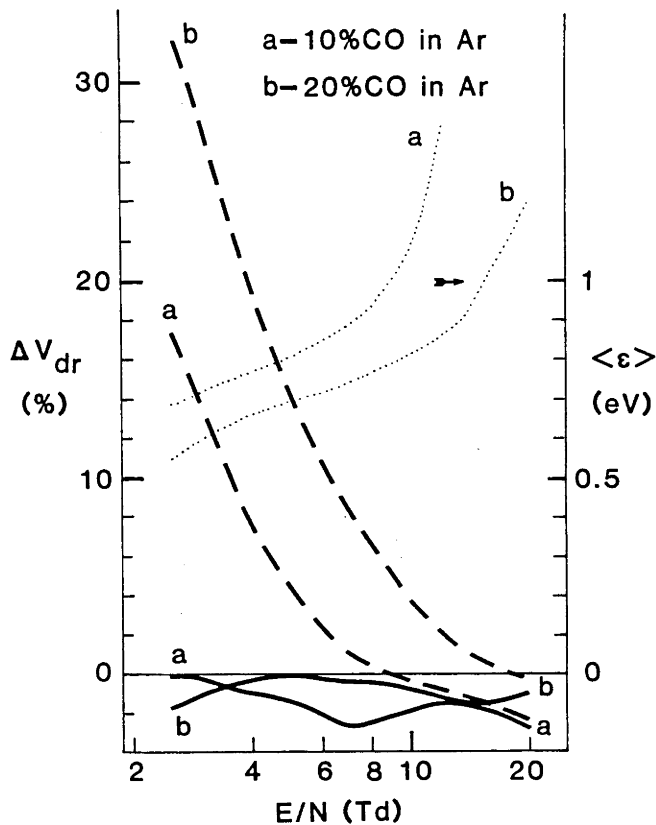


Figure 11.5 Differences between calculated and experimental drift velocities in (a) 10% and (b) 20% mixtures of CO in Ar. Dashed lines represent results calculated without the contribution from non-resonant vibrational excitation. The average electron energies are also shown (dotted line).

11.4: Conclusion

This Chapter reports an extension of the work of Haddad and Milloy (1983) which they initiated to derive accurate cross sections for vibrational excitation of CO using multiterm transport theory. It is a good example of at least three points that were discussed in Chapter 2. First, the TTT is not sufficiently accurate for an analysis of transport data for this gas and its application leads to errors that are as large as 10% for the calculated values of D_T/μ ; it may therefore lead to even larger errors in the derived cross sections. Second, since many inelastic

processes are playing a significant role at some energies the cross sections for these processes cannot be determined uniquely over the entire energy range from available transport data even when the data for pure CO is supplemented with data for mixtures of CO with other gases. Third, the work demonstrates that, if some input from beam experiments and/or theory is used, a high degree of uniqueness can be achieved.

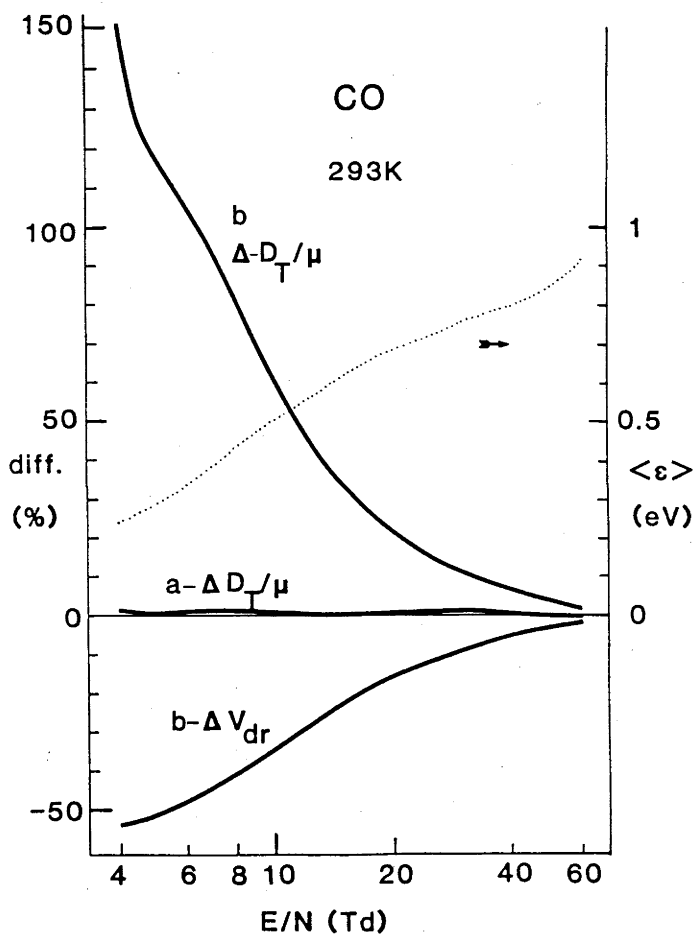


Figure 11.6 Differences between the calculated and experimental values for v_{dr} and for D_T/μ with (a) and without (b) the non-resonant excitation cross section (see text). Only the differences of D_T/μ values are shown when the calculations were made which included the non-resonant cross section. Average electron energies are also shown (dotted line).

The present set of experimental results for D_T/μ and v_{dr} provides additional and therefore more stringent constraints on the derived vibrational excitation (and momentum transfer) cross sections than the more limited data available to Haddad and Milloy. Therefore the present results

should be an improvement on the results of Haddad and Milloy even though it must be said that the modifications that were made as a result of the present analysis lie within the error bounds that can be assigned to their cross sections.

It was not possible to extend the analysis to lower values of E/N for two reasons. First a large number of rotational transitions exists in CO at room temperature. The corresponding cross sections are known only approximately while their large number dictates the use of some simple analytical formula to represent them adequately. Second, the D_T/μ data obtained in the present work do not extend to sufficiently low values of E/N that, when used in conjunction with the measured v_{dr} data, they enable a satisfactory analysis to be made in this low energy region.

CHAPTER 12: LOW ENERGY ELASTIC SCATTERING OF ELECTRONS BY ARGON12.1: Introduction

Argon is one of the most important gases for the physics of gas discharges. Being an atomic gas it has no inelastic losses at low energies and the existence of the Ramsauer-Townsend minimum (RTM) makes it possible for electrons to reach high energies for relatively low values of density-normalized electric field strengths. It is not possible to give here a detailed review of the many investigations that require a knowledge of electron scattering in argon, which includes data for the elastic scattering cross section at low energies, and only a short list will be given: modelling of positive columns (Ingold 1978; Smits and Prins 1979; Ferreira 1983; and many more); nonequilibrium phenomena in low pressure gas discharges (Hayashi 1982); modelling of gas lasers (see Werner and George 1976; Garscadden 1981; Tellinghuisen 1982;...); electron energy thermalization and thermal mobility calculations (Mozumder 1981, Hayashi and Usheroda 1983; McMahon and Shizgal 1985). Especially interesting are the studies of various gas mixtures containing argon (Long et al. 1976; Al-Dargazelli et al. 1981; Winkler et al. 1983; Davies et al. 1984; and many more).

In most applications advantage is taken of the fact already mentioned that for relatively low fields high electron energies are easily achieved and consequently a large proportion of the energy is deposited in the metastable levels through electron excitation (Ismail and Garamoon 1979; Bozin et al. 1983). The energy stored in metastable levels can be converted to various other forms through heavy particle collisions (see

Hill et al. 1974; Golde 1976 and many more).

Argon is also important for theoretical electron scattering physics because it has been studied more than most other gases experimentally and therefore it is possible to test various approximations that must be made in any theoretical discussion of such a complicated atom.

Data for H₂-Ar mixtures have already been used in this thesis, together with other sources of data, to derive the vibrational excitation cross sections for H₂. In this chapter results for the drift velocity in an Ar-H₂ mixture will be used to derive the low energy cross section for Ar. There seems to be a conflict between these two applications of mixture data, but in fact there is none. In Chapter 9 data obtained at relatively large values of E/N (and therefore relatively high average electron energies, between 200 meV and 1.5 eV) were used. In that energy range the cross sections for vibrational excitation are important and in fact make the largest contribution to the energy loss, making it possible to determine the cross sections for this process from an analysis of these data.

In this chapter the measurements of v_{dr} were made in Ar-H₂ mixtures at low values of E/N with average energies between 30 and 300 meV. In that range of energies the major energy loss is rotational excitation for which the cross sections are thought to be known very accurately, there being agreement between the swarm-derived and the theoretical values (see Chapter 9). The contribution of rotational excitation above 0.5 eV and of vibrational excitation is small and a high accuracy for the cross sections for these processes is not required to achieve high accuracy in the analysis of the mixture data in this range of E/N. Therefore the discrepancies that exist between swarm-derived and theoretical vibrational

excitation cross sections will not affect the present analysis to determine the argon momentum transfer cross section at very low energies.

12.2: Cross Sections for Electron-Argon Scattering

12.2.1: Theoretical results. Argon is much more difficult to treat theoretically than helium. Therefore, so far, cross sections for elastic scattering that match the accuracy of the theoretical cross sections for electron-helium scattering (Nesbet 1979) have not been produced.

The earliest theoretical work that will be mentioned here is the work of Thompson (1966; 1971). This author included the effects of polarisation and exchange in his work, and derived elastic scattering cross sections for argon (and other gases) and also a formula that gives a good estimate of the contribution of the higher order phase shifts to the total elastic and momentum transfer cross sections. Thompson's formula was used in the present work. A similar theoretical approach to that of Thompson (i.e. a polarised orbital approximation) was adopted by Gabarty and LaBahn (1971) and Walker (unpublished personal communication), while McCarthy et al. (1977) and Amusia et al. (1982) used an optical potential model in their calculations. The most accurate calculations performed to date are the R-matrix calculations of Fon et al. (1983), extended to low energies by Bell et al. (1984), and the calculations of McEachran and Stauffer (1983) who also applied a polarised orbital method. McEachran and Stauffer carried out *ab initio* calculations of the phase shifts for various multipole interactions. The best agreement with the experimental data of Andrick and Bitsch (see McEachran and Stauffer 1983) and Williams (1979) was found when only the dipole part of the polarisation potential was used.

The position of the RTM in their calculations changes considerably when the dipole interaction is supplemented by multipole terms.

12.2.2: Modified effective range theory. Modified effective range theory (MERT) was used in the present work to represent analytically the form of the low energy cross section. This theory will therefore be briefly outlined here.

The form of effective range theory that is frequently used in nuclear physics was modified by O'Malley et al. (1961; 1962 see also O'Malley 1963; 1964) to include the long range polarisation potential and therefore it was possible to apply the theory to electron-atom scattering. As mentioned in Chapter 9 the theory was also extended to quadrupole interactions and applied to electron non-polar molecule scattering (Chang 1974; 1981; Fabrikant 1981; 1984). It has also been extended to electron-permanent dipole interactions and applied to electron-polar molecule scattering (Fabrikant 1977; 1978).

Nevertheless MERT has been most successfully applied to electron-atom scattering at low energies. It is particularly suited to the analysis of swarm data because it makes it possible to reduce the number of adjustable parameters in the analysis.

The formulae used in the present analysis will be summarized next. The two lowest order phase shifts are given by (see Haddad and O'Malley 1982):

$$\eta_0 = -A k \left\{ 1 + \frac{4\alpha}{3a_0} k^2 \ln(ka_0) \right\} - \frac{\pi\alpha}{3a_0} k^2 P D k^3 + F k^4, \quad (12.1)$$

$$\eta_1 = \frac{\pi}{15} \alpha k^2 \left\{ 1 - \left(\frac{\epsilon}{\epsilon_1} \right)^{1/2} \right\} \quad (12.2)$$

or alternatively

$$\eta_1 = \frac{\pi}{15} \alpha k^2 - A_1 k^3$$

where A, D, F and ϵ_1 ($A_1 = \pi\alpha/13.605/15\sqrt{\epsilon_1}$) are the adjustable parameters, $\epsilon = 13.605 (ka_0)^2$, a_0 is the Bohr radius, and α is the polarizability (in a_0 units). The higher order phase shifts are given to a satisfactory accuracy by the Born formula:

$$\eta_l = \frac{\pi}{(2l+3)(2l+1)(2l-1)a_0} \alpha k^2 \quad (12.3)$$

There is a certain degree of uncertainty about the upper limit of validity of MERT. This limit (ϵ_{\max}) is hard to set and O'Malley (O'Malley and Crompton 1980) proposed an alternative form of the phase shift formulae in an attempt to extend its validity to 2 eV. Haddad and O'Malley (1982), in their reanalysis of swarm data for argon, used the standard MERT formulae but they varied ϵ_{\max} and found that when ϵ_{\max} is less than 1.5 eV the results obtained were independent of the energy range, and that good agreement could be obtained between the calculated and experimental values. These authors considered 1 eV to be the optimum choice for ϵ_{\max} . Their MERT parameters are $A = -1.488$; $D = 65.4$; $F = -84.3$ and $\epsilon_1 = 0.883$.

12.2.3: Experimental results obtained using electron beams. In contrast to the situation for molecular gases, the application of MERT enables one to make a comparison between beam and the swarm-derived results for atomic gases over an extended energy range. MERT can be used to calculate the phase shifts from beam data for the total or differential cross sections which in turn can be used to calculate the momentum transfer cross section, enabling the transport data to be calculated and checked for consistency with the experimental swarm data. This provides an important

check of the quality of the beam results.

It is usually considered that Golden and Bandel (1966) were the first to apply modern experimental techniques to determine the total scattering cross section in Ar, although it should be noted that the old results of Ramsauer and Kollath 1929 have withstood the test of time amazingly well. The results of Golden and Bandel extended to 100 meV and it was therefore possible to fit their data using MERT. The value of the scattering length obtained by these authors was $A=-1.65$, and on the basis of the MERT parameters derived in a subsequent analysis of their data Golden (1966) derived a momentum transfer cross section. This cross section differed considerably from the cross section of Frost and Phelps (1964). (It is interesting to note that O'Malley (1963) fitted the data of Ramsauer and Kollath using MERT and obtained $A=-1.70$.)

Gus'kov et al. (1978) measured the total cross section to the lowest energy achieved so far by beam methods - namely to 25 meV. Their result is in good agreement with the results of Golden and Bandel, especially the position and the depth of the RTM.

On the other hand, recent measurements of the total cross section by Ferch et al. (1984) and Jost et al. (1983) are in disagreement with the results of Golden and Bandel (1966) especially in the position and the depth of the RTM (and are more consistent with the swarm-derived cross section of Haddad and O'Malley 1982). It has been suggested that at the RTM, where the s-wave becomes zero, the scattering is strongly anisotropic (i.e. forward scattering is enhanced) and therefore the angular discrimination of the experiments of Golden and Bandel (1966) and Gus'kov et al. (1978) might not have been good enough to distinguish between the unscattered and the forward scattered electrons.

The total error of the data of Ferch et al. is less than $\pm 4\%$. The MERT fit to their data gives the following values: $A=-1.449$, $D=73.1$, $F=-115.8$ and $A_1=8.50$. However these authors observed a dependence of the scattering length on the choice of ϵ_{\max} . The results presented above correspond to an ϵ_{\max} of 500 meV. For $\epsilon_{\max}=1.0$ eV the resulting scattering length is in good agreement with the result of Haddad and O'Malley (1982).

Measurements of the differential cross sections have also been made in the low energy range. Until recently, however, the differential cross sections had not been measured in the range of energies below the RTM (see Williams 1979). However, Weyhreter et al. (1983) solved the formidable problems that are encountered in the sub-eV range and managed to complete measurements of the differential cross sections for Ar, Kr and Xe between 50 meV and 2 eV. These authors fitted their results for argon in the range up to 300 meV with MERT and obtained $A=-1.64$, $D=51.9$ and $A_1=8.8$ ($\epsilon_1=0.986$).

The present work was partially motivated by a desire to use the swarm-derived cross section in conjunction with the results of Weyhreter et al. (1983) to determine definitive differential, total and momentum transfer cross sections for argon. Weyhreter et al. calibrated their energy scale using the $^2P_{2/3}$ resonance at the energy of 11.098 eV. It is, however, questionable whether this calibration still holds at 50 meV. If the energy scale of Weyhreter et al. is shifted by 20 meV their result for A is in good agreement with the swarm value (Linder - personal communication). It is therefore important to establish limits to the swarm-derived value of A that are as firm and as narrow as possible if it is to be used to calibrate the low energy scale of the beam experiments.

In Fig. 12.1 some of the recently derived or measured cross sections for Ar are shown.

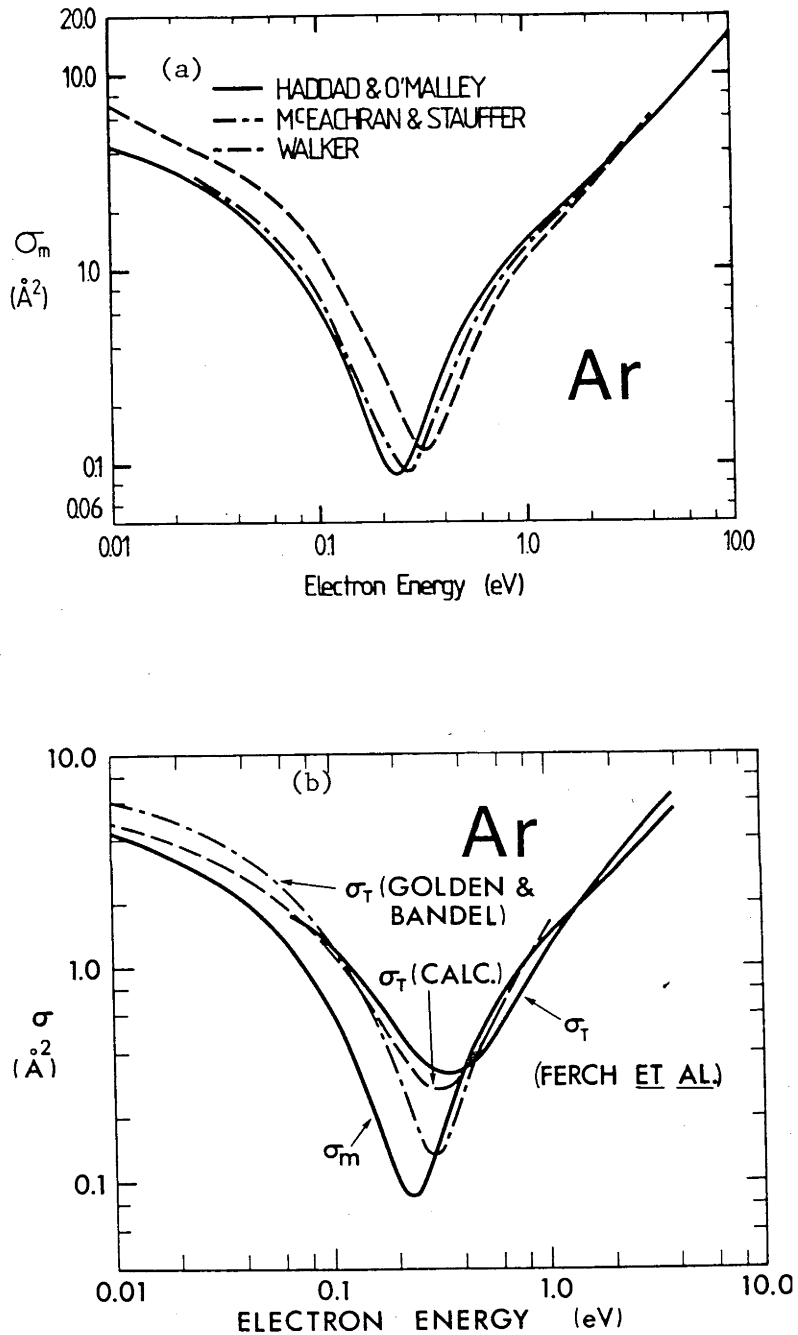


Figure 12.1 a) Recently derived theoretical momentum transfer cross sections compared to the swarm-derived cross section of Haddad and O'Malley.

b) Recently measured total cross sections for Ar compared to the total cross section $\sigma_T(\text{calc.})$ that was calculated using the MERT fit to the swarm derived σ_m .

12.2.4: Swarm-derived cross sections. The first derivation of the momentum transfer cross section from transport data was made by Frost and Phelps (1964). Milloy et al. (1977) used the high precision transport data obtained at IDU to derive σ_m in the energy range from 0 to 4 eV. A reanalysis of the same set of data was carried out by Haddad and O'Malley (1982) in an attempt to extend the range of application of MERT (Milloy et al. used MERT only up to 0.32 eV). The results of Haddad and O'Malley have already been presented in Section 12.2.2.

It is of interest to point out that Milloy (1975) showed that the effects of inelastic processes in Ar become appreciable only above 2 Td.

12.3: Data used in the Present Analysis

12.3.1: Drift velocities and D_T/μ values in pure argon. The drift velocities measured at 90 K by Robertson (1977) were used. Robertson assessed the error bars for these results as $\pm 4\%$ below 0.005 Td, between ± 4 and $\pm 1\%$ in the range between 0.005 and 0.01 Td, and between ± 1 and $\pm 2\%$ in the range between 0.01 and 0.1 Td. The error bounds were made as large as this because of the comparatively large values of the diffusion correction, but more realistic error bounds are probably less than $\pm 2\%$, especially when the pressure correction due to multiple scattering effects is taken into account (see Section 12.3.2).

D_T/μ values measured at 293 K by Milloy and Crompton (1977b) were also used. The error limits assigned to their data are $\pm 2\%$ below 0.0035 Td and $\pm 1.5\%$ above 0.004 Td. The data obtained by these authors are believed to be unaffected by collective effects (see Section 12.3.2).

12.3.2: Pressure dependence of the transport coefficients. The non-existence of low energy inelastic losses and a very low value of the cross section at the RTM are, as mentioned above (see Section 12.1), an advantage in numerous applications, but on the other hand these characteristics are a source of major difficulties when the low energy cross section is to be determined from the transport data. In order to reach very low electron energies, extremely low values of E/N must be used, which in turn means that the pressures used in the experiments have to be very high. With such high pressures, however, it was found that the drift velocities become pressure dependent (Lowke 1963; Robertson 1970 and many more).

Many attempts have been made to provide a satisfactory theoretical explanation of the pressure dependence. Frommhold (1968) suggested that resonance scattering leads to a situation where the electrons spend a part of their transit time quasi-bound to the molecules. However the existence of the pressure dependence for rare gases, where there are no low energy resonances, and the positive pressure dependence for CH_4 could not be explained by Frommhold's hypothesis. A multiple scattering model was suggested by Legler (1970) based on the fact that at high pressure the electron wavelength becomes comparable to the mean free path and the gas can therefore be treated as a continuous medium.

Further investigations include those of Atrazhev and Iakubov (1977; see also Khrapak and Yakubov 1979), O'Malley (1980), and many more. Especially successful in interpreting both positive and the negative pressure dependence in a wide range of gases was the theory of Braglia and Dallacasa (1978; 1982). These authors proposed a quantum mechanical theory of

electron motion through high density gas. The gas is not treated as a continuum and therefore their theory has an advantage over that of Legler for intermediate pressures. Further improvements to the theory along similar lines were made by numerous authors (Gryko and Popielawski 1979; Polischuk 1983 and especially Kirkpatrick and Dorfman 1983).

It is also worth mentioning that O'Malley (1983) has recently analysed the density dependence of the thermal value of D/μ in relation to the density dependence of μ^{th} . His work is of great importance for understanding the Nernst-Townsend (Einstein) relations.

The most interesting theoretical results relating to the present work are those that provide a means to extend the analysis of the pressure dependence to non-thermal electron mobilities. It was shown theoretically that as the field increases the mobility rapidly attains the low density value (which is pressure independent) (Atrazhev 1984). It has also been found that it is possible to modify the momentum transfer cross section in such a way that it gives a good representation of the pressure dependence of the electron mobility.

It might be thought that it would be possible to carry out measurements of drift velocities at different pressures and extrapolate the results to the value corresponding to zero pressure. However, the diffusion corrections for Ar are quite large even at such high pressures and it is not possible to apply theoretical values for the diffusion correction (see Section 2.4) without making significant errors. In order to eliminate the errors from this source one has to extrapolate the results obtained at different pressures to infinite pressure. Therefore it is necessary to estimate the pressure dependent correction due to multiple collisions by calculation in order to overcome the conflicting requirements for the

extrapolations.

The pressure dependence of the drift velocity can be estimated (Braglia 1984 - personal communication) by replacing the momentum transfer cross section σ_m with:

$$\sigma_m \rightarrow \frac{\sigma_m(\epsilon)}{1 - \frac{\lambda(\epsilon)}{\ell(\epsilon)}} \quad (12.4)$$

where $\lambda(\epsilon)$ is the deBroglie wavelength of the electron and $\ell(\epsilon)$ is the mean free path. If the ratio λ/ℓ is very small one obtains:

$$\sigma_m(\epsilon) = \sigma_m(\epsilon) \left(1 + 3.904 \cdot 10^{-24} N \sigma(\epsilon)/\sqrt{\epsilon} \right) . \quad (12.5)$$

Using equation (12.5) and the momentum transfer cross section of Haddad and O'Malley (1982) the drift velocities (at 90 K) were calculated with and without the correction for pressures in the range between 0 and 800 Torr (which was the highest pressure used by Robertson 1977). All the differences were smaller than 1%, i.e. smaller than the diffusion corrections at the lowest values of E/N. Therefore a correction procedure was adopted that is equivalent to correcting each experimental point for the effect of multiple collisions and then extrapolating the corrected points to infinite pressure to account for the effect of diffusion. In Table 12.1 the drift velocities in pure argon at 89.6 K (Robertson 1977) are displayed that were obtained with and without the corrections for the effects of multiple collisions. It can be seen that the maximum correction to the v_{dr} data at 89.6 K is at the lowest value of E/N (as expected) and is 1.24%. The corrections rapidly get smaller as the value of E/N increases and are negligible above 0.006 Td. The corrections to the room temperature v_{dr} and D_T/μ data are negligible (less than 0.1%).

12.3.3: Drift velocities in Ar-H₂ mixtures. To supplement the existing data in pure Ar, measurements of drift velocities were made in an Ar-H₂ mixture containing 5.45% of H₂. The basic reasons for using the Ar-H₂ mixture are the following:

1) In such a mixture it is possible to achieve an average electron energy which is of the order of 40 meV at pressures that are sufficiently low that multiple scattering effects are negligible (the present calculations indicate that for this mixture at 590 Torr and at the lowest value of E/N used the pressure effect on v_{dr} is 0.06%). As can be seen from Fig. 12.2 the average energy of the EDF for the Ar-H₂ mixture is much lower than that for pure Ar at the same E/N.

2) Hydrogen was chosen as the electron energy moderator because the very low energy cross sections for H₂ are known better than the cross sections for any other molecular gas (see Chapter 9). For the present application very accurate cross sections are required only for rotational excitation in order to analyze transport data for the mixture. At very low energies the momentum transfer cross sections for Ar and H₂ are similar in magnitude. Therefore an uncertainty of $\pm 5\%$ in σ_m^{SW} for H₂ results in negligible uncertainty in σ_m for the mixture, and therefore in the momentum transfer cross section for Ar derived from it.

3) The measurements in Ar-H₂ mixtures at 293 K and at moderately low values of E/N are easier than in pure Ar at 89.6 K (because they can be carried out using lower pressures and without the use of a coolant) while the diffusion corrections are smaller. Consequently the error bounds on the mixture data are expected to be smaller.

Table 12.1 Drift velocities in pure argon and the corresponding corrections for multiple scattering.

E/N	Original Data of Robertson V_{dr} (10^5 cm/s)	Pressure Correction (%)	Final Data V_{dr} (10^5 cm/s)	$\langle \epsilon \rangle$ calculated (meV)	D_T/μ (mV)
0.002	1.49	1.24	1.508	17	14
0.0025	2.04	1.18	2.064	24	30
0.003	2.86	1.18	2.894	40	68
0.0035	4.01	1.0	4.05	70	119
0.004	5.20	0.79	5.24	107	170
0.005	7.10	0.36	7.126	112	253
0.006	8.100	0.18	8.115	215	318
0.008	9.060	0	9.060	263	418
0.010	9.61	0	9.61	292	497
0.015	10.45			344	646
0.020	11.07			384	759
0.030	12.18			450	928
0.040	13.05			506	1056
0.050	13.82			558	1158
0.060	14.50			605	1245
0.080	15.69			693	1389
0.10	16.68			773	1510
0.12	17.56			845	1618
0.15	18.68			945	1763

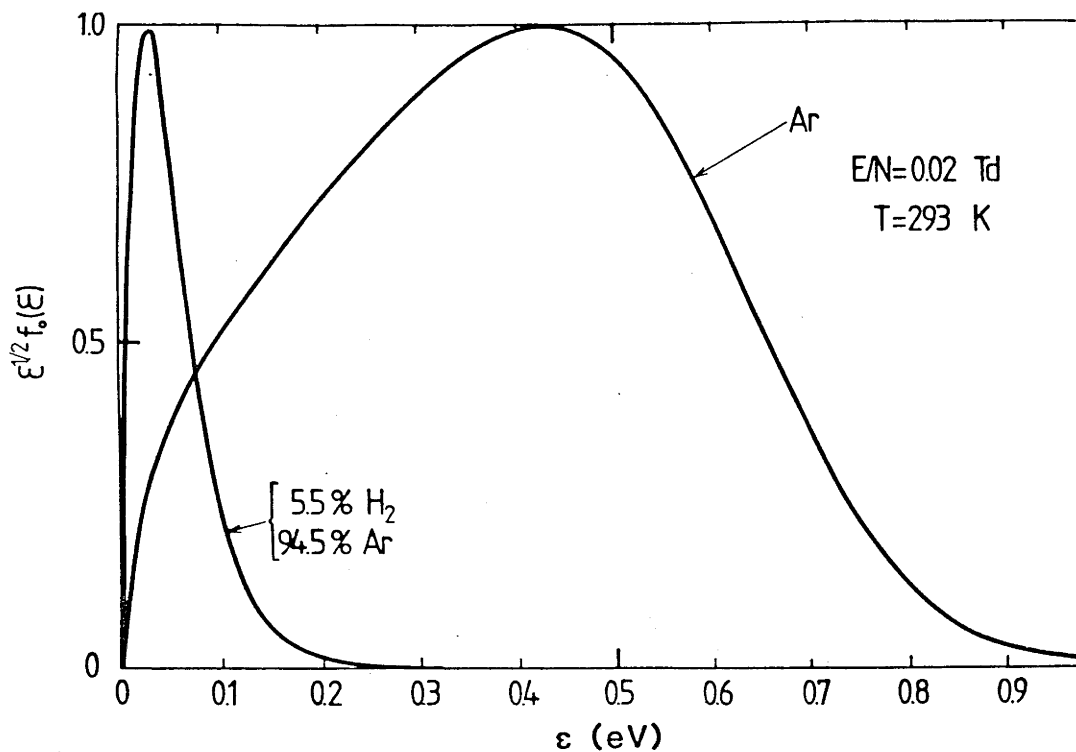


Figure 12.2 EDF in pure Ar and in the Ar-H₂ mixture for the same value of $E/N(=0.02$ Td).

The results obtained using the Bradbury-Nielsen drift tube (see Chapter 8) are shown in Table 12.2. The maximum diffusion correction was 0.4%, but normally it was of the order of 0.1-0.2%. The final results were obtained both by extrapolating the pressure dependence to infinite pressure and by calculating the diffusion correction with $C=5$ (see Section 8.2). Good agreement was found between these two methods for the present results. The estimated maximum error bounds are $\pm 1.5\%$ over the entire E/N range used in the present work.

E/N (Td)	(Calculated)		V_{dr} (10^5 cm s $^{-1}$)			Diffusion Correction $\frac{5D_T/\mu}{U}$	Pressure Dependence Extrapolated
	$\langle \epsilon \rangle$ (meV)	D_T/μ (mV)	77	68	53		
0.017	47	31	1.252	1.254		1.253	
0.020	50	33	1.489	1.489	1.488	1.489	1.490
0.025	55	36	1.895	1.895	1.895	1.895	1.895
0.030	61	40	2.308	2.308	2.308	2.308	2.308
0.035	68	45	2.723	2.723	2.722	2.722	2.726
0.040	75	50	3.131	3.131	3.133	3.131	3.133
0.050	90	60	3.911		3.910	3.912	3.908
0.060	106	72	4.606	4.610	4.605	4.608	4.604
0.070	123	84	5.201	5.206	5.202	5.203	5.200
0.080	139	97	5.697	5.698	5.697	5.697	5.696
0.10	170	123	6.445	6.442	6.445	6.444	6.446
0.12	197	149	6.956	6.959	6.960	6.958	6.958
0.14	221	174			7.336	7.334	
0.17	254	209			7.775	7.771	

Table 12.2 Measured drift velocities in the Ar-H₂ mixture. Also shown are the average energies calculated using σ_m^{sw} .

12.4: Analysis

12.4.1: Introduction. In the present work several cross sections were used to calculate the transport coefficients and these results were then compared to experimental results. The aim was first to check the compatibility of some recently derived cross sections with the transport data and second to establish the limits of accuracy of the swarm-derived scattering length.

12.4.2: Method of calculation. The standard two-term code was used in the present work. Multiterm calculations were carried out for the Ar-H₂ mixture and it was shown that the corrections to the TTT results did not exceed 0.1%. Various multi-term and Monte Carlo calculations for pure argon (see Lin et al 1979; Makabe and Mori 1982 and many more) have led to the conclusion that the TTT is accurate for argon. However, several problems need to be examined or overcome when the transport coefficients for argon are to be calculated even with a highly accurate theory.

The inadequacy of the definition of the diffusion coefficient as discussed in Section 2.5 does not affect the present analysis. Makabe and Mori (1984) calculated the difference between ND_T and ND_V (see Section 2.5 for definitions). At the highest values of E/N used in the present work the difference is of the order of 1% - still within the experimental uncertainty. Since the situation regarding the inadequacy of the TTT formula for ND_T is still uncertain, no corrections for this effect were applied. Had they been applied the corrections would have only affected a few values of D_T/μ at the highest E/N and not the data that are important for determining the scattering length.

In the work of Haddad and O'Malley (1982), a two term-code was used that was developed by O'Malley (O'Malley and Crompton 1980) to analyse electron transport in neon. This code has a logarithmic rather than a linear energy mesh, that is, each step in the mesh is obtained by multiplying the preceding step by a constant (>1) and therefore the step size increases with increasing energy. The reason for adopting such a procedure is to have a small step size close to zero energy but not to have a correspondingly large number of points over the entire energy range. (As an example, for $E/N=0.002$ and an integration range of 0.28 eV, if the first energy step is 0.06 meV only 50-70 logarithmic steps are used over the entire energy range.) If a large number of points is used the computer time necessary to perform the calculations becomes long and it would make the automatic fitting procedure very slow. However, this approach was thought to be inadequate for argon at the lowest values of E/N because the energy steps in the range of the RTM, where σ_m changes rapidly, would be relatively large. In the present work, therefore, a standard two-term code with equal energy steps was used. The number of steps was increased initially to 6000 so that the same energy resolution was achieved at low energies as in the work of Haddad and O'Malley but at the upper end of the integration range the energy resolution was equally high. The maximum difference between the results obtained using the two codes was significant (although less than 1%) and occurred at 0.005 Td where there is a significant number of electrons in the swarm in the RTM.

Although 6000 points are needed to have the same energy resolution as Haddad and O'Malley at their lowest energy it was found that when the number of points was reduced to 2500 the calculated results were still in excellent agreement with the data calculated with the larger number of

points.

In addition to making a careful choice of the mesh size one had to be careful to ensure that the energy integration range was not too large and that the EDF did not become smaller than the smallest number available on the computer. In that case any extension of the integration range resulted in an unnecessary loss of energy resolution for a given number of mesh points. The "rule of thumb" adopted for most gases is to choose an energy range of approximately $10eD_T/\mu$. However, one needs to be careful when calculations in Ar are being made. The value of eD_T/μ in Ar is not normally smaller than $\langle \epsilon \rangle$ contrary to the situation in most other gases. Moreover, in Ar the EDF does not extend to very high energies as can be expected for other atomic gases. On the contrary the EDF decreases very rapidly at higher energies due to a sudden increase of σ_m above the RTM. Therefore the integration ranges should sometimes be as low as $3eD_T/\mu$.

In the present work the integration ranges were chosen so that the ratio of the EDF at zero energy to its value at the end of the energy range was not less than 10^{-25} . For the E/N values where the EDF extends to relatively high energies as compared to the value of $\langle \epsilon \rangle$ (i.e. the lowest few values of E/N) the decision about the integration range was made by varying the range and checking whether the results changed. During these tests the energy resolution, that is the mesh size, was kept fixed.

Another important point in relation to the argon calculations is that it is sometimes not adequate to use the tabulated values of the cross sections and then to interpolate linearly between the points. Even when over 40 points were used to tabulate σ_m below 1 eV a difference of up to 0.7% in the transport coefficients was observed between the calculations that used the analytical formula (MERT) for the cross section and those

that used the tabulated data. When the more sparsely tabulated data of McEachran and Stauffer (1983) were used the errors in the calculated transport coefficients due to linear interpolation of the cross section were up to 10%. This example illustrates the importance of having a large number of tabulated points for σ_m or preferably an analytical expression.

In the present analysis the MERT formulae were used to calculate η_0 and η_1 , and the Born formula to calculate η_2 and η_3 . The formula derived by Thompson (1966) was used to determine the contribution of the higher-order phase shifts to σ_m . The cross section obtained using this formula was compared with that obtained when the first 20 higher-order phase shifts were calculated using the Born formula (Buckman - personal communication). It was found that the contribution of the higher order phase shifts was very small and therefore that the method of calculation using the Thompson formula was adequate. The maximum relative contribution of the higher order phase shifts is in the region of the RTM. Table 12.3 shows the errors that are made when the contribution from η_3 , and from higher order phase shifts calculated using the Thompson's formula, are neglected.

Table 12.3 Errors in the calculated cross section when higher order phaseshifts are neglected.

ϵ (eV)	error in the cross section in (%) when the series expansion for σ_m is limited to terms containing the phase shift differences shown	
	$\eta_0 - \eta_1, \eta_1 - \eta_2, \eta_2 - \eta_3$	$\eta_0 - \eta_1, \eta_1 - \eta_2$
0.20	0.9	9.0
0.23	1.26	12.7
0.25	1.3	13.1
0.30	1.0	9.9
1.00	0.33	3.1

From Table 12.3 it can be seen that the accuracy of the calculation of the phase shifts above η_2 is not critical, but they have to be represented. The phase shifts η_2 calculated using the Born formula are in good agreement with the results of McEachran and Stauffer (1983) in the region of the RTM (at 0.136 and 0.544 eV, two of the energies for which the theoretical data are tabulated, the difference are 1.6 and 4.8% respectively). The resulting errors in the calculated differences $\eta_1 - \eta_2$ and $\eta_2 - \eta_3$ are small in the region where some uncertainty in η_2 could cause significant uncertainty of the calculated σ_m because $\eta_0 - \eta_1$ is close to zero. Therefore it may be concluded that the difference between the higher order phase shifts used in the present work and the theoretical values, or the values derived from beam experiments, are unimportant for the accuracy of the calculated σ_m .

If some objections are raised to the use of the MERT formula in the swarm analysis it can be countered by saying that it is simply used as a convenient representation of the momentum transfer cross section and that the cross section is no less accurate because of a possible inadequacy of MERT. However, although σ_m may be sufficiently accurately represented it does not follow that the phase shifts are sufficiently accurate to calculate differential and total cross sections with adequate accuracy. In situations where MERT breaks down valid comparisons of experimental cross sections with those calculated with these phase shifts are clearly not possible.

12.4.3: Comparison of cross sections. Three sets of cross sections were initially chosen for the comparisons: σ_m^{WBL} obtained from the MERT fit to the crossed beam data of Weyhreter et al. (1984), σ_m^{F} obtained from the MERT fit to the total cross section of Ferch et al. (1984), and the

theoretical results σ_m^{MS} obtained by McEachran and Stauffer (1983).

MERT parameters obtained by Weyhreter et al. (1984) and Ferch et al. (1984) were used in the energy range suggested by the authors, which in both cases included the RTM and the low energy part of the cross section (which is especially important for the present analysis). Above ϵ_{max} for MERT the swarm-derived tabulated cross section was used. The theoretical results were used over the entire energy range needed for the calculations. Because of the insufficient number of the available theoretical points the data of McEachran and Stauffer (1983) were fitted using the MERT formulae (only their scattering length $A = -1.506$, corresponding to their zero energy limit of n_0/k was retained). The following MERT parameters were obtained: $D=69.71$; $F=-97.94$ and $\epsilon_1=0.9338$. Using these parameters values of σ_m and σ_T could be recovered that were not more than 2.5% different from the original values; normally the difference was much smaller. The energy range for the MERT fit was 0 - 1 eV.

Calculations were also carried out using a MERT fit to the recently published theoretical data of Bell et al. (1984). MERT fits were made to both the total and momentum transfer cross sections. However, because only a limited number of data were available below 1 eV the accuracy of the fits was reduced. Similar MERT parameters were obtained from fitting to each cross section ($A=-1.676$, $D=63.81$, $F=-74.25$ and $\epsilon_1=1.1605$). It was not possible to obtain additional values of the cross sections from the authors in order to perform a more reliable MERT fit and therefore the results for this cross section and the comparison with the swarm data should be regarded just as an indication rather than a final comparison.

In addition to the comparisons described above others were carried out using the MERT parameters derived by Haddad and O'Malley (1982) and also

with some modifications to their results. The modifications were made by changing A by 1 or 2% and then adjusting the other MERT parameters to achieve the best possible agreement between the calculated and experimental transport data.

The results of all the comparisons are shown in Fig. 12.3, Fig. 12.4 and Fig. 12.5.

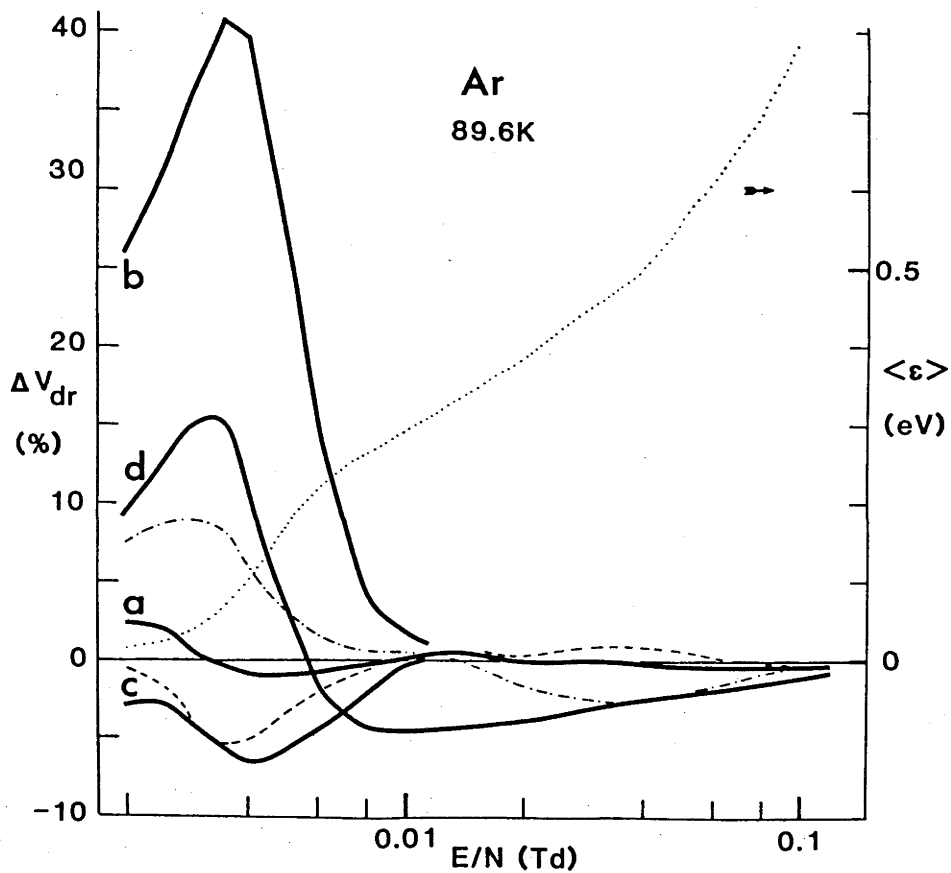


Figure 12.3 Differences between the calculated and experimental drift velocities in Ar at 89.6 K. The cross sections used in the calculations are : a) Haddad and O'Malley; b) Weyhreter et al.; c) Ferch et al.; d) McEachran and Stauffer. The dashed line corresponds to a scattering length reduction of 1% and the dot-dashed line to an increase of 2%. The values of the average energy are also shown as a (dotted line).

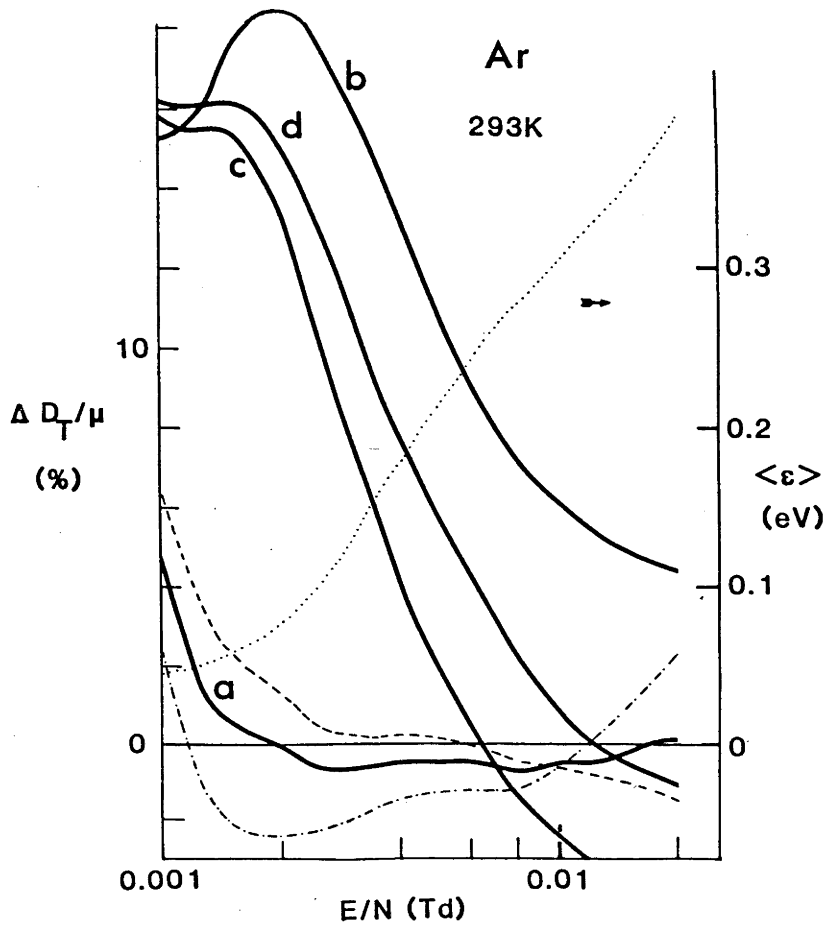


Figure 12.4 Differences between the calculated and experimental D_T/μ values in Ar at 293 K. The cross sections used in calculations are : a) Haddad and O'Malley; b) Weyhreter et al.; c) Ferch et al.; d) McEachran and Stauffer. The dashed line corresponds to scattering length reduction of 2% and the dot-dashed line to an increase of 2%. The values of the average energy are also shown.

First the cross section of Weyhreter et al. will be discussed. At the lowest values of E/N the calculated transport coefficients are significantly different from the experimental data. In all cases the disagreement is more than ten times the claimed error bounds. It is therefore evident that the scattering length derived by Weyhreter et al. is

too large. This can be checked by keeping A fixed and by varying all other parameters. It is not possible to achieve a major improvement of the fit by that procedure. The fit apparently improves with increasing E/N in all cases. However, this is because the swarm-derived σ_m was used above ϵ_{\max} and therefore the improved agreement is misleading (the same is true for the comparison using the cross section of Ferch et al.).

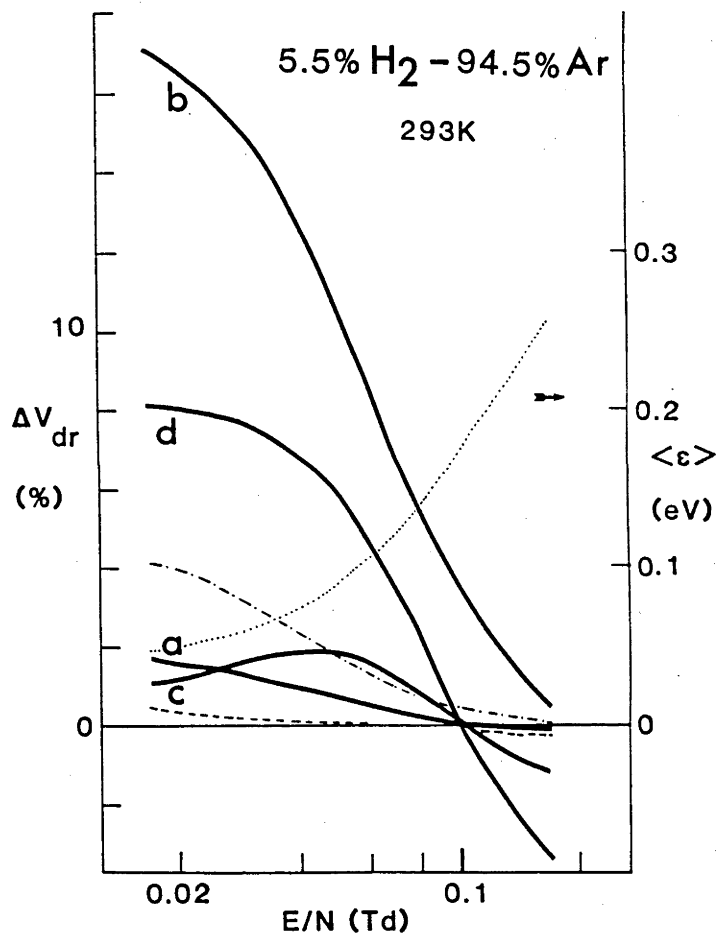


Figure 12.5 Differences between the calculated and experimental drift velocities in the Ar-H₂ mixture. The cross sections used in the calculations are : a) Haddad and O'Malley; b) Weyhreter et al.; c) Ferch et al.; d) McEachran and Stauffer. The dashed line corresponds to a scattering length reduction of 1% and the dot-dashed line to an increase of 2%. The values of the average energy are also shown.

The results calculated using the MERT parameters of Ferch et al. (1984) are in good agreement with the experimental data for drift velocities. At some values of E/N the results lie outside the error bounds, but not by very much. The difference between the calculated D_T/μ values and the experimental data, which is not seen in the v_{dr} data, is due to the fact that D_T/μ values are more sensitive to the position and the shape of the RTM than v_{dr} values (Milloy and Crompton 1977b) and indicates that there is still some incompatibility between the beam-derived σ_m and the experimental transport data. This could reflect inadequacy of the MERT analysis as described above. However, the scattering length obtained by Ferch et al. is in good agreement with the result of Haddad and O'Malley.

Even though McEachran and Stauffer (1983) provided a large number of calculated values of the cross section below 1 eV in addition to the values published in their paper, the tabulation below 1 eV was still insufficiently dense to minimize the interpolation errors (see Section 12.4.2). Therefore their data were fitted using MERT as discussed in this section. The results presented in the figures were obtained using MERT up to 1 eV and the tabulated values of σ_m above 1 eV.

The error due to interpolation was estimated and subtracted when the calculations were performed using the tabulated values over the entire energy range. Both procedures led to similar results.

Even though the scattering length obtained by McEachran and Stauffer (1983) is in agreement with the value obtained by Haddad and O'Malley (1982) other parameters and consequently the position of the RTM are different. Therefore the calculated transport coefficients are sometimes in significant disagreement with the experimental data.

The transport coefficients calculated using the MERT fit to the theoretical results of Bell et al. are not presented in the figures. Of all the cross sections used in these comparisons, this cross section leads to poorest agreement with the experimental swarm data. The maximum differences are: 55% for v_{dr} (90 K) data, 45% for the D_T/μ data, and 27% for the mixture data. The results show that the cross section is too large.

The results calculated using the MERT parameters obtained by Haddad and O'Malley agree best with the presently available data including the newly measured drift velocities for the H₂-Ar mixture and could not be improved upon. This is because the inaccuracy in the calculations using the logarithmic energy steps, as implemented in the code used by these authors (see Section 12.4.2), was partially compensated by the corrections for multiple collisions. For all the data except the lowest E/N results for D_T/μ the agreement with experimental transport data for pure Ar is within the error bounds. For the mixture data the calculated values lie outside the error bounds only for the two lowest E/N values, and then not by much. The best agreement for the mixture data is achieved when A is reduced by 1%, but in that case the calculated drift velocities in pure Ar are 1% outside the error bounds. Therefore it was decided not to adjust the MERT parameters of Haddad and O'Malley but to suggest the following error bounds for the scattering length namely +0.5 and -1.5%.

12.5: Conclusion

None of the cross sections used in the present analysis apart from that of Haddad and O'Malley (1982) is consistent with the transport data. Two

of the cross sections predict scattering lengths that are just outside the presently derived error bounds for the swarm-derived scattering length, but in these cases other features of the cross sections give rise to the differences between the calculated and the experimental transport data.

A virtue of the swarm technique is that absolute values of cross sections can be derived very accurately. On the other hand it is hard to analyse cross sections with sharply changing features, and the RTM is such a feature. It has been suggested (Crompton 1984a) that a combination of the swarm-derived scattering length with the data from crossed beam experiments (both differential and total cross sections) should provide the most reliable cross section for low energy electron scattering in Ar. The beam data may require normalization of both the energy scale and the absolute magnitude. The present analysis is the first step in that direction.

Despite differences that remain, it can be concluded that the agreement between the swarm-derived, beam-derived, and theoretical cross sections is now much better than three years ago. The results of the comparisons reported in this chapter should be regarded as encouraging, even though the remaining discrepancies are still outside the limits claimed for the swarm analysis.

Finally a comment should be made about some recent studies of electron thermalization in pure Ar. McMahon and Shizgal (1985) found that the cross section of Haddad and O'Malley (1982), if used in their analysis, gives rise to thermalization times that are in disagreement with some of the experimental data (see Appendix 2) and that the cross section of Mozumder (1981) was superior. Their most striking prediction based on the cross section of Haddad and O'Malley is that the mobility may become

significantly negative for a short period of time, which has not been observed experimentally. However, it is not certain which part of the cross section is responsible for the predicted occurrence of this effect; moreover the accuracy of the thermalization data is not as high as the accuracy of the experimentally derived transport data. Therefore no attempt has been made to include the thermalization data in the present analysis.

Appendix 1: Requirements for the Computer-Interface System for
Controlling the CDE

The original computer controlled system, that was used for some of the present measurements was based on the DEC PDP 8/e computer connected to a specialized interface. However, since the system was designed and built before 1973, there were a number of restrictions on the usage of the system due to limitations in the technology that was used both in the PDP 8/e and in the interface. The most undesirable restrictions for the operation of the CDE were:

1) a limited range of S and D values, especially at the higher end ($S+D < 2$ ms) which, for instance, made the measurements in pure H₂O impossible;

2) difficulties in modifying, storing and retrieving programs; the programs were written using assembler and stored on cassettes, and modifications had to be written in the computer memory using the keyboard with hexadecimal numbers;

3) the small memory of the computer, which limited optional calculations and also made it impossible to start a number runs with different parameters without intervention of the operator;

4) the loss of the collected data and parameters for a run if the system "crashes" ;

5) inconvenient input/output, and impossibility to have the current status of the experiment displayed.

Nevertheless the old system proved to be very reliable and has been operating continuously for more than ten years.

The new controller was built to overcome all the restrictions mentioned

above and to extend the possibilities of the experiment even further. The controller is "a disk based STD BUS microcomputer running the CP/M operating system" (Cullen 1985). The system as presently configured is shown in Fig. A.1.1.

The controller is used to perform the following tasks:

1) to input/output the parameters for the run from the terminal or from the disk;

2) to execute a shot (see Chapter 4) by triggering the X-ray tube, by setting the sampling amplitude, and by triggering the sampling pulse at appropriate times (at S, with and without the X-ray pulse and at S+D with and without the X-ray pulse);

3) to digitize the analogue signal amplitude and to store the value at the appropriate memory location;

4) to control the time between the two pulses (the repetition time);

5) to control the number of shots and to group the collected data into experiments and runs;

6) to carry out the calculations for the continuously updated display (current status) of the time constant (for the current experiment), and to display the levels of the signal at times S and S+D (with or without the subtraction of the noise pulse) together with the standard deviations of the signal amplitudes up to that point, to calculate the remaining number of shots, and the time required to complete the experiment (run, series);

7) to carry out calculations of the time constant for each experiment and to store the number of shots having signal amplitudes that were below or above the range of the linear response of the detection chain and therefore not included in the calculations;

8) to carry out the calculations of the average time constant for the

run and of its standard deviation;

9) to store the data on the disk after certain time intervals in order to protect the data against system "crashes";

10) to edit, recall, rename, print out, display and update the files from the disk and to give the directory of the disk without exiting the main program;

11) to adjust the sampling amplitude from the keyboard while the experiment is running;

12) to stop, continue or terminate the experiment;

The program that, in conjunction with the interface carries out the tasks mentioned above was written in Pascal MT⁺ by Cullen (1985). It is a menu driven program that uses an overlay technique.

The new system also provides facilities to test the linearity of the detection chain, to apply clearing pulses (if the metal sampling pulse electrodes are located inside the cell) and to connect two additional analog signals for continuous monitoring, AD conversion, storing, and use in further calculations. In order to use the third facility the software would need to be extended. The additional acquisitions would be used if for example the variations of the temperature were to be monitored or if the RF heating were applied and the stability of the field needed to be monitored and its variations accounted for. In addition it is possible to make further calculations with the data that are stored in the computer memory or to include some other parameters in the analysis of the raw experimental data. The system could be upgraded by additions to the software to satisfy most of the requirements that may be made in the future.

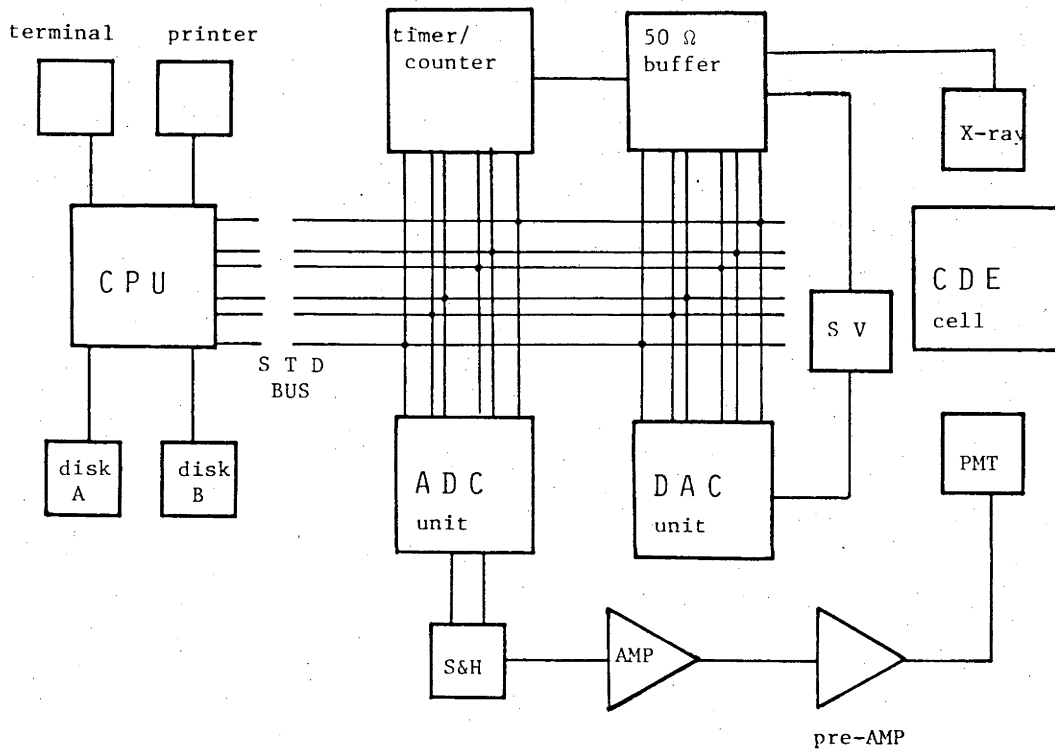


Figure A.1.1 The new computer controlled system as connected to the CDE. CPU - the central processing unit, AMP - amplifier and shaper, ADC - analog to digital conversion unit, DAC - digital to analog conversion unit, PMT - photo-multiplier tube, S&H - sample and hold circuit.

Appendix 2: Electron Thermalization

The Electron thermalization time τ_{th} is usually defined as the time it takes electrons, starting from some energy well above thermal, to reach the energy 10% above thermal energy and is an important parameter for the application of the CDE technique. It is important to check the value of τ_{th} for every gas that is being used in the CDE because electrons in that experiment are formed by X-rays that have an energy of the order of 20 keV and are therefore capable of producing high energy electrons which in turn produce many electrons with energies of the order of 20 eV (Rhymes 1976).

The sampling of the number of electrons in the CDE should only start when all the electrons have reached thermal equilibrium with the gas. The relaxation of electron energy to about 1 eV is very fast and therefore the most of the thermalization time is taken up by the slow approach of the energy from about 1 eV to the thermal energy.

Information about thermalization times can be obtained from the swarm data (Christophorou et al. 1975; Rhymes 1976), by direct calculations (Mozumder 1980; 1982; Tembe and Mozumder 1983; Shizgal and McMahon 1984; McMahon and Shizgal 1985), by Monte Carlo Simulations (Koura 1983; 1984), and by measurements (e.g. Dean et al. 1974; Dean and Smith 1975; Warman and Sauer 1975; Warman and deHaas 1975). Rigorous analysis based on the moment method for solving BE was carried out by Knierim et al. (1982) for two model gases (constant collision frequency and constant cross section) and it was found that the approximate theory of Mozumder was less than 25% in error for the two cases studied. Such an accuracy is sufficient for the present purpose.

Table A.2.1 contains thermalization times for electrons in gases that

were either used or considered to be used in the present work with the CDE. Instead of the usual presentation of the results as N_{1th} or as τ_{th} at 1 Torr the results are presented as τ_{th} at 1 kPa.

Table A.2.1 Thermalization times for electrons in various gases at 1 kPa and 300 K.

τ_{th} (μs)							
gas	a	b	c	d	e	f	g
N ₂			1.5	1.4		2.7	1.0
H ₂	0.2		0.3	0.45			0.2
CO ₂					0.01		0.04
H ₂ O					0.004		
He	4.0	7.4	5.3				3.5
Ne	160	400	210			50	90
Ar	1600	740	400			50	170
Kr		240	150			13	
Xe		200	90				

a Rhymes (1976)

b Shizgal and McMahon (1984)

c Mozumder (1980; 1981) and Tembe and Mozumder (1983)

d Koura (1983; 1984)

e Christophorou et al. (1975)

f Dean et al. (1974) and Smith and Dean (1975)

g Warman and Sauer (1975) and Warman and deHaas (1975)

Appendix 3: The Experimental Data used in the Analysis to Determine the Cross Sections in Hydrogen

Table A.3.1 Transport data for parahydrogen at 77 K

E/N (Td)	v_{dr} (10^5 cm/s)	D_T/μ (mV)
0.002		6.83 ^{b)}
0.0025		6.89
0.0030		6.95
0.0035		6.99
0.004		7.05
0.005		7.16
0.006		7.30
0.007		7.45
0.008	0.274 ^{a)}	7.61
0.010	0.330	7.95
0.012	0.384	8.30
0.014	0.437	8.66
0.017	0.511	9.24
0.020	0.579	9.83
0.025	0.682	10.68
0.030	0.779	11.48
0.035	0.871	12.23
0.040	0.959	12.90
0.050	1.131	14.10
0.060	1.296	15.07
0.070	1.457	15.93
0.080	1.614	16.73
0.100	1.913	18.14
0.12	2.20	19.41
0.14	2.46	20.60
0.17	2.83	22.5
0.20	3.17	24.3
0.25	3.67	27.3

0.30	4.11	30.3
0.35	4.51	33.3
0.40	4.85	36.4
0.50	5.42	42.8
0.60	5.89	49.6
0.70	6.29	56.5
0.80	6.62	63.8
1.00	7.15	78.6
1.20	7.56	93.5
1.40	7.93	107.7
1.70	8.45	131.8
2.00	8.93	153.9
2.50	9.68	189.1
3.00	10.39	220
3.50	11.07	250
4.00	11.73	276
5.00	13.03	323
6.00	14.30	365
7.00	15.52	
8.00	16.70	
10.00	18.90	
12	20.90	
14	22.80	
17	25.60	
20	28.10	
25	32.20	
26	33.10	
27.3	34.20	
30	36.60	

a) Robertson (1971)

b) Crompton and McIntosh (1968)

Table A.3.2 Transport data for normal hydrogen at 77 K

E/N (Td)	v_{dr} (10^5 cm/s)	D_T/μ (mV)	E/N (Td)	v_{dr} (10^5 cm/s)	D_T/μ (mV)
0.002		6.76 ^{b)}	0.30	3.61	36.4
0.0025		6.81	0.35	3.97	39.8
0.003		6.85	0.4	4.29	43.3
0.0035		6.90	0.5	4.86	50.2
0.004		6.96	0.6	5.33	57.2
0.005		7.09	0.7	5.75	64.2
0.006		7.23	0.8	6.11	71.3
0.007		7.38	1.0	6.71	86.0
0.008	0.274 ^{a)}	7.55	1.2	7.21	100.8
0.010	0.328	7.90	1.4	7.64	115.7
0.012	0.382	8.27	1.7	8.20	138.0
0.014	0.433	8.67	2.0	8.70	159.5
0.017	0.504	9.26	2.5	9.48	192.9
0.020	0.568	9.86	3.0	10.21	224
0.025	0.666	10.84	3.5	10.92	252
0.030	0.757	11.79	4	11.60	278
0.035	0.843	12.68	5	11.92	325
0.040	0.922	13.53	6	14.20	366
0.05	1.070	15.08	7	15.43	405
0.06	1.213	16.49	8	16.60	440
0.07	1.347	17.77	10	18.80	506
0.08	1.478	18.93	12	20.9	565
0.1	1.725	21.0	14	22.8	
0.12	1.958	22.9	17	25.5	
0.14	2.18	24.7	20	28.1	
0.17	2.49	27.0	25	32.2	
0.20	2.78	29.4			
0.25	3.21	32.9			

a) Robertson (1971)

b) Crompton and McIntosh (1968)

Table A.3.3 Transport data for normal hydrogen at 293 K.

E/N(Td)	$v_{dr}(10^5\text{cm/s})$	$D_T/\mu(\text{mV})$	E/N(Td)	$v_{dr}(10^5\text{cm/s})$	$D_T/\mu(\text{mV})$
0.012	0.1862 ^{a)}		1.4	7.20	124.8
0.014	0.217		1.7	7.82	146.5
0.017	0.264		2.0	8.37	167.6
0.020	0.311	25.9 ^{b)}	2.5	9.22	201
0.025	0.385	26.2	3.0	10.01	231
0.03	0.459	26.5	3.5	10.76	259
0.035	0.530	26.8	4.0	11.47	284
0.04	0.600	27.1	5.0	12.85	330
0.05	0.737	27.8	6.0	14.15	371
0.06	0.870	28.5	7.0	15.35	410
0.07	0.998	29.2	8.0	16.50	446
0.08	1.124	30.0	10.0	18.70	511
0.10	1.366	31.4	12.0	20.70	573
0.12	1.578	32.9	14.0	22.7	630
0.14	1.777	34.4	17.0	25.5	710
0.17	2.07	36.6	20	28.1	787
0.20	2.35	38.7	25	32.2	916
0.25	2.76	42.3	30	36.6	1051
0.30	3.13	45.7	35	40.7	1199
0.35	3.47	49.0	40	45.3	1374
0.40	3.78	52.4	50	57.0	1714
0.50	4.33	59.3	60	69.5	1983
0.60	4.82	66.3	70	82.9	2190
0.70	5.24	73.6	80	98.2	2370
0.80	5.60	80.9	100	128.0	2670
1.0	6.23	95.3	120	165.9	2930
1.2	6.74	110.2	140	194.7	3190

a) Robertson (1971)

b) Crompton and McIntosh (1968)

Table A.3.4 Transport data for the mixture of 0.5% H₂ in Ar at 293 K.

E/N (Td)	v_{dr} (10^5 cm sec ⁻¹)	D_T/μ (V)
0.005		0.0346 ^{c)}
0.006		0.0390
0.007		0.0446
0.008		0.0512
0.010	1.9 ^{c)}	0.0667
0.012	2.4	0.0844
0.014	2.8	0.103
0.017	3.34	0.133
0.020	3.62	0.162
0.025	3.87	0.211
0.030	3.96	0.256
0.035	4.01	0.299
0.04	4.03	0.338
0.05	4.06	0.411
0.06	4.11	0.473
0.07	4.18	0.528
0.08	4.24	0.579
0.10	4.37	0.667
0.12	4.50	0.741
0.14	4.62	0.807
0.17	4.80	0.894
0.20	4.97	0.969
0.25	5.23	1.077
0.30	5.46	1.172
0.35	5.66	1.252
0.40	5.9	1.325
0.50	6.2	1.464

c) Haddad and Crompton (1980)

Table A.3.5 Transport data for the mixture of 4% H₂ in Ar at 293 K.

E/N (Td)	v_{dr} (10^5 cm sec ⁻¹)	D_T/μ (V)
0.012		0.0300 ^{c)}
0.014		0.0315
0.017		0.0339
0.020	1.72 ^{c)}	0.0368
0.025	2.23	0.0421
0.03	2.74	0.0484
0.035	3.26	0.0552
0.04	3.75	0.0627
0.05	4.63	0.0788
0.06	5.33	0.0964
0.07	5.88	0.114
0.08	6.29	0.132
0.10	6.85	0.168
0.12	7.22	0.201
0.14	7.50	0.233
0.17	7.85	0.276
0.20	8.15	0.315
0.25	8.61	0.373
0.30	9.02	0.424
0.35	9.41	0.470
0.40	9.77	
0.50	10.5	
0.60	11.0	
0.70	11.6	
0.80	12.1	
1.00	13.0	

c) Haddad and Crompton (1980)

Appendix 4: Scaling Factors for Rotational Cross Sections

In this Appendix the formulae used to scale the rotational cross sections for H₂ and for D₂ will be summarized. Here it is assumed that the cross section for a certain transition J to J' is known and it is required to determine the cross section for another transition with the same ΔJ but different J. The procedure and the relevant references were published in greater detail by Morrison (1979). The theoretical basis for the formulae is the so called "adiabatic nuclear rotation theory". The main assumption inherent in this approximate theory is that the duration of the electron - molecule collision is short compared to the period of nuclear rotation. Consequently close to the threshold and near the resonance this approach is expected to be inadequate. The extent of the failure near threshold for H₂ was illustrated by the theoretical calculations of Morrison and coworkers (Morrison et al. 1984b).

The ratio of the cross sections for transitions J₁ → J₁' and J₂ → J₂' with ΔJ = 2 (quadrupole transitions) derived on the basis of the adiabatic nuclear rotation theory is:

$$\frac{\sigma_{\text{rot}}(J_2 \rightarrow J_2')}{\sigma_{\text{rot}}(J_1 \rightarrow J_1')} = R(J_1, J_1'; J_2, J_2') = \left(\frac{\epsilon - \epsilon_{T_2}}{\epsilon - \epsilon_{T_1}} \right)^{1/2} \left[\frac{C(J_2, 2J_2'; 000)}{C(J_1, 2J_1'; 000)} \right]^2 \quad (\text{A.4.1})$$

where ϵ_{T_l} is the threshold energy for the transition $l \rightarrow l+2$ and $C(\dots)$ are Clebsch-Gordan coefficients. For the excitations $J \rightarrow J+2$ the ratio is:

$$R(J_1, J_1+2; J_2, J_2+2) = \left(\frac{\epsilon - \epsilon_{T_2}}{\epsilon - \epsilon_{T_1}} \right)^{1/2} \frac{(J_2+2)(J_2+1)(2J_1+1)(2J_1+3)}{(J_1+2)(J_1+1)(2J_2+1)(2J_2+3)} \quad (\text{A.4.2})$$

and for the deexcitations $J \rightarrow J-2$:

$$R(J_1, J_1-2; J_2, J_2-2) = \left(\frac{\varepsilon - \varepsilon_{T_2}}{\varepsilon - \varepsilon_{T_1}} \right)^{1/2} \frac{J_2(J_2-1)(2J_1+1)(2J_1-1)}{J_1(J_1-1)(2J_2+1)(2J_2-1)} \quad (\text{A.4.3})$$

In the second case the principle of detailed balancing has been used to determine the cross section for the superelastic process from the inelastic cross section.

Appendix 5: Energy Losses in Rotationally Inelastic Vibrational
Transitions

The difference between the term values for the two different levels 1 and 2 is (in this appendix the notation of Herzberg 1950 will be followed):

$$\Delta T^{12} = \Delta T_{\text{vib}} + \Delta T_{\text{rot}} + \dots \quad (\text{A.5.1})$$

The difference due to rotational levels only is :

$$\begin{aligned} \Delta T_{\text{rot}} = & [B_e - \alpha_e (v_1 + 1/2)] J_1(J_1+1) \\ & - [B_e - \alpha_e (v_2 + 1/2)] J_2(J_2+1) . \end{aligned} \quad (\text{A.5.2})$$

a) For quadrupole transitions $\Delta J=2$ from an arbitrary rotational level J_1 ($J_2=J_1+2$) accompanied by an arbitrary vibrational transition $\Delta v (=v_2 - v_1)$:

$$\begin{aligned} \Delta T_{\text{rot}} = & [B_e - \alpha_e (v_1 + 1/2)] (4J_1 + 6) \\ & + \alpha_e \Delta v (J_1^2 + 5J_1 + 6) . \end{aligned} \quad (\text{A.5.3})$$

Data for hydrogen for B_e and α_e , taken from Herzberg (1950), are:

$$\begin{aligned} B_e &= 60.80 \text{ cm}^{-1} \\ \alpha_e &= 2.993 \text{ cm}^{-1} . \end{aligned}$$

=====

It follows that, for

$$J_1 = 0 \quad v_1 = 0 \quad \Delta v = 1$$

the energy difference due to rotational transition is

$$\Delta \epsilon_{\text{rot}} = 46 \text{ meV} \quad (\Delta \epsilon_{\text{vib}} = 516 \text{ meV})$$

and for

$$J_1 = 1 \quad v_1 = 0 \quad \Delta v = 1$$

$$\Delta \epsilon_{\text{rot}} = 77 \text{ meV}$$

b) For quadrupole transitions $\Delta J = 0$ with arbitrary rotational level J_1 (i.e. $J_1 = J_2$) and arbitrary vibrational transition $\Delta v (=v_2 - v_1)$:

$$\Delta T_{\text{rot}} = \alpha_e \Delta v J_1 (J_1 + 1) ;$$

=====

$$\text{for } J_1 = 0 \quad \Delta \epsilon = 0$$

$$\text{and for } J_1 = 1 \quad \Delta v = 1 \quad \Delta \epsilon = 0.7 \text{ meV.}$$

Appendix 6: Populations of the Rotationally Excited Levels in
Molecules

In the analysis of the molecular gases it is important to specify the populations of the rotationally excited levels because the cross sections for various rotational transitions are quite different, and therefore cannot be summed to give a single effective cross section that could be used at different temperatures or compared to other sources of data. Therefore in the present work the rotational cross sections were treated separately and were weighted by the number representing the abundance of the lower rotational level in the transition at the given temperature.

The abundance of the level J is given by:

$$\frac{N_J}{N} = \frac{p_J \exp(-\epsilon_J/kT)}{\sum_{J=0}^{\infty} p_J \exp(-\epsilon_J/kT)} \quad (\text{A.6.1})$$

where ϵ_J is the energy of the rotational level J and:

$$p_J = (2I + 1) (I+a) (2J+1) \quad . \quad (\text{A.6.2})$$

In (A.6.2) I is the nuclear spin, and $a = 0$ when J is even and 1 when J is odd for some molecules like H_2 and O_2 , while $a = 1$ when J is even and 0 when J is odd for other molecules like D_2 , N_2 and O_2 (see Gilardini 1972; Huxley and Crompton 1974). Hydrogen and deuterium have ortho- and para-molecules. Under normal conditions the ratio of the para- to ortho- states for normal hydrogen is 1:3 while for deuterium the ratio is 2:1. Therefore for hydrogen ($I=1/2$):

$$p_J = 2J + 1 \quad (\text{for } J \text{ even})$$

$$p_J = 3(2J + 1) \quad (\text{for } J \text{ odd}) \quad (\text{A.6.3})$$

while for deuterium ($I=1$):

$$p_J = 6(2J + 1) \quad (\text{for } J \text{ even})$$

$$p_J = 3(2J + 1) \quad (\text{for } J \text{ odd}) \quad (\text{A.6.4})$$

Using the formulae (A.6.1)-(A.6.4) the following table was prepared.

Table A.6.1 Abundances of the rotational levels in H_2 and D_2 ,

	J=0	J=1	J=2	J=3	J=4	J=5
p- H_2 77 K	0.9946	0	0.0054	0	0	0
n- H_2 77 K	0.2487	0.75	0.0013	0	0	0
n- H_2 293 K	0.135	0.67	0.112	0.079	0.003*	0
n- D_2 77 K	0.5721	0.3307	0.0945	0.0026	0	0
n- D_2 293 K	0.1832	0.2060	0.3858	0.1137	0.0924	0.0134

* In the actual analysis this abundance was added to the abundance of the next lower J of the same parity.

The abundances of the rotationally excited levels in CO were calculated from (A.6.1) and (A.6.2).

REFERENCES

- Ahtye W F (1972), J. Chem. Phys. 57 5543.
- Ajello J M and Chutjian A (1979), J. Chem. Phys. 71 1079.
- Al-Dargazelli S S, Ariyaratne T R, Breare J M and Nandi B C (1981), Nucl. Instrum. Methods 176 523.
- Alge E, Adams N G and Smith D (1984) J. Phys. B 16 1433.
- Allis W P (1956), "Motions of Ions and Electrons" In Handbuch der Physik (Ed. S Flugge) 21 413 (Springer Verlag: Berlin).
- Allis W P (1983), In "Electrical Breakdown and Discharges in Gases" (Ed.s E E Kunhardt and L H Luessen)Pt A p 187 (Plenum Press: New York).
- Altshuler S (1957), Phys. Rev. 107 114.
- Amusia M Ya, Cherepkov N P, Chernyshova L V, Davidović D M and Radojević V (1982), Phys. Rev A 25 219.
- Andrick D and Bitsch A (1975), J. Phys. B 8 393.
- Atrazhev V M (1984), J. Phys. D 17 889.
- Atrazhev V M and Iakubov I T (1977), J. Phys. D 10 2155.
- Audibert M M, Joffrin C and Ducuing J (1974), Chem. Phys. Lett. 25 158.
- Ault E R (1975), Appl. Phys. Lett. 26 619.
- Ault E R, Bhaumik M and Olson N (1974), IEEE J. Quantum Electron. QE-10 624.
- Ayala J A, Wentworth W E and Chen E C M (1981), J. Phys. Chem. 85 3889.
- Bacal M (1982), Physica Scripta T2/2 467.
- Bansal K M and Fessenden R W (1972), Chem. Phys. Lett. 15 21.
- Baraff G A and Buchsbaum S J (1963), Phys. Rev. 130 1007.
- Bardsley J N and Wadehra J M (1979), Phys. Rev. A 20 1398.

- Bartell D M, Hurst G S and Wagner E B (1973), Phys. Rev. A 7 1068.
- Beaty E C, Dutton J and Pitchford L C (1979) JILA Information Center Report 20.
- Belić D S, Landau M and Hall R I (1981), J. Phys. B. 14 175.
- Bell K L, Scott N S and Lennon M A (1984), J. Phys. B 17 4757.
- Black G, Wise H, Schechter S and Sharpless R L (1974), J. Chem. Phys. 60 3526.
- Blanc M A (1908), J. Phys. (Paris) 7 825.
- Blaunstein R P and Christophorou L G (1968), J. Chem. Phys. 49 1526.
- Blevin H A and Fletcher J (1984), Aust. J. Phys. (to be published)
- Blevin H A, Fletcher J and Hunter S R (1976), J. Phys. D 9 471 and 1671
see also (1978) ibid 11 1653 and 2295.
- Blevin H A, Fletcher J and Hunter S R (1978a), Aust. J. Phys. 31 299.
- Blevin H A, Fletcher J and Hunter S R (1978b), J. Phys. D 11 1653.
- Boeuf J P and Marode E (1982), J. Phys. D 15 2169.
- Boeuf J P and Marode E (1984), J. Phys. D 17 1133.
- Boness M J W and Schulz G J (1973), Phys. Rev. A 8 2883.
- Bozin J V, Urosević V V and Petrović Z Lj (1983), Z. Phys. A 312 349.
- Bradbury N E and Tatel H E (1934), J. Chem. Phys. 2 835.
- Braglia G L (1970), Nuovo Cimento 70 B 169 see also Braglia G L and Caraffini G L (1974), Riv. Mat. Univ. Parma 3 81.
- Braglia G L (1977), Physica 92C 91.
- Braglia G L (1980), Beitr. Plasma Phys. 20 147.
- Braglia G L (1981a), Lett. Nuovo Cimento 31 183.
- Braglia G L (1981b), J. Chem. Phys. 74 2990.
- Braglia G L and Baiocchi A (1978), Physica 95C 227.
- Braglia G L and Caraffini G L (1980), Lett. Nuovo Cimento 27 145.

- Braglia G L and Dallacasa V (1978), Phys. Rev. A 18 711.
- Braglia G L and Dallacasa V (1982), Phys. Rev. A 26 902.
- Braglia G L and Lowke J J (1979), J. Phys. D 12 1831.
- Braglia G L, Bruzzese R, Solimeno S, Martellucci S and Quantieri J (1981), Lett. Nuovo Cimento 30 459.
- Braglia G L, Romano L and Roznerski W (1983), Nuovo Cimento 2D 898.
- Braglia G L, Romano L and Diligenti M (1984), Nuovo Cimento 79B 93.
- Braglia G L, Wilhelm J and Winkler R (1984b), Nuovo Cimento 80 21.
- Brunet H and Vincent P (1979), J. Appl. Phys. 50 4700 and 4708.
- Buckman S and Phelps A V (1985), to be published.
- Bulos B R and Phelps A V (1976), Phys. Rev. A 14 615.
- Burch D S and Whealton J H (1977), J. Appl. Phys. 48 2213.
- Bychkov Yu I, Korolev Yu D and Mesyats G A (1980), Sov. Phys. Usp. 21 944.
- Capitelli M, Gorse C, Berardini M and Braglia G L (1981), Lett. Nuovo Cimento 31 231.
- Capitelli M, Gorse C, Wilhelm J and Winkler R (1982), Nuovo Cimento 70 163.
- Capitelli M, Gorse C and Ricard A (1983), J. Physique Lett. 44 L-251.
- Carnahan B L and Zipf E C (1977), Phys. Rev. A 16 991.
- Cavalleri G (1969), Phys. Rev. 179 186.
- Cavalleri G (1981), Aust. J. Phys. 34 361.
- Cavalleri G, Gatti E and Redaelli G (1962), Nuovo Cimento 25 1282.
- Cavalleri G, Gatti E and Principi P (1964), Nuovo Cimento 31 302.
- Cavalleri G, Gatti E and Interlenghi A M (1965), Nuovo Cimento 40B 450.
- Chang E S (1974), Phys. Rev. A 9 1644.
- Chang E S (1981), J. Phys. B 14 893.

- Chang E S and Wong S (1977), Phys Rev. Lett. 38 1327.
- Chantry P J (1963), Proc. III ICPEAC J. McDowell Ed. North Holland Amsterdam 565.
- Chantry P J (1982a), Phys. Rev. A 25 1209; see also Braglia G L (1982), Phys. Rev. A 25 1214.
- Chantry P J (1982b), In "Applied Atomic Collisions Physics Vol 3" (Volume Editors E W McDaniel and W L Nighan)p 35 (Academic Press: New York).
- Chantry P J (1983), personal communication.
- Chapman S and Cowling T G (1960), "The Mathematical Theory of Non-Uniform Gases" (University Press: Cambridge).
- Chen C L and Chantry P J (1979), J. Chem. Phys. 71 3897.
- Chen Z F and Jones H G (1984), J. Phys. D 17 337.
- Chen E, George R D and Wentworth W E (1968), J. Chem. Phys. 49 1973.
- Chapman S and Cowling T G (1960), "The Mathematical Theory of Non-Uniform Gases" (University Press:Cambridge).
- Cherrington B E (1979) "Gaseous Electronics and Gas Lasers" (Pergamon Press: Oxford).
- Christodoulides A A and Christophorou L G (1971) J. Chem. Phys. 54 4691.
- Christophorou L G (1971), "Atomic and Molecular Radiation Physics" (Wiley Interscience: New York).
- Christophorou L G (1978), In "Advances in Electronics and Electron Physics" (Ed. L Marton; Academic Press: New York), 46 55.
- Christophorou L G (1980), Environmental Health Perspectives 36 3.
- Christophorou L G and Hunter S R (1984), In "Electron Molecule Interactions" (Ed L G Christophorou, Academic Press: New York) 317.

- Christophorou L G and Pittman D (1970), J. Phys. B 3 1252.
- Christophorou L G, McCorkle D L and Carter J G (1971a), J. Chem. Phys. 54 253.
- Christophorou L G, McCorkle D L and Anderson V E (1971b), J. Phys. B 4 1163.
- Christophorou L G, Gant K S and Baird J K (1975), Chem. Phys. Lett. 30 104.
- Christophorou L G, Mathis R A, James D R and McCorkle D L (1981), J. Phys. D 14 1889.
- Christophorou L G, Hunter S R, Carter J G and Mathis R A (1982a), Appl. Phys. Lett. 41 147.
- Christophorou L G, James D R and Pai R Y (1982b), In "Applied Atomic Collision Physics Vol 5" (Volume Editors H S W Massey, E W McDaniel and B Bederson)p 87 (Academic Press: New York).
- Christophorou L G, Mathis R A and James D R (1983), J. Appl. Phys. 54 3098.
- Chutjian A (1981), Phys. Rev. Lett. 46 1511 see also (1982), Phys. Rev. Lett. 48 289.
- Chutjian A (1982), J. Phys. Chem. 86 3518.
- Chutjian A and Alajajian S H (1985), to be published in Phys. Rev. and personal communication.
- Chutjian A and Tanaka H (1980), J. Phys. B 13 1901.
- Compton R N, Christophorou L G, Hurst G S and Reinhardt R W (1966), J. Chem. Phys. 45 4634.
- Compton R N and Christophorou L G (1967), Phys. Rev. 154 110.
- Corrigan S J B (1965), J. Chem. Phys. 43 4381.
- Creaser R P (1967), Aust. J. Phys. 20 547.

- Crompton R W (1967), J. Appl. Phys. 38 4093.
- Crompton R W (1969), Advan. Electron. Electron Phys. 27 1.
- Crompton R W (1972), Aust. J. Phys. 25 409.
- Crompton R W (1979), In Proc. 1st Swarm Seminar (Ed. I Ogawa) p 1.
- Crompton R W (1980), IDU Internal Report 1980/3 (ANU: unpublished).
- Crompton R W (1983), In Invited Papers Proc. ICPIG - XVI Dusseldorf
Ed.s Botticher, Wenk and Schulz-Gulde, p 58.
- Crompton R W (1984a), Proc 4th ESCAMPIG (Ed. M Capitelli, Bari).
- Crompton R W (1984b), In Invited Lectures Proc 12th SPIG (Ed. M M
Popović, Institute of Physics: Belgrade).
- Crompton R W and Elford M T (1962), J. Sci. Instrum. 39 480.
- Crompton R W and Haddad G N (1983), Aust. J. Phys. 36 15.
- Crompton R W and Jory R L (1962), Aust. J. Phys. 15 451.
- Crompton R W and McIntosh A I (1967), Phys. Rev. 18 527.
- Crompton R W and McIntosh A I (1968), Aust. J. Phys. 21 637.
- Crompton R W and Morrison M A (1982), Phys. Rev. A 26 3695.
- Crompton R W and Robertson A G (1971), Aust. J. Phys. 24 543.
- Crompton R W, Hall B I H and Macklin W C (1957), 10 366.
- Crompton R W, Elford M T and Gascoigne J (1965), Aust. J. Phys. 18 409.
- Crompton R W, Liley B S, McIntosh A I and Hurst C A (1966), In Proc 7th
ICPIG (Ed.s B Perović and D Tosić Gradjevinska Knjiga: Beograd).
- Crompton R W, Elford M T and Jory R L (1967), Aust. J. Phys. 20 369.
- Crompton R W, Elford M T and McIntosh A I (1968), Aust. J. Phys. 21 43.
- Crompton R W, Gibson D K and McIntosh A I (1969), Aust. J. Phys. 22
715.
- Crompton R W, Elford M T and Robertson A G (1970), Aust. J. Phys. 23
667.

- Crompton R W, Gibson D K and Robertson A G (1970b), Phys. Rev. 2 1386.
- Crompton R W, Hegerberg R and Skullerud H R (1980), J. Phys. B L455.
- Crompton R W, Haddad G N, Hegerberg R and Robertson A G (1982), J. Phys. B 15 L483.
- Csanak G, Cartwright D C, Srivastava S K and Trajmar S (1983), LA-UR-83-445 (Los Alamos Scientific Laboratory) to be published in (1984) "Electron-Molecule Interactions and their Applications" (Ed. L Christophorou, Academic Press: New York).
- Cullen A (1985), "Cavalleri Controller Report" Electronics Unit (R. S. Phys. S. ANU: Canberra-unpublished).
- Davies A R, Smith K, Thomson R M (1975), Comp. Phys. Comm. 10 117 and (1976) J. Appl. Phys. 47 2037.
- Davies A J, Dutton J, Evans C J, Goodings A and Stewart P K (1979), J. Phys. (Paris) Coll. 40 C7-63.
- Davies A J, Dutton J, Evans C J, Goodings A and Stewart P K (1984), J Phys. D 17 287.
- Davis F J and Nelson D R (1969), Chem. Phys. Lett. 3 461.
- Davis F J and Nelson D R (1970), Chem. Phys. Lett. 6 277.
- Davis F J, Compton R N and Nelson D R (1973), 59 2324.
- de Heer F J (1981), Physica Scripta 23 170.
- Dean A G, Smith D and Adams N G (1974), J. Phys. B. 7 644.
- Dincer M S and Govinda Raju G R (1983), J. Appl. Phys. 54 6311.
- Doyennette L, Margotin-Maclou M, Gueguen H, Corion A and Henry L (1974), J. Chem. Phys. 60 697.
- Dutton J (1975), J. Phys. Chem. Ref. Data 4 577.
- Ehrhardt H, Langhans L, Linder F and Taylor H S (1968), Phys. Rev. 173 222.

- Elford M T (1972), In "Case studies in Atomic Collision Physics II" (Ed. E W McDaniel and M R C McDowell)p 91 (North Holland: Amsterdam).
- Elford M T (1980), Aust. J. Phys. 33 231 and 251.
- Elford M T (1984), Personal communication.
- Elford M T and Robertson A G (1973), 26 685.
- El-Hakeem N and Mathieson E (1978), Proc. 3rd Int. Meeting on Drift and Proportional Chambers, Dubna.
- Engelhardt A G and Phelps A V (1963), Phys. Rev. 131 2115.
- Engelhardt A G and Phelps A V (1964), Phys. Rev. 133 A 375.
- Engelhardt A G, Phelps A V and Risk C G (1964), Phys. Rev. 135 A 1566.
- Englert G W (1971), Z. Naturforsch 26a 836.
- Erwin D A and Kunc J A (1983), IEEE PS-11 266.
- Fabrikant I I (1977a), Sov. Phys. JETP 44 77.
- Fabrikant I I (1977b), J. Phys. B 10 1761.
- Fabrikant I I (1980), Phys Lett. 77A 421.
- Fabrikant I I (1981), J. Phys. B 14 335.
- Fabrikant I I (1983), J. Phys. B 16 1253.
- Fabrikant I I (1984), J. Phys. B 17 4223.
- Fehsenfeld F C (1970), J. Chem. Phys. 53 2000.
- Feldt A N and Morrison M A (1984), Phys. Rev. A 29 401.
- Ferch J, Raith W and Schroder K (1980), J. Phys. B 13 1481.
- Ferch J, Granitza B, Masche C and Raith W (1984), J. Phys. B submitted.
- Ferrari L (1975), Physica 81A 276.
- Ferrari L (1977), Physica 85C 161.
- Ferreira C M and Ricard A (1983), J. Appl. Phys. 54 2261.
- Fessenden R W and Bansal K M (1970), J. Chem. Phys. 53 3468.
- Foltz G W, Latimer C J, Hildebrandt G F, Kellert F G, Smith K A, West W

- P, Dunning F B and Stebbings R F (1977), J. Chem. Phys. 57 1352.
- Fon W C, Burke P G, Berrington K A and Hibbert A H (1983) J. Phys. B 16 307.
- Foreman L, Kleban P, Schmidt L D and Davis H T (1981), Phys. Rev. A 23 1553.
- Fox R E, Malmberg P R and Grosser R B (1961), Rev. Sci. Instrum. 32 898.
- Francey J L A (1976), J. Phys. D 9 457.
- Freeman G R (1968) Radiation Res. Rev. 1 1.
- Friedland L (1977), Phys. Fluids 20 1461.
- Frommhold L (1968), Phys. Rev. 172 118.
- Frost L S and Phelps A V (1962), Phys. Rev. 127 1621.
- Frost L S and Phelps A V (1964), Phys. Rev. 136 A 1538.
- Fujimoto G, Nitzan A and Weitz E (1976), Chem. Phys. 15 217.
- Furst J, Magherefti M and Golden D E (1984), Phys. Rev. A 30 2256.
- Gallagher J W, Beaty E C, Dutton J and Pitchford L C (1982), JILA Information Center Report 22 and (1983) J. Phys. Chem. Ref. Data 12 109.
- Gant K S and Christophorou L G (1976), J. Chem. Phys. 65 2977.
- Garamoon A A and Ismail I A (1977), J. Phys. D 10 991.
- Garbaty E A and LaBahn R W (1971), Phys. Rev. A 4 1425.
- Garscadden A (1981), In "Electron and Ion Swarms" (Ed. L G Christophorou)p 251 (Pergamon: New York).
- Garscadden A, Duke G A and Bailey W F (1980), Bull. Am. Phys. Soc. 26 724.
- Gascoigne J (1970), Vacuum 21 21.
- Gauyacq J P and Herzenberg A (1984), J. Phys. B 17 1155.

- Gerjuoy E and Stein S (1955), Phys. Rev. 97 1071, 98 1848.
- Gibson D K (1970), Aust. J. Phys. 23 683.
- Gibson T L and Morrison M A (1981), J. Phys. B 14 727.
- Gibson T L and Morrison M A (1984), Phys. Rev. A 29 2497.
- Gibson D K, Crompton R W and Cavalleri G (1973), J. Phys. B 6 1118.
- Gibson T L, Lima M A P, Takatsuka K and McKoy V (1984), Phys. Rev. A 30 3005.
- Gilardini A L (1972), "Low Energy Electron collisions in Gases" (Wiley Interscience: New York).
- Ginzburg V L and Gurevich A V (1960), Usp. Fiz. Nauk 70 201 and 393.
- Giraud P and Krebs V (1982), Chem. Phys. Lett. 86 85.
- Goans R E and Christophorou L G (1975) J. Chem. Phys. 63 2821.
- Golde M F (1976), Specialists Periodical Reports "Gas Kinetic and Energy Transfer" Chem. Soc. London 2 123.
- Golden D E (1966), Phys. Rev. 151 48.
- Golden D E (1984), Phys. Rev. 30 1247.
- Golden D E and Bandel H W (1966), Phys. Rev. 149 58.
- Golden D E, Bandel H W and Salerno J A (1966), Phys. Rev. 146 40.
- Gorse C, Capitelli M and Ricard A (1984), J. Chem. Phys. 80 149.
- Gould R J (1974), Ann. Phys. (NY) 84 480.
- Govinda Raju G R and Hackam R (1982), J. Appl. Phys. 53 5557.
- Gradshteyn S and Ryzhik I M (1980), "Tables of Integrals, Series and Products", (Academic Press: New York).
- Gryko J and Popielawski J (1979), Phys. Rev. A 21 1717 and (1981) Phys. Rev. A 24 1129.
- Gundersen M and Guha S (1982), J. Appl. Phys. 53 1190.
- Gus'kov Yu K, Savvov R V and Slobodyanyuk V A (1978), Sov. Tech. Phys.

23 167.

- Haas R A (1973) Phys. Rev. A 8 1017.
- Haddad G N (1983), Aust. J. Phys. 36 297.
- Haddad G N (1984), Aust. J. Phys. 37 487.
- Haddad G N (1985), Aust. J. Phys. (to be submitted).
- Haddad G N and Crompton R W (1980), Aust. J. Phys. 33 975.
- Haddad G N and Milloy H B (1983), Aust. J. Phys. 36 473.
- Haddad G N and O'Malley (1982), Aust. J. Phys. 35 35.
- Haddad G N, Lin S L and Robson R E (1981), Aust. J. Phys. 34 243.
- Hall B I H (1955), Aust. J. Phys. 8 468.
- Hall C A and Lowke J J (1975), J. Comp. Phys. 19 297.
- Hake R D and Phelps A V (1967), Phys. Rev. 158 70.
- Hansen D, Jungblut H and Schmidt W F (1983), J. Phys. D 16 1623.
- Hasted J B (1972), "Physics of Atomic Collisions" 2nd Edition, p 557-9
(Butterworths: London)
- Hasted J B and Beg S (1965), Brit. J. Appl. Phys. 16 74.
- Hay D J (1982), J. Chem. Phys. 76 502.
- Hayashi M (1981), IPPJ-AM-19 (Nagoya Institute of Technology: Nagoya).
- Hayashi M (1982), J. Phys. D 15 1411.
- Hayashi M (1983a), J. Phys. D 16 591.
- Hayashi M (1983b), J. Phys. D 16 581.
- Hayashi M and Ushiroda S (1983), J. Chem. Phys. 78 2621.
- Haydon S (1985), personal communication.
- Healey R H and Reed J W (1941), "The Behaviour of Slow Electrons in Gases " (AWA: Sydney).
- Hegerberg R and Crompton R W (1980), Aust. J. Phys. 33 989.
- Hegerberg R and Crompton R W (1983), Aust. J. Phys. 36 831 (See also

- Crompton R W, Hegerberg R and Skullerud H R (1980) J. Phys. B 13 L455).
- Hegerberg R, Elford M T and Crompton R W (1980), Aust. J. Phys 33 895.
- Henry R J W and Lane N F (1969), Phys. Rev. 183 221 and (1971) Phys. Rev. A 4 410.
- Herzberg G (1950), "Spectra of Diatomic Molecules" (Van Nostrand: Princeton)
- Hill R M, Gutcheck R A, Huestis D L, Mukherjee D and Lorents D C (1974) SRI Technical Report 3 (Stanford Research Institute: unpublished) and Gutcheck R A, Hill R M, Lorents D C, Huestis D L, McCusker M V and Nakano H H (1975), J. Appl. Phys. 46 1306.
- Hiskes J R, Karo A M, Bacal M, Bruneteau A M and Graham G (1982), J. Appl. Phys. 53 3469; see also Karo A M, Hiskes J R, Olwell K D, DeBoni T M and Hardy R J (1984), In Proc. Production and Neutralization of Negative Ions and Beams, 3rd Int. Symposium, Brookhaven (Ed. K Prelec) p 197 (AIP: New York)
- Hodgson R T (1970), Phys. Rev. Lett. 25 494.
- Hodgson R T and Dreyfus R W (1972), Phys. Rev. Lett. 28 536.
- Holstein T (1946), Phys Rev. 70 367.
- Hughes M H (1970), J. Phys. B 3 1544.
- Hunter S R (1977a), Ph.D Thesis (Flinders University of South Australia: Adelaide-unpublished).
- Hunter S R (1977b), Aust. J. Phys. 30 83.
- Hunter S R (1984), personal communication.
- Hunter S R, Christophorou L G, McCorkle D L, Sauers I, Ellis H W and James D R (1983), J. Phys. D 16 573.
- Hurst G S (1974), Radiation Research 59 350.

- Hurst G S, Stockdale J A and O'Kelly L B (1963), J. Chem. Phys. 38 2572.
- Huxley L G H (1972a), Aust. J. Phys. 25 523.
- Huxley L G H (1972b), Aust. J. Phys. 25 43.
- Huxley L G H (1973), Aust. J. Phys. 26 135.
- Huxley L G H (1981), "The Ginsburg Gurevich Treatment of the Maxwell-Boltzmann Equation as Applied to the Motions of Electrons in Gases" IDU Internal report (unpublished) (1981/1).
- Huxley L G H and Crompton R W (1962), In "Atomic and Molecular Processes" (Ed. D R Bates) p 335 (Academic Press: New York).
- Huxley L G H and Crompton R W (1974), "The Diffusion and Drift of Electrons in Gases" (Wiley-Interscience: New York).
- Huxley L G H, Crompton R W and Elford M T (1966), Bull. Inst. Phys. and Phys. Society 17 251.
- Ikuta N (1984), Proc. 4th ESCAMPIG (Ed. M Capitelli, Bari).
- Ikuta N and Itoh H (1982), Bull. of Faculty of Engineering (Tokushima University) 19 73.
- Ikuta N, Itoh H and Toyota K (1983), Jap. J. Appl. Phys 22 117.
- Ingold J H (1978), in "Gaseous Electronics" (Ed. Hirsh and Oskam) p 19 (Academic Press: New York).
- Ingold J H (1984), Proc. 3rd GEM p 25.
- Ismail I A and Garamoon A A (1979), J. Phys. D 12 1117.
- Itikawa Y (1978), Phys. Rep. 46 118.
- Itoh T and Musha T (1960), J. Phys. Soc. Japan 15 1675.
- Itoh H, Ikuta N and Toyota K (1983), J. Phys. D 16 293.
- Jacob J H and Mangano J A (1976), Appl. Phys. Lett. 29 467.
- Johnson G R A, Sauer Jr M C and Warman J M (1969), J. Chem. Phys. 50

- 4933.
- Jost K, Bisling P G F, Eschen F, Felsmann M and Walther L (1983), In Proc XIII ICPEAC, Berlin, p 91.
- Judd O (1976) J. Appl. Phys. 47 5297.
- Kaufman Y and Kagan Yu M (1981), J. Phys. D 14 2215; see also Kagan Yu M and Kaufman Y (1983), J. Phys. D 16 1687.
- Kellert F G, Higgs C, Smith K a, Hildebrandt G F, Dunning F B and Stebbings R F (1980), J. Chem. Phys. 72 6312.
- Khrapak A G and Yakubov I T (1979) Sov. Phys Usp. 22 703.
- Kieffer L J (1973), JILA Information Center Report No. 13.
- Kirkpatrick T R and Dorfman J R (1983) J. Stat. Phys. 30 67.
- Kitamori K, Tagashira H and Sakai Y (1978) J. Phys. D 11 283.
- Kitamori K, Tagashira H and Sakai Y (1980) J. Phys. D 13 535.
- Kleban P and Davis H T (1977), Phys. Rev. Lett. 39 456.
- Kleban P and Davis H T (1978), J. Chem. Phys. 68 2999.
- Kleban P, Foreman L and Davis H T (1980), J. Chem. Phys. 73 519.
- Kleban P, Foreman L and Davis H T (1981), Phys. Rev. A 23 1546.
- Kline L J, Davies D K, Chen C L and Chantry P J (1979), J. Appl. Phys. 50 6789.
- Klonover A and Kaldor U (1979), J. Phys. B 12 3797.
- Klots C E (1976), Chem. Phys. Lett. 38 61.
- Klots C E and Reinhardt P W (1970), J. Phys. Chem. 74 2848.
- Knierim K D, Waldman M and Mason E A (1982), J. Chem. Phys. 77 943.
- Koizumi T, Murakoshi H, Yamamoto S and Ogawa I (1984), J. Phys. B 17 4387.
- Kontoleon N, Lucas J and Virr L E (1973), J. Phys. D 6 1237.
- Koura K (1983), J. Chem. Phys. 79 3367.

- Koura K (1984), J. Chem. Phys. 80 5709 and 81 303.
- Kovacs M, Ramachandra Rao D and Javan A (1968), J. Chem. Phys. 48 3339.
- Kucukarpaci H N and Lucas J (1979), J. Phys. D 12 2123.
- Kucukarpaci H N, Saelee H T and Lucas J (1981), J. Phys. D 14 9.
- Kuffel E (1959), Proc. Phys. Soc. 74 297.
- Kumar K (1980), Aust. J. Phys. 33 449 and 469.
- Kumar K (1981), J. Phys. D 14 2199.
- Kumar K (1984), Phys. Rep. 112 320.
- Kumar K and Robson R E (1973), Aust. J. Phys. 26 157.
- Kumar K, Skullerud H R and Robson R E (1980), Aust. J. Phys. 33 343.
- Kunc J A (1983), J. Appl. Phys. 54 3788.
- Kunc J A and Gundersen M A (1982), IEEE PS-10 315.
- Kunhardt E E and Tzeng Y (1984), to be published in Phys. Rev.
- Lambert J D (1977), "Vibrational and Rotational Relaxation in Gases"
(Clarendon Press: Oxford).
- Lane N F (1980), Rev. Modern Phys. 52 29.
- Land J E (1978), J. Appl. Phys. 49 5716.
- Lawton S A and Phelps A V (1978), J. Chem. Phys. 69 1055.
- Lee T G (1963) J. Phys. Chem. 67 360.
- Leemon H I and Kumar K (1975), Aust. J. Phys. 28 25.
- Legler W (1970), Phys. Lett. 31A 129.
- Levich B G (1973) "Theoretical Physics Vol.4" (North-Holland:
Amsterdam).
- Liboff R L (1969), "Introduction to the Theory of Kinetic Equations"
(Wiley: New York).
- Lin S L and Bardsley J N (1977), J. Chem. Phys. 66 435.
- Lin S L and Bardsley J N (1978), Comp. Phys. Comm. 15 161.

- Lin S L, Robson R E and Mason E A (1979), J. Chem. Phys. 71 3483.
- Linder F (1974), Endeavour 33 124.
- Linder F and Schmidt H (1971), Z Naturf. 26a 1603.
- Loeb L B (1955), "Basic Processes of Gaseous Electronics" (University of California Press: Berkeley).
- Long W H Jr, Bailey W F and Garscadden A (1976), Phys. Rev. A 13 471.
- Lopantseva G B, Pal' A F, Persiatsev I G, Polushkin V M, Starostin A N, Timofeev M A and Treneva E G (1979), Sov. J. Plasma Phys. 5 767.
- Lowke J J (1962), Aust. J. Phys. 15 39.
- Lowke J J (1963), Aust. J. Phys. 16 115.
- Lowke J J (1973), Aust. J. Phys. 26 469.
- Lowke J J and Parker J H (1969), Phys. Rev. 181 302.
- Lowke J J and Rees J A (1963), Aust. J. Phys. 16 447.
- Lowke J J, Parker Jr J H and Hall C A (1977), Phys. Rev. A 15 1237.
- Lucas J (1967), Int. J. Electron. 22 529.
- Lucas J (1969), Int. J. Electron. 27 201.
- Lucas J (1970), Int. J. Electron. 29 465.
- Luft P E (1975), JILA Information Center Report 14.
- McCarthy I E, Noble C J, Phillips B A and Turnbull A D (1977), Phys. Rev. A 15 2173.
- McCorkle D L, Christodoulides A A, Christophorou L G and Szamrej I (1980), J. Chem. Phys. 72 4049.
- McDaniel E W (1964), "Collision Phenomena in Ionized Gases", p 455-7 (Wiley Interscience: New York,).
- McDaniel E W and Mason E A (1973), "The Mobility and Diffusion of Ions in Gases" (Wiley: New York).
- McEachran R P and Stauffer A D (1983), 16 4023 and personal

- communication.
- McIntosh A I (1966), Aust. J. Phys. 19 805.
- McIntosh A I (1969), Ph. D. Thesis (ANU: unpublished).
- McIntosh A I (1974), Aust. J. Phys. 30 73.
- McMahon D R A (1983a) "Comparisons of Multi-Term and Monte Carlo Calculation of Electron Transport Coefficients" IDU-ANU Internal Report (1983/2) (unpublished).
- McMahon D R A (1983b), Aust. J. Phys. 36 163.
- McMahon D R A (1983c), Aust. J. Phys. 36 27 and 45.
- McMahon D R A (1985), Phys. Rev. to be published.
- McMahon D R A and Crompton R W (1983), J. Chem. Phys. 78 603.
- McMahon D R A and Shizgal B (1985), to be published.
- Mahan B H and Young C E (1966), J. Chem. Phys. 44 2192.
- Makabe T and Mori T (1980), J. Phys. D 13 387.
- Makabe T and Mori T (1982), J. Phys. D 15 1395.
- Makabe T and Mori T (1984), J. Phys. D 17 699.
- Margottin-Maclou M, Doyennette L and Henry L (1971), Appl. Optics. 10 1768.
- Massey H (1976), "Negative Ions" (University Press Cambridge).
- Mathieson E and El-Hakeem N (1979), Nucl. Instrum. Methods. 159 489.
- Milloy H B (1975), J. Phys. B 8 L414.
- Milloy H B and Crompton R W (1977a), Phys. Rev. A 15 1847.
- Milloy H B and Crompton R W (1977b), Aust. J. Phys. 30 51 see also (1982) *ibid.* 35 105.
- Milloy H B and Crompton R W (1982), Aust. J. Phys. 35 105.
- Milloy H B and Robson R E (1973), J. Phys. B 6 1139.
- Milloy H B and Watts R O (1977), Aust. J. Phys. 30 73.

- Milloy H B, Crompton R W, Rees J A and Robertson A G (1977), Aust. J. Phys. 30 61.
- Morgan W L (1979), JILA Information Center Report 19.
- Morgan W L and Fisher E R (1977), Phys. Rev. A 16 1186.
- Morgan C G , Powell W D and W T Williams (1967), Brit. J. Appl. Phys. 18 939.
- Morrison M A (1979), IDU - Internal Report 1979/3.
- Morrison M A (1983), Aust. J. Phys. 36 238.
- Morrison M A, Gibson T L and Austin D (1984a), J. Phys. B 17 2725.
- Morrison M A, Feldt A N and Saha B C (1984b), Phys. Rev. A 30 2811.
- Morrison M A ,Feldt A N and Austin D (1984c), Phys. Rev. A 29 2518.
- Moruzzi J L (1967), Rev. Sci. Instr. 38 1284.
- Mothes K G and Schindler (1971), Ber. Bunsenges. Phys. Chem. 75 936.
- Mothes K G, Schultes E and Schindler R N (1972), J. Phys. Chem. 76 3758.
- Motz H and Wise H (1960), J. Chem. Phys. 32 1893.
- Mozumder A (1980), J. Chem. Phys. 72 1657 and 6289.
- Mozumder A (1981), J. Chem. Phys. 74 6911.
- Mozumder A (1982), J. Chem. Phys. 76 3277.
- Muller III C H and Phelps A V (1980), J. Appl. Phys. 51 6141.
- Nelson R D, Jr Lide D R Jr and Maryott A A (1967), "Selected Values of Electric Dipole Moments for Molecules in the Gas Phase" NSRDS- NBS 10.
- Nelson D R and Davis F J (1969), J. Chem. Phys. 51 2322, (see also: 1968 Oak Ridge National Laboratory Report TM-2222).
- Nesbet R K (1979), Phys. Rev. A 20 58.
- Nesbet R K, Noble C J, Morgan L A and Weatherford C A (1984), J. Phys.

- B 17 L891, see also Nesbet R K (1984), J. Phys. B 17 L897.
- Ness K F (1977), Hon. thesis, (James Cook University of North Queensland: Townsville - unpublished).
- Ness K F (1984a), Proc. 3rd GEM p 13.
- Ness K F (1984b), personal communication.
- Nighan W L (1970), Phys. Rev. A 2 1989.
- Nighan W L (1977), Phys. Rev. A 16 1209.
- Norcross D W (1982), In "Applied Atomic Collision Physics Vol 5" (Volume Editors H S W Massey, E W McDaniel and B Bederson)p 69 (Academic Press: New York).
- Norcross D W and Collins L A (1982), In "Advances in Atomic and Molecular Physics" (Ed. D R Bates and B Bederson) p 341 (Academic Press: New York).
- Odom R W, Smith D L and Futrell J H (1975), J. Phys. B 8 1349.
- O'Malley T F (1963), Phys. Rev. 130 1020.
- O'Malley T F (1964), Phys. Rev. 134 A1188.
- O'Malley T F (1980), J. Phys. B 13 1491.
- O'Malley T F (1983), Phys. Lett. 95A 32.
- O'Malley and Crompton R W (1980), J. Phys. B 13 3451.
- O'Malley T F, Spruch L and Rosenberg L (1961), J. Math. Phys. 2 491
- O'Malley T F, Rosenberg L and Spruch L (1962), Phys. Rev. 125 1300.
- O'Malley T F, Burke P G and Berrington K A (1979) J. Phys. B 12 953.
- Pack J L and Phelps A V (1961), Phys. Rev. 121 798.
- Pack J L and Phelps A V (1966), J. Chem. Phys. 44 1870 and 45 4316.
- Pack J L Voshall R E and Phelps A V (1962), Phys. Rev. 127 2084.
- Parker Jr J H and Lowke J J (1969), Phys. Rev. 181 290.
- Payne M G, Klots C E and Hurst G S (1975), J. Chem. Phys. 63 1422.

- Penetrante B M and Bardsley J N (1983), J. Appl. Phys. 54 6150.
- Penetrante B M and Bardsley J N (1984), J. Phys. D 17 1971.
- Petrović Z Lj and Crompton R W (1982), Ion Diffusion Unit Quarterly Report QR90 (unpublished).
- Petrović Z Lj, Crompton R W and Haddad G N (1984), Aust. J. Phys. 37 23.
- Petrushevich Yu V and Starostin A N (1981), Sov. J. Plasma Phys. 7 463.
- Phelps A V (1968), Rev. Mod. Phys. 40 399.
- Phelps A V (1979), In Proc. 1st Swarm Seminar (Ed I Ogawa) p 23.
- Phelps A V (1984), Proc 3rd GEM p 8.
- Phelps A V, Pack J L and Frost L S (1960) 117 470.
- Pitchford L C (1983), In "Electrical Breakdown and Discharges in Gases" (Ed.s E E Kunhardt and L H Luessen) Pt A p 313 (Plenum Press: New York).
- Pitchford L C and Phelps A V (1982), Phys. Rev. A 25 540.
- Pitchford L C, O'Neil S V and Rumble Jr J R (1981), Phys. Rev. A 23 294.
- Polischuk A Ya (1983), J. Phys. B 16 3845.
- Pouvesle J M, Bouchoule A and Stevefelt J (1982), J. Chem. Phys. 77 817.
- Prelec K ed.(1984), Proc. AIP Conf. on "Production and Neutralization of Negative Ions and Beams", (AIP: New York).
- Ramsauer C E and Kollath R (1929), Ann. Phys. 3 536.
- Rapp D and Englander-Golden P (1965), J. Chem. Phys. 43 1464.
- Rees H D (1969) J. Phys. Chem. Solids 30 643.
- Reid I D (1977), Ph.D thesis (ANU-unpublished).
- Reid I D (1979), Aust. J. Phys. 32 231, see also (1982) *ibid.* 35 473.

- Reid I D and Hunter S R (1979), Aust. J. Phys. 32 255.
- Reif F (1965) "Fundamentals of Statistical and Thermal Physics" (McGraw Hill: New York).
- Resbois R and Leener M de (1977), "Classical Kinetic Theory of Fluids" (Wiley Interscience: New York).
- Rhymes T (1976), Ph.D thesis (ANU-unpublished).
- Rhymes T and Crompton R W (1975), Aust. J. Phys. 28 675.
- Rhymes T, Crompton R W and Cavalleri G (1975), Phys. Rev. A 12 776.
- Roberts S A (1979), Comp. Phys. Comm. 18 353, 363 and 377.
- Robertson A G (1970), Ph.D. Thesis (ANU: unpublished).
- Robertson A G (1971), Aust. J. Phys. 24 445.
- Robertson A G (1977), Aust. J. Phys. 30 39.
- Robson R E (1972), Aust. J. Phys. 25 685.
- Robson R E (1973), Aust. J. Phys. 26 203.
- Robson R E (1976a), J. Phys. B 9 L337.
- Robson R E (1976b), Phys Rev A 13 1536.
- Robson R E (1981), Aust. J. Phys. 34 223.
- Robson R E (1983), personal communication.
- Robson R E (1984), Aust. J. Phys. 37 35.
- Rockwood S D and Greene A E (1980), Comp. Phys. Comm. 19 377; see also LA-UR-79-2166 report Los Alamos Scientific Laboratory.
- Roznerski W and Leja K (1984), J. Phys. D 17 279; and personal communication.
- Roznerski W and Mechlinska-Drewko J (1979), Phys. Lett. 70A 271.
- Saelee H T and Lucas J (1977), J. Phys. D 10 343.
- Saelee H T, Lucas J and Limbeek J W (1977), solid state an Electron Devices 1 111.

- Sakai Y, Tagashira H and Sakamoto S (1972), J. Phys. B 5 1010.
- Sakai Y, Tagashira H and Sakamoto S (1977), J. Phys. D 10 1035.
- Salvini S, Burke P G and Noble C J (1984), J. Phys. B 17 2549.
- Sauers I, Havens T J and Christophorou L G (1980), J. Phys. D 16 1283.
- Savel'ev V L (1983) J. Phys. B 16 141.
- Schneider B I and Collins L A (1983), Phys. Rev. A 27 2847.
- Schoenbach K H, Schaefer G, Kunhardt E E, Kristianson M, Hatfield L L and Guenther A H (1982), IEEE Trans. Plasma Sci. PS-10 246.
- Schoenbach K H, Schaefer G, Kristiansen M, Hatfield L L and Guenther A H (1983), In "Electrical Breakdown and Discharges in Gases" (Ed.s E E Kunhardt and L H Luessen) Pt B p 313 (Plenum Press: New York).
- Schryer N L (1976), Bell Laboratories; Computer Science Technical Report No. 52.
- Searles S K (1974), Appl. Phys. Lett. 25 735.
- Segur P, Bordage M, Balaguer J and Yousfi M (1983a) J. Comp. Phys. 50 116.
- Segur P, Yousfi M, Boeuf J P, Marode E, Davies A J and Evans J G (1983b), In "Electrical Breakdown and Discharges in Gases" (Ed.s E E Kunhardt and L H Luessen) Pt A p 331 (Plenum Press: New York).
- Segur P, Yousfi M and Bordage M (1984), J. Phys. D 17 2199.
- Sherman B (1960) J. Math. Analysis and Application 1 342.
- Shimamori H and Fessenden R W (1979), J. Chem. Phys. 71 3009.
- Shizgal B and McMahon D R A (1984), J. Phys. Chem. 88 4854.
- Shkarofsky I P, Johnston T W and Bachynski M P (1966), "The Particle Kinetics of Plasmas" (Addison-Wesley: Reading).
- Shyn T W and Sharp W E (1981), Phys. Rev. A 24 1734.
- Skinker M F and White J V (1923), Philos. Mag. 46 630.

- Skullerud H R (1968), J. Phys. D 1 1567.
- Skullerud H R (1969), J. Phys. B 2 696.
- Skullerud H R (1972), Norwegian Institute of Technology Technical Report EIP 72-1 (Trondheim).
- Skullerud H R (1973), J. Phys. B 6 728.
- Skullerud H R (1974), Aust. J. Phys. 27 195.
- Skullerud H R (1983), Aust. J. Phys. 36 845.
- Skullerud H R (1984), J. Phys. B 17 913.
- Skullerud H R and Kuhn S (1983), J. Phys. D 16 1225.
- Smirnov B M (1981), "Physics of Weakly Ionized Gases" (Mir Publishers: Moscow).
- Smith D (1983), personal communication.
- Smith D and Dean A G (1975), J. Phys. B 8 997.
- Smith D, Adams N G and Alge E (1984), J. Phys. B 17 461.
- Smits R M M and Prins M (1979), Physica C 96 243 and 262.
- Specht L T, Lawton S A and DeTemple T A (1980), J. Appl. Phys. 51 166.
- Spence D and Schultz G J (1973), J. Chem. Phys. 58 1800.
- Srivastava S K, Tanaka H, Chutjian A and Trajmar S (1981), Phys. Rev. A 23 2156.
- Stockdale J A, Davis F J, Compton R N and Klots C E (1974), J. Chem. Phys. 60 4279.
- Strait G E (1982), J. Chem. Phys. 77 826.
- Swanson N, Celotta R J, Kuyatt C E and Cooper J W (1975), J. Chem. Phys. 62 4880.
- Tachibana K and Phelps A V (1979), J. Chem. Phys. 71 3544.
- Tagashira H (1981), In Proceeding of the XV ICPIG Invited Talks (unpublished), Minsk p 377 and the references therein.

- Tagashira H, Taniguchi T, Kitamori K and Sakai Y (1978), J. Phys. D 11 L43.
- Takayanagi K (1966), J. Phys. Soc. Jpn. 21 507.
- Takeda S and Dougal A (1960), J. Appl. Phys. 31 412.
- Tellinghuisen J (1982), In "Applied Atomic Collisions Physics Vol 3" (Volume Editors E W McDaniel and W L Nighan)p 251 (Academic Press: New York).
- Tembe B L and Mozumder A (1983), Phys. Rev. A 27 3274.
- Tembe B L and Mozumder A (1984), J. Chem. Phys. 81 2492.
- Thomas W R L (1969) J. Phys. B 2 551.
- Thomas R W L and Thomas W R L (1969), J. Phys. B 2 562.
- Thompson D G (1966), Proc. R. Soc. 294 160.
- Thompson D G (1971), J. Phys. B 4 468.
- Thompson D G (1983), Adv. Atomic and Molecular Physics 19 309.
- Thomson R M, Smith K and Davies A R (1976), Comp. Phys. Comm. 11 369.
- Townsend J (1947), "Electrons in Gases" (Hutchinson's: London).
- Trajmar S and Cartwright D F (1982), LA-UR-82-2598 (Los Alamos Scientific Laboratory) to be published in (1984) "Electron-Molecule Interactions and their Applications" (Ed. L G Christophorou, Academic Press: New York).
- Trajmar S, Register D F and Chutjian A (1983), Phys. Rep. 97 219.
- Urosević V V, Bozin J V and Petrović Z Lj (1983), Z. Phys. A 309 293.
- Varracchio E F and Lamanna U T (1984), J. Phys. B 17 4395.
- Verbeek T G and Drop P C (1974), J. Phys. D 7 1677.
- Wada T and Freeman G R (1981), Phys. Rev. A 24 1066.
- Wagner E B, Davis F J and Hurst G S (1967), J. Chem. Phys. 47 3138.
- Warman J M and Sauer M C Jr (1970), J. Chem. Phys. 52 6428.

- Warman J M and Sauer M C Jr (1975), J. Chem. Phys. 62 1971.
- Warman J M and Haas M P de (1975), J. Chem. Phys. 63 2094.
- Warren R W and Parker J H (1962), Phys. Rev. 128 2661.
- Weinert U (1982), Phys. Rep. 91 297.
- Weinert U (1983), Physica 121A 150.
- Wentworth W E, George R and Keith H (1969), J. Chem. Phys. 51 1791.
- Werner C W and George E V (1976), In "Principles of Laser Plasmas" (Ed. G Bekefi) p 421 (Wiley Interscience: New York).
- West R C ed. (1982), "Handbook of Chemistry and Physics" 63rd edition (C.R.C. Press).
- West W P, Cook T B, Dunning F B, Rundel R D and Stebbings R F (1975) J. Chem. Phys. 63 1237.
- West W P, Foltz G W, Dunning F B, Latimer C J and Stebbings R F (1976), Phys. Rev. Lett. 36 854.
- Weyhreter M, Barzick B and Linder F (1984), J. Phys. B to be published, personal communication; and Weyhreter M (1983), Diplomarbeit (Universitat Kaiserslautern: Kaiserslautern-unpublished).
- Whealton J H, Mason E A and Robson R E (1974), Phys. Rev. A 9 1017.
- Wilhelm J and Winkler R (1969), Ann. Physik 23 28.
- Willett C S (1974), "Introduction to Gas Lasers: Population Inversion Mechanisms" (Pergamon: Oxford).
- Williams J F (1979), J Phys. B 12 265.
- Wilson J F, Davis F J, Nelson D R, Compton R N and Crawford O H (1975), J. Chem. Phys. 62 4204.
- Winkler R B, Wilhelm J and Winkler R (1983), Ann. Physik (Leipz) 40 90 and 119.
- Yardley J T (1971), Appl. Opt. 10 1760.

Yardley J T (1980), "Introduction to Molecular Energy Transfer"
(Academic press: New York).

Yoshida S, Phelps A V and Pithford L C (1983), Phys. Rev. A 27 2858.

Young C E (1966), UCRL Rep. No. UCRL-17171.

Zollars B G, Smith K A and Dunning F B (1984) J. Chem. Phys. 81 3158.